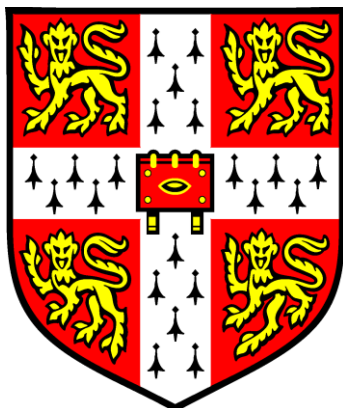


University of Cambridge

Dynamic Combinatorial Synthesis of Donor-Acceptor Catenanes



Fabien B. L. Cougnon

Fitzwilliam College

September 2011

A dissertation submitted to the University of Cambridge in partial fulfilment of the requirements for the degree of Doctor of Philosophy

Declaration

This dissertation is an account of research work carried out in the University Chemical Laboratory, Cambridge, between October 2008 and September 2011. Except where otherwise stated, either directly or by reference, it is the author's own work. It has not, either in part or as a whole, been submitted for a degree, diploma or other qualification at any other university. It does not exceed 60,000 words in length.

Fabien B. L. Cougnon

23 September 2011

Abstract

Dynamic combinatorial chemistry (DCC) is a powerful method for synthesising complex molecules and identifying unexpected receptors. Chapter 1 gives an overview of the concept of DCC and its applications, and discusses its evolution to date.

Chapter 2 describes the discovery of a new generation of donor-acceptor [2]catenanes in aqueous dynamic combinatorial systems. The assembly of these [2]catenanes is promoted by a high salt concentration (1 M NaNO₃), which raises the ionic strength and encourages hydrophobic association. More importantly, a mechanism that explains and predicts the structures formed is proposed, giving a fundamental insight into the role played by hydrophobic effect and donor-acceptor interactions in this process.

Building on these results, Chapter 3 describes the assembly in high salt aqueous libraries of a larger structure: a [3]catenane. Remarkably, the [3]catenane exhibits strong binding interactions with a biologically relevant target – spermine – in water under near-physiological conditions. Its synthesis is improved if the salt is replaced by a sub-mM concentration of spermine, acting as a template.

Chapter 4 explores in further detail how subtle variations in the building block design influence the selective formation of either [2] or [3]catenanes. This last section underlines both the advantages and the limitations of the method developed in Chapter 3.

After a short conclusion (Chapter 5), Chapter 6 gives experimental details.

Acknowledgements

I would like to thank Professor Jeremy Sanders for his kind supervision and guidance. He has given me both the freedom and the inspiration that made my PhD a fulfilling and enjoyable experience. I am grateful for his accessibility and genuine care for his students, and I will cherish the high quality of the scientific emotions that we shared over three years in Cambridge, Warsaw and Bürgenstock. The opportunity that he gave me to work with him has been a real privilege.

I want to express my gratitude to Dan Pantoş for not only his ‘day-to-day’ supervision in the lab, but also for the long NMR sessions in the evenings and weekends, and for the many stimulating discussions which ensured the smooth progression of my PhD.

I also want to thank my Part III student, Nick Jenkins; supervising him has been a tremendous and rewarding experience. Some parts of this thesis have benefited from his hard work and enthusiasm.

I must acknowledge all the members of lab 354, present and past, who made the lab such a friendly and unique place. Special thanks go to Ernie, who guided my first steps into the world of catenanes; my dear fellow Kouj for endless proof-readings and for our common passion for Taio Cruz; Yana for introducing me to Rakia and Bulgarian pop-folk; Victoria for introducing me to climbing and for moving mattresses all across Cambridge; Xavier, Jörg and Matej for the tough squash sessions that (occasionally) distracted me from chemistry; Miguel for an unforgettable journey into the jungle of Mexico; Geneva and Sophie for their steady good mood and for being such talented cooks; Michael for interesting scientific discussions at the *Free Press*; Emiliano for being Italian and for the table tennis game that he

gave to us; Artur for organising an amazing leaving dinner at *Polonia*; Naoki for making the office such a fun place to work in; Ana and Rosy for their help with the HPLC and the LC-MS.

I would like to thank particularly Nandhini for her support and patience, mostly during the last year of my PhD. My time in Cambridge would have not been as enjoyable without her.

I would like to show my gratitude to my parents and siblings for being so supportive, and to Sijbren Otto and Charles Tanielian, without whom I would have never started this PhD in Cambridge.

Finally, I would like to acknowledge the technical staff of the Department of Chemistry, Fitzwilliam College for the quality of its facilities and support, and EPSRC for funding.

Abbreviations

A	Acceptor
COSY	Correlation spectroscopy
Cys	Cysteine
D	Donor
DCC	Dynamic combinatorial chemistry
DCL	Dynamic combinatorial library
DMF	Dimethylformamide
DMSO	Dimethylsulfoxide
DN	Dioxynaphthalene
DNA	Deoxyribonucleic acid
ESI-MS	Electrospray ionisation mass spectroscopy
FA	Formic acid
Gly	Glycine
GSH	Glutathione
HRMA	High resolution mass spectroscopy
HPLC	High performance liquid chromatography
<i>K</i>	association constant
LC-MS	Liquid chromatography – mass spectroscopy
<i>m/z</i>	mass to charge ratio
MS	Mass spectroscopy
MS/MS	Tandem mass spectroscopy
NDI	Naphthalenediimide
nOe	Nuclear Overhauser effect
NOESY	Nuclear Overhauser enhancement spectroscopy
RDCC	Resin-bound dynamic combinatorial library
TFA	Trifluoroacetic acid
UV-Vis	Ultra-violet visible

Table of Contents

Declaration	i
Abstract	ii
Acknowledgements	iii
Abbreviations	v
Table of Contents	vi

CHAPTER 1

Evolution of Dynamic Combinatorial Chemistry	1
1.1. A successful but naive idea	3
1.2. Unexpected and delicate architectures	10
1.3. Expanding the scope of dynamic combinatorial chemistry	14
1.4. Conclusion	21
References	22

CHAPTER 2

Exploring the Formation Pathways of Donor-Acceptor Catenanes in Aqueous Dynamic Combinatorial Libraries	26
2.1. Introduction	27
2.1.1. Brief overview on donor-acceptor interactions	27
2.1.2. Scope of this Chapter	29
2.2. Mechanism of formation of donor-acceptor catenanes	32
2.2.1. Design of the building blocks used in this Chapter	32
2.2.2. Test for thermodynamic equilibrium	35
2.2.3. Proposed mechanism of catenanes formation in aqueous DCLs	38
2.3. Exploring Pathway I	41

2.3.1. Identification of the first DADA catenane: Cat-4	42
2.3.2. Improving the synthesis of DADA catenanes: from Cat-4 to Cat-6	44
2.3.3. ¹ H NMR characterisation of Cat-6	45
2.3.4. Improving further the synthesis of DADA catenanes: Cat-7	48
2.3.5. ¹ H NMR characterisation of Cat-7	49
2.3.6. Conclusion: synthesising DADA catenanes from Pathway I	51
2.4. Exploring Pathway II	53
2.5. Exploring Pathway III	56
2.5.1. Identification of the first AADA catenane: Cat-8	57
2.5.2. ¹ H NMR characterisation of Cat-8 and of its isomeric macrocycle 24	59
2.5.3. Identification of a second AADA catenane: Cat-10	64
2.5.4. ¹ H NMR characterisation of Cat-10	66
2.5.5. Identification of other AADA catenanes	68
2.6. Competing Pathways	71
2.7. Conclusion	73
References	75

CHAPTER 3

Templated Dynamic Synthesis of a [3]catenane	78
3.1. Introduction	79
3.1.1. Synthesis of donor-acceptor [3]catenanes	79
3.1.2. Dynamic combinatorial synthesis: from [2] to [3]catenanes	79
3.2. Discovery of the first [3]catenane	82
3.3. Investigating the mechanism of formation of 4,4-[3]Cat	85
3.4. Stepwise addition of one of the building blocks	87
3.5. ¹ H NMR characterisation of 4,4-[3]Cat	88
3.6. Amplification of 4,4-[3]Cat with spermine	92
3.7. Amplification of 4,4-[3]Cat with other polyamines	94
3.8. ¹ H NMR titration of 4,4-[3]Cat with spermine	95

3.9. Conclusion	97
References	99

Chapter 4

Versatile Formation of Donor-Acceptor [2] and [3]Catenanes in Water	102
4.1. Introduction	103
4.1.1. Scope of this Chapter	103
4.1.2. Design of the building blocks used in this Chapter	105
4.2. Effect of the length of the aliphatic linker	107
4.2.1. Manifestation of an odd-even effect	108
4.2.2. Identification of new unexpected [2]catenanes	111
4.2.3. ¹ H NMR characterisation of the isolated catenanes	116
4.2.3.1. ¹ H NMR characterisation of 7-[2]Cat	116
4.2.3.2. ¹ H NMR characterisation of 7,7-A, 7,7-[2]Cat and 7,7-[3]Cat	119
4.3. Influence of the building block chirality	122
4.3.1. Effect of chirality on the yield of catenanes	122
4.3.2. Exploring the differences between two diastereomeric catenanes	125
4.3.2.1. Kinetics of formation	125
4.3.2.2. ¹ H NMR spectra	127
4.3.2.3. Interaction with spermine	129
4.3.3. Conclusion on the effect of chirality	131
4.4. Conclusion	132
References	134

Chapter 5

Conclusion	137
-------------------	-----

Chapter 6

Experimental	138
6.1. General information	138
6.1.1. Chemicals and solvents	138
6.1.2. DCL preparations	138
6.1.3. NMR	139
6.1.4. LC-MS	140
6.1.5. Preparative HPLC	140
6.1.6. UV-Vis	141
6.1.7. Other analytical methods	141
6.2. Synthesis of the building blocks	142
6.2.1. Synthesis of building block A4	142
6.2.2. Synthesis of building block A5	145
6.2.3. Synthesis of the extended building blocks n-A	147
6.2.4. Synthesis of building block D2a'	163
6.3. LC-MS analysis of the DCLs	165
6.3.1. LC-MS methods for Chapter 2	165
6.3.2. LC-MS methods for Chapters 3 and 4	167
6.4. MS and MS/MS spectra of the new catenanes	168
6.5. NMR data of the isolated macrocycles and catenanes	183
6.6. UV-Vis spectra of the isolated macrocycles and catenanes	191

CHAPTER 1

Evolution of Dynamic Combinatorial Chemistry

Since its inception in the mid-1990s, dynamic combinatorial chemistry (DCC) — the chemistry of complex systems under thermodynamic control — has proved valuable in identifying unexpected molecules with remarkable binding properties, and in providing effective synthetic routes to complex molecules. In essence, it is an approach in which one designs the experiment, rather than the molecule. It has also provided us with a tool for gaining insights into how some chemical systems respond to external stimuli. Using examples from the work of the Sanders group and others, this introduction shows how the concept of DCC, inspired by the evolution of living systems, has found an increasing range of applications in diverse areas, and has itself evolved conceptually and experimentally.

A dynamic combinatorial library (DCL) is a thermodynamically controlled mixture of interconverting species that can respond to various stimuli. For example, an added template can select and stabilize a strongly binding member which is then amplified at the expense of the unsuccessful library members, minimizing the free energy of the system. Thus, the Cambridge version of dynamic combinatorial chemistry was initially inspired by the example of the mammalian immune system and conceived as a way to create and identify new unpredictable receptors, but it has been exploited in a variety of other ways.¹ DCC has contributed significantly to the evolution of chemistry over the past two decades as its range of applications have increased in diverse fields including catalysis, fragrance release, and responsive materials. Among these applications, the ability of complex chemical systems to reach a high level of organisation has been exploited to build intricate and well-defined architectures such as catenanes or hydrogen-bonded nanotubes. In addition, it has proved a powerful tool for the study of complex molecular networks and systems.

Dynamic combinatorial chemistry is actively contributing to the improvement of our understanding of chemical and biological systems. The study of folding or self-replicating macrocycles in DCLs has been applied as a model to help us appreciate how complex organisations such as life can emerge from a pool of simple chemicals. Today, DCC is no longer restricted to thermodynamic control, and new systems have recently emerged in which kinetic and thermodynamic control co-exist. Expanding the realm of DCC to unexplored and promising new territories, these hybrid systems show that the concept of dynamic combinatorial chemistry continues to evolve.

1.1. A successful but naive idea

Evolution has long been associated with the idea of a blind, random emergence of the best-adapted organism. However, in recent decades, many scientists have questioned whether evolution is truly random, and have shown it to be strongly constrained by the laws of physics and chemistry: in 1993, in his book *The Origins of Order*,² Kauffman used the perspective of mathematics to show that complex disordered systems (including, amongst others, living organisms) display an inherent property to self-organise and evolve in a way that was described as a “combinatorial optimisation process”. Building on this notion, Williams and Fraústo Da Silva³ proposed — from a purely biochemical point of view — that evolution can be predictably driven both by the nature of the chemicals accumulated within organisms and the way they interact with a changing environment.

Such concepts offer the opportunity of using complex networks of interactions to access highly organised structures and chemists, taking inspiration from nature, have since designed many artificial evolutionary systems. Amongst them, dynamic combinatorial chemistry (DCC)^{1, 4} has proven to be a particularly fruitful approach: instead of designing a molecule to target a specific problem, the dynamic combinatorial chemist designs a system in which the most successful molecule is automatically selected and amplified from a pool of potential targets. In the beginning, DCC appeared to be a simple way to access many different and unpredictable receptors from a single pool of relatively simple components; chemists soon realised that it was a good way of discovering complex architectures and receptors that are normally inaccessible or unimaginable by rational design, and also a powerful tool for the study of systems chemistry.⁵

In dynamic combinatorial chemistry, simple molecular units (building blocks) are held together by non-covalent or reversible covalent bonds, generating a complex mixture of products which continuously

interconvert: ideally, the composition of the mixture at equilibrium is thermodynamically controlled and is referred to as a dynamic combinatorial library (DCL, Figure 1.1).^{1, 4} However, the definition of dynamic combinatorial systems has also been extended to more complex systems that are not purely under thermodynamic control.

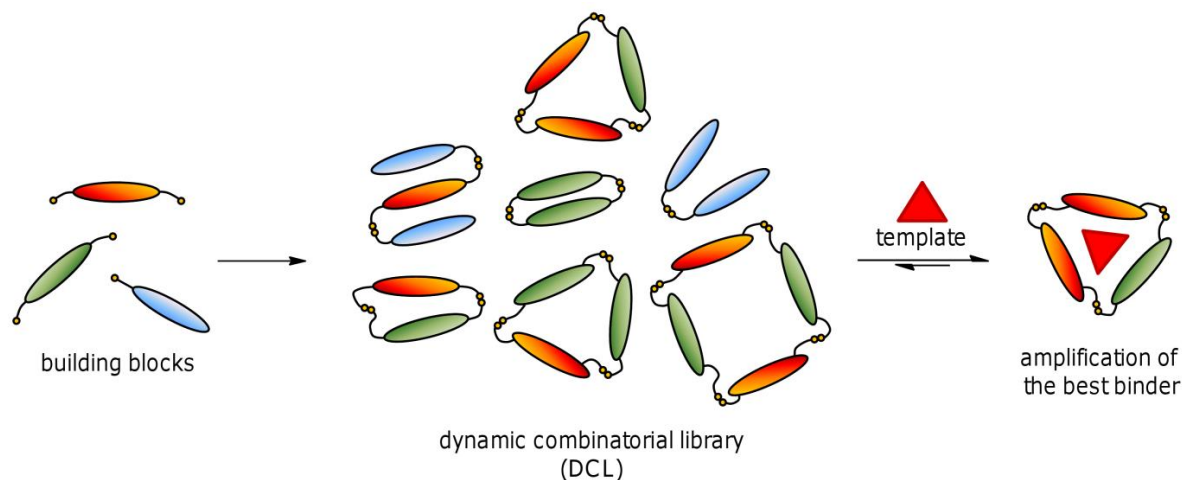


Figure 1.1. Schematic representation of a dynamic combinatorial library and amplification of the best binder in the presence of a template.

As a dynamic system, a library can respond to various stimuli that drive the constituents to reorganize in order to minimise the total free energy of the system. The stimuli that have been investigated include change of pH, temperature, or electric field, but the most exploited stimulus involves the introduction of a chemical template: libraries of macrocycles, for example, provide as many potential receptors as library members, and addition of a guest which binds strongly to one of the library components shifts the equilibrium towards its formation, resulting in the amplification of the successful receptor at the expense of the less successful. This concept constitutes an elaborated version of the metal-ion templated macrocycle synthesis proposed by Busch in the 1960s,⁶ and was independently developed by the

Sanders⁷ and Lehn⁸ group in the mid-1990s. Allowing easy screening of potential receptors with different features, this approach has made DCC a powerful tool for the discovery of new receptors.

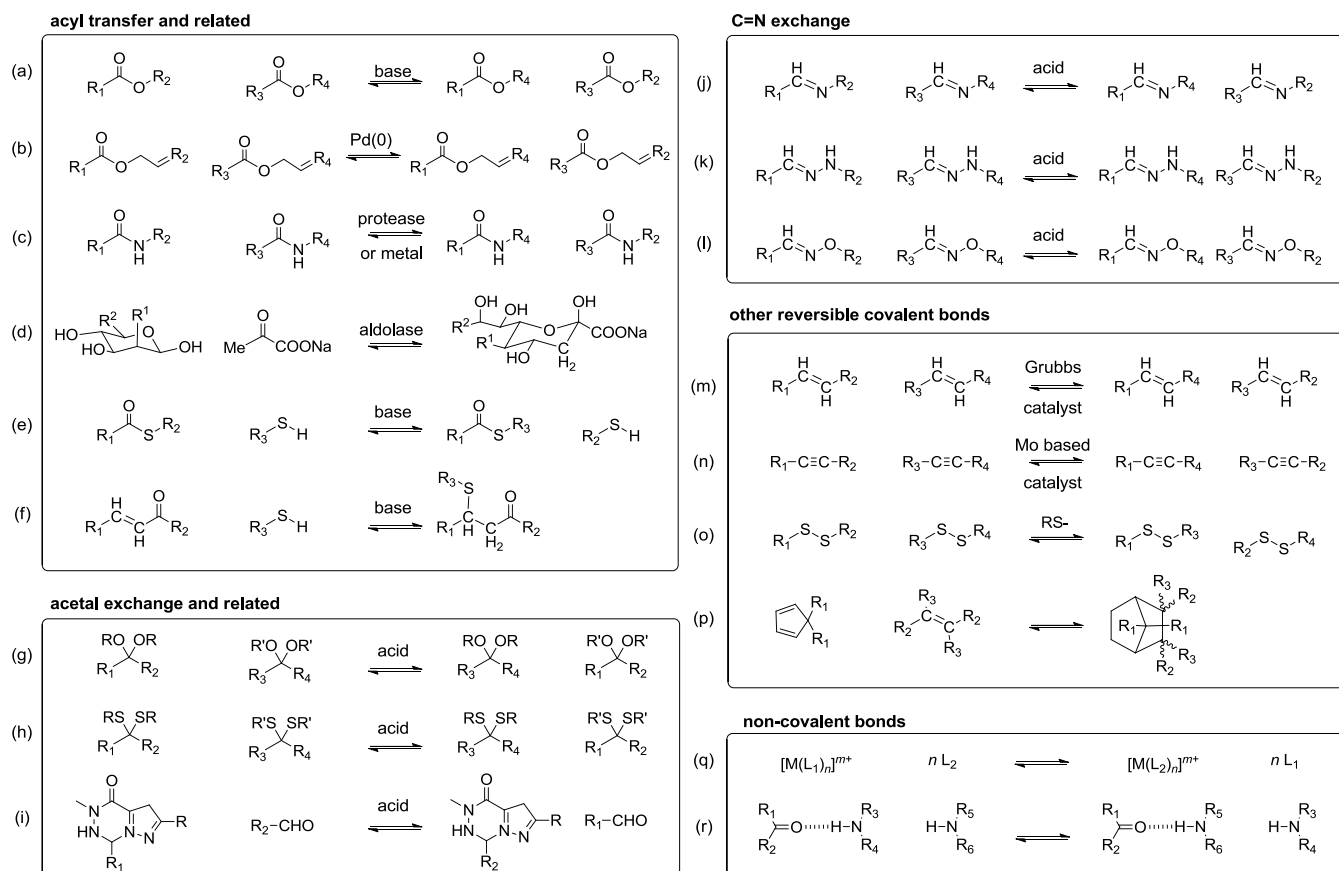


Figure 1.2. Some of the reversible reactions used in DCLs: (a) transesterification, (b) transallylesterification, (c) transamidation, (d) aldol exchange, (e) transthioesterification, (f) Michael / retro-Michael reactions (g) acetal exchange, (h) thioacetate exchange, (i) pyrazolotriazone metathesis, (j) imine exchange, (k) hydrazone exchange, (l) oxime exchange, (m) alkene metathesis, (n) alkyne metathesis, (o) disulfide exchange, (p) Diels-Alder / retro-Diels-Alder reactions, (q) metal-ligand exchange, and (r) hydrogen-bond exchange.¹

Most of the reversible reactions used in DCC have been summarised elsewhere,^{1, 4} although the range of reversible bonds used continues to grow. Some of them are shown in Figure 1.2. Disulfide exchange has

been much exploited in our laboratory because it offers several attractions: the disulfide bond is relatively robust but it exchanges under mild conditions.

Disulfide DCLs can be generated simply by dissolution of thiol building blocks in water at pH 8.0 under air, allowing for the screening of biologically relevant target under near-physiological conditions. The exchange is generally accepted to proceed through the nucleophilic attack of a thiolate anion on the disulfide bond formed by the slow oxidation of the thiol building blocks (Figure 1.3). The process is reversible as long as thiolate anions are present in solution, but the oxidation process is irreversible, and the exchange stops after the building blocks are fully oxidized, allowing for easy purification of the macrocycles formed.

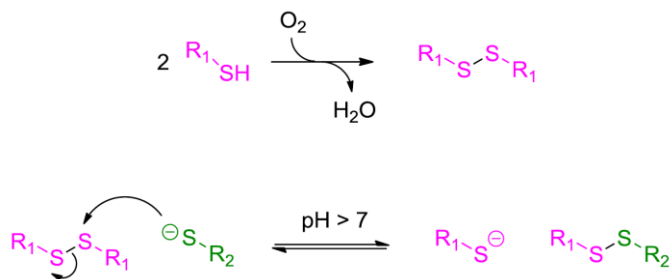


Figure 1.3. Proposed mechanism of disulfide exchange.

Complex libraries can easily be prepared with a limited number of building blocks. A library composed of only three building blocks (**1**, **2** and **3**, Figure 1.4), for example, contains a large number of macrocycles, forty-five of which could be differentiated by LC-MS.⁹ The complexity of this particular library is further increased by the fact that **1** was synthesised as a racemic mixture, and most macrocycles were consequently present as a mixture of stereoisomers. The building blocks were inspired by a family of cyclophane receptors developed earlier by the Dougherty group.¹⁰

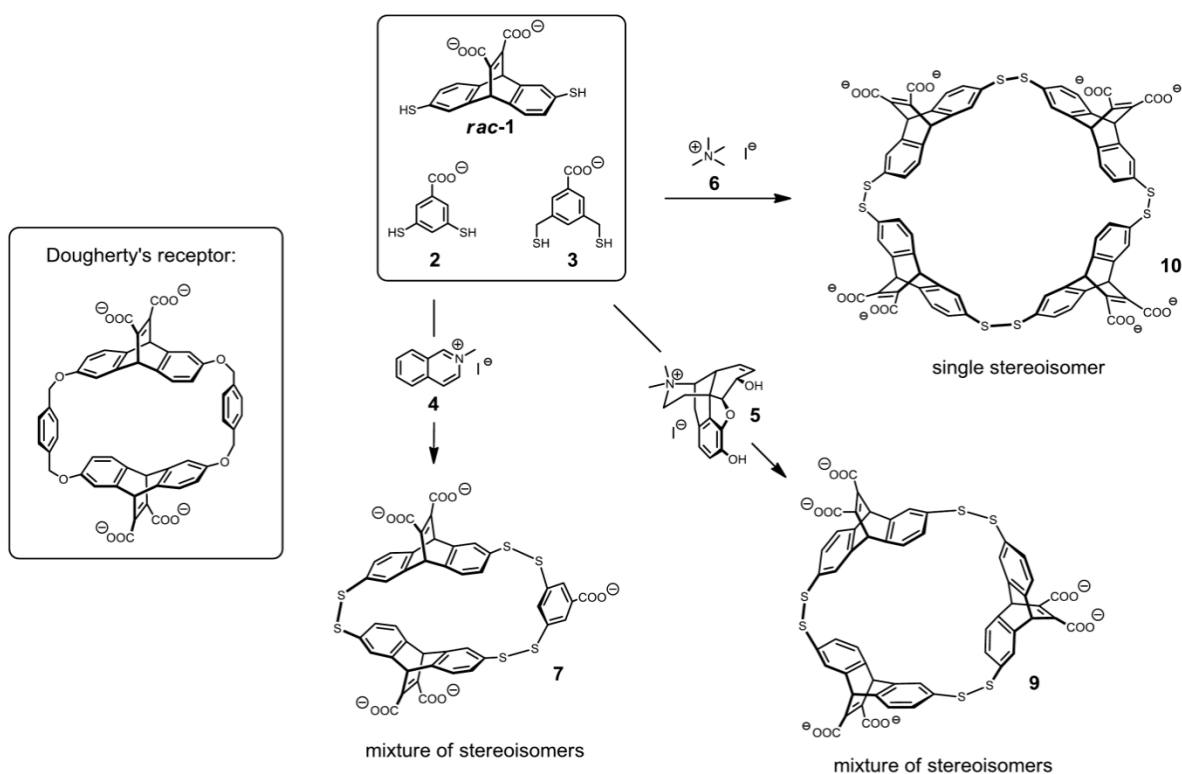


Figure 1.4. Amplification of three different receptors from one single library.⁹

Upon addition of the ammonium guest **4**, one of the best known binders to the negatively charged receptor developed by Dougherty, the cyclic trimer **7** was amplified. Although the receptor selected in the library shares many features with Dougherty's, it is striking that **7** is not its exact analogue, thus demonstrating the power of DCC to uncover unexpected receptors. Moreover, addition of two other ammonium guests, **5** and **6**, resulted in the amplification of two different macrocyclic receptors, trimer **9** and tetramer **10**, showing that one single library with a sufficient diversity can be used to amplify more than one receptor, and that a small difference in binding affinity is sufficient to amplify selectively from a large number of similar structures.

The 1000-fold amplification of the large tetramer **10** by the small tetramethylammonium iodide guest^{9b} is particularly surprising; even more remarkably, there are four diastereomers of the tetramer but only

one is amplified in the presence of the ammonium guest as it is the only one that can efficiently fold around the template. In the absence of a template, macrocycle **10** adopts a variety of exchanging conformations and consequently displays extremely broad NMR resonances; these sharpen dramatically in the presence of the template, thereby highlighting the discriminating power of DCC through the induced-fit selection of not only one diastereomer but also just one specific conformation. The main attraction of this system was that it provided access to many new receptors without the need for long synthesis. Moreover, in optimised conditions, the yield of the amplified macrocycles was remarkably high, a noteworthy feat given the low yields commonly associated with macrocyclisation reactions.

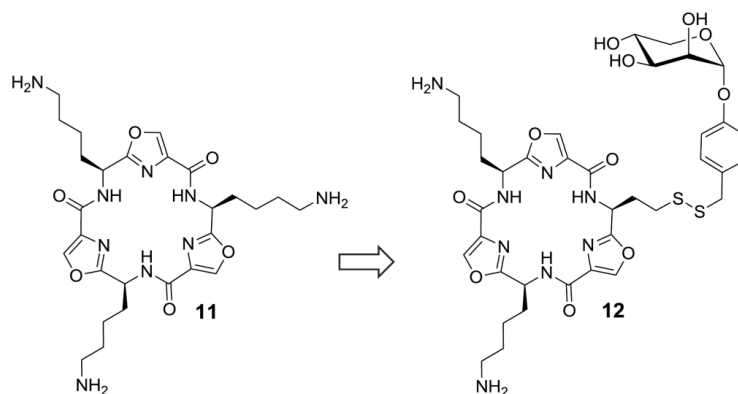


Figure 1.5. G-quadruplex ligands: a known binder (**11**), and an improved version (**12**) amplified from a DCL in the presence of c-Kit21.¹¹

The scope of DCC rapidly extended to more complex target structures. Our group demonstrated in collaboration with the Balasubramanian group that a DCL of small molecules could be templated by DNA G-quadruplexes.¹¹ The DCC approach enabled a high level of discrimination between different G-quadruplex targets with a disulfide library inspired by macrocycle **11**. The binding affinity of the ligands amplified in the libraries (such as **12**, Figure 1.5) was superior to the binding affinity of the similar macrocycle **11**. However, these libraries are of relatively modest size: a similar level of discrimination

could be obtained using regular parallel synthesis, and for this reason, increasing the size of the libraries soon became a topic of major interest.¹²⁻¹⁶

As one might expect, increasing the size of the library increases the probability of generating potential binders, but as the concentration of the library members decreases in large libraries, the limit of analytical instrumentation is rapidly reached and the fear of entropy increases. Otto *et al.* recently showed that the size of the library could be extended to up to 9,000 members by using equimolar amounts of eight building blocks.¹³ In this large library, addition of ephedrine resulted in the unexpected amplification of macrocycles which were previously undetectable in the absence of template. The experiment clearly showed that a receptor does not need to be significantly present in the untemplated library to be amplified. As in the previous case, the amplification correlated well with a good binding affinity between the isolated receptor and the guest, and the amplified receptors turned out to have among the highest affinities reported for ephedrine in water. The analytical challenge posed by such large libraries has been met by Miller *et al.*,¹⁴ who developed a RBDCC (resin-bound dynamic combinatorial library) technology that allows identification of effective binders for fluorescently labelled target RNA in a library of small peptides with a theoretical size of 11,325 members.

While the above examples imply that library size is limited only by technological constraints, other factors need to be considered in order to understand the response of a DCL to the addition of template. For example, the Severin group and ours showed that, when the concentration of template is too high, the amplification of weaker binders may compete with the amplification of stronger binders.¹⁵ More specifically, the amplification of weaker-binding mixed-macrocycles may be favoured over stronger-binding homo-macrocycles, and the amplification of small macrocycles that are weak binders may be favoured over the amplification of better but larger receptors in order that the whole system gains maximum free energy. Although these problems can be avoided at low template concentration, using

DCC to study host-guest interactions appears to be more complicated than initially expected.¹³ Furthermore, the composition of the library and its behaviour may also be complicated by other issues described below.

In spite of these limitations, DCC exhibits an amazing propensity to form complex architectures, and some most surprising examples are depicted in the following section: DCC offers a unique approach for exploring and exploiting the properties of templating, self-folding or self-replicating molecules, and has rapidly grown as an ideal testing ground to improve our understanding of complex reversible systems.

1.2. Unexpected and delicate architectures

Although the above example shows that large macrocycles can fold in a suitable conformation in order to optimize their interaction with a guest,⁹ macrocyclic receptors often lack flexibility. Our group recently reported the amplification of highly flexible linear oligomers at the expense of macrocycles by dihydrogen phosphate anion acting as template.¹⁷ A hydrazone-based library was formed in a mixed chloroform/methanol solvent using commercial mono- and di-aldehydes, and a di-hydrazide building block, composed of a ferrocene unit coupled to an amino acid (valine). The library contains both linear and cyclic oligomers. However, in the presence of the anion, only the linear species were amplified. The presence of the chiral *L*-Valine induces a *P* helicity of the peptide chains around the ferrocene unit, which dictates the structure of the linear oligomers: being simultaneously organised and flexible, they can easily adopt a suitable conformation to wrap efficiently around the anion.

The amplified linear oligomers are unusually large and incorporate five, seven or nine building blocks. Intuitively, the fear of entropic costs would have inhibited the design of such large and flexible anion receptors, and the formation of these large oligomers should be entropically unfavorable in the library. Their formation can only be explained by the cooperative binding of multiple dihydrogen phosphate anions: indeed, the pentamer **13** (Figure 1.6) binds two anions, and the more complex and larger oligomers are thought to bind more than two anions.

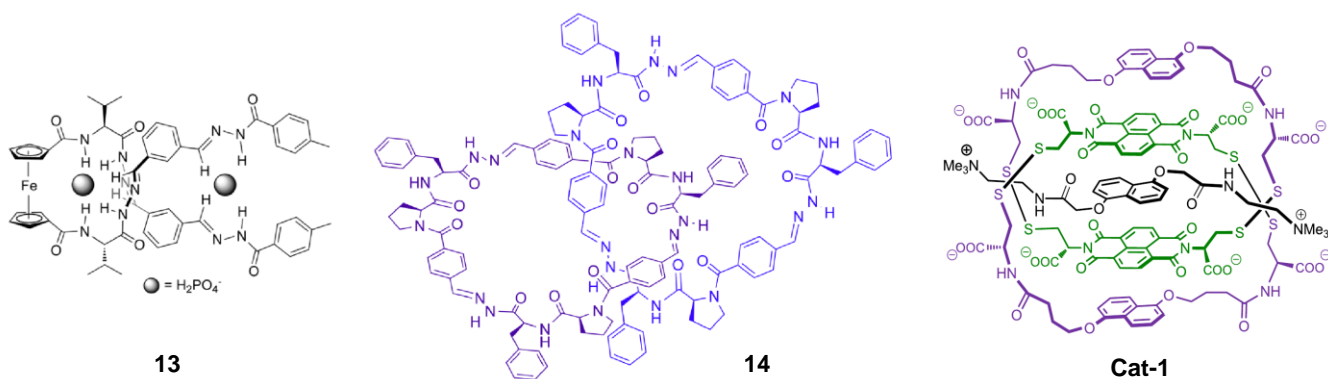


Figure 1.6. Unexpected receptors discovered by DCC: a helical linear receptor for dihydrogen phosphate ions (**13**),¹⁷ a peptide-based catenane binding to acetylcholine (**14**),¹⁸ and a donor-acceptor catenane binding to a donor-template (**Cat-1**).²⁰

Surprisingly, complex structures such as catenanes, can also turn out to be good receptors. The amplification of an acetylcholine-binding [2]catenane (**14**, Figure 1.6) in a hydrazone-based DCL is perhaps one of the most striking examples.¹⁸ As the previous example showed, peptide moieties in synthetic building blocks can serve as scaffolds with useful recognition properties. In the presence of the neurotransmitter acetylcholine, a library composed of only one peptide-based building block (derived from phenylalanine and proline) resulted in the formation of a hexameric [2]catenane originally not

detectable in the untemplated library. Because of the presence of chiral centres in the initial building block, two diastereomeric [2]catenanes are possible. However, acetylcholine promotes the formation of only one of these diastereomers. Moreover, although this diastereomer can adopt many conformations, only one of these conformations binds acetylcholine.

Recently, Gagné *et al.* have reported the dynamic combinatorial syntheses of several [2]catenanes derived from similar building blocks, in which the phenylalanine unit was replaced by non-natural amino acids such as dimethylglycine or amino(1-naphthyl)acetic acid.¹⁹ In this case, octameric [2]catenanes spontaneously formed under the dynamic combinatorial conditions. The [2]catenane self-templation is very dependent on both the amino acid incorporated in the building block and its chirality; also, the complementarities of the H-bonding motifs and of other non-covalent interactions, such as CH- π interactions, are important features of the self-assembly of these [2]catenanes.

The dynamic combinatorial donor-acceptor [2]catenane **Cat-1** (Figure 1.6) also exhibits interesting binding properties.²⁰ This [2]catenane has an unusual stacking arrangement of the donor (D) and acceptor (A) units, and its formation in aqueous medium hints that its assembly is governed mainly by hydrophobic effects. However, donor-acceptor interactions can be favourably used to form a host-guest complex in the presence of a donor template, allowing the formation of a stable DADAD stack. Further stabilization of the complex apparently comes from the interaction between the ammonium cations of the guest and the carboxylic anions of the host catenane.

In all these cases, access to these remarkably complex architectures is the result of both the recognition of the catenanes' components with themselves (self-recognition) and host-guest recognition (template effect). These two phenomena are not necessary complementary and can be antagonistic: dynamic combinatorial systems have been reported in which the spontaneous assembly of [2]catenanes is reversed by the presence of a template that binds preferentially to simpler macrocycles.²¹

The intricate network of interactions in dynamic combinatorial systems has been exploited to self-assemble many other receptors and complex structures.^{1, 4} Subtle differences in the building block structure or in the library conditions can be reflected in the library diversity, leading to the formation of either simple or complex libraries. The flexibility (or lack thereof) of the building blocks may affect their properties of molecular recognition, self-aggregation, or self-replication within the library, but it seems that the most successful building blocks tend to possess both a rigid and a flexible component.

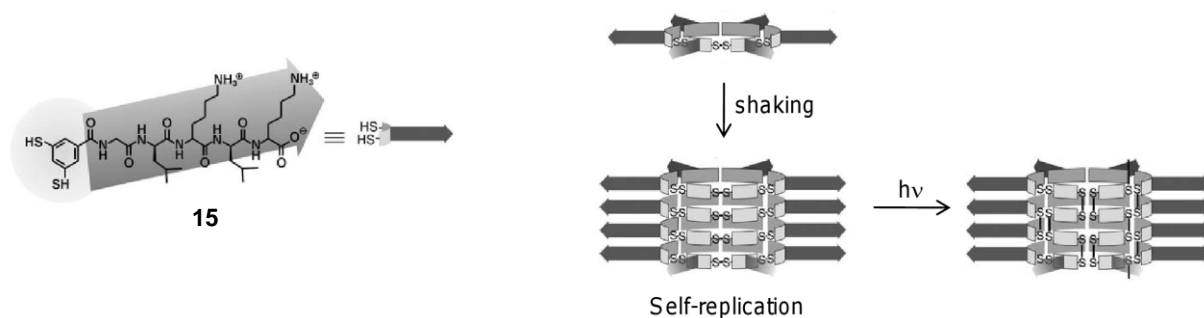


Figure 1.7. Self-replication of a hexamer and covalent capture of the fibres upon UV irradiation.²³

The aptitude of peptide-based building blocks to organise into complex dynamic combinatorial systems has brought a valuable insight into the rules governing biomolecular processes.²² Otto *et al.* recently showed that a hexamer formed from a fully synthetic peptide-based building block (**15**) can self-replicate through the formation of three dimensional fibres (Figure 1.7).²³ These fibres, held together by β sheets, are fragile, breaking when subjected to moderate shear forces, but they can be covalently captured upon UV irradiation. The ability to replicate is an essential characteristic of life, and such self-assembly processes could, plausibly, lie at the origin of living systems. As such, the scope of dynamic systems can be expanded far beyond the initial realms of dynamic combinatorial chemistry.

1.3. Expanding the scope of dynamic combinatorial chemistry

Dynamic combinatorial chemistry has been extended to several other fields, such as drug delivery,¹ two-phase transport,²⁵ fragrance delivery,^{4, 26} or biosensing.²⁷ The Sanders group described how DCC can be used as an approach to finding new catalysts, inspired by the example of catalytic antibodies.²⁸ Used as a template, **17** (Figure 1.8) amplified significantly two macrocycles in the disulfide DCL shown earlier in Figure 1.4.

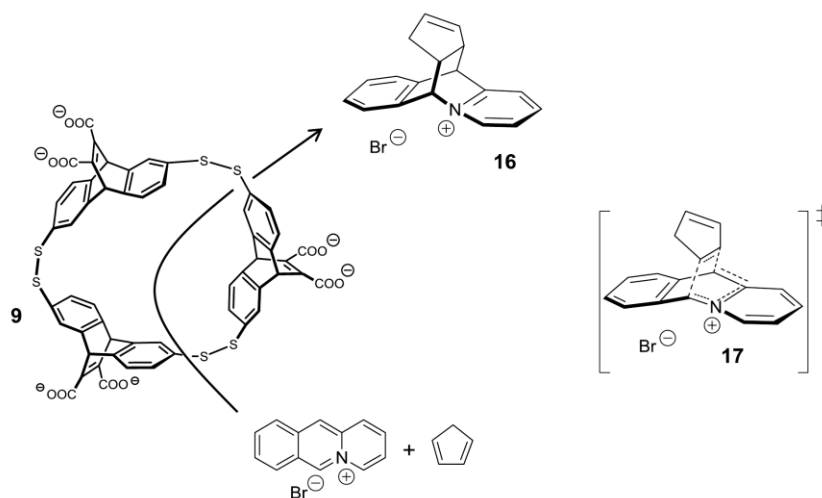


Figure 1.8. Towards an application of DCC for the discovery of catalysts.²⁸

Template **17** is the product of the Diels-Alder reaction shown in Figure 1.8, and may be considered as a stable analogue of the transition state **16**. The envisaged stabilising interaction between the amplified macrocycles and the transition state of this reaction led us to reason that these macrocycles may act as catalysts: the two macrocycles were isolated and their potential to catalyse the Diels-Alder reaction was evaluated. While the first macrocycle was found to bind better to the starting material than to the product and thus be catalytically inactive, the second macrocycle (**9**, Figure 1.8) induced a modest acceleration of the reaction rate. Although this macrocycle exhibits a limited catalytic activity, it showed

that a correlation exists between the observed amplification and the catalytic activity. A similar strategy was also applied to the catalysis of acetal hydrolysis. Prins *et al.* have further developed this approach to screen and understand catalytic processes, using phosphonate as a model for the transition state of carboxylic ester hydrolysis.²⁹

Templates are not necessarily limited to small molecules: large templates such as enzymes can induce the self-assembly of the best substrate, as demonstrated by Huc and Lehn in 1997.³⁰ This seductive approach provides an alternative strategy for fragment-based drug discovery, and has been recently expanded by Greaney *et al.*³¹

The knowledge produced by dynamic combinatorial systems may also be used to access quantitative assembly of well-defined molecular structures. Sleiman *et al.* developed complementary DNA-branched building blocks that generate a library of macrocycles under thermodynamic control, including the dimer, tetramer, and hexamer (Figure 1.9.a).³² Addition of the ruthenium template $\text{Ru}(\text{bpy})_3^{2+}$ produced the quantitative reorganisation of the library into the square tetramer **18**. Based on this result, the Sleiman group designed a new generation of building blocks which formed, in the presence of the ruthenium template, the DNA-based ladder **19**, a single nanostructure based on the previously amplified square.

This latest example shows how the understanding and control of self-assembly at a molecular level can result into the formation of precisely controlled micrometer DNA-fibres. Lehn *et al.* recently demonstrated that dynamic systems could be used to form reversible thermoresponsive polymers (Figure 1.9.b),³³ or to switch between macrocycles and polymers in the presence or absence of Zn^{2+} .³⁴ More generally, the adaptative response of reversible systems to external stimuli offers a method of altering the properties of a system on the macroscopic scale, leading to the recent emergence of dynamic materials whose formation and properties can be triggered by diverse stimuli.³⁵

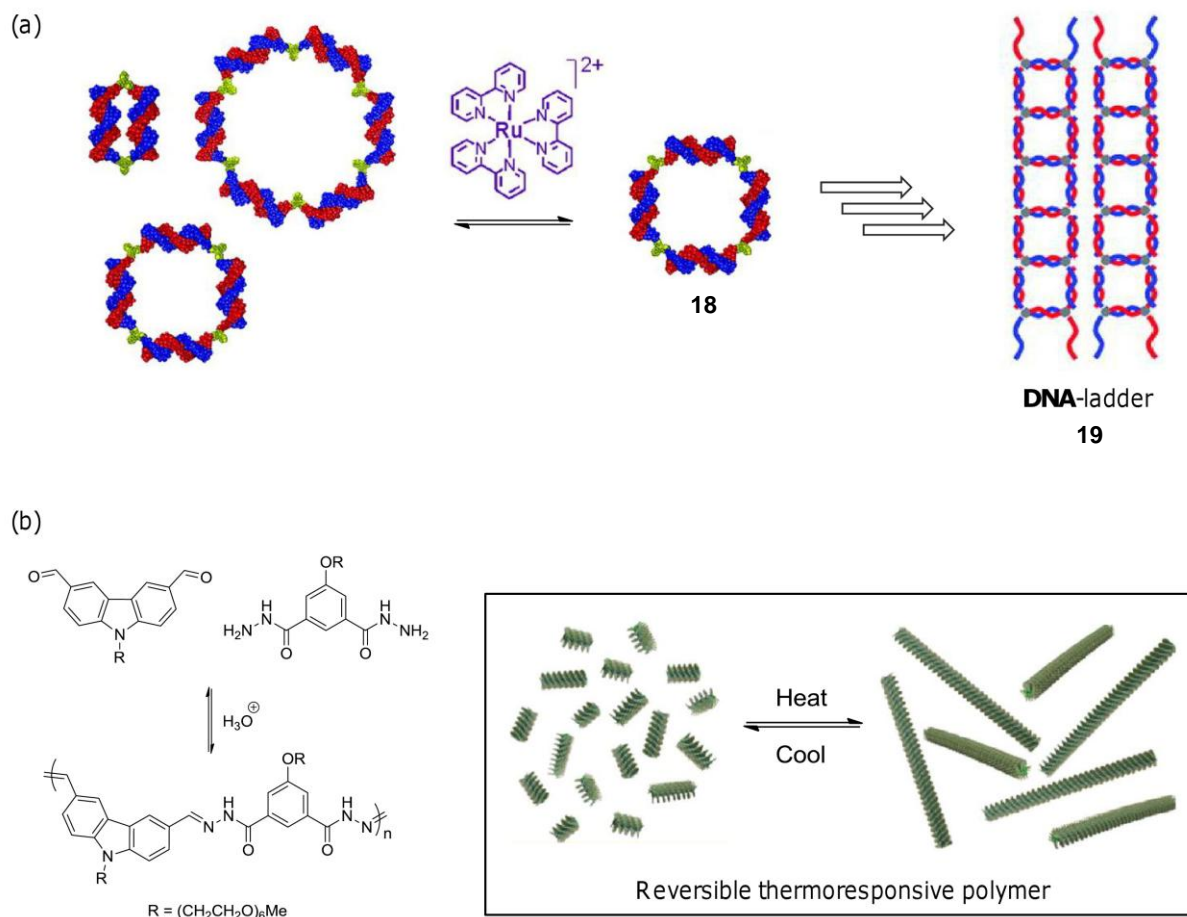


Figure 1.9. From molecular level to macroscopic scale. These two examples show that the control of reversible systems on the molecular level can be used to create much larger assembly: (a) a DNA-based ladder³² or (b) thermo-responsive polymers.³³

Dynamic combinatorial chemistry has promoted the evolution of knowledge and new technologies, but its scope may be limited by its intrinsic requirements. Above all, thermodynamic control is a key requirement to generate a truly dynamic combinatorial system. Our group proved that thermodynamic equilibrium could be reached in a variety of conditions, in organic or aqueous media, and recently even in the solid state.³⁶ To generate a sufficiently diverse library under thermodynamic control, different conditions must be fulfilled: the linkage between the building blocks must be fully reversible and the energy landscape of the library must be relatively shallow to allow rapid interconversion. Hydrogen

bonding may be used for this purpose, but unlike the covalent and slow metal exchange processes described above, the exchange process cannot be turned off, making the isolation of the individual library members impossible.

One of the most representative examples might be the fully reversible and highly dynamic formation of supramolecular nanotubes (Figure 1.10).³⁷ In halogenated solvents, 1,4,5,8-naphthalenetetracarboxylic diimide functionalised with amino acids (**20**) formed a library of hollow organic nanotubes of different sizes through carboxylic acid dimerisation.

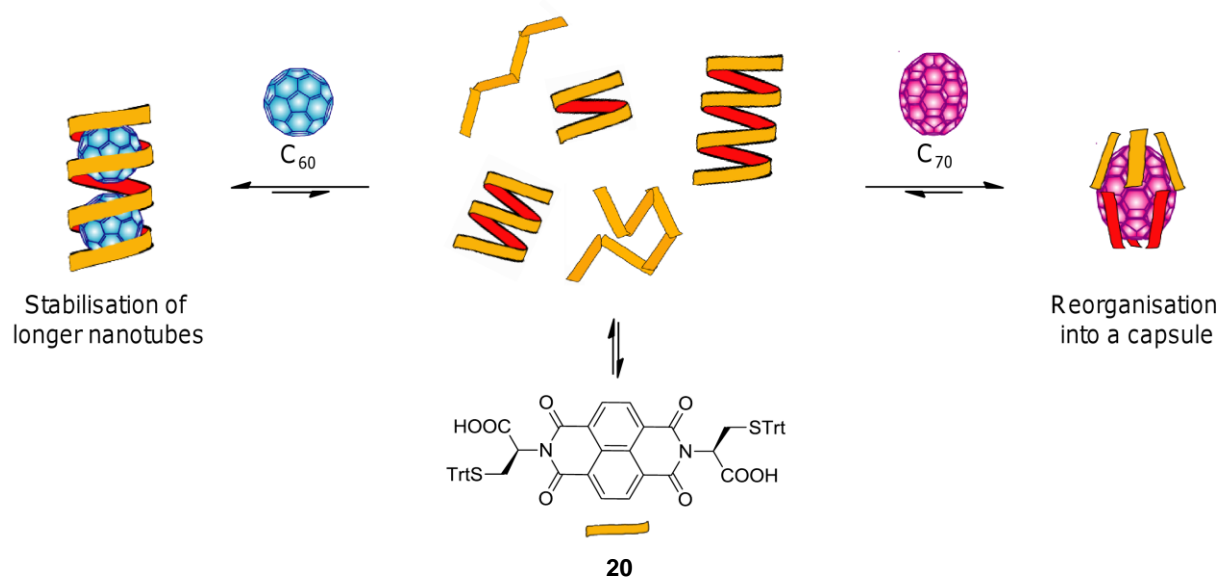


Figure 1.10. A library of hydrogen-bonded helical nanotubes. Addition of C₆₀ or C₇₀ allows amplification of longer nanotubes or of a hexameric capsule, respectively.³⁷

Studies of the thermodynamic parameters of the nanotubes brought valuable insight into the possibility of forming non-classical hydrogen bonds (C-H...O) in solution. Due to the delicate balance between the enthalpic gain and the entropic loss necessary to the formation of the nanotubes, our group demonstrated

that the free energy of shorter helical oligomers was equivalent to the free energy of the longer ones, leading to a statistical distribution of chain length. Upon addition of C_{60} , which fills the nanotubes' cavity and dramatically stabilises them, our group observed the amplification of longer nanotubes, shifting the degree of polymerisation from 5.3 to 15.7 (1 mM solution in 1,1,2,2-tetrachloroethane at 273 K). Addition of C_{70} led to a complete restructuring of the whole library, from nanotubes to a hexameric capsule wrapped around the solvophobic surface of the fullerene. Moreover, the reversible nature of the system allows a pH-dependent and selective binding of C_{60} or C_{70} in a mixture of both guests.

However, in most libraries, the library members do not interconvert so easily. Indeed, if one of the library members is particularly stabilised, for example by intramolecular interactions, it can act as a kinetic trap, accumulating at the expense of the other library members. Furthermore, high effective molarity within the macrocycles promotes intramolecular reaction, and the macrocycles may consequently be located in a relatively deep energetic well, inhibiting the exchange necessary for thermodynamic control. Our group recently described such a system,³⁸ in which hydrazone-based macrocycles are kinetically trapped and do not freely exchange. In this case, a small excess of monoaldehyde was shown to favour the formation of linear oligomers and facilitate the exchange between the macrocycles.

Kinetic control is not always a constraint and it has been used as a complementary alternative to thermodynamic control to expand the limits of dynamic combinatorial chemistry. Ashkenasy *et al.* have described in detail the kinetic behaviour of replicating peptide-based DCLs under partial thermodynamic control,³⁹ and the possibility of manipulating the replication processes either with light or by addition of a template. The contrast between kinetically and thermodynamically controlled libraries has been elegantly illustrated by Krishnan and Balasubramanian.⁴⁰ As mentioned above,

disulfide exchange can be easily promoted by slow oxidation of thiol building blocks under air. However, the exchange stops after the thiol building blocks are completely oxidised into disulfides, and these libraries do not always reach thermodynamic equilibrium. Under air oxidation, a library composed of two peptide-based thiol building blocks reached the kinetically controlled statistical distribution. When the same library was prepared under thermodynamic control (redox buffer under argon), a significant amplification of one of the library members was observed. This amplification, which would have not been obvious if the experiment had only been run under thermodynamic control, is due to the self-recognition between two building blocks with a complementary peptide sequence allowing for the formation of a stable β -hairpin.

These latest examples clearly show that apparent limitations of dynamic combinatorial chemistry, instead of acting as a hindrance, can promote its evolution towards new promising horizons.

The Sanders group was faced with a similar conundrum involving π -acceptor (A) 1,4,5,8-naphthalenetetracarboxylic diimide and π -donor (D) dialkoxynaphthalene thiol building blocks. This project was initiated by Dr Ho Yu Au-Yeung, who discovered that the donor-acceptor libraries formed in water under air oxidation lead to a variety of donor-acceptor catenanes.^{20, 41} These [2]catenanes exhibit previously unobserved stacking arrangements: DAAD (**Cat-2**) and DADD (**Cat-3**), as shown in Figure 1.11. Surprisingly, the conventional alternating DADA catenane was never found in these libraries.

Not only do these catenanes have unusual structures, but some of them exhibit remarkable conformations⁴¹ and binding properties (**Cat-1**, Figure 1.6).²⁰ The pioneering work of Dr Ho Yu Au-Yeung will be described in more detail in Chapter 2.

The next Chapter demonstrates that these catenanes are only part of a wider family, containing the AADA, DADA, DAAD and DADD catenanes. In this system, the exchange stops before reaching thermodynamic equilibrium, placing the libraries in a previously unexplored region between kinetic and thermodynamic control. These libraries present some advantages compared to traditional thermodynamically controlled libraries, allowing the elucidation of the mechanism of catenane formation, and an evaluation of the role played by donor-acceptor interactions and hydrophobic effect at each step of their formation (Chapter 2). Building on these observations, a series of new building blocks was designed to access more complex structures, such as [3]catenanes (Chapters 3 and 4).

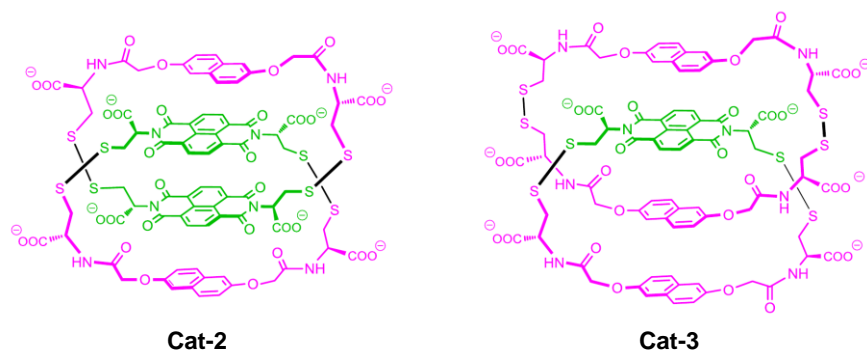


Figure 1.11. Two of the unusual donor-acceptor catenanes identified by Dr Ho Yu Au-Yeung.⁴¹

1.4. Conclusion

Inspired by the evolutionary systems found in nature, dynamic combinatorial chemistry has broadened our knowledge of complex chemical interactions. Two apparently general conclusions emerging from these adventures in DCC are that large, highly flexible linears and macrocycles are better receptors than small rigid macrocycles, and that (certain) catenanes are actually rather easy to prepare. The first of these conclusions should not surprise any chemist familiar with molecular recognition by biopolymers, but it contradicts received wisdom in much of the supramolecular community. From a purely ‘chemical’ point of view, DCC has offered a new route for the synthesis of complex architectures and understanding and control of reversible systems, giving rise to new technologies in diverse fields, from molecular recognition to material sciences.

The original idea of DCC is still used for a variety of purposes, but chemists can also increasingly appreciate, with more subtlety, its complexity and explore its limitations. Therefore, dynamic combinatorial chemistry will probably engender a new generation of ingenious concepts and lead to new, as yet unpredictable, discoveries.

Along those lines, the present thesis shows how hybrid systems, which cannot be classified as purely dynamic combinatorial, can be exploited to widen our understanding of donor-acceptor interactions and hydrophobic effect, and assemble complex [2] and [3]catenanes.

References:

1. For a more complete history, see: Corbett, P. T.; Leclaire, J.; Vial, L.; West, K. R.; Wietor, J.-L.; Sanders, J. K. M.; Otto, S. *Chem. Rev.* **2006**, *106*, 3652.
2. Kauffman, S. A. *The Origins of Order*. Oxford University Press, 1993.
3. Williams, R. J. P.; Fraústo Da Silva, J. J. R. *J. Theor. Biol.* **2003**, *220*, 323.
4. (a) Rozenman, M. M.; McNaughton, B. R.; Liu, D. R. *Curr. Opin. Chem. Biol.* **2007**, *11*, 259; (b) Ladame, S. *Org. Biomol. Chem.* **2008**, *6*, 219; (c) Herrmann, A. *Org. Biomol. Chem.* **2009**, *7*, 3195; (d) Lehn, J.-M. *Chem. Soc. Rev.* **2007**, *36*, 151; (e) de Bruin, B.; Hauwert, P.; Reek, J. N. H. *Angew. Chem. Int. Ed.* **2006**, *45*, 2660.
5. Ludlow, R. F.; Otto, S. *Chem. Soc. Rev.* **2008**, *37*, 101.
6. Thompson, M. C.; Busch, D. H. *J. Am. Chem. Soc.* **1962**, *84*, 1762.
7. (a) Brady, P. A.; Bonar-Law, R. P.; Rowan, S. J.; Suckling, C. J.; Sanders, J. K. M. *Chem. Commun.* **1996**, 319; (b) Brady, P. A.; Sanders, J. K. M. *J. Chem. Soc., Perkin Trans. I* **1997**, 3237. Structural corrections: *J. Chem. Soc., Perkin Trans. I* **1998**, 2119.
8. Hasenknopf, B.; Lehn, J.-M.; Boumediene, N.; Dupont-Gervais, A.; Van Dorsselaer, A.; Kneisel, B.; Fenske, D. *J. Am. Chem. Soc.* **1997**, *119*, 10956.
9. (a) Otto, S.; Furlan, R. L. E.; Sanders, J. K. M. *Science* **2002**, *297*, 590; Corbett, P. T.; Tong, L. H.; Sanders, J. K. M.; Otto, S. *J. Am. Chem. Soc.* **2005**, *127*, 8902.
10. Ngola, S. M.; Kearney, P. C.; Mecozzi, S.; Russel, K.; Dougherty, D. A. *J. Am. Chem. Soc.* **1999**, *121*, 1192.

11. Bugaut, A.; Jantos, K.; Wietor, J.-L.; Rodriguez, R.; Sanders, J. K. M.; Balasubramanian, S. *Angew. Chem. Int. Ed.* **2008**, *47*, 2677.
12. Corbett, P. T.; Otto, S.; Sanders, J. K. M. *Org. Lett.* **2004**, *6*, 1825.
13. Ludlow, R. F.; Otto, S. *J. Am. Chem. Soc.* **2008**, *130*, 12218.
14. Gareiss, P. C.; Sobczak, K.; McNaughton, B.R.; Palde, P. B.; Thornton, C.A.; Miller, B. L. *J. Am. Chem. Soc.* **2008**, *130*, 16254.
15. (a) Corbett, P. T.; Sanders, J. K. M.; Otto, S. *J. Am. Chem. Soc.* **2005**, *127*, 9390; (b) Severin K. *Chem. Eur. J.* **2004**, *10*, 2565.
16. (a) Ludlow, R. F.; Liu, J.; Li, H.; Roberts, S. L.; Sanders, J. K. M.; Otto, S. *Angew. Chem. Int. Ed.* **2007**, *46*, 5762; (a) Corbett, P. T.; Otto, S.; Sanders, J. K. M. *Chem. Eur. J.* **2004**, *10*, 3139.
17. Beeren, S. R.; Sanders, J. K. M. *J. Am. Chem. Soc.* **2011**, *133*, 3804.
18. (a) Lam, R. T. S.; Belenguer, A.; Roberts, S. L.; Naumann, C.; Jarrosson, T.; Otto, S.; Sanders, J. K. *M. Science* **2005**, *308*, 667.
19. Chung, M.-K.; White, P. S.; Lee, S. J.; Gagné, M. R. *Angew. Chem. Int. Ed.* **2009**, *48*, 8683.
20. Au-Yeung, H. Y.; Pantoş, G. D.; Sanders, J. K. M. *Proc. Natl. Acad. Sci. USA.* **2009**, *106*, 10466.
21. West, K. R.; Ludlow, R. F.; Corbett, P. T.; Besenius, P.; Mansfeld, F. M.; Cormack, P. A. G.; Sherrington, D. G.; Goodman, J. M.; Stuart, M. C. A.; Otto, S. *J. Am. Chem. Soc.* **2008**, *130*, 10834.
22. Sadownik, J.W.; Ulijn, R. V. *Curr. Opin. Biotech.* 2010, *21*, 401.

23. (a) Carnall, J. M. A.; Waudby, C. A.; Belenguer, A. M.; Stuart, M. C. A.; Peyralans, J. J.-P.; Otto, S. *Science* **2010**, 327, 1502; (b) Li, J.; Carnall, J. M. A.; Stuart, M. C. A.; Otto, S. *Angew. Chem. Int. Ed.* DOI: 10.1002/anie.201103297.
24. (a) West, K.; Bake, K.; Otto, S. *Org. Lett.* **2005**, 2615; (b) West, K.; Otto, S. *Curr. Drug. Disc. Techn.* **2005**, 2, 123.
25. Pérez-Fernández, R.; Pittelkow, M.; Belenguer, A. M.; Lane, L.; Robinson, C. V.; Sanders, J. K. M. *Chem. Commun.* **2009**, 3708.
26. Herrmann, A.; Giuseppone, N.; Lehn, J.-M. *Chem. Eur. J.* **2009**, 15, 117.
27. (a) Otto, S.; Severin, K. *Topics Curr. Chem.* **2007**, 277, 267; (b) Buryak, A.; Severin, K. *Angew. Chem. Int. Ed.* **2005**, 44, 7935.
28. (a) Brisig, B.; Sanders, J. K. M.; Otto, S. *Angew. Chem. Int. Ed.* **2003**, 42, 1270; (b) Vial, L.; Otto S.; Sanders, J. K. M. *New J. Chem.* **2005**, 29, 1001.
29. Gasparini, G.; Prins, L. J.; Scrimin, P. *Angew. Chem. Int. Ed.* **2008**, 47, 2475.
30. Huc, I. ; Lehn, J.-M. *Proc. Natl. Acad. Sci. USA.* **1997**, 94, 2106.
31. Bhat, V. T.; Caniard, A. M.; Luksch, T.; Brenk, R.; Campopiano, D. J.; Greaney, M. F. *Nature Chem.* **2010**, 2,490.
32. Aldaye, F.; Sleiman, H. F. *J. Am. Chem. Soc.* **2007**, 129, 10070.

33. Folmer-Andersen, J. F.; Lehn, J.-M. *J. Am. Chem. Soc.* **2011**, *133*, 10966.
34. (a) Ulrich, S.; Lehn, J.-M. *J. Am. Chem. Soc.* **2009**, *131*, 5546; (b) Ulrich, S.; Lehn, J.-M. *Angew. Chem. Int. Ed.* **2008**, *47*, 2240.
35. Wojtecki, R. J.; Meador, M. A.; Rowan S. J. *Nature Mater.* **2011**, *10*, 14.
36. Belenguer, A.; Friščić, T.; Day G. M.; Sanders, J. K. M. *Chem. Sci.* **2011**, *2*, 696.
37. (a) Pantoş, G. D.; Pengo P.; Sanders, J. K. M. *Angew. Chem. Int. Ed.* **2007**, *46*, 194; (b) Ponnuswamy, N.; Pantoş, G. D.; Smulders, M. M. J.; Sanders, J. K. M. *J. Am. Chem. Soc.* *accepted for publication*; (c) Pantoş, G. D.; Wietor, J.-L.; Sanders, J. K. M. *Angew. Chem. Int. Ed.* **2007**, *46*, 2338; (d) Wietor, J.-L.; Pantoş, G. D.; Sanders, J. K. M. *Angew. Chem. Int. Ed.* **2008**, *47*, 2689; (e) Tamanini, E.; Ponnuswamy, N.; Pantoş, G. D.; Sanders, J. K. M. *Faraday Discussions* **2010**, *145*, 205; (f) Tamanini, E.; Pantoş G. D.; Sanders, J. K. M. *Chem. Eur. J.* **2010**, *16*, 81; (g) Stefankiewicz, A. R.; Tamanini, E.; Pantoş G. D.; Sanders, J. K. M. *Angew. Chem. Int. Ed.* **2011**, *50*, 5725.
38. (a) Beeren, S. R.; Pittelkow, M.; Sanders, J. K. M. *Chem. Commun.* **2011**, 7359; (b) Beeren S. R.; Sanders, J. K. M. *Chem. Sci.* **2011**, *2*, 1560.
39. Dadon, Z.; Samiappan, M.; Wagner, N.; Ashkenasy G. *Chem. Commun.*
DOI: 10.1039/C1CC14301H.
40. Krishnan-Ghosh, Y.; Balasubramanian, S. *Angew. Chem. Int. Ed.* **2003**, *42*, 2171.
41. (a) Au-Yeung, H. Y.; Pantoş, G. D.; Sanders, J. K. M. *J. Org. Chem.* **2011**, *76*, 1257; (b) Au-Yeung, H. Y.; Pantoş, G. D.; Sanders, J. K. M. *Angew. Chem. Int. Ed.* **2010**, *49*, 5331; (c) Au-Yeung, H. Y.; Pantoş, G. D.; Sanders, J. K. M. *J. Am. Chem. Soc.* **2009**, *131*, 16030.

CHAPTER 2

Exploring the Formation Pathways of Donor-Acceptor Catenanes in Aqueous Dynamic Combinatorial Libraries

The discovery through dynamic combinatorial chemistry of a new generation of donor-acceptor [2]catenanes highlights the power of DCC to access unprecedented structures. While conventional thinking has limited the scope of donor-acceptor catenanes to strictly alternating stacks of donor (D) and acceptor (A) aromatic units, DCC is demonstrated in this chapter to give access to unusual DAAD, DADD, and ADAA stacks. Each of these catenanes has specific structural requirements, allowing control of their formation. Based on these results, and on the observation that the catenanes represent kinetic bottlenecks in the reaction pathway, a mechanism that explains and predicts the structures formed is proposed. Furthermore, the spontaneous assembly of catenanes in aqueous dynamic systems gives a fundamental insight into the role played by hydrophobic effect and donor-acceptor interactions when building such complex architectures.

2.1. Introduction

The discovery of new donor-acceptor [2]catenanes is presented in this Chapter. These catenanes are assembled from simple electron-donor (D) and electron-acceptor (A) building blocks using disulfide chemistry. Moving on from our previous dynamic combinatorial syntheses of catenanes with unusual DAAD and DADD stacking arrangements (see Chapter 1), this Chapter now describes the formation of catenanes with DADA and unprecedented AADA stacks under the same conditions. These four types of catenanes form a complete set, and can be viewed as a whole new generation of donor-acceptor [2]-catenanes. More importantly, perhaps, a mechanism is outlined, which explains and predicts the formation of each of these catenanes, which turn out to be kinetic bottlenecks on the reaction pathway.

2.1.1. Brief overview on donor-acceptor interactions

Interactions between aromatic molecules are mainly described in term of electrostatic interactions between electron-deficient and electron-rich π -systems.¹ The complementary alternating stack of electron-deficient and electron-rich aromatic moieties, leading to the optimum electronic overlap, has always been thought to be the most favourable arrangement. Alternating D-A stacks adopt a parallel and compact face-to-face geometry, and have been extensively used as scaffolds for complex structures such as foldamers,² rotaxanes,³ and catenanes.⁴

The formation of stacked structures reduces the total solvent-exposed surface area, so efficient desolvation of the aromatic systems plays a crucial role in this process (Figure 2.1). Iverson *et al.*⁵ showed that the effective strength of donor-acceptor interactions is closely related to the solvent environment: association constants between the electron-rich 1,5-dialkoxynaphthalene (DN) and the

electron-deficient 1,4,5,8-naphthalenetetracarboxylic diimide (NDI) vary with the polarity of the solvent, from *ca.* 2 M^{-1} in chloroform to *ca.* 2000 M^{-1} in water. As expected, alternating donor-acceptor interactions are clearly dominant over weaker A-A ($K < 1 \text{ M}^{-1}$ in chloroform, *ca.* 200 M^{-1} in water) or donor-donor interactions ($K < 1 \text{ M}^{-1}$ in chloroform, *ca.* 20 M^{-1} in water).⁵ From these results it is generally believed that the strong solvophobic component of aromatic interactions can be used to dramatically increase the effectiveness of electrostatic interactions, and that the alternating D-A stack is favoured in any solvent.

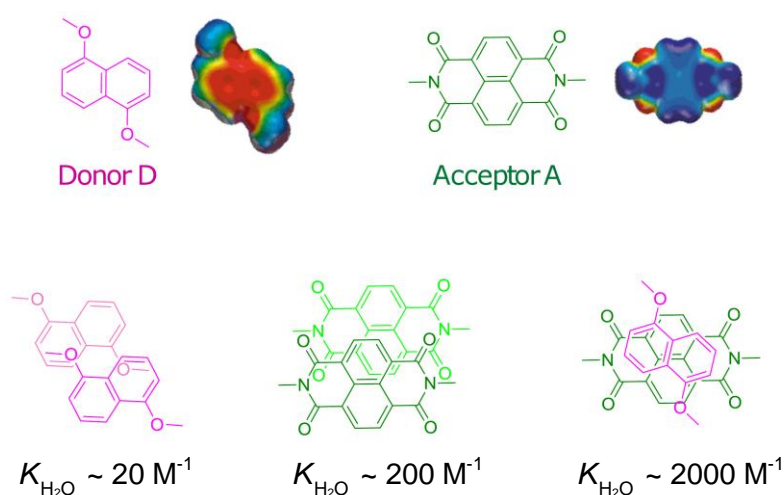


Figure 2.1. Calculated electrostatic surface potential for the electron-rich 1,5-dialkoxy-naphthalene and the electron-deficient 1,4,5,8-naphthalenetetracarboxylic diimide (the relatively high electron density is shown in red and the shortage of electron density is shown in blue), and illustration of the possible stacking arrangements coming from X-ray crystals with the corresponding association constants in water.⁵ For clarity, the substituents are omitted.

2.1.2. Scope of this Chapter

In light of these numbers, it is perhaps surprising that in recent years A-A and D-D stacks have spontaneously emerged from the self-assembly of donor and acceptor units in polar media.⁶⁻⁸ In these cases, the solvophobic effect seems to overcome, at least partially, pure electrostatic interactions between donor and acceptor units, although it remains difficult to evaluate to what extent the two phenomena cooperate and/or compete.

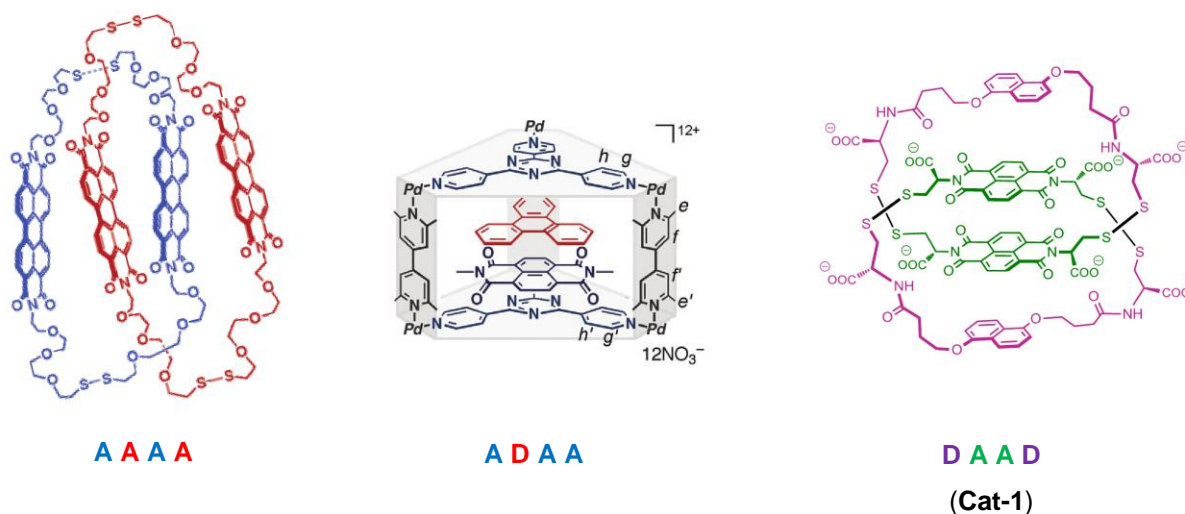


Figure 2.2. Atypical donor-acceptor architectures: an AAAA [2]catenane (Li),^{6a} a AADA assembly within a box (Fujita),^{6b} and DAAD catenane **Cat-1** (Sanders).^{8d}

To our knowledge, only a few examples of these unconventional architectures have been reported in the literature.^{6, 7} Amongst the most representative examples, illustrated in Figure 2.2, Li and co-workers reported the synthesis of an AAAA [2]-catenane based on perylene-3,4,9,10-tetracarboxylic diimide.^{6a} Most recently, Fujita *et al.* showed that discrete ADDA and AADA stacks could be obtained within a box-shaped cavity.^{6b} Our group reported the dynamic combinatorial synthesis of DAAD and DADD catenanes⁸ at the expense of

the expected DADA structure. According to the D-A stacking model, the DADD stack would be unlikely to be formed in significant quantities in competition with the more obvious D-A stacks. By expanding the range of building blocks, the possibility of accessing a larger variety of donor-acceptor catenanes, such as: DDDD, DADD, DADA, DAAD, AADA, or AAAA (Figure 2.3) is now open.

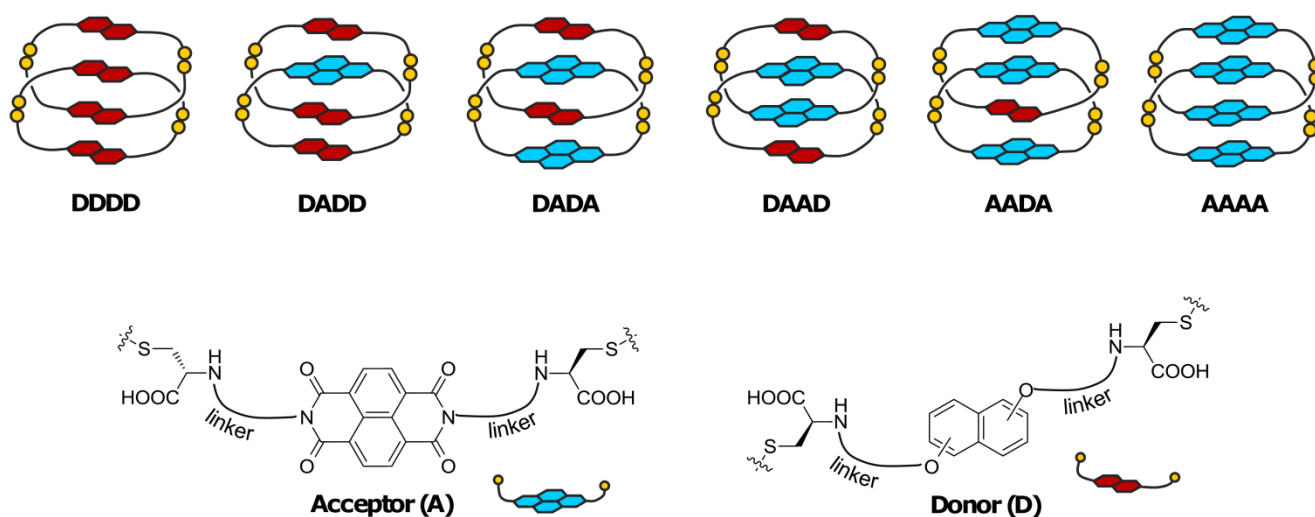


Figure 2.3. Possible arrangements of the π units of a donor-acceptor [2]-catenane. Aromatic π -donor and π -acceptor are represented by red and blue cartoons, respectively.

Each catenane presented in Figure 2.3 represents a major synthetic challenge from a classical approach but can, in principle, be achieved using dynamic combinatorial chemistry.^{9, 10} Out of the six possible arrangements, four were obtained, with the AAAA and DDDD stacks remaining elusive at present. The size and geometry of the building blocks influences dramatically the composition of the dynamic combinatorial libraries, such as to allow a precise control over the type of catenane formed based on its structural requirements.

The new generation of donor-acceptor [2]catenanes reported in this work not only constitutes a success in the synthesis of topologically complex targets, but it may also open new horizons for the use of catenanes as molecular machines, as one of the DAAD catenanes was recently shown to exhibit two switchable conformations, with a parallel arrangement of the π -units or a Gemini-sign (II)-like conformation.^{8b} Hence, these catenanes present a major advance in understanding, designing, and using complex architectures based on donor and acceptor units. These systems also demonstrate a complex environment in which both thermodynamic and kinetic factors play a role in determining the composition of the library.

We present first a proposed mechanistic pathway for the synthesis of the donor-acceptor [2]catenanes which rationalizes our earlier results and predicts the composition of new libraries. The remainder of this Chapter explores and confirms these predictions experimentally.

2.2. Mechanism of formation of donor-acceptor catenanes

2.2.1. Design of the building blocks used in this Chapter

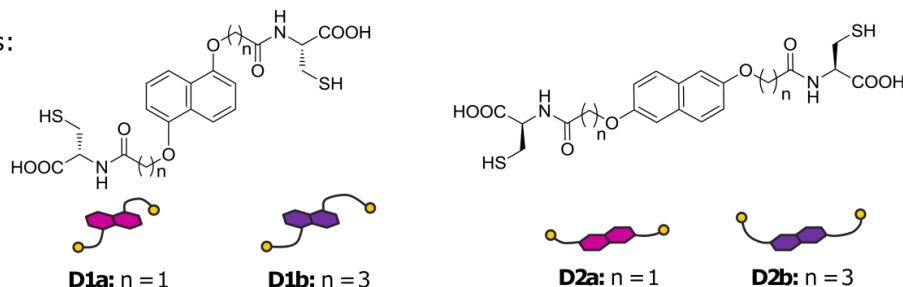
To explore the mechanism of formation of donor-acceptor catenanes in aqueous libraries, a set of building blocks, shown in Figure 2.4, was designed. All the building blocks are constructed on a similar design: a large hydrophobic π -surface, either NDI as electron-acceptor (A) or DN as electron-donor (D), to which are attached two cysteine-terminated hydrophilic side-chains of various lengths. The cysteine-derived side-chains provide easy access to building blocks of different sizes, along with the thiol necessary for the disulfide exchange and carboxylic acids for water solubility.

The donor building blocks, previously synthesised by Dr Ho Yu Au-Yeung,⁸ differ in the substitution pattern of the central core (1,5- or 2,6-) and the length of the side-chains. The acceptor building blocks differ in the length, hydrophilicity and bulk of the side-chains. **A1**, **A2** and **A3** were also synthesised by Dr Ho Yu Au-Yeung.⁸ **A4** was synthesised according to a similar procedure, from the 1,4,5,8-naphthalenetetracarboxylic dianhydride and trityl protected glutathione, followed by the deprotection of the trityl protecting groups (Scheme 2.1). **A5** was synthesised in a similar fashion in three steps, involving the mono-substitution of the 1,4,5,8-naphthalenetetracarboxylic dianhydride with the trityl protected glutathione, reaction with the trityl protected cysteine, and deprotection of the trityl protecting groups (Scheme 2.2). More details on the synthesis of these building blocks are given in the experimental section, Chapter 6.

Screening of libraries containing different combinations of these donor and acceptor building blocks allows us to investigate the extent to which all of these parameters play a role in the formation of catenanes. Aqueous disulfide DCLs were created by dissolving the building blocks to a total concentration of 5 mM in water at pH 8. The pH was adjusted with aqueous NaOH and the libraries

were stirred under air in capped vials to allow oxidation of the thiol building blocks. After 5 days, the libraries were fully oxidized and analyzed by HPLC and LC-MS. Absorbance was recorded at the optimum wavelength for each building block: acceptor units at 383 nm, and donor units at 292 nm (1,5-substituted **D1a** and **D1b**) or 260 nm (2,6-substituted **D2a** and **D2b**). Only the most significant results are shown here.

Donor building blocks:



Acceptors building blocks:

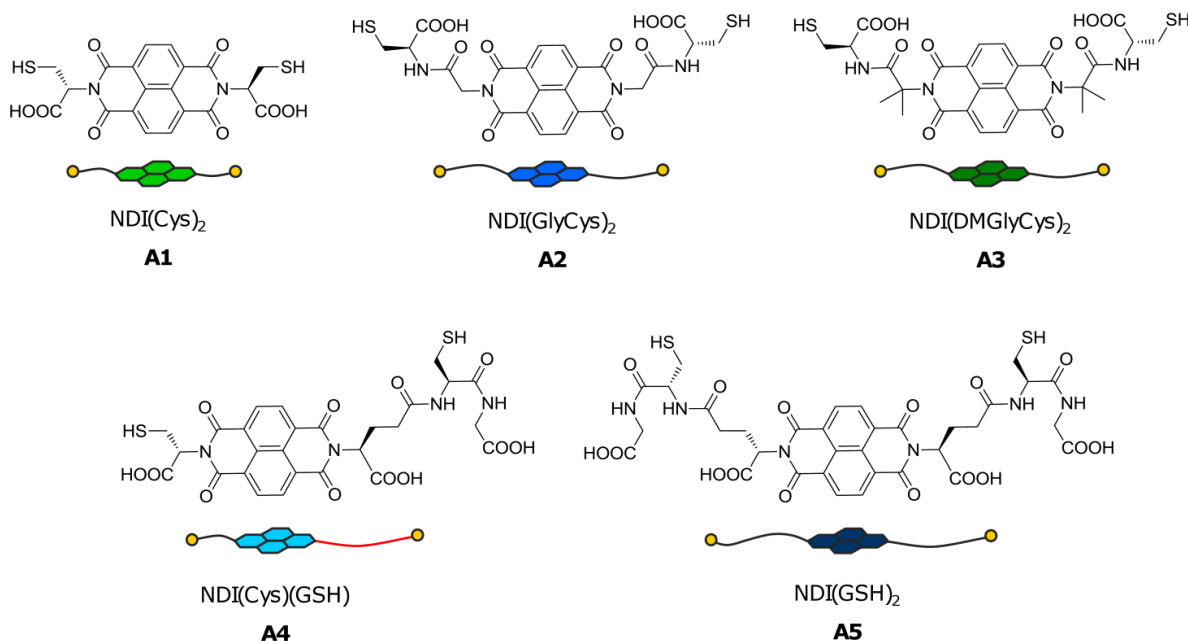
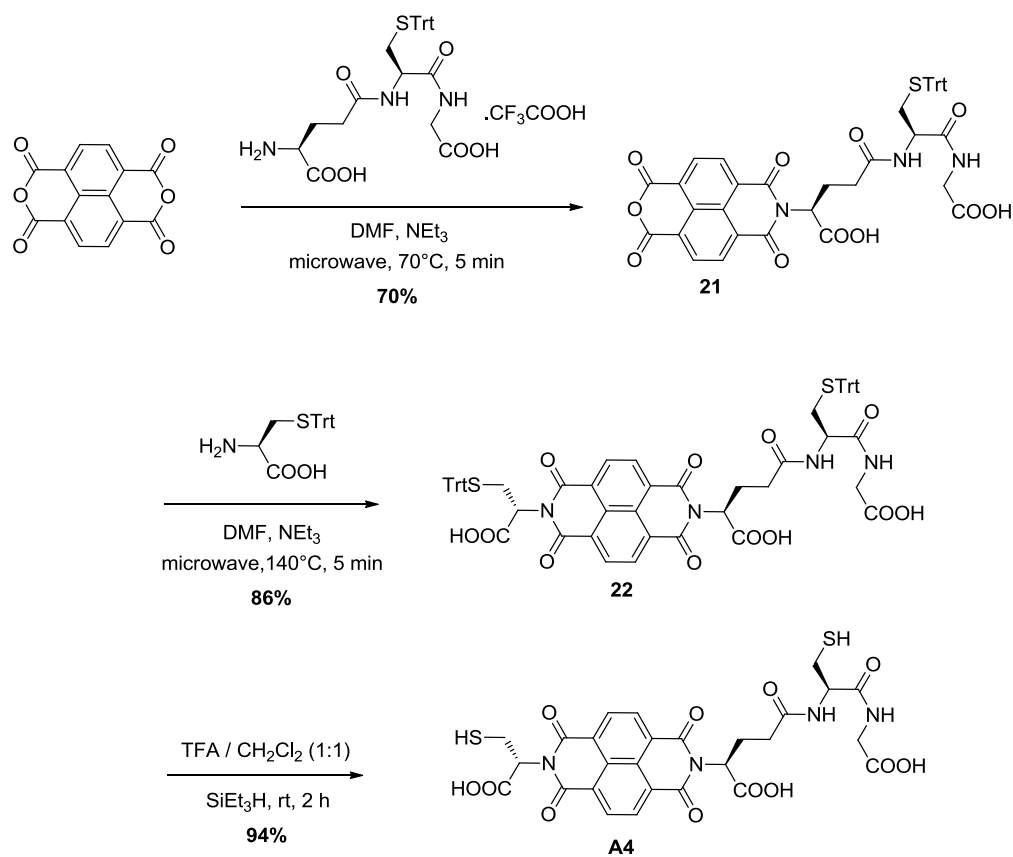
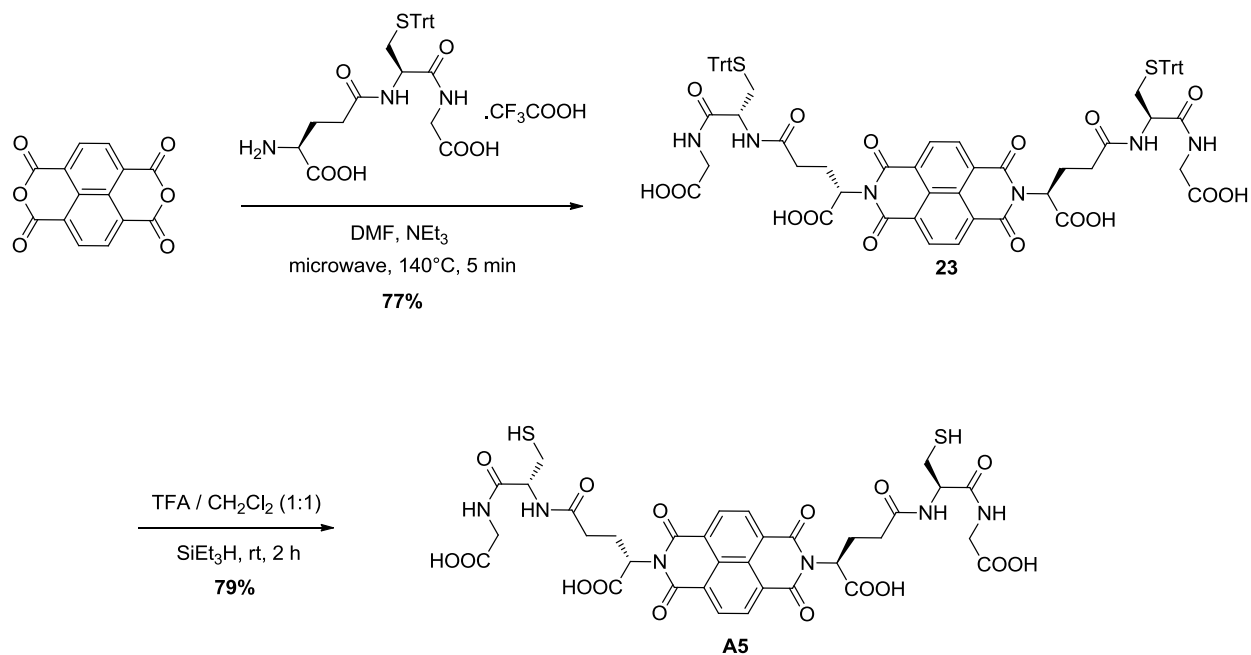


Figure 2.4. Donor (D) and acceptor (A) building blocks used in this Chapter, and their cartoon representations.

Scheme 2.1. Synthetic route to building block **A4**.Scheme 2.2. Synthetic route to building block **A5**.

2.2.2. Test for thermodynamic equilibrium

Contrary to our initial thoughts,⁸ the dithiol building blocks used in this work are fully oxidized into disulfide, and stop exchanging, before the libraries reach thermodynamic equilibrium.

The thermodynamic equilibrium was tested on the first library in which a donor-acceptor catenane was identified,^{8d} originally designed by Dr Ho Yu Au-Yeung. Two separate libraries were prepared, composed of **A1** and **D1b** (5 mM total) in water pH 8, in the presence of 1 M NaNO₃. These two libraries were individually analysed after one day of stirring (Figure 2.5.a and b). No significant change was observed in the library distribution when the libraries were analysed after 5 and 10 days of stirring, suggesting that either thermodynamic equilibrium or full oxidation of the library was reached after one day.

These two libraries were mixed in a 1:1 (v/v) ratio immediately after they were prepared (Figure 2.5.c) and after they have been separately stirred for one day (Figure 2.5.d). When the freshly prepared libraries were mixed, the LC-MS revealed a library of varied macrocycles, containing one catenane (**Cat-1**). On the other hand, when the two libraries were mixed after being stirred separately for one day, the LC-MS of the new library appeared to be a simple superimposition of the original libraries showed in Figures 2.5.a and b, and did not contain any catenane.

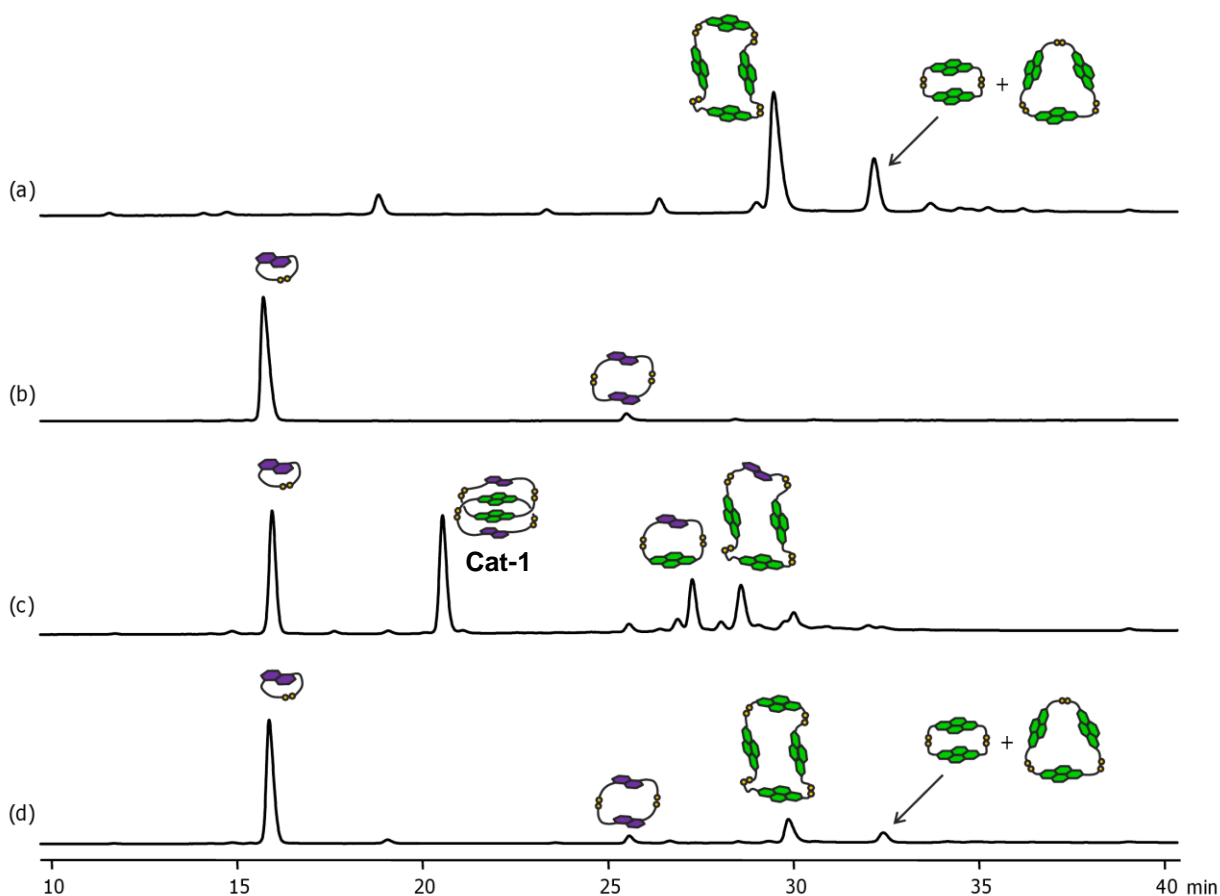


Figure 2.5. HPLC analyses of aqueous libraries composed of (a) **A1**, (b) **D1b**. The libraries were set up in the presence of 1 M of NaNO_3 , with a total concentration of building blocks of 5 mM. These two libraries were mixed (c) just after preparation and (d) after 1 day of separate stirring in a 1:1 (v/v) ratio to produce new libraries containing **A1** and **D1b** (1:1 molar ratio, 5 mM total). Absorbance was recorded at 292 nm.

This observation unambiguously shows that the disulfide exchange stops after one day of oxidation: the catenane is progressively formed in the library until it reaches a steady state, corresponding to the full oxidation of the thiols. The quantity of catenane **Cat-1** formed could be further increased by adding 20% of dithiothreitol to reinitiate the exchange process, showing that thermodynamic equilibrium had not been reached yet (Figure 2.6).

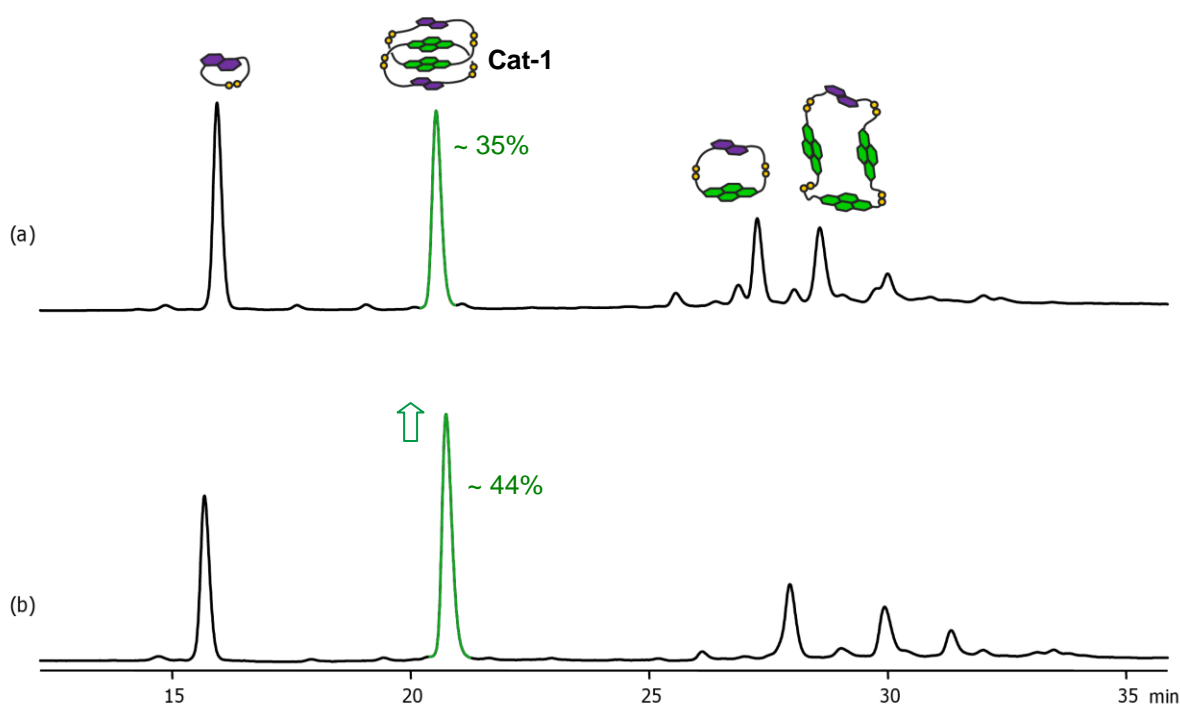


Figure 2.6. (a) HPLC analysis of an aqueous library composed of **A1** and **D1b** (1:1 molar ratio). The library was set up in the presence of 1 M of NaNO_3 , with a total concentration of building blocks of 5 mM, and analyzed after 5 days of stirring. (b) After this library has been fully oxidized, the exchange process was reinitiated by adding 10% of dithiothreitol. The library was analyzed again after 1 day of stirring. Absorbance was recorded at 292 nm.

The kinetics of formation of the library members consequently plays a major role. Although seemingly trivial, this observation is of major importance: because the libraries are not under thermodynamic control, it is possible to map out the pathways leading to the different types of catenanes. For each of these pathways, the intermediates involved can be traced, and the role played by hydrophobic and donor-acceptor interactions in each step of the catenation process can be evaluated.

2.2.3. Proposed mechanism of catenanes formation in aqueous DCLs

The formation of catenanes in aqueous donor-acceptor DCLs occurs through three successive steps: formation of a dimer, threading of a linear species into the dimer's cavity, and closing of the catenane. The key elements in the formation of catenanes are the donor-acceptor interactions and the polarity of the medium, manipulated by the addition of salt.

In pure water, DCLs composed of donor and acceptor building blocks do not usually lead to the formation of catenanes, although traces can be observed in some isolated cases. This indicates that in water, in the timeframe of the libraries' oxidation, the sum of donor-acceptor and hydrophobic interactions is insufficient to bring stacks of building blocks into the close proximity necessary for catenation.

In high salt^{8, 11} (1 M NaNO₃) libraries, the increased polarity of the medium promotes the decrease of solvent-exposed hydrophobic surfaces; this is achieved by a building block or linear oligomer sliding into the hydrophobic cavity of a preformed cyclic dimer (equivalently, the complexation of linear oligomers and single building blocks can lead to their cyclisation to give the same intermediates). This threaded species is the first intermediate in the formation of a catenane. Besides the threading mechanism described above, it can also be formed by the templated cyclization of a linear precursor in the presence of a complementary linear template.¹² If the donor-acceptor interactions have a significant role, then the [-A-A-] cyclic dimer should preferentially bind a donor over an acceptor unit; similarly, the [-D-D-] and the [-A-D-] cyclic dimers are more likely to interact with an acceptor rather than a donor moiety. Each of the three favourable threaded species corresponds to the initial step of a different pathway for formation of catenanes: *Pathways I, II, and III*, respectively (Figure 2.7).

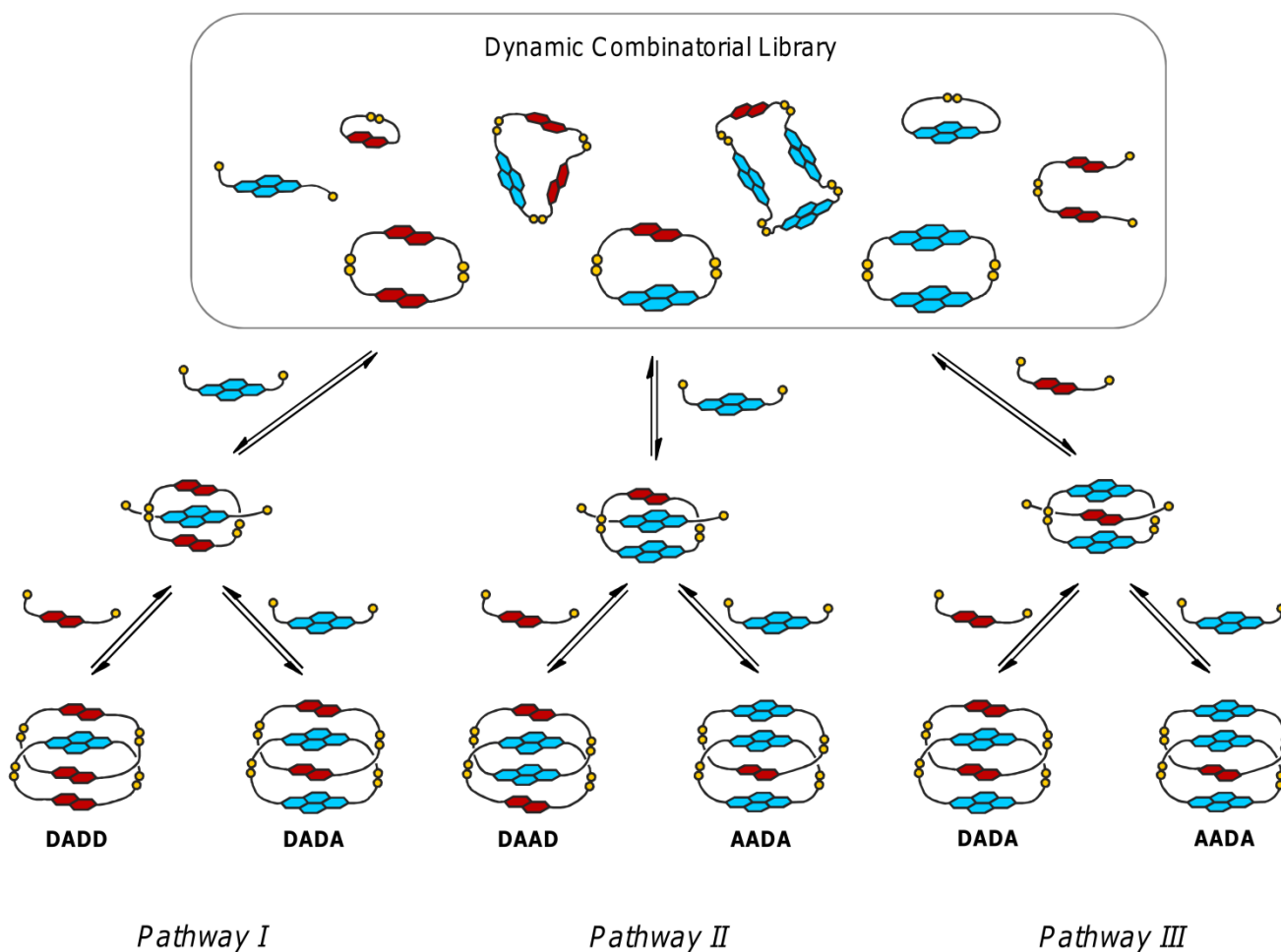


Figure 2.7. Proposed mechanism for formation of dynamic combinatorial donor-acceptor [2]-catenanes. For clarity, the mechanistically equivalent possibilities of threading a linear oligomer through each cyclic dimer, or of forming complexes between linear dimers before cyclization, are not shown.

Once a threaded complex is formed through *Pathway I*, *II*, or *III*, linking a fourth building block completes the catenane formation. The factors involved in the closing step are more difficult to predict, but electrostatic interactions are expected to play a lesser role than in the threading step: in the closing step there are only two π surfaces interacting while in the threading step there are four. The catenanes can then be closed with either an acceptor or a donor building block, depending on which event leads to the maximum stabilization. Therefore, each pathway should lead to a characteristic pair of catenanes:

DADD and DADA catenanes from *Pathway I*, DAAD and AADA catenanes from *Pathway II*, DADA and AADA catenanes from *Pathway III* (Figure 2.7).

This mechanism predicts that no homocatenane (AAAA or DDDD) will be formed in this system: although the formation of catenanes is dominated overall by the hydrophobic effect, donor-acceptor interactions play a determining role in the first step of threading. However, further increasing the polarity of our medium or increasing the surface area of the hydrophobic core⁶ could potentially lead to the formation of homocatenanes.

Based on this set of intermediates and interactions involved in the mechanism, it is possible to identify the parameters promoting efficient formation of the catenanes in the libraries. First, the [-A-D-], [-D-D-] and [-A-A-] dimers constitute the cornerstone for the formation of any catenane, so their abundance in the DCL is paramount. To form a catenane, a dimer needs to fulfil two requirements: it must be formed efficiently in the library, and be large enough to accommodate an aromatic thread. Catenane formation will be favoured when an optimum overlap of the aromatic moieties favours both donor-acceptor and hydrophobic interactions in the two steps of threading and closing. This happens when each ring forming the catenane is tight; when the rings are too flexible, the enthalpic gain is low and cannot compensate for the entropic costs derived from the catenation process, so the catenane is not formed.

We can take advantage of these factors by designing the libraries carefully, not only to form one type of catenane selectively, but to also select the pathway by which it will be formed.

2.3. Exploring Pathway I

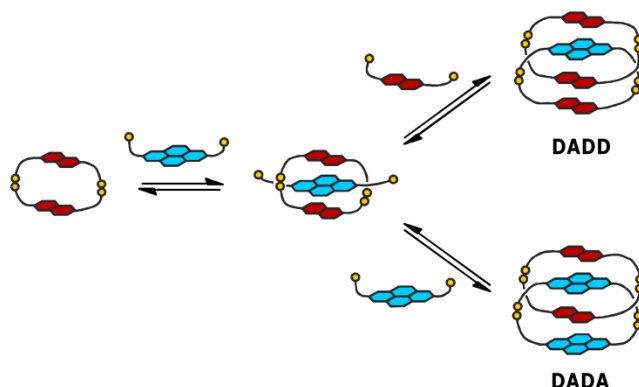


Figure 2.8. Formation of catenanes *via Pathway I*.

The efficient formation of a [-D-D-] dimer required in *Pathway I* (Figure 2.8) is achieved using donor building blocks with short side-chains.^{8a, c, 13a} The short side-chains of the building block result in a [-D-D-] dimer whose small cavity size enables a relatively good interaction with an acceptor moiety, favouring the threading mechanism described above. The geometry of the 1,5-isomer **D1a** favours the formation of the [-D-] cyclic monomer over the [-D-D-] dimer, so does not lead to the formation of any catenane. On the other hand, the 2,6-isomer **D2a** forms a stable [-D-D-] dimer, which leads to the formation of catenanes through *Pathway I*. Hence, all the following libraries were prepared with the **D2a** donor building block and different acceptor building blocks or mixtures of acceptor building blocks. Only the significant results are shown here.

To summarize the results described in this section, the synthesis of three DADA catenanes is described, all containing a [-**D2a-D2a**-] dimer interlocked with either [-**A2-A2**-], [-**A1-A2**-] or [-**A1-A4**-] acceptor dimers. Their respective paired DADD catenanes were also identified. The different yields of DADA catenanes suggest that the size of the acceptor dimer influences their efficiency of formation, with the

tightest dimer [-A1-A4-] leading to a 70% yield of the corresponding [2]-catenane. A detailed discussion of the libraries that follow *Pathway I* is presented below.

2.3.1. Identification of the first DADA catenane: Cat-4

Acceptor A1, with short side-chains, forms an extremely tight [-A1-A1-] dimer, which cannot possibly lead to the formation of alternating DADA catenanes.^{8,13} Hence, the first DADA catenane (**Cat-4**) was identified, along with its predicted DADD paired catenane (**Cat-5**), in a library containing the slightly longer acceptor A2 and D2a (Figure 2.9).

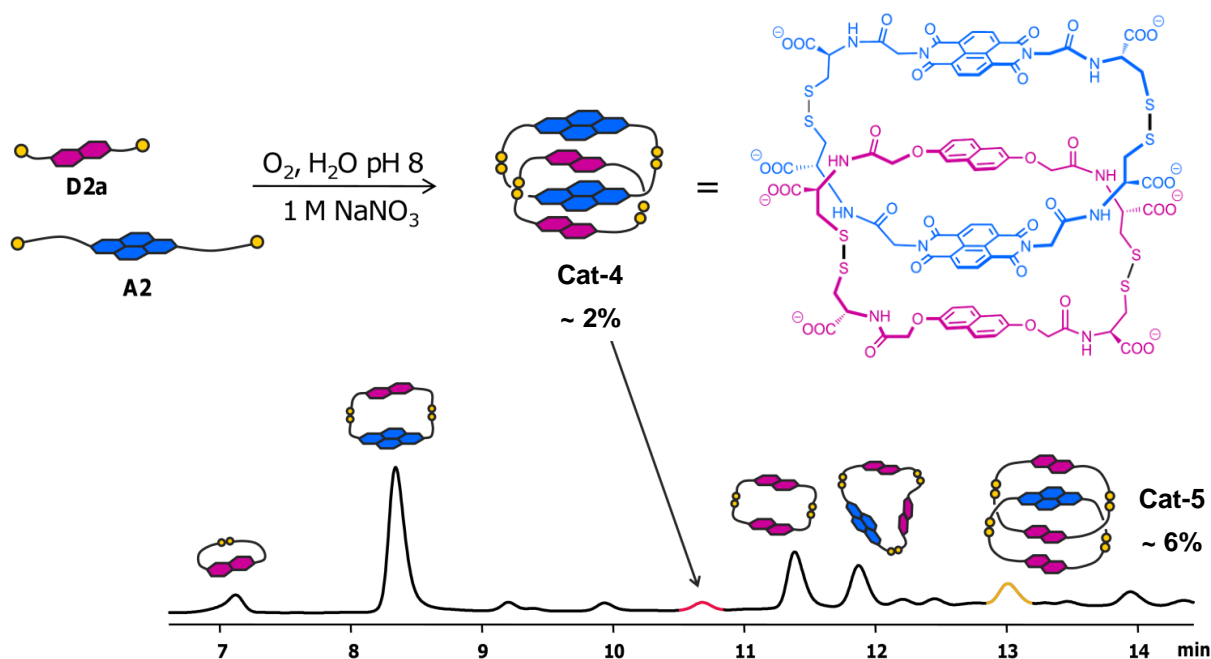


Figure 2.9. HPLC analysis of an aqueous library composed of **D2a** and **A2** (1:1 molar ratio, 5 mM total), in the presence of 1 M of NaNO₃. Absorbance was recorded at 260 nm.

Cat-4, was characterized by Mass Spectrometry (MS and MS/MS), as shown in Figure 2.10. The ESI-MS (negative ion) shows a doubly charged molecular ion (m/z of 1065.0), corresponding to the mass of a tetramer composed of two donor and two acceptor units. The largest fragments observed in MS/MS have an m/z of 1171.0 and 959.0, corresponding to the mass of the acceptor and donor homodimer respectively. This fragmentation pattern is characteristic for a DADA catenane, i.e. a ring containing two acceptors interlocked with another ring consisting of two donors.

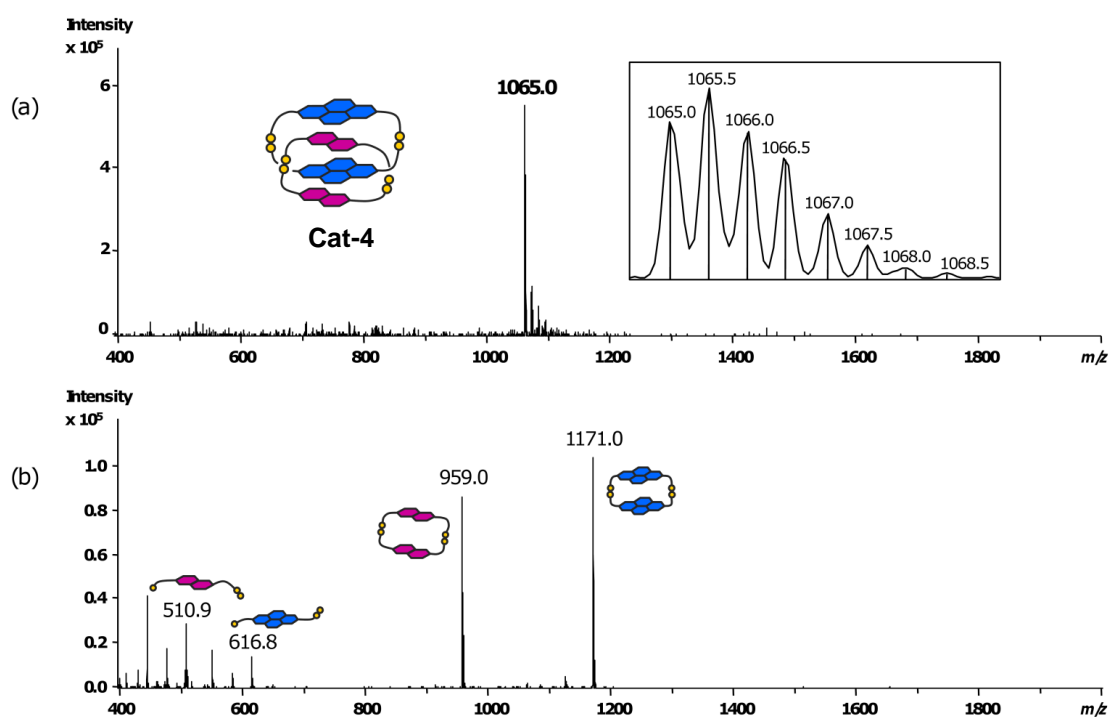


Figure 2.10. Tandem (a) MS and (b) MS/MS fragmentation of DADA catenane **Cat-4**. The yellow cartoon dots represent the sulfur atoms of the cysteine.

The presence of the two paired catenanes (**Cat-4** and **Cat-5**) supports the proposed mechanism, whereby the choice of the threaded building block is directed by donor-acceptor interactions, while the

closing step of catenation is driven by hydrophobic effects. The low yield of both catenanes (**Cat-4**: 2% and **Cat-5**: 6% of the library) is unsurprising; as their respective rings are relatively large, the likelihood of a strong interaction between the aromatic units is small. Furthermore, even though the building block ratio (1:1) should not favour the formation of a structure containing three donor units, the DADD catenane **Cat-5** is more efficiently formed, indicating that the overall catenation process is not dominated by donor-acceptor interactions.

2.3.2. Improving the synthesis of DADA catenanes: from **Cat-4** to **Cat-6**

Considering the size of the [-A-A-] dimer, if [-A1-A1-] is too tight, the larger [-A2-A2-] dimer is too loose to allow formation of a DADA catenane efficiently. Therefore, it was not surprising to observe that replacing **A2** by similarly sized **A3** did not bring much improvement (catenanes were also observed in very low yields). The behaviour of the longer **A4** is relatively complex and will be discussed in the end of this chapter, but as expected, in the case of the acceptor building block with the longest side-chains, **A5**, no catenane was observed: only a limited number of small macrocycles, including the cyclic acceptor monomer, were identified.

Introducing two acceptor building blocks in the presence of donor **D2a** allowed easy access to [-A-A-] dimers of intermediate sizes to explore further the formation of catenanes *via Pathway I*. This is illustrated by a library composed of **D2a**, **A1** and **A2** in a 2:1:1 molar ratio, shown in Figure 2.11. In this library the only DADA catenane formed is **Cat-6** which contains the tight mixed acceptor dimer [-A1-A2-]. The yield (15%) of this catenane is higher than that of **Cat-4**. Once again, the DADD paired catenane, **Cat-3**, is present in the library, supporting the proposed formation pathway.

Naturally, increasing the complexity of the DCLs opens the possibility for other pathways to compete with *Pathway I*. This explains the formation of other types of catenanes, such as the DAAD **Cat-2**, which will be discussed later.

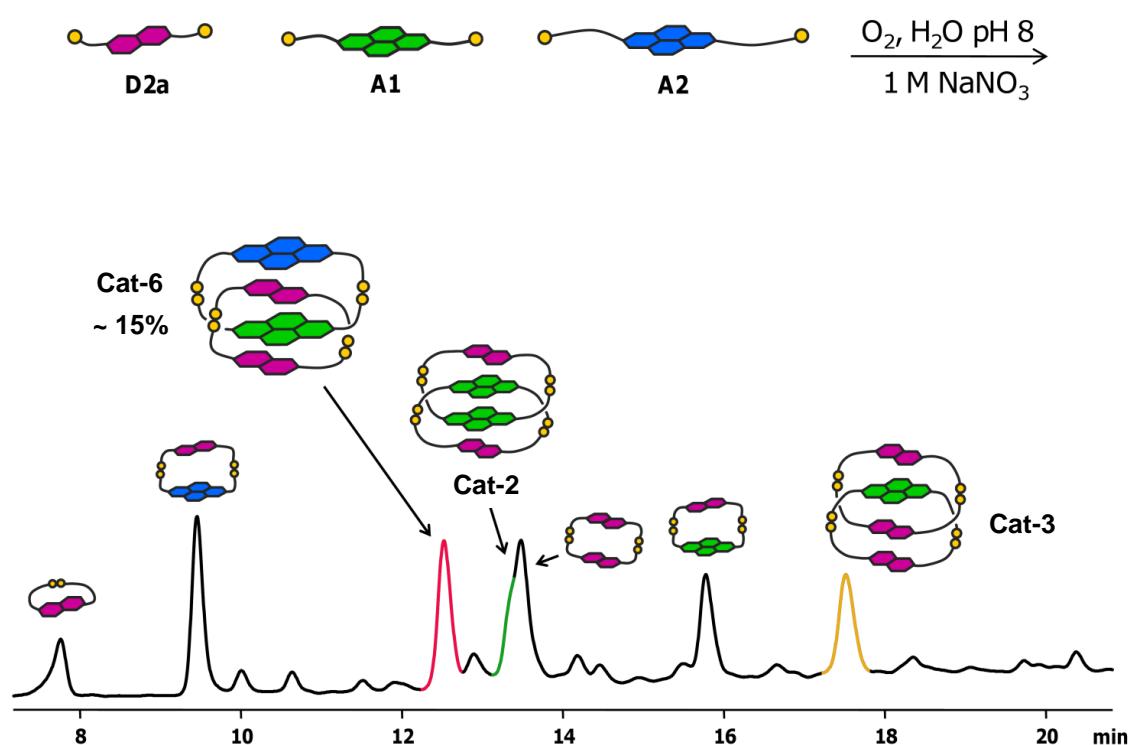


Figure 2.11. HPLC analysis of an aqueous library composed of **D2a**, **A1** and **A2** (2:1:1 molar ratio, 5 mM total), in the presence of 1 M of $NaNO_3$. Absorbance was recorded at 260 nm.

2.3.3. 1H NMR characterisation of Cat-6

Cat-6 was isolated and characterized by 1H NMR (Figures 2.12 to 2.14). It displays two conformations in a molar ratio of 2:1, as either **A1** or **A2** can be situated in the inner or outer positions of the catenane. 1H NMR (500 MHz, 298 K, D_2O) shows two sets of signals for each conformation in the acceptor region (7.55 to 8.15 ppm, Figure 2.13.a), assigned by correlation spectroscopy (COSY): one upfield shifted (inner NDI) and one downfield shifted (outer NDI). A similar pattern, with two sets of signals

for each conformation was observed in the donor region (5.55 to 7.05 ppm, Figure 2.13.b). At low temperature (278 K), cross-peaks between the donor and acceptor units of the major conformation were observed in NOESY spectra, confirming the alternating DADA structure of **Cat-6** (Figure 2.14).

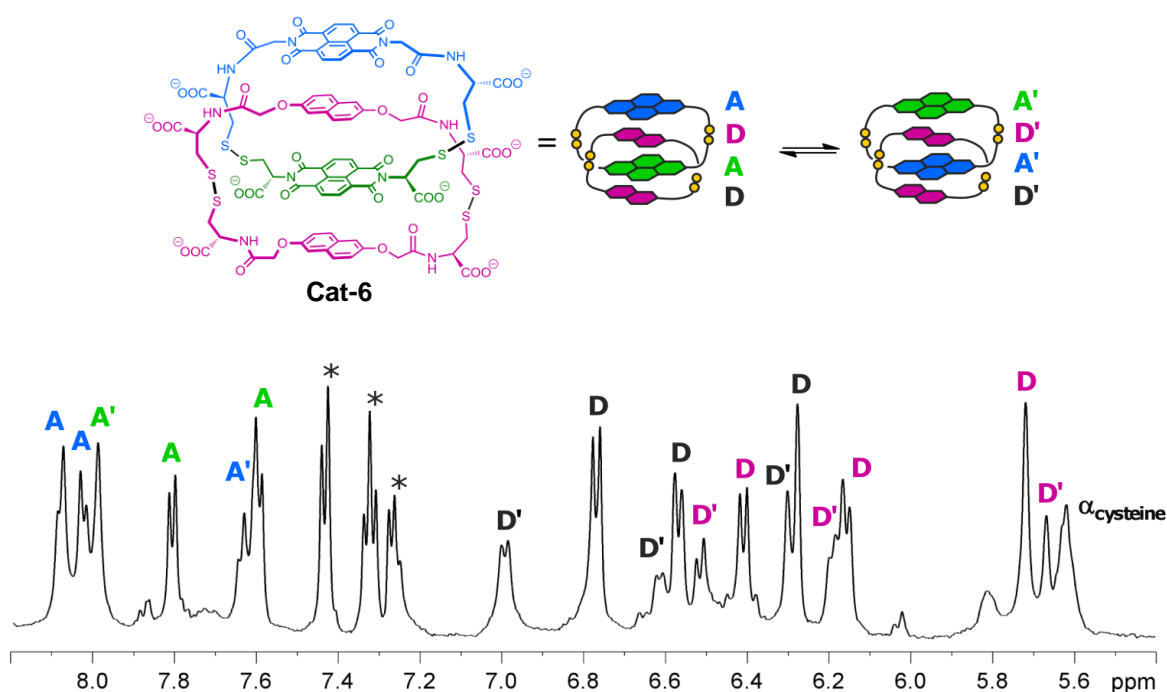


Figure 2.12. Partial ^1H NMR spectrum (D_2O , 298 K, 500 MHz) of DADA catenane **Cat-6** (the peaks labelled with * are associated with a [-A1-A2-] dimer impurity). The outer NDI, corresponding to the singlet at 8.0 ppm, was assigned arbitrarily to **A1**.

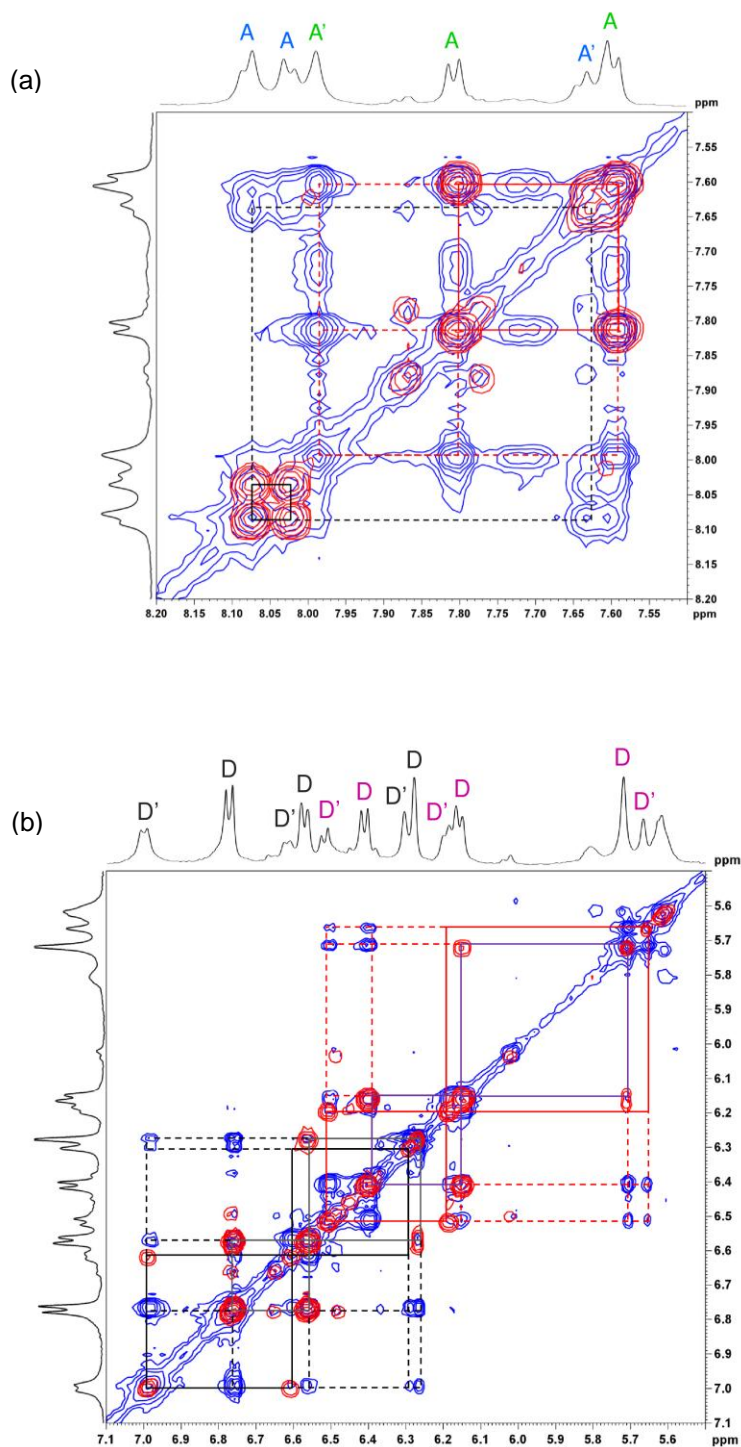


Figure 2.13. Partial COSY (red) and NOESY (blue) spectra of **Cat-6** between (a) 7.50 ppm and 8.20 ppm and (b) between 5.50 ppm and 7.10 ppm (D_2O , 298 K, 500 MHz, mixing time = 800 ms). The dotted lines highlight peaks connected through chemical exchange. The solvent peak was referenced at 4.79 ppm.

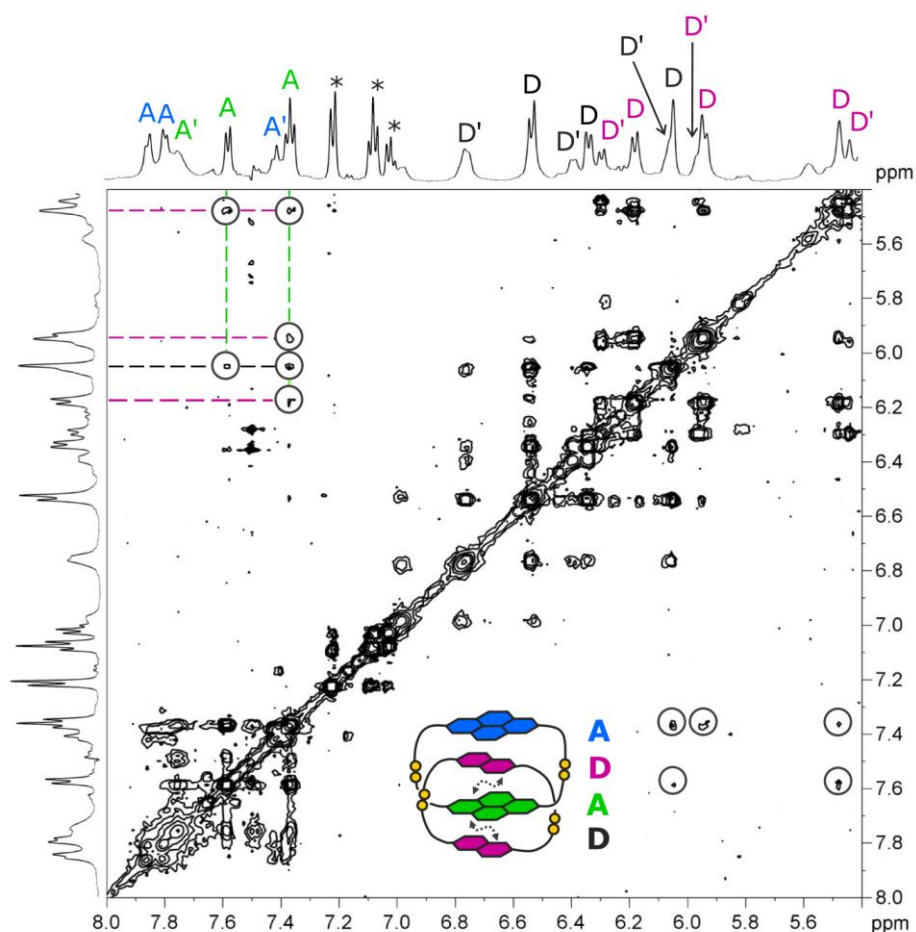


Figure 2.14. Expanded region of the NOESY spectrum (D_2O , 278 K, 500 MHz, mixing time: 800 ms) of DADA catenane **Cat-6** (the peaks labelled with * are associated with a [-A1-A2-] dimer impurity). The outer NDI, corresponding to the broad singlet at 7.8 ppm, was assigned arbitrarily to A1.

2.3.4. Improving further the synthesis of DADA catenanes: Cat-7

A library composed of **D2a**, **A1** and **A4** in a 2:1:1 molar ratio (Figure 2.15) further illustrates the link between the size of the acceptor ring and the efficiency of the formation of DADA catenanes in the libraries. The [-A1-A4-] acceptor ring is very tight, and the corresponding catenane **Cat-7** is now formed in the unusually high yield of 70%. The DADD paired catenane **Cat-3** is still present, but is now

a minor product. The formation of **Cat-7** in such high yield indicates a combination of optimal donor-acceptor and hydrophobic interactions and their efficient cooperation, leading to this particularly favourable catenane.

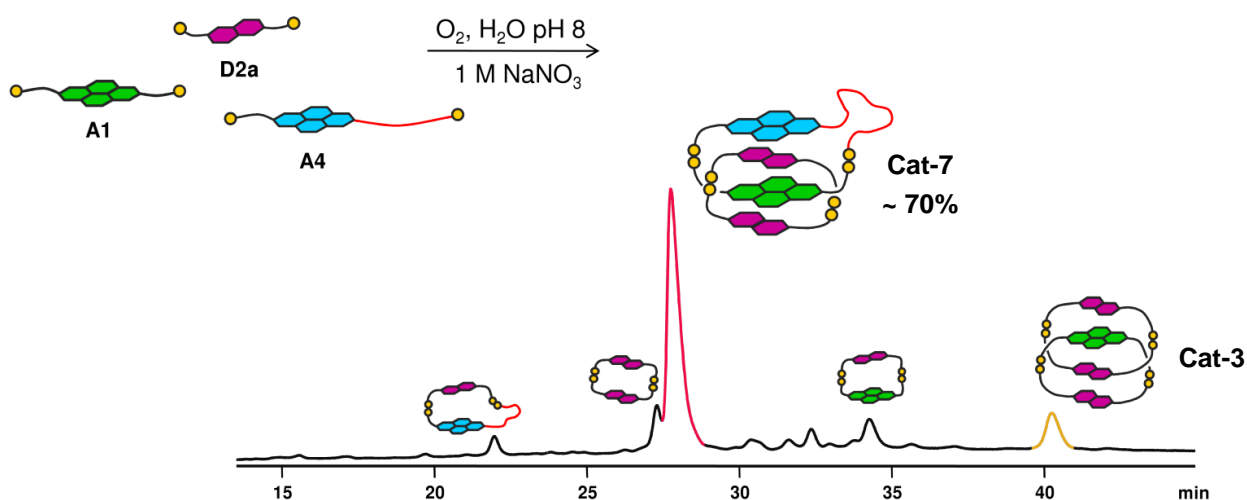


Figure 2.15. HPLC analysis of an aqueous library composed of **D2a**, **A1** and **A4** (2:1:1 molar ratio, 5 mM total), in the presence of 1 M of NaNO_3 . Absorbance was recorded at 260 nm.

2.3.5. ^1H NMR characterisation of **Cat-7**

Because of its lack of symmetry, **Cat-7** is produced as a pair of diastereomers, each having two conformers, as either acceptor can be situated in the inner or outer positions of the catenane. The ^1H NMR of **Cat-7** is consequently extremely complex (Figure 2.16). However, analysis of the acceptor region by a combination of the COSY and NOESY spectra (7.10 to 8.15 ppm) allowed correlation of the signals expected from a mixture of four isomeric catenanes (Figure 2.17).

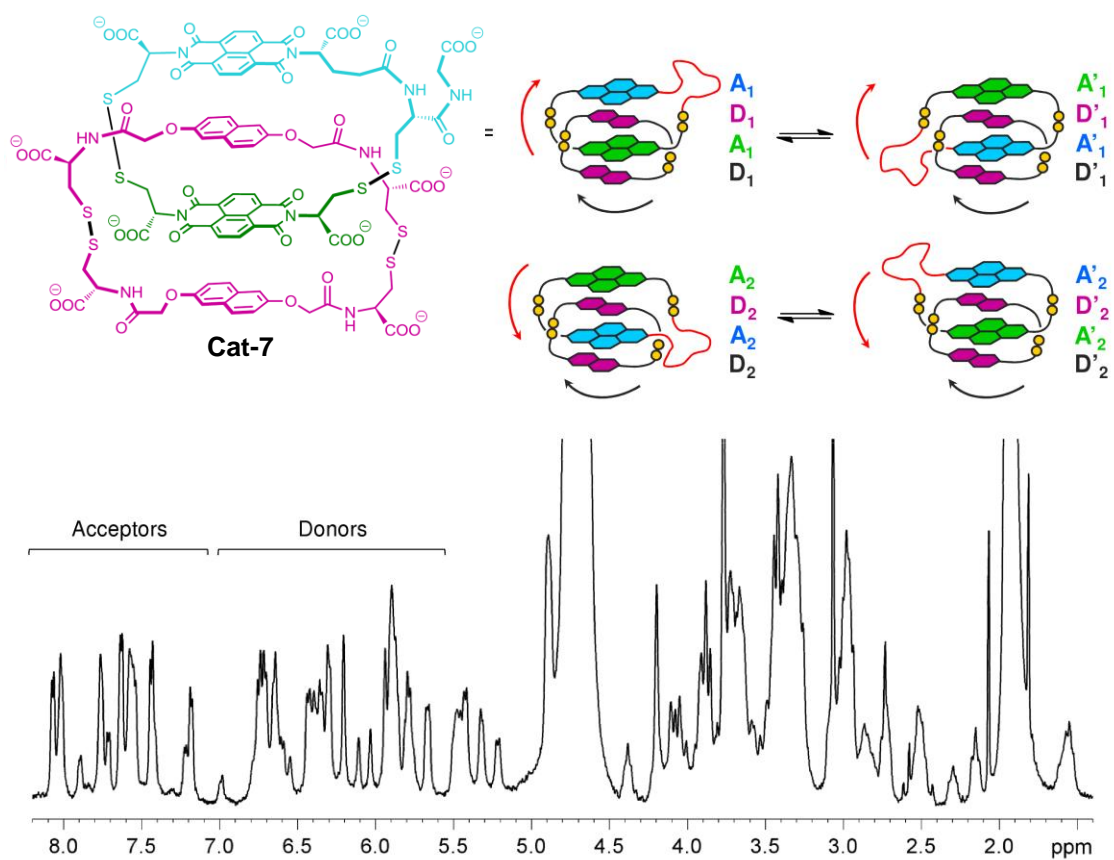


Figure 2.16. ^1H NMR spectrum (D₂O, 278 K, 500 MHz) of Cat-7. The solvent peak was referenced at 4.79 ppm.

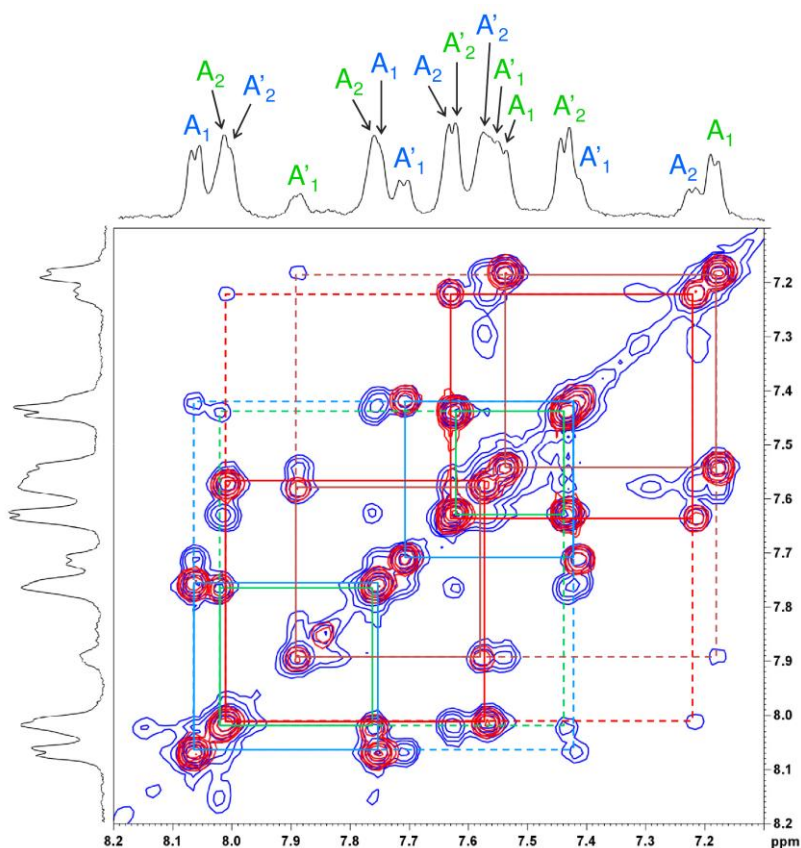


Figure 2.17. Partial COSY (red) and NOESY (blue) spectra **Cat-7** between 7.10 ppm and 8.20 ppm (D_2O , 278 K, 500 MHz, mixing time = 800 ms). The dotted lines highlight peaks connected through chemical exchange. The solvent peak was referenced at 4.79 ppm.

2.3.6. Conclusion: synthesising DADA catenanes from Pathway I

In conclusion, the **D2a** donor building block forms a stable [-D-D-] dimer, which is the key intermediate for the formation of DADA and DADD catenanes *via Pathway I*. The efficiency of the DADA catenane formation is directly linked to the tightness of the acceptor ring (Figure 2.18) as reflected by the yields that vary from 2% to 70% of the library. **Cat-6** and **Cat-7** are deep red in color in aqueous solution which is indicative of the presence of charge-transfer interactions between the complementary aromatic units.

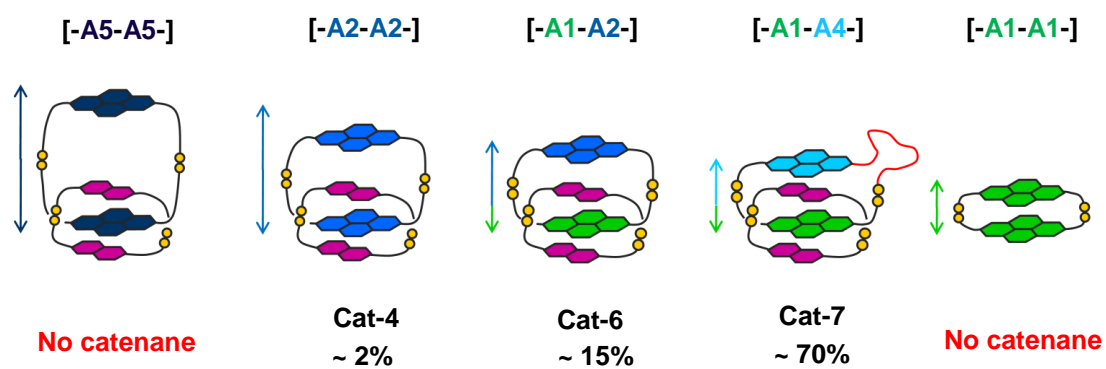


Figure 2.18. Relationship between the size of the acceptor ring and the efficiency of DADA catenane formation. The donor ring is [-D2a-D2a-] in each case.

2.4. Exploring Pathway II

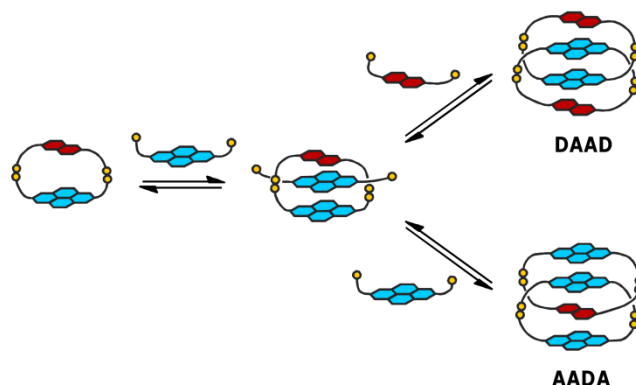


Figure 2.19. Formation of catenanes *via Pathway II*.

Pathway II (Figure 2.19) occurs under two circumstances. First, the donor building block must have rather long side-chains (**D1b** or **D2b**) so that it favours the formation of the [-D-] cyclic monomer and restricts the formation of a stable [-D-D-] dimer,^{8a,b,d, 12} thus preventing the formation of catenanes through *Pathway I*. Second, the formation of the threaded complex into the cavity of the [-A-A-] dimer must be prevented, blocking the formation of catenanes *via Pathway III*. This is the case when using **A1**: as the [-A1-A1-] dimer is too tight to allow threading through its cavity,^{8, 12} the [-D-A-] heterodimer becomes the only species which can potentially form a catenane. Composed of a long donor building block and a short acceptor, the [-D-A-] dimer has a relatively small cavity, suitable for strong interactions with an acceptor building block. A pair of ADAA and DAAD catenanes should be formed through *Pathway II*. However, the necessity of having a tight [-A-A-] dimer implies that the ADAA catenane cannot actually be formed, hence only one type of catenane, DAAD, was observed.

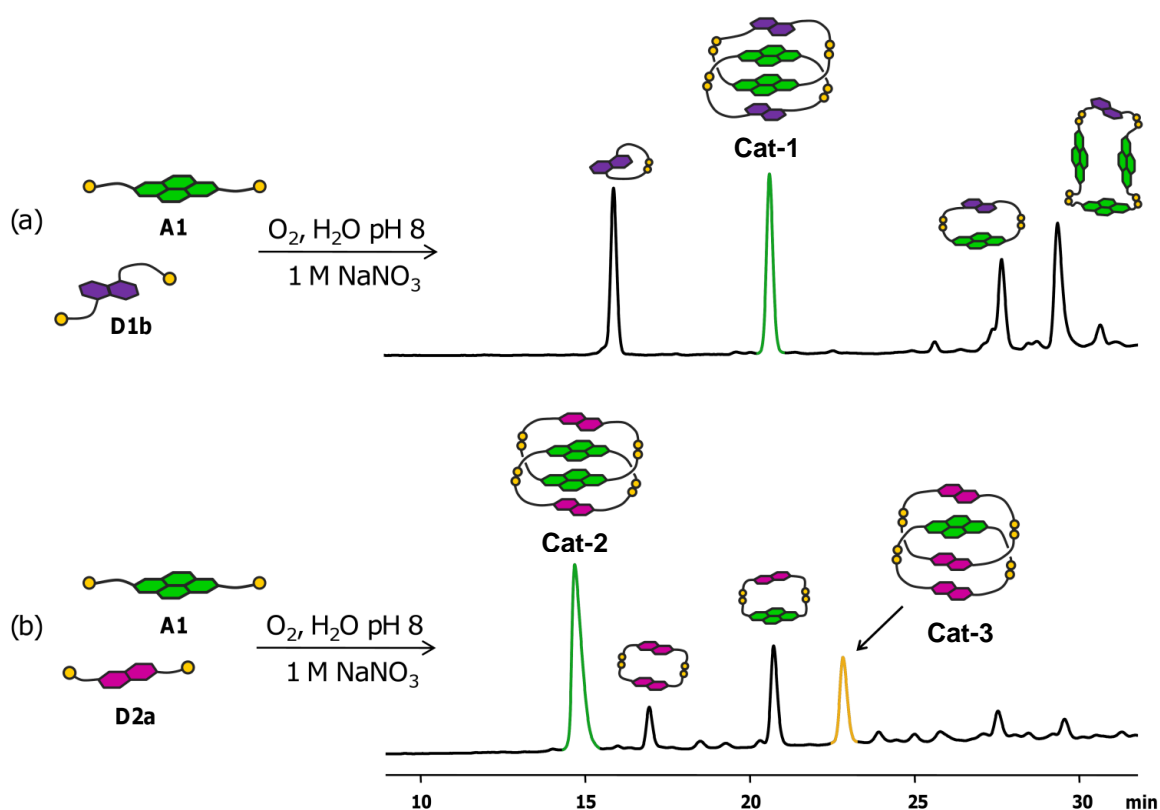


Figure 2.20. HPLC analysis of aqueous libraries composed of (a) **D1b** and **A1** (1:1 molar ratio, 5 mM total), and (b) **D2a** and **A1** (1:1 molar ratio, 5 mM total). The libraries were prepared with 1 M of NaNO_3 . Absorbance was recorded at (a) 292 nm, and (b) 260 nm.^{8c,d}

Many of these DAAD catenanes have previously been published by our group,^{8b,c,d} and now find their place in the generic mechanism described here, such as **Cat-1**, formed in a library of **D1b** and **A1** (1:1 molar ratio),^{8d} (Figure 2.20.a). A similar catenane was observed when replacing **D1b** by its 2,6-isomer **D2b**.^{8b}

The short donor **D2a** is also suitable for the formation of a DAAD catenane *via Pathway II* when mixed with **A1** (Figure 2.20.b).^{8c} However, **D2a** has also been shown to favour *Pathway I*, and the two pathways now compete. According to our mechanism, *Pathways I* and *II* should lead to two pairs of two catenanes, respectively DADD / DADA, and DAAD / ADAA. Once again, because the [-**A1-A1**-] does

not allow threading of an aromatic group through its cavity, only one type of catenane can actually be observed for each pathway: DAAD **Cat-2** (*Pathway II*), DADD **Cat-3** (*Pathway I*). Both catenanes, composed of short donor and acceptor building blocks, are the tightest catenanes obtained to date for these two types of structures, and are consequently formed in the best yields (55% for DAAD **Cat-2** in a D:A=1:1 molar ratio, and 50% for DADD **Cat-3** in a D:A = 3:1 molar ratio). This agrees with our previous observation that tight rings are necessary for the efficient formation of catenanes.

The two catenanes were previously isolated and characterized by Dr Ho Yu Au-Yeung.^{8c} Interestingly, the green DAAD catenane **Cat-2** and the orange DADD catenane **Cat-3**, exhibit different UV-Vis spectra^{8c} from the DADA catenanes described above, due to the particular arrangement of their donor and acceptor units.

2.5. Exploring Pathway III

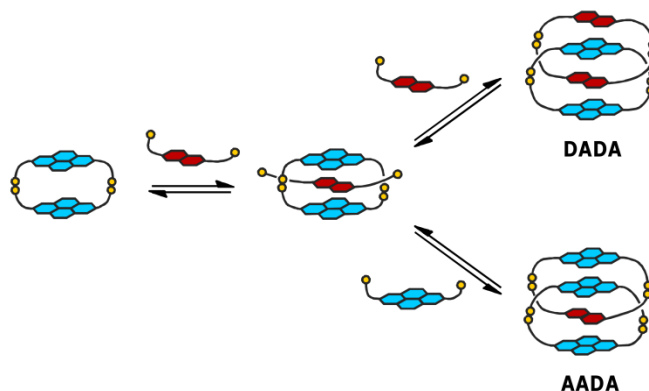


Figure 2.21. Formation of catenanes *via Pathway III*.

Pathway III (Figure 2.21), which leads to the formation of the new pair of catenanes DADA and AADA, occurs under particular conditions. The donor building block must have long side-chains (**D1b** or **D2b**), to limit the formation of the [-D-D-] dimer. The acceptor building block must also have long enough side-chains, so that the [-D-A-] dimer is too loose to form any stable threaded complex. However, it must be able to form a [-A-A-] dimer tight enough to allow a favourable interaction with a donor moiety. Therefore, the size of the acceptor building block is critical to the formation of catenanes through *Pathway III*. Unfortunately, it is not the only limitation for this mechanism. In the previous cases described (*Pathways I* and *II*), the smallest and most rigid donor and/or acceptor building blocks were necessary to lead efficiently to the most compact catenanes. The libraries were consequently quite simple, composed of catenanes and small macrocycles. To access catenanes through *Pathway III*, more flexible building blocks are necessary, increasing the complexity of the libraries: large macrocycles, such as trimers or tetramers, which can fold and thus bury some of their large hydrophobic surfaces intramolecularly, become serious competitors for the formation of the catenanes.

2.5.1. Identification of the first AADA catenane: Cat-8

The first library that follows *Pathway III* was composed of donor **D1b** with the acceptor building blocks **A1** and **A2** in a 2:1:1 molar ratio (Figure 2.22a). The DADA **Cat-9** is formed from the tightest possible acceptor ring in this system [-**A1-A2**-], interlocked with the donor ring which is much larger than in previous catenanes of this type, leading to a very low yield. This shows that both the size of the acceptor and the donor rings play a role in the efficiency of formation of the DADA catenane.

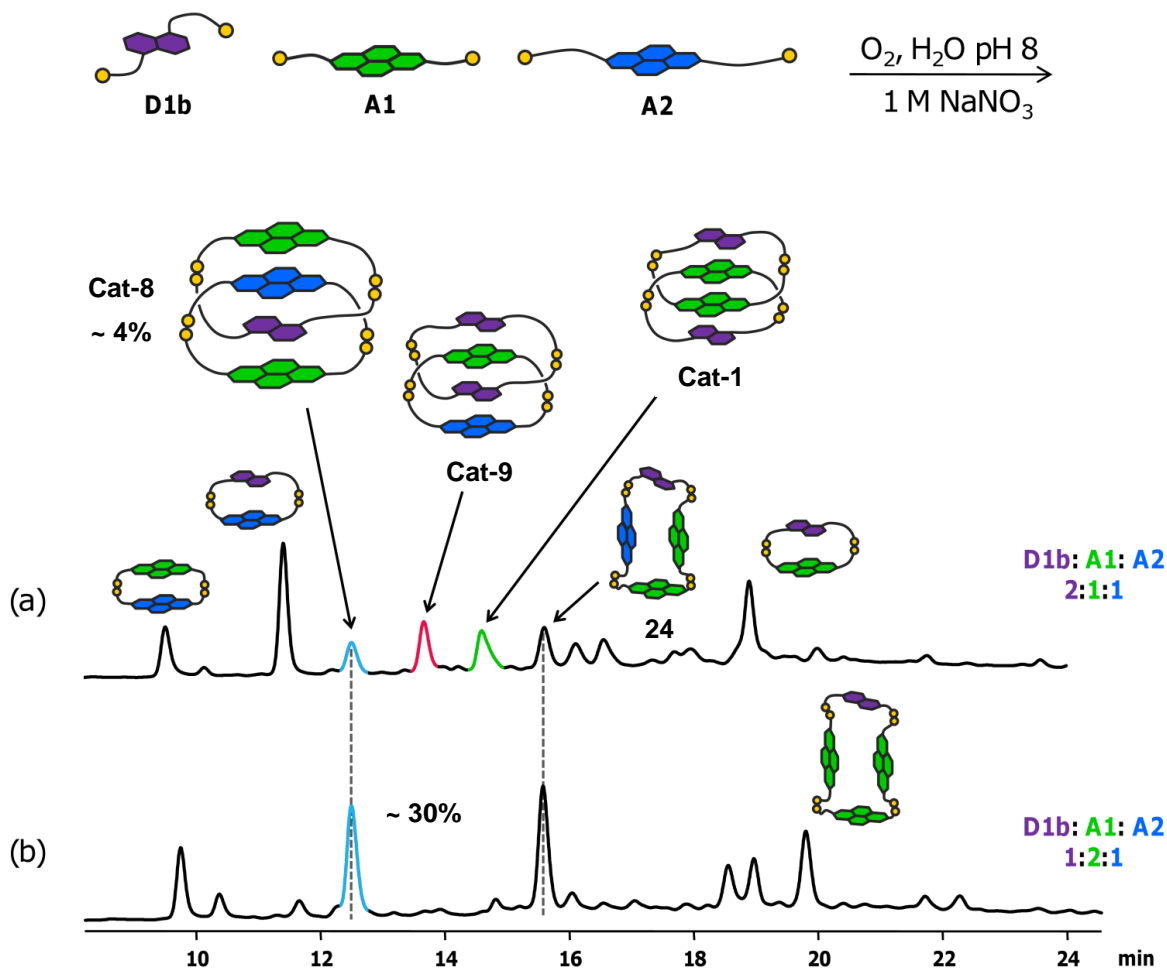


Figure 2.22. HPLC analysis of aqueous libraries composed of **D1b**, **A1** and **A2** (5 mM total): (a) 2:1:1 molar ratio, and (b) 1:2:1 molar ratio. DCLs were prepared with 1 M of $NaNO_3$. Absorbance was recorded at 383 nm.

Its paired AADA catenane **Cat-8** is observed for the first time, and identified by tandem MS and MS/MS (Figure 2.23). The library also contained the DAAD **Cat-7** formed via *Pathway II*.

ESI-MS (negative ion) of **Cat-8** shows a doubly charged molecular ion (m/z of 1031.7), corresponding to the mass of a tetramer containing only one donor and three acceptor units. The fragmentation pattern in MS/MS of **Cat-8** (Figure 2.23.b) is significantly different to the one of its isomeric macrocycle **24** (Figure 2.23.c), with the largest fragments observed have an m/z of 1056.5 and 1006.6, corresponding to the mass of the [-A1-A2-] homodimer and the [-D2b-A1-] heterodimer respectively.

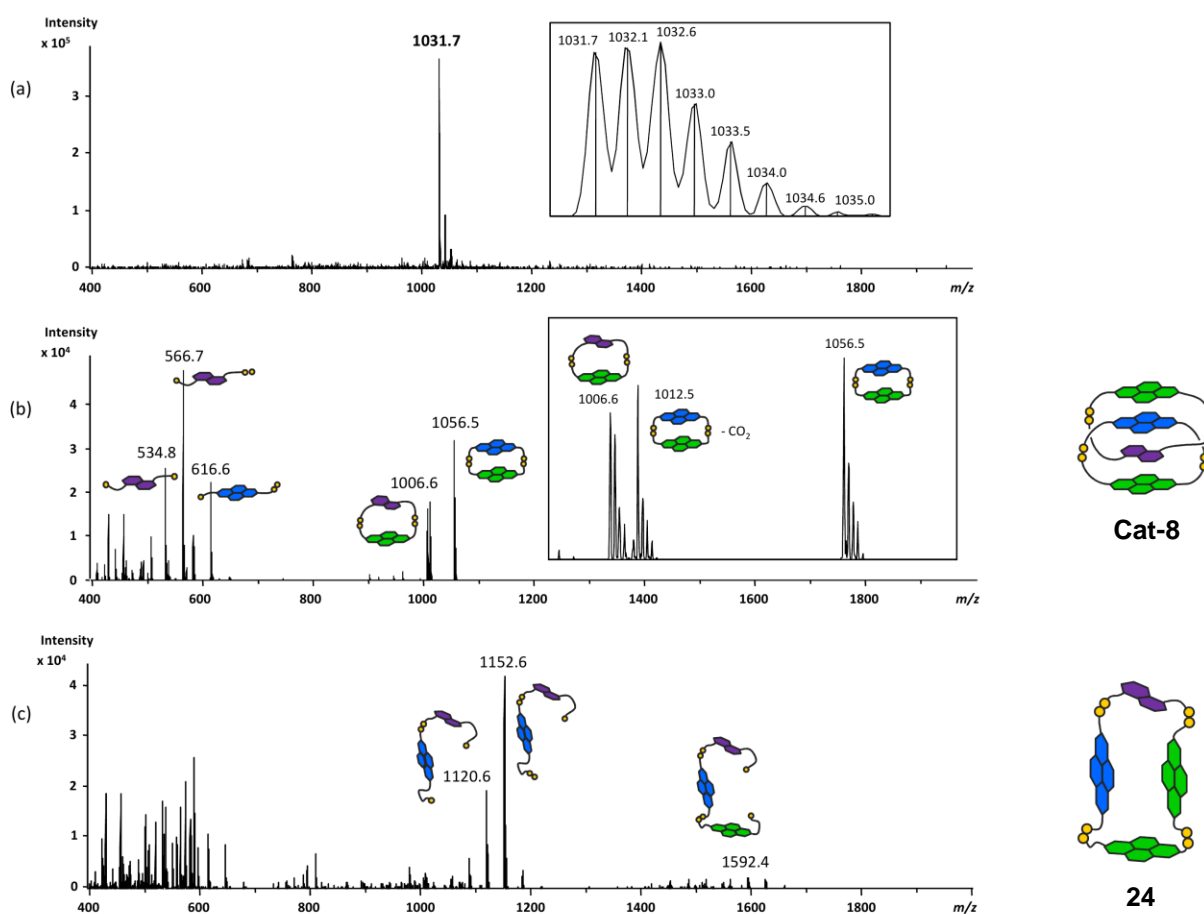


Figure 2.23. Tandem (a) MS, (b) MS/MS fragmentation **Cat-8**, and (c) of its macrocyclic isomer **24**. The yellow cartoon dots represent the sulfur atoms of the cysteine.

The AADA **Cat-9** could be amplified up to 30% yield, along with its isomeric macrocycle **24**, by using a biased ratio of building blocks (Figure 2.22.b). The amplification of this tetramer clearly shows that large macrocycles can fold to minimize hydrophobic exposure and be in direct competition with the formation of the corresponding catenanes.

2.5.2. ^1H NMR characterisation of **Cat-8** and of its isomeric macrocycle **24**

Both **Cat-8** and its isomeric tetramer **24** were isolated and analyzed by ^1H NMR spectroscopy (Figures 2.24 to 2.28). The two compounds exhibit significantly different ^1H NMR spectra (500 MHz, D_2O), with the spectrum of the catenane displaying the expected upfield shifts for the aromatic protons due to the stacked structure (Figure 2.24).

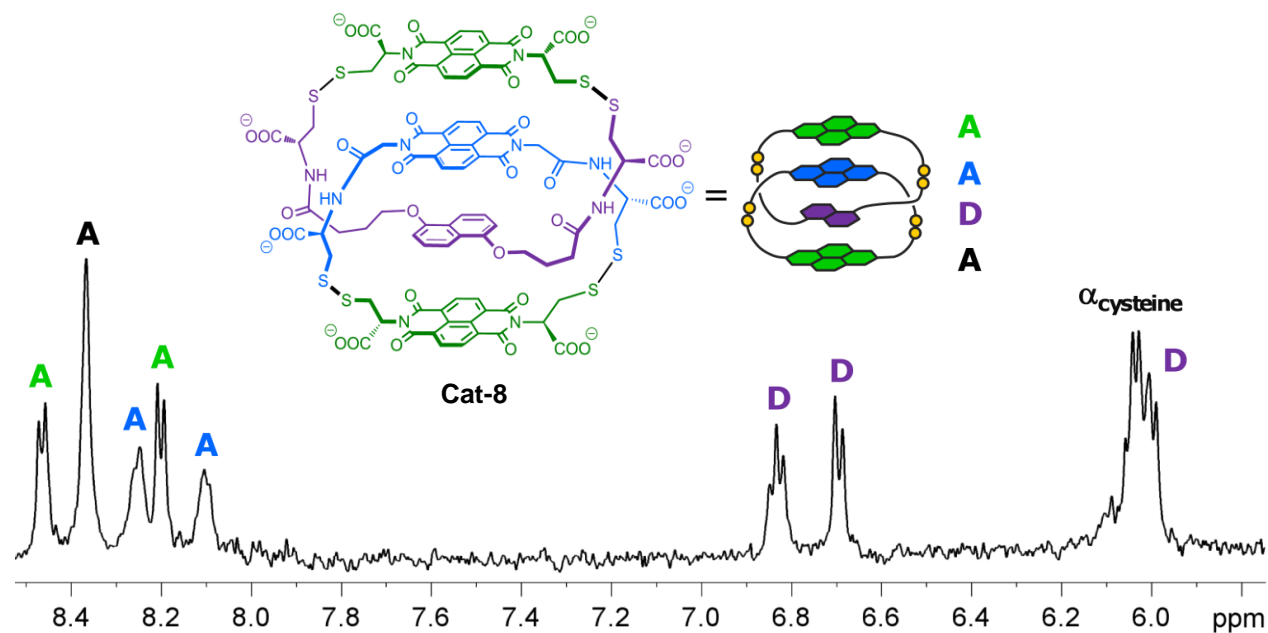


Figure 2.24. Partial ^1H NMR spectrum (D_2O , 333 K, 500 MHz) of AADA catenane **Cat-8**. The inner NDI, corresponding to the doublets at 8.25 and 8.10 ppm, was assigned arbitrarily to **A2**.

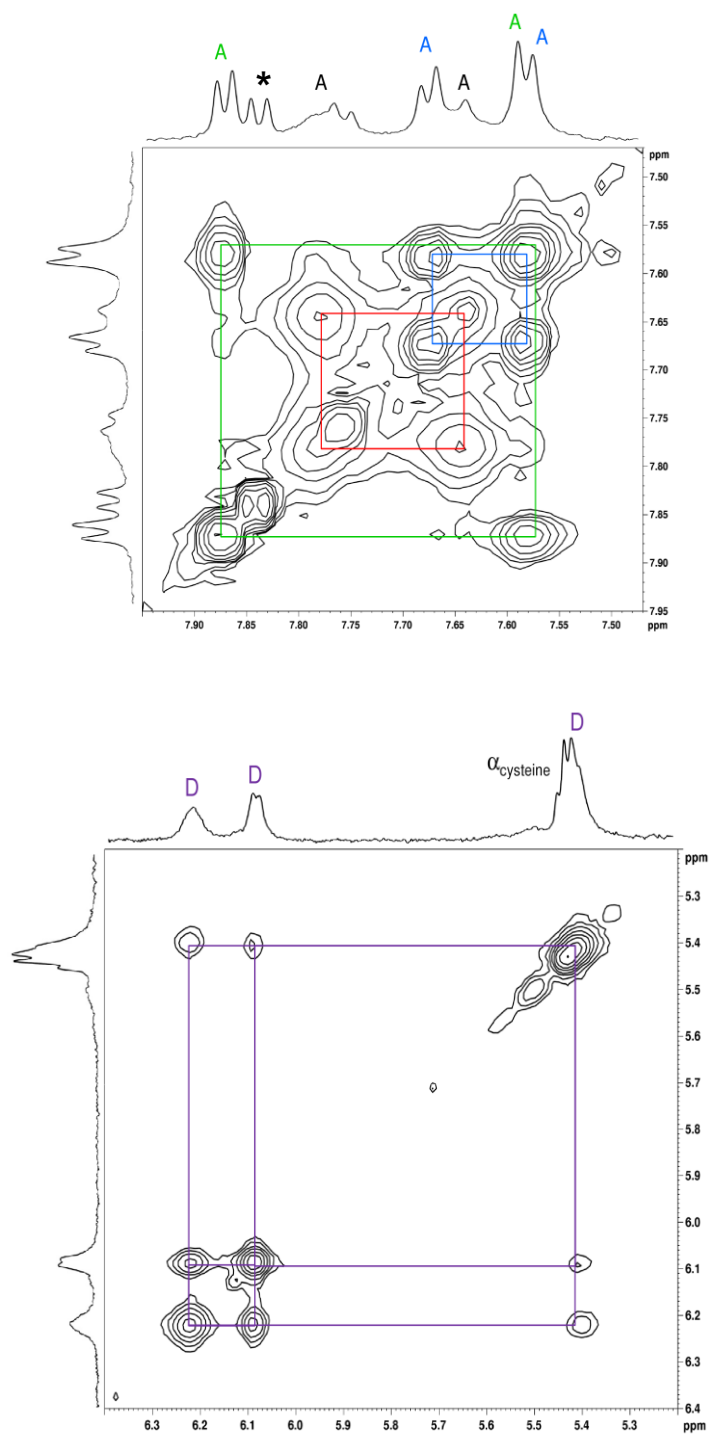


Figure 2.25. Partial COSY spectrum (D_2O , 278 K, 500 MHz) of **Cat-8** between (a) 7.45 ppm and 7.95 ppm and (b) 5.20 ppm and 6.40 ppm. The solvent peak was referenced at 4.79 ppm.

Only one conformation was observed for the AADA catenane **Cat-8**. Three sets of signals were correlated by COSY in the acceptor region (8.05 to 8.50 ppm, Figure 2.25.a), corresponding to the two outer and one inner NDIs. Only one set of signals corresponding to one DN unit was found in the donor region (5.95 to 6.90 ppm, Figure 2.25.b). At 278 K, cross-peaks between the aromatic units were observed by NOESY, confirming the unusual AADA structure of **Cat-8** (Figure 2.26).

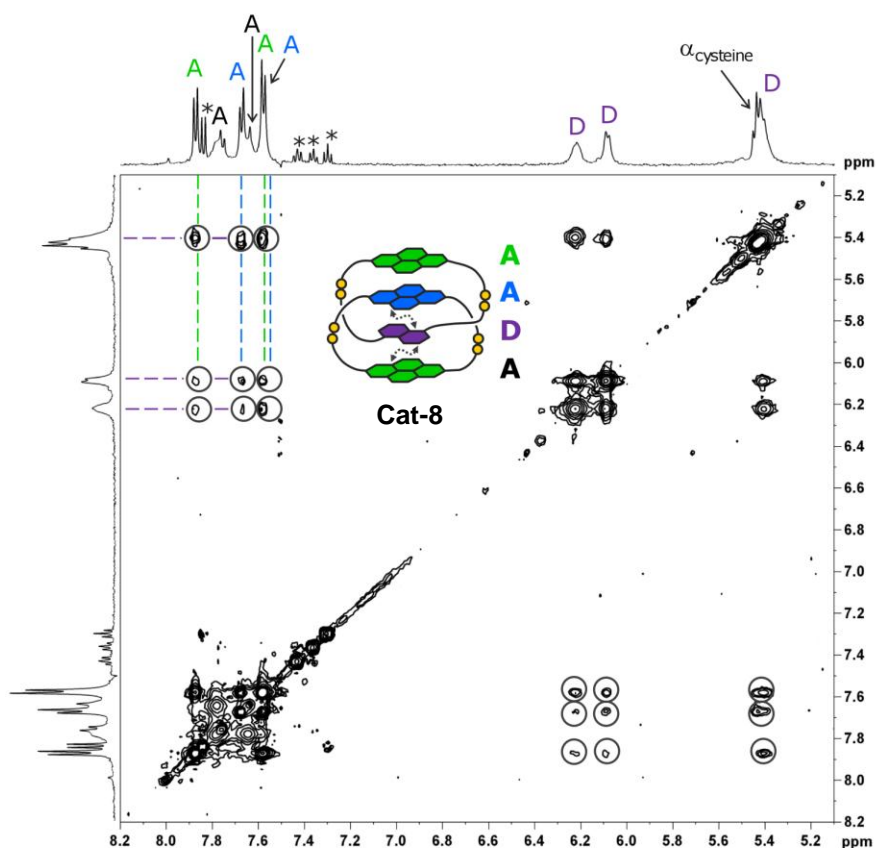


Figure 2.26. Expanded region of the NOESY spectrum (D_2O , 278 K, 500 MHz, mixing time = 800 ms) of AADA catenane **Cat-8** (the peaks labelled with * are associated with a [-A1-A2-] dimer impurity).

The resonances of the catenane are clearly assignable at 278 K and slightly broaden upon increasing the temperature (Figure 2.27.a). In sharp contrast, the resonances of macrocycle **24** at 278 K are extremely broad and dramatically sharpen upon increasing the temperature up to 333 K (Figure 2.27.b).

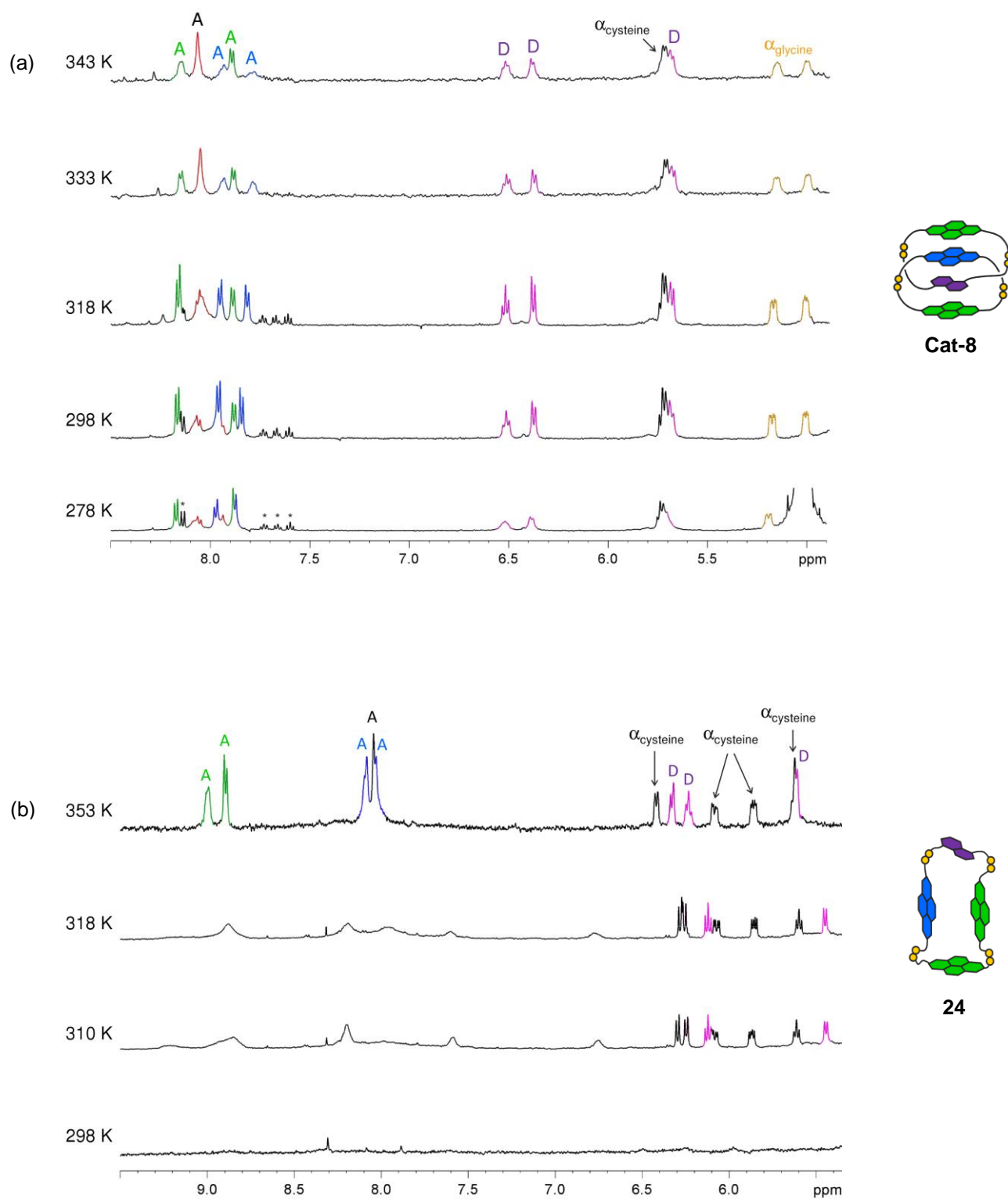


Figure 2.27. Partial ^1H NMR spectrum (D₂O, 500 MHz) of (a) **Cat-8** at 343 K, 333 K, 318 K, 298K, and 278 K and (b) its isomeric macrocycle **24** at 353 K, 318 K, 310 K, and 298K. The solvent peak was referenced at 4.79 ppm at 298K. The peaks labelled with * are associated with a [-A1-A2-] dimer impurity.

As for **Cat-8**, the aromatic protons of macrocycle **24** were assigned by COSY spectroscopy (Figure 2.28). The confirmation by ^1H NMR of the structural difference between catenane **Cat-8** and macrocycle **24** verifies the reliability of our identifications by tandem MS and MS/MS.

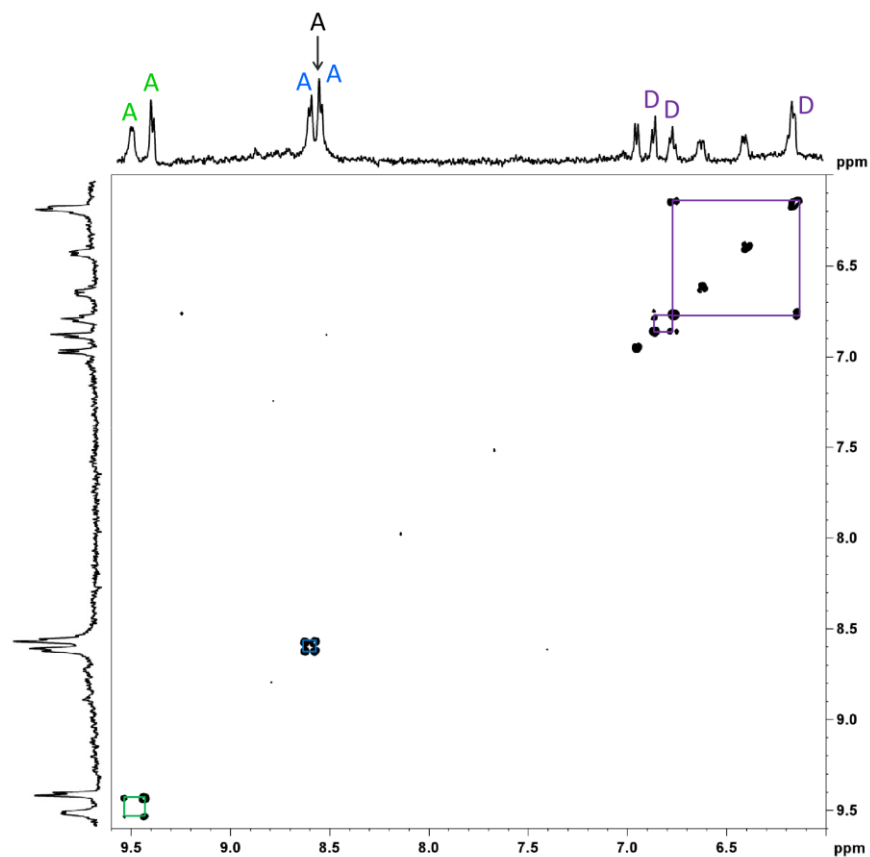


Figure 2.28. Partial COSY spectrum (D_2O , 353 K, 500 MHz) of macrocycle **24** between 6.00 ppm and 9.60 ppm. The solvent peak was referenced at 4.79 ppm.

2.5.3. Identification of a second AADA catenane: **Cat-10**

As expected, a library composed of **D2b**, **A1** and **A2** (2:1:1 molar ratio, Figure 2.29.b) contains the DADA catenane **Cat-11** and its paired AADA catenane **Cat-10**. The presence of **Cat-9** again indicates that *Pathway II* is competing with *Pathway III*.

In a biased library with a ratio of **D2b:A1:A2** of 1:2:1 in 1 M NaNO₃ (Figure 2.29.c) the yield of this catenane increased up to 10% of the library, allowing for its isolation. In this case, higher amplification of **Cat-10** was observed in the presence of 1 M Na₂SO₄, up to 20% of the library. This amplification is most likely due to the higher ionic strength of the solution (Figure 2.29.d). However, no difference of behaviour had been observed when replacing NaNO₃ by Na₂SO₄ in the previous libraries. The better amplification of **Cat-10** in the presence of Na₂SO₄ was attributed to the particularly high complexity of the library and the presence of large macrocycles.

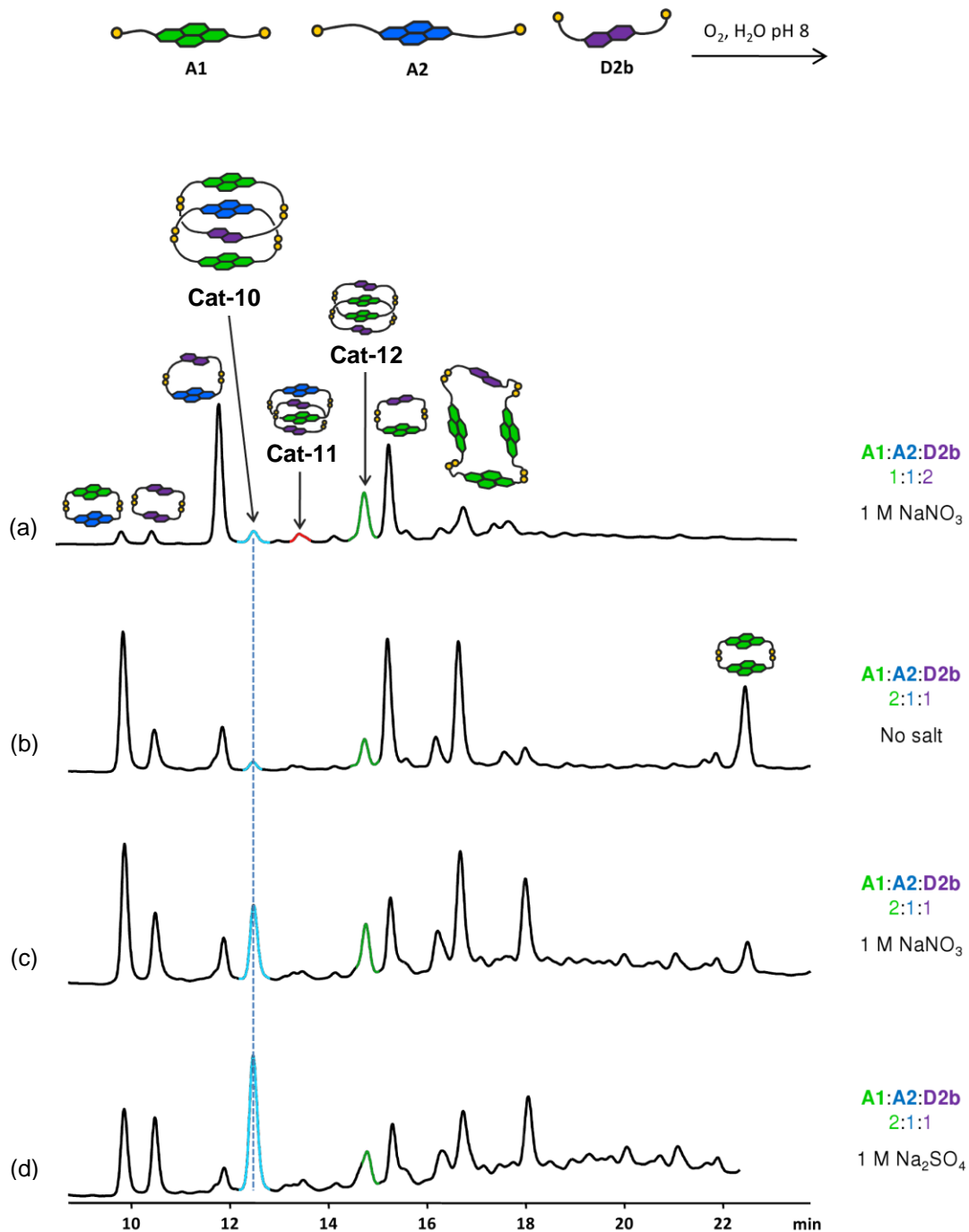


Figure 2.29. HPLC analyses of aqueous libraries composed of **A1**, **A2** and **D2b** (total concentration of building blocks of 5 mM): (a) **A1:A2:D2b** = 1:1:2 molar ratio in the presence of 1 M of $NaNO_3$, (b) **A1:A2:D2b** = 2:1:1 molar ratio in the absence of salt, (c) **A1:A2:D2b** = 2:1:1 molar ratio in the presence of 1 M of $NaNO_3$, (d) **A1:A2:D2b** = 2:1:1 molar ratio in the presence of 1 M of Na_2SO_4 . Absorbance was recorded at 383 nm.

2.5.4. ^1H NMR characterisation of **Cat-10**

Cat-10 was characterized by ^1H NMR (500 MHz, 298 K, D_2O , Figures 2.30 to 2.32). While the slightly shorter **Cat-8** displays only one conformation, **Cat-10** displays two conformations, which could be assigned with the help of COSY and NOESY spectra (Figure 2.31). This observation can only be attributed to the slight difference of size and geometry of the donor units incorporated in **Cat-8** and **Cat-10**. Once again, cross-peaks between the donor and acceptor units of the major conformation were observed in NOESY spectra, confirming the AADA structure of **Cat-10** (Figure 2.32).

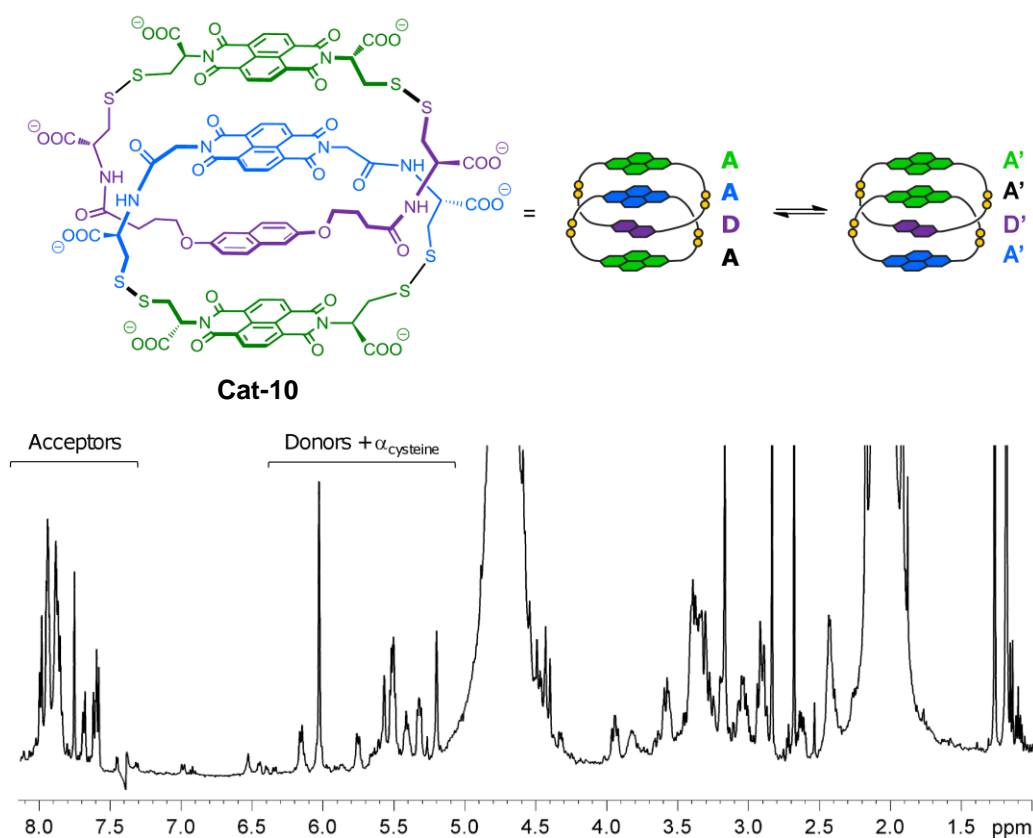


Figure 2.30. ^1H NMR spectrum (D_2O , 298 K, 500 MHz) of **Cat-10**. The solvent peak was referenced at 4.79 ppm.

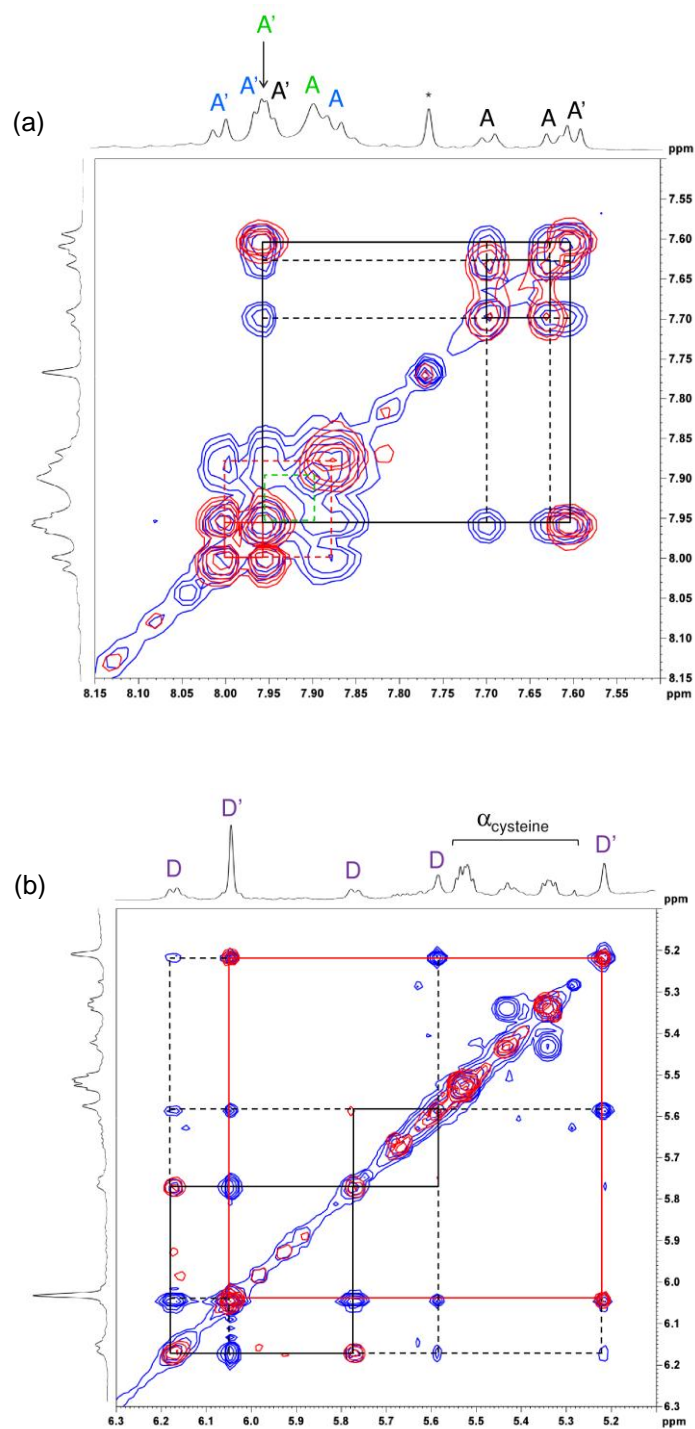


Figure 2.31. Partial COSY (red) and NOESY (blue) spectra of **Cat-10** between (a) 7.50 ppm and 8.15 ppm and (b) 5.10 ppm and 6.30 ppm (D_2O , 298 K, 500 MHz, mixing time = 800 ms). The dotted lines highlight peaks connected through chemical exchange. The solvent peak was referenced at 4.79 ppm.

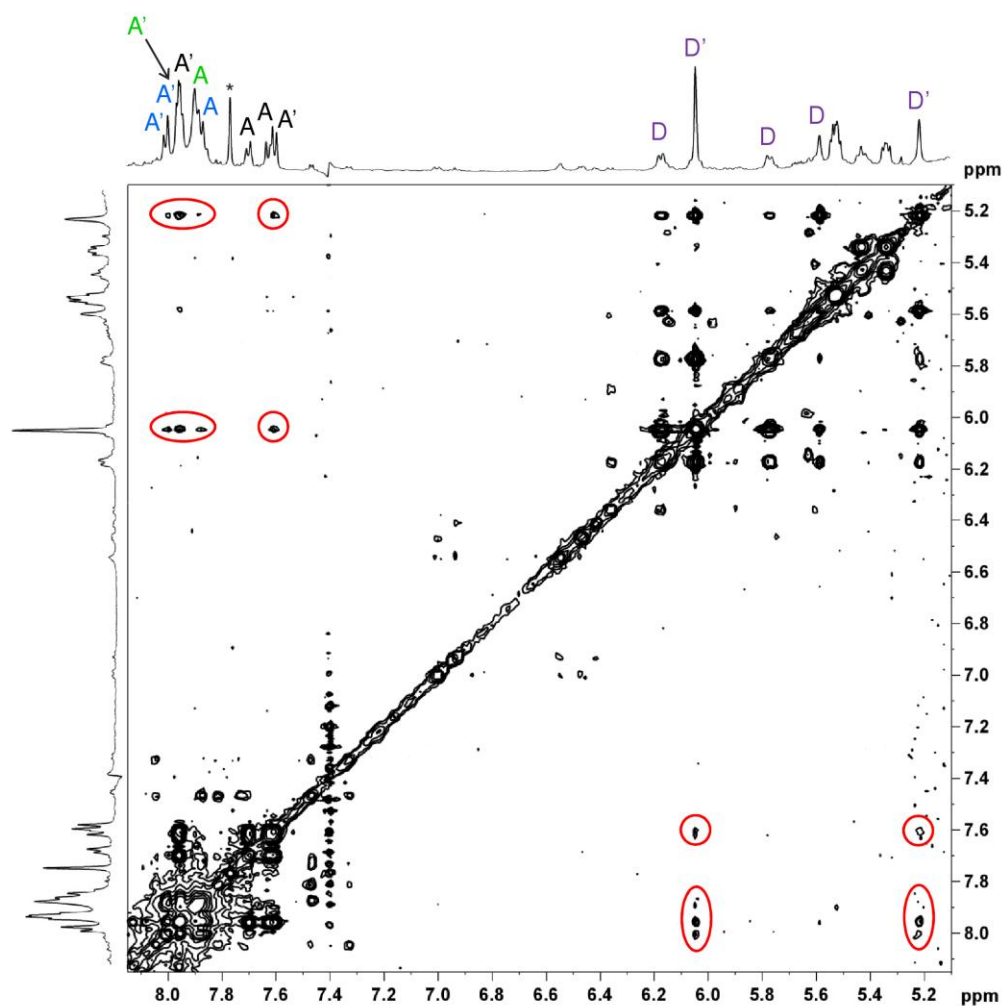


Figure 2.32. Partial NOESY spectrum of **Cat-10** between 5.10 ppm and 8.20 ppm (D_2O , 298 K, 500 MHz, mixing time = 800 ms). An impurity was labelled by *. The solvent peak was referenced at 4.79 ppm.

2.5.5. Identification of other AADA catenanes

Many other AADA catenanes were identified in libraries based on either long donors **D1b** or **D2b**: only one example is shown in Figure 2.33. As expected, only the smallest acceptor rings lead to the formation of AADA catenanes, but most of the libraries producing catenanes from *Pathway III* are

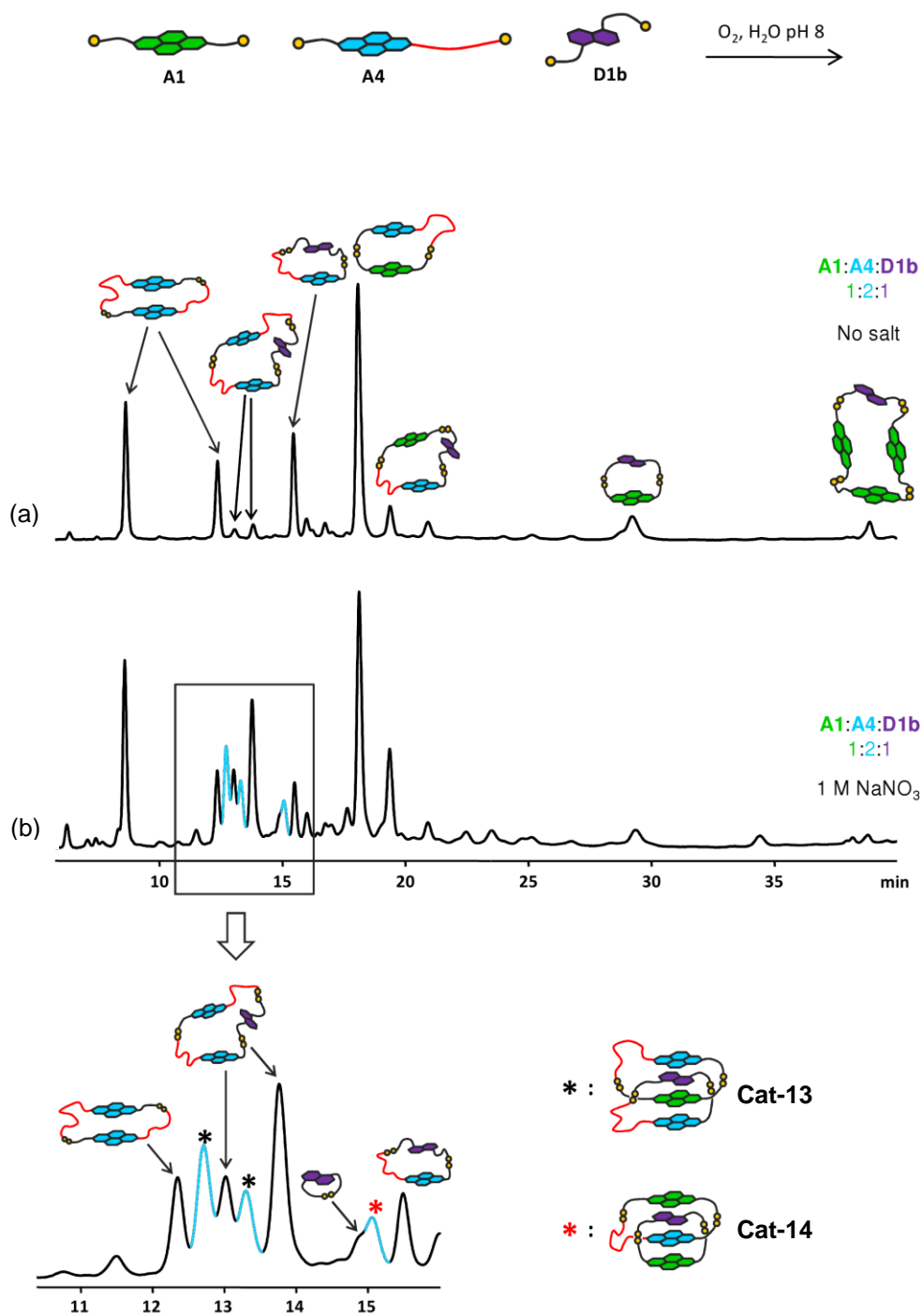


Figure 2.33. HPLC analyses of aqueous libraries composed of **A1**, **A4** and **D2b** (total concentration of building blocks of 5 mM): (a) **A1:A4:D2b** = 1:2:1 molar ratio in the absence of salt, (b) **A1:A4:D2b** = 1:2:1 molar ratio in the presence of 1 M of NaNO₃. Absorbance was recorded at 383 nm.

relatively complex and the formation of large macrocycles seems to be favoured over the formation of the catenanes, which are only present, in most cases, as traces. In the library depicted in Figure 2.33, two AADA catenanes (**Cat-13** and **Cat-14**) could be identified in the presence of NaNO_3 , in an otherwise extremely complex library. The presence of two peaks on the HPLC trace for **Cat-13** can be explained by the existence of different isomers, due to the asymmetry of building block **A4**.

2.5.6. Conclusion: synthesising AADA catenanes from Pathway III

To conclude, using flexible donors **D1b** or **D2b** leads to the formation of DADA and AADA catenanes through *Pathway III*. The formation of DADA catenanes is not favoured through this mechanism, because the donor ring is too large to allow an optimum overlap of the complementary aromatic units. There is a delicate balance in the formation of AADA catenanes as they are in competition with the formation of large macrocycles such as trimers and tetramers. However, optimizing the choice of the building blocks, in order to the access the tightest possible acceptor and donor rings, can lead to AADA catenanes such as **Cat-8**, that can be amplified up to 30%. Both **Cat-8** and **Cat-10** were isolated as yellow-brown products, showing that AADA catenanes exhibit different optical properties than the other types of catenanes described above.

2.6. Competing Pathways

The previous section described design protocols that access catenanes selectively *via Pathways I, II, or III*, but we also observed in the most complex systems that catenanes can be formed *via* two simultaneous *Pathways*. It is therefore conceivable that a library fulfilling the conditions of all three *Pathways* will generate all the types of catenanes. This is beautifully illustrated in Figure 2.34 by a library containing the short donor building block **D2a** and the asymmetric acceptor building block **A4** (1:1 molar ratio, 5 mM).

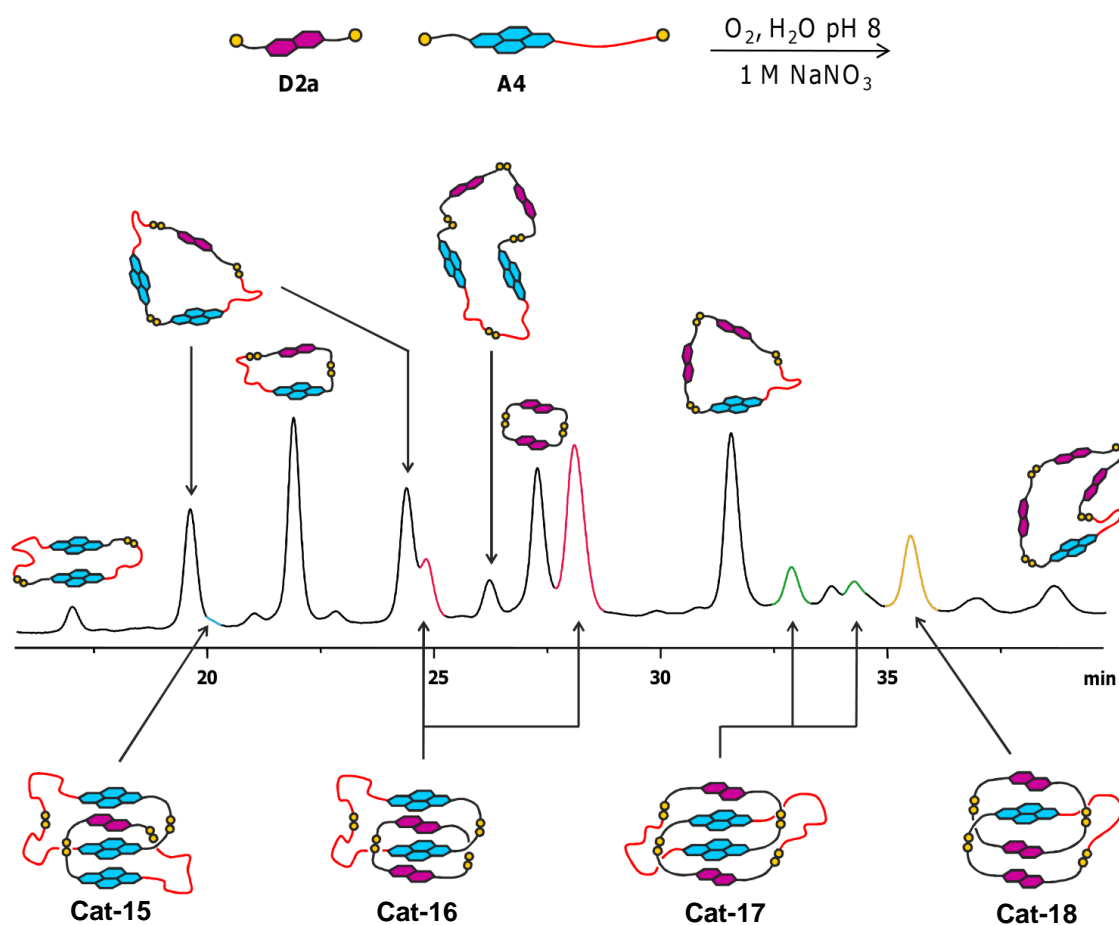


Figure 2.34. HPLC analysis of an aqueous library composed of **D2a** and **A4** (1:1 molar ratio, 5 mM total), in the presence of 1 M of $NaNO_3$. Absorbance was recorded at 260 nm.

The behaviour of **A4** is driven by its shorter side-chain, making the formation of a DAAD catenane possible (*Pathway II*). However, the [-A-A-] homodimer is now large enough to allow the formation of DADA and AADA catenanes (*Pathway III*), and the use of **D2a** allows the formation of a DDAD catenane (*Pathway I*). Indeed, all the four possible catenanes DAAD (**Cat-17**), DADD (**Cat-18**), DADA (**Cat-16**) and AADA (**Cat-15**), were observed in the same library.

Here again, the presence of two peaks on the HPLC trace for each of **Cat-16** and **Cat-17** can be explained by the existence of different isomers or of slowly interconverting conformations. The synthesis of all four types of catenanes in the same library clearly shows that there is little energetic difference between them. This allows us to conclude beyond doubt that the formation of the unusual AADA, DAAD and AADA stacked catenanes is not significantly disfavoured when compared to the typical DADA catenane.

2.7. Conclusion

A variety of new donor-acceptor [2]catenanes with different arrangements of the aromatic units (DAAD, DDAD, DADA, and AADA) have been identified by dynamic combinatorial chemistry. The observation that complete oxidation freezes exchange in such a way that the catenanes become kinetic bottlenecks (or traps) takes this work away from pure dynamic combinatorial chemistry into a hybrid realm where there is a complex interplay of kinetics and thermodynamics. While this is in some sense disappointing, it is not entirely surprising and it also provides an opportunity to probe reaction pathways that are necessarily invisible in a truly thermodynamic equilibrium.

Donor-acceptor interactions, which conventionally lead to DADA catenanes only, were partially overcome by using a highly polar medium, allowing efficient access to catenanes with unusual DADD, DAAD and ADAA stacking sequences. The formation of these previously exotic catenanes in the DCLs can be convincingly explained by taking into account the relative contributions of donor-acceptor and hydrophobic effects in their assembly. A close analysis of the DCLs studied allowed us to propose a mechanistic pathway for their synthesis and also to predict the outcome of libraries *a priori*. Donor-acceptor interactions are crucial in the mechanism but the hydrophobic effect determines the overall outcome of catenation process. Catenanes containing different stacking sequences of the donor and acceptor units can be selectively formed following one of the three synthetic pathways proposed simply by choosing the correct building blocks in the DCL setup.

These results challenge conventional thinking that has limited the scope of donor-acceptor [2]catenanes to strictly alternating stacks of donor and acceptor aromatic units. They indicate that an approach to catenane synthesis that takes into account only donor-acceptor interactions is unnecessarily limiting. To date, aromatic interactions have been satisfactorily described in terms of electrostatic interactions, which can only be enhanced by solvophobic effect. This work shows that the solvophobic effect can overcome

and direct syntheses based on supramolecular interactions between aromatic moieties. This observation will allow chemists to design and indeed synthesize complex structures that were previously inaccessible.

References:

1. (a) Hunter, C. A.; Lawson, K. R.; Perkins, J.; Urch, C. J. *J. Chem. Soc., Perkin Trans. 2* **2001**, 651; (b) Hunter C. A. *Chem. Soc. Rev.* **1994**, *23*, 101; (c) Hunter, C. A.; Sanders, J. K. M. *J. Am. Chem. Soc.* **1990**, *112*, 5525.
2. (a) Ramkumar, S. G.; Ramakrishnan, S. *Macromolecules* **2010**, *43*, 2307; (b) Zhang, W.; Dichtel, W.R.; Stieg, A. Z.; Benítez, D.; Gimzewski, J. K.; Heath, J. R.; Stoddart, J. F. *Proc. Natl. Acad. Sci. USA.* **2008**, *105*, 6514; (c) Bradford, V. J.; Iverson, B. L. *J. Am. Chem. Soc.* **2008**, *130*, 1517; (d) Zhou, Q.-Z.; Jia, M.-X.; Shao, X.-B.; Wu, L.-Z.; Jiang, X.-K.; Li, Z.-T.; Chen, G.-J. *Tetrahedron* **2005**, *61*, 7117; (e) Zhao, X.; Jia, M.-X.; Jiang, X.-K.; Wu, L.-Z.; Li, Z.-T.; Chen, G.-J. *J. Org. Chem.* **2004**, *69*, 270; (f) Ghosh, S.; Ramakrishnan, S. *Angew. Chem. Int. Ed.* **2004**, *43*, 3264; (g) Zhou, Q.-Z.; Jiang, X.-K.; Shao, X.-B.; Chen, G.-J.; Jia, M.-X.; Li, Z.-T. *Org. Lett.* **2003**, *5*, 1955; (h) Gabriel, G. J.; Iverson, B. L. *J. Am. Chem. Soc.* **2002**, *124*, 15174; (i) Ngyuen, J. Q.; Iverson, B. L. *J. Am. Chem. Soc.* **1999**, *121*, 2639; (j) Lokey, R. S.; Iverson, B. L. *Nature* **1995**, *375*, 303.
3. For some recent examples: (a) Mullen, K. M.; Davis, J. J.; Beer, P. D. *New J. Chem.* **2009**, *33*, 769; (b) Lin, T.-C. Lai, C.-C.; Chiu, S.-H. *Org. Lett.* **2009**, *11*, 613; (c) Ikeda, T.; Higuchi, M.; Kurth, D. G. *Chem. Eur. J.* **2009**, *15*, 4906; (d) Yoon, I.; Benítez, D.; Zhao, Y.-L.; Miljanić, O. Š.; Kim, S.-Y., Tkatchouk, E.; Leung, K. C.-F.; Khan, S. I.; Goddard III; W. A.; Stoddart, J. F. *Chem. Eur. J.* **2009**, *15*, 1115; (e) Ikeda T.; Higushi, M.; Kurth, D. G. *J. Am. Chem. Soc.* **2009**, *131*, 9158; (f) Cagulada, A. M.; Hamilton, D. G. *J. Am. Chem. Soc.* **2009**, *131*, 902; (f) Pascu, S. I.; Naumann, C.; Kaiser, G.; Bond, A. D.; Sanders, J. K. M.; Jarroson, T. *Dalton Trans.* **2007**, 3874; (g) Pascu, S. I.; Jarroson, T.; Naumann, C.; Otto, S.; Kaiser, G.; Sanders, J. K. M. *New J. Chem.* **2005**, *29*, 80.

4. For some recent examples: (a) Wang, C.; Olson, M. A.; Fang, L.; Benítez, D.; Tkatchouk, E.; Basu, S.; Basuray, A. N.; Zhang, D.; Zhu, D.; Goddard, W. A.; Stoddart, J. F. *Proc. Natl. Acad. Sci. USA* **2010**, *107*, 13991; (b) Stoddart, J. F. *Chem. Soc. Rev.* **2009**, *38*, 1802; (c) Zhao, Y.-L.; Trabolsi, A.; Stoddart, J. F. *Chem. Commun.* **2009**, 4844; (d) Spruell, J. M.; Paxton, W. F.; Olsen, J.-C.; Benítez, D.; Tkatchouk, E.; Stern, C. L.; Trabolsi, A.; Friedman, D. C.; Goddard, W. A. III; Stoddart, J. F. *J. Am. Chem. Soc.* **2009**, *131*, 11571; (e) Ramos, S.; Alcalde, E. Stoddart, J. F.; White, A. J. P.; Williams, D. J.; Pérez-García, L. *New J. Chem.* **2009**, *33*, 300; (f) Cao, D.; Amelia, M.; Klivansky, L. M.; Koshkakarayan, G.; Khan, S. I.; Semeraro, M.; Silvi, S.; Venturi, M.; Credi, A.; Liu, Y. *J. Am. Chem. Soc.* **2010**, *132*, 1110; (g) Li, S.; Liu, M.; Zheng, B.; Zhu, K.; Wang, F.; Li, N.; Zhao, X.-L.; Huang, F. *Org. Lett.* **2009**, 3350; (h) Liu, M.; Li, S.; Zhang, M.; Zhou, Q.; Wang, F.; Hu, M.; Fronczek, F. R.; Li, N.; Huang, F. *Org. Biomol. Chem.* **2009**, *7*, 1288; (i) Blanco, V.; Abella, D.; Pía, E.; Platas-Iglesias, C.; Peinador, C.; Quintela, J. M. *Inorg. Chem.* **2009**, *48*, 4098; (j) Koshkakarayan, G.; Parimal, K.; He, J.; Zhang, X.; Abliz, Z.; Flood, A. H.; Liu, Y. *Chem. Eur. J.* **2008**, *14*, 10211; (k) Liu, Y.; Bruneau, A.; He, J.; Abliz, Z. *Org. Lett.* **2008**, *10*, 765; (l) Raehm, L.; Hamilton, D. G.; Sanders, J. K. M. *Synlett* **2002**, *11*, 1743; (m) Hansen, J. G.; Feeder, N.; Hamilton, D. G.; Gunter, M. J.; Becher, J.; Sanders, J. K. M. *Org. Lett.* **2000**, *2*, 449; (n) Zheng, Q.; Hamilton, D. G.; Feeder, N.; Teat, S. J.; Goodman, J. M.; Sanders, J. K. M. *New J. Chem* **1999**, *23*, 897; (o) Hamilton, D. G.; Prodi, L.; Feeder, N.; Sanders, J. K. M. *J. Chem. Soc., Perkin Trans. 1* **1999**, 1057.

5. Cubberley, M. S.; Iverson, B. L. *J. Am. Chem. Soc.* **2001**, *123*, 7560.

6. (a) Wang, W.; Wang, L.; Palmer, B. J.; Exarhos, G. J.; Li, A. D. Q. *J. Am. Chem. Soc.* **2006**, *128*, 11150. (b) Murase, T.; Otsuka, K.; Fujita M. *J. Am. Chem. Soc.* **2010**, *132*, 7864.

7. For other examples of unconventional donor-acceptor architectures, see: (a) Peinador, C.; Blanco, V.; Quintela, J. M. *J. Am. Chem Soc.* **2009**, *131*, 920; (b) Blanco, V.; Chas, M.; Abella, D.; Peinador, C.;

Quintela, J. M. *J. Am. Chem. Soc.* **2007**, *129*, 13978; (c) Chas, M.; Blanco, V.; Peinador, C.; Quintela, J. M. *Org. Lett.* **2007**, *9*, 675.

8. (a) Au-Yeung, H. Y.; Pantoş, G. D.; Sanders, J. K. M. *J. Org. Chem.* **2011**, *76*, 1257; (b) Au-Yeung, H. Y.; Pantoş, G. D.; Sanders, J. K. M. *Angew. Chem. Int. Ed.* **2010**, *49*, 5331; (c) Au-Yeung, H. Y.; Pantoş, G. D.; Sanders, J. K. M. *J. Am. Chem. Soc.* **2009**, *131*, 16030; (d) Au-Yeung, H. Y.; Pantoş, G. D.; Sanders, J. K. M. *Proc. Natl. Acad. Sci. USA.* **2009**, *106*, 10466.

9. (a) Herrmann, A. *Org. Biomol. Chem.* **2009**, *7*, 3195; (b) Ladame, S. *Org. Biomol. Chem.* **2008**, *6*, 219; (c) Lehn, J.-M. *Chem. Soc. Rev.* **2007**, *36*, 151; (d) Rozenman, M. M.; McNaughton, B. R.; Liu, D. R. *Curr. Opin. Chem. Biol.* **2007**, *11*, 259; (e) Corbett, P. T.; Leclaire, J.; Vial, L.; West, K. R.; Wietor, J.-L.; Sanders, J. K. M.; Otto, S. *Chem. Rev.* **2006**, *106*, 3652; (f) de Bruin, B.; Hauwert, P.; Reek, J. N. H. *Angew. Chem. Int. Ed.* **2006**, *45*, 2660.

10. Other examples of catenane discovery from DCLs: (a) Chung, M.-K.; White, P. S.; Lee, S. J.; Gagné, M. R. *Angew. Chem. Int. Ed.* **2009**, *48*, 8683; (b) West, K. R.; Ludlow, R. F.; Corbett, P. T.; Besenius, P.; Mansfeld, F. M.; Cormack, P. A.G.; Sherrington, D. G.; Goodman, J. M.; Stuart, M. C. A.; Otto, S. *J. Am. Chem. Soc.* **2008**, *130*, 12218; (c) Lam, R. T. S.; Belenguer, A.; Roberts, S. L.; Naumann, C.; Jarrosson, T.; Otto, S.; Sanders, J. K. M. *Science* **2005**, *308*, 667.

11. (a) Fujita, M.; Ibukuro, F.; Hagihara, H.; Ogura, K. *Nature* **1994**, *367*, 720; (b) Fujita, M.; Ibukuro, F.; Ogura, K. *J. Am. Chem. Soc.* **1995**, *117*, 4175.

12. (a) Au-Yeung, H. Y.; Cougnon, F. B. L.; Pantoş, G. D.; Sanders, J. K. M. *Chem. Sci.* **2010**, 567; (b) Au-Yeung, H. Y.; Pengo, P.; Pantoş, G. D.; Otto, S.; Sanders, J. K. M. *Chem. Commun.* **2009**, 419.

CHAPTER 3

Templated Dynamic Synthesis of a [3]Catenane

The self-assembly of a water-soluble [3]catenane from a library composed exclusively of linear building blocks is described. This process is promoted by a high salt concentration (1 M NaNO₃). Even more remarkably, the synthesis is improved if the salt, which raises the ionic strength and encourages hydrophobic association, is replaced by a sub-mM concentration of spermine acting as a template. The spermine-templated synthesis of the [3]catenane shows for the first time that such structures can exhibit strong binding interactions with a biologically relevant target, in water under near-physiological conditions.

This work was initiated in collaboration with an undergraduate student, Nicholas A. Jenkins.

3.1. Introduction

3.1.1. Synthesis of donor-acceptor [3]catenanes

Although of potential interest in the context of nanoscience,¹ donor-acceptor [3]catenanes have remained relatively unexplored because of their challenging synthesis. Stoddart *et al.* showed that donor-acceptor interactions could be efficiently used to reversibly assemble preformed macrocycles into the thermodynamically more stable [3]catenane (Figure 3.1).^{2a, b}

This approach is not trivial: careful design of the size and geometry of the rings is necessary and, while the assembly of the catenane is nearly quantitative, the synthesis of each of the rings involves a series of delicate steps, ultimately leading to an overall low yield. Apart from a few variations and improvements to the method developed by the Stoddart group, these constraints have made examples of donor-acceptor [3]catenanes rare in the literature.²⁻⁴

3.1.2. Dynamic combinatorial synthesis: from [2] to [3]catenanes

Chapter 2 illustrates that dynamic combinatorial chemistry⁵ can lead to an unexpected variety of donor-acceptor [2]catenanes.^{6, 7} To investigate the possibility of forming higher order interlocked structures through dynamic combinatorial chemistry, we designed building block **4-A**, composed of two large hydrophobic NDI electron-deficient π -systems, connected *via* a flexible butyl chain (Figure 3.2). The notation **4-A** refers to the four CH₂ of the butyl chain linking the acceptor units, and will be generalised in the next Chapter to a whole series of acceptor building blocks.

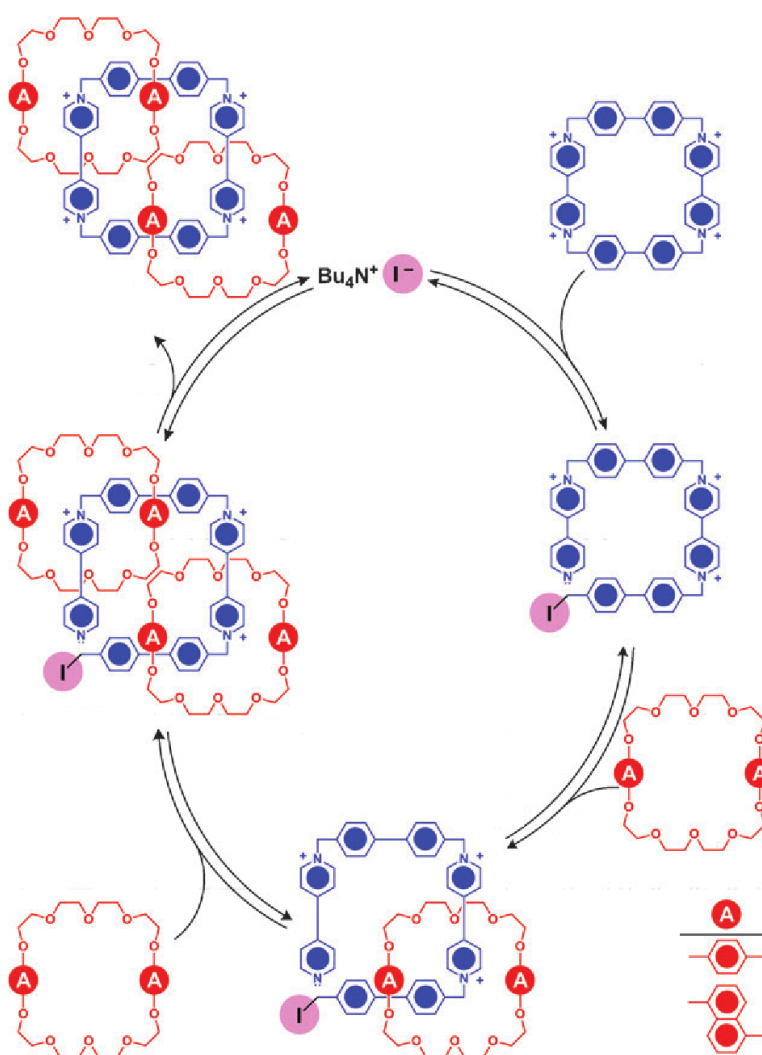


Figure 3.1. Iodine-catalysed reversible self-assembly of a donor-acceptor [3]catenane (Stoddart).^{2a}

Building block **4-A** is terminated by two cysteine components which, once again, provide both the thiol necessary for disulfide exchange and carboxylate anions for water solubility. It was synthesised in three steps, involving the mono-substitution of the 1,4,5,8-naphthalenetetracarboxylic dianhydride with the trityl protected cysteine,⁸ reaction with 1,4-diaminobutane, and deprotection of the trityl protecting groups (Scheme 3.1). **4-A** was synthesised for the first time by Nicholas A. Jenkins, undergraduate student.

The objective was to explore its behaviour in the presence of the electron-rich dialkoxynaphthalene building block **D2a**, which has been thoroughly studied in Chapter 2: **D2a** forms a [-D-D-] dimer whose cavity size is best suited to interact with an acceptor moiety, favoring the formation of an alternating DAD stack.^{6a, d}

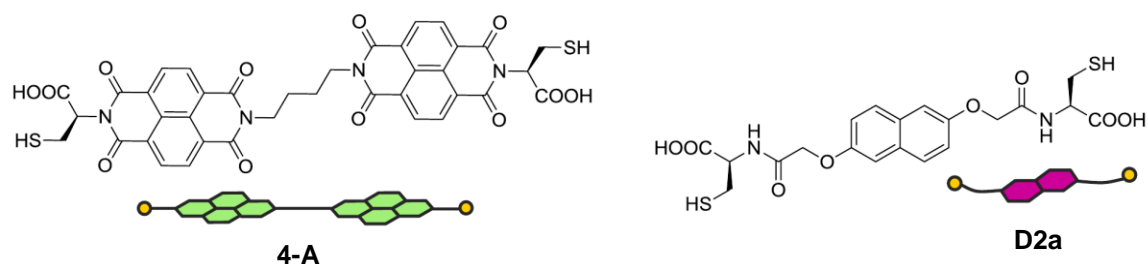
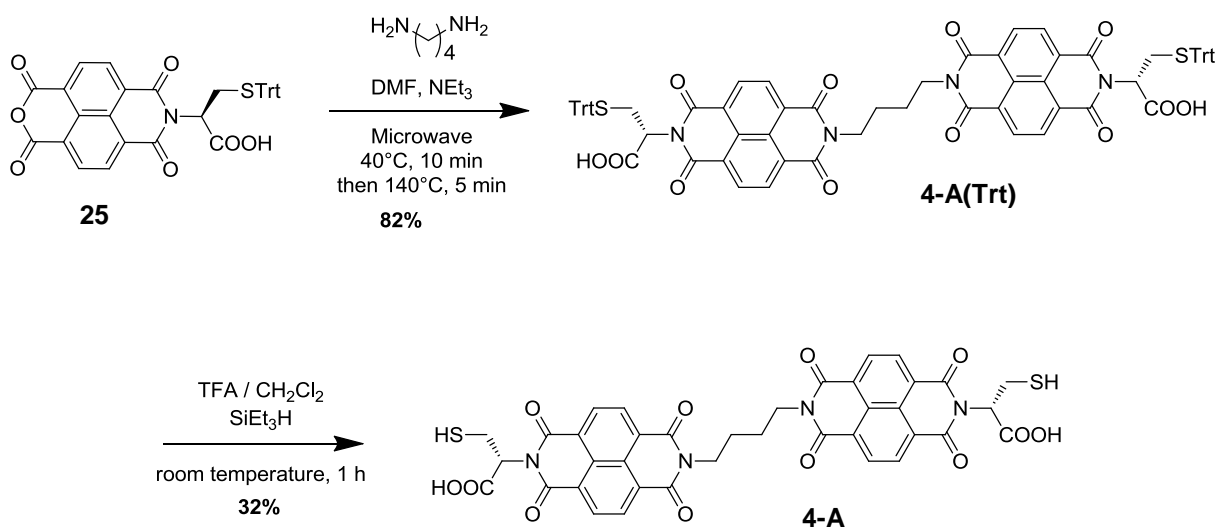


Figure 3.2. Building blocks used in this Chapter and their cartoon representations.



Scheme 3.1. Synthetic route to building block **4-A**.

3.2. Discovery of the first [3]catenane

The first library was prepared by dissolving **4-A** and **D2a** to a total concentration of 5 mM (1:2 molar ratio) in water at pH 8 in the presence of 1 M NaNO₃, as the formation of catenanes is known^{6,9} to be promoted upon addition of salt. The library was stirred for one day under air in capped vials to allow oxidation of the thiol building blocks.

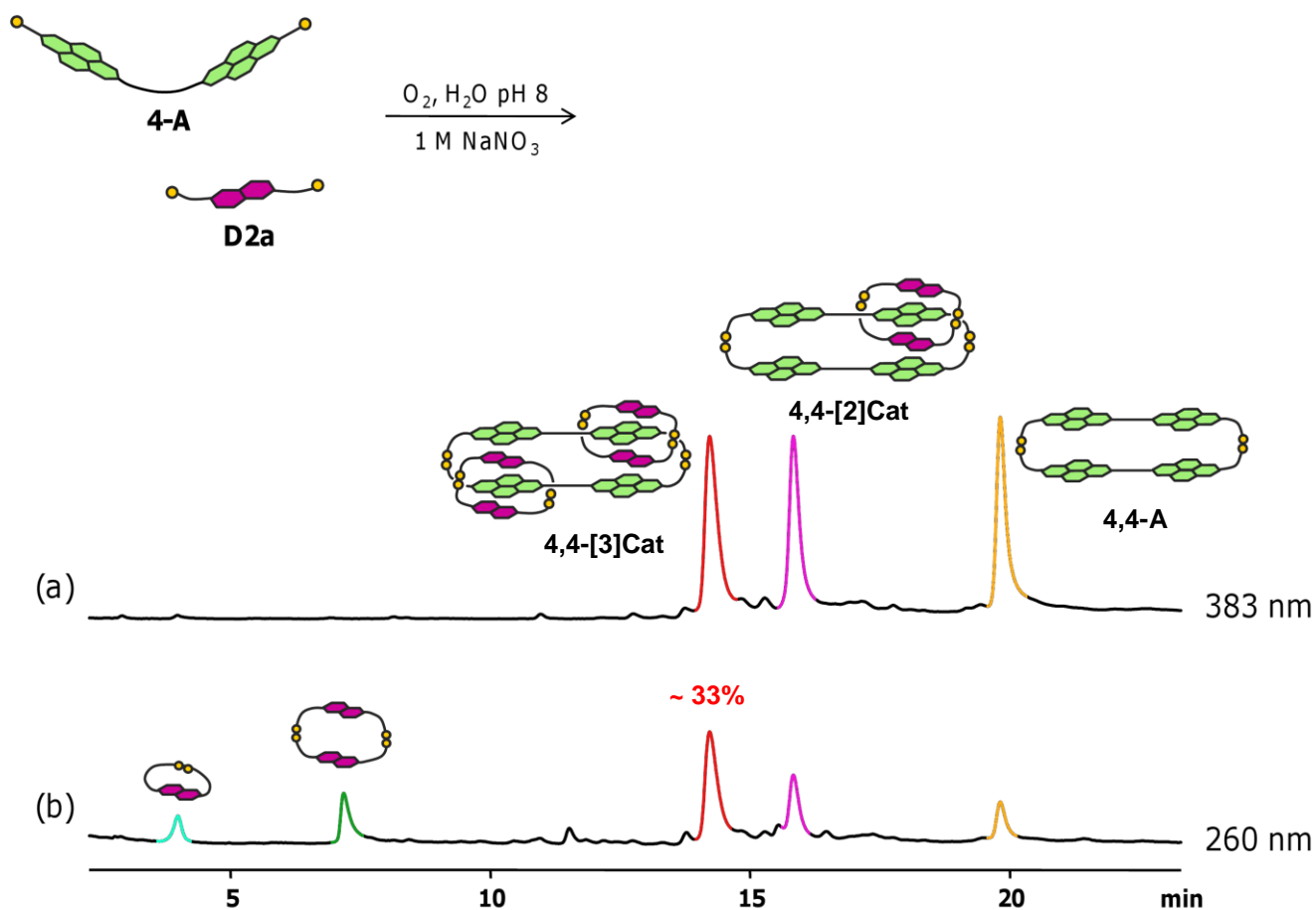


Figure 3.3. HPLC analysis of an aqueous library composed of **4-A** and **D2a** (1:2 molar ratio, 5 mM total), in the presence of 1 M of NaNO₃. Absorbance was recorded at (a) 383 nm and (b) 260 nm.

Far from the diversity expected from such flexible building blocks, LC-MS analysis revealed that the fully oxidised library contains a relatively small number of significant components. The only detectable members of this library are the closed monomer [-D2a-], the donor [-D2a-D2a-] and acceptor **4,4-A** dimers, as well as two catenanes composed of one and two donor dimers interlocked with an acceptor dimer, **4,4-[2]Cat** and **4,4-[3]Cat** respectively (Figure 3.3). The **4,4-** notation was chosen to indicate that these structures are based on the macrocycle composed of two acceptor building blocks **4-A**.

Both catenanes were unambiguously identified by tandem ESI-MS and MS/MS. The [3]catenane displays doubly and triply charged molecular ions (m/z 1752.5 and 1167.8), corresponding to a species composed of two acceptor and four donor building blocks (Figure 3.4.a).

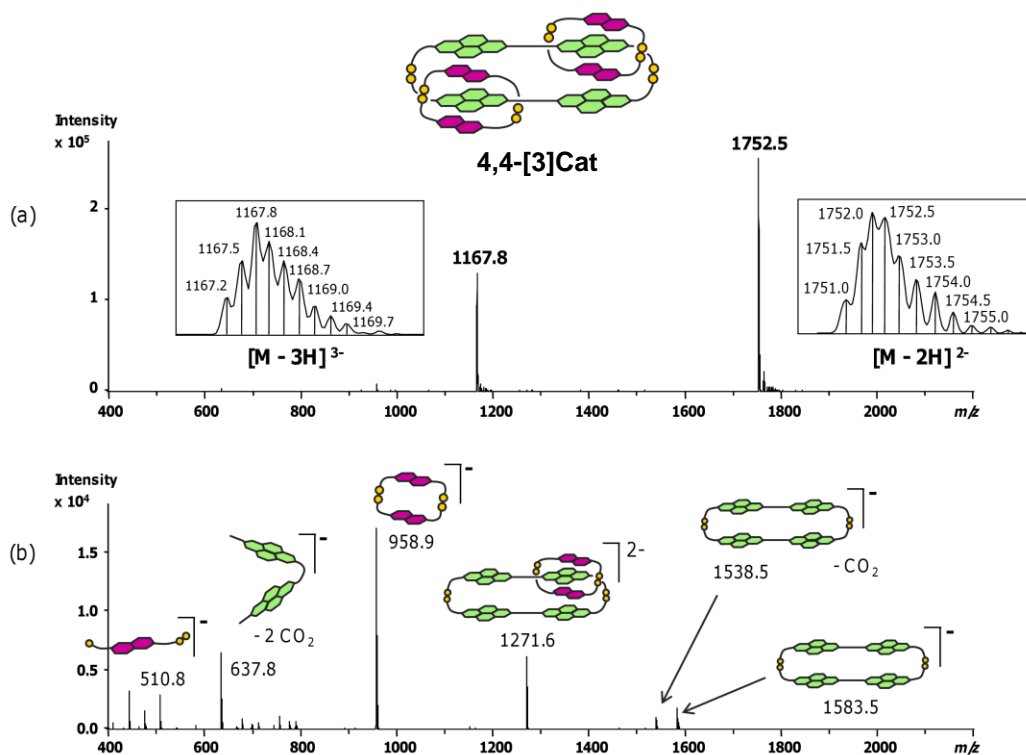


Figure 3.4. Tandem (a) MS and (b) MS/MS fragmentation of **4,4-[3]Cat**. The yellow cartoon dots represent the sulfur atoms of the cysteine.

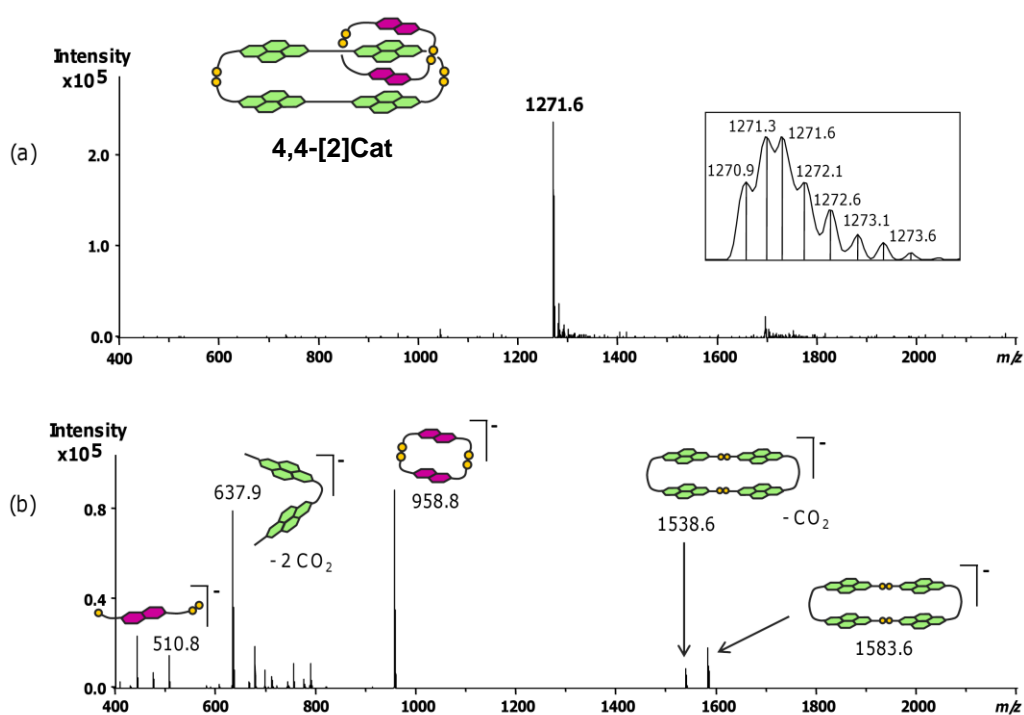


Figure 3.5. Tandem (a) MS and (b) MS/MS fragmentation of **4,4-[2]Cat**. The yellow cartoon dots represent the sulfur atoms of the cysteine.

Its fragmentation pattern is characteristic of that expected for a [3]catenane, with the loss of one or both rings producing the intermediate **4,4-[2]Cat** (m/z 1271.6, doubly charged), dimers **4,4-A** (m/z 1583.5) and **[-D2a-D2a-]** (m/z 958.9), and smaller fragments (Figure 3.4.b). A similar fragmentation pattern was observed for **4,4-[2]Cat** (Figure 3.5).

The presence of **4,4-[2]Cat** along with remaining non-interlocked dimers, suggested that the library is fully oxidized before thermodynamic equilibrium is reached. This hypothesis is consistent with previous observations^{6a} and was confirmed by a series of kinetic analyses.

3.3. Investigating the mechanism of formation of 4,4-[3]Cat

The kinetics of a library in a 1:1 molar ratio (Figure 3.6 and 3.7) was studied in order to compare the rates of oxidation of building blocks **4-A** and **D2a**.

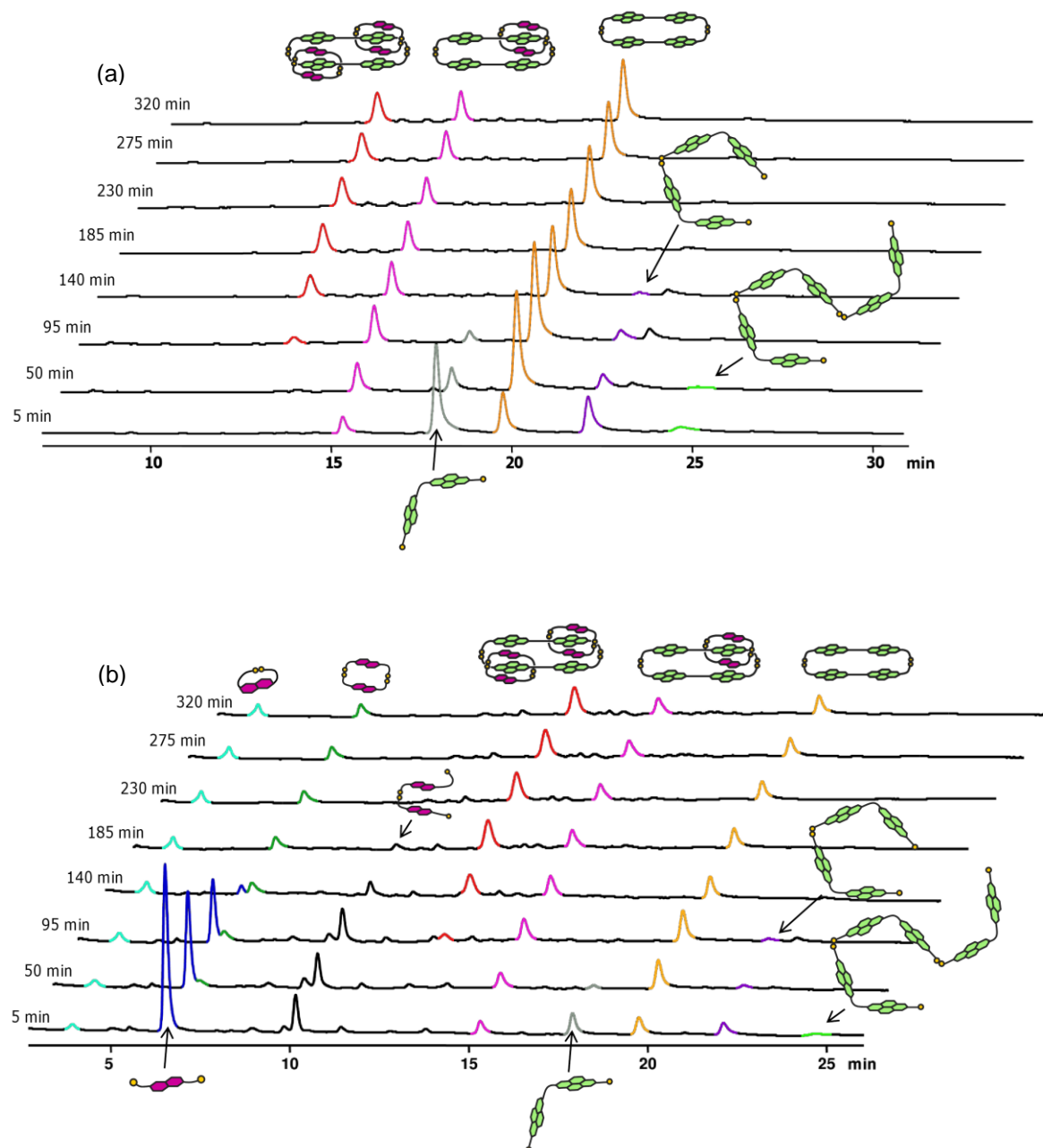


Figure 3.6. LC-MS analysis of a library composed of **4-A** and **D2a** (5mM total, 1:1 molar ratio) at different time intervals. Absorbance was monitored at (a) 383 nm and (b) 260 nm.

This study showed that the acceptor **4-A** oxidises faster than donor **D2a** (Figure 3.7.a), rapidly forming the acceptor dimer **4,4-A**. Although the rate of oxidation of the thiols should be similar for the two building blocks, it is perhaps not surprising that favourable hydrophobic and π - π interactions¹⁰ make the formation of **4,4-A** a pseudo-intramolecular process and therefore faster, unlike the electron-rich and hence unfavourable donor dimer.

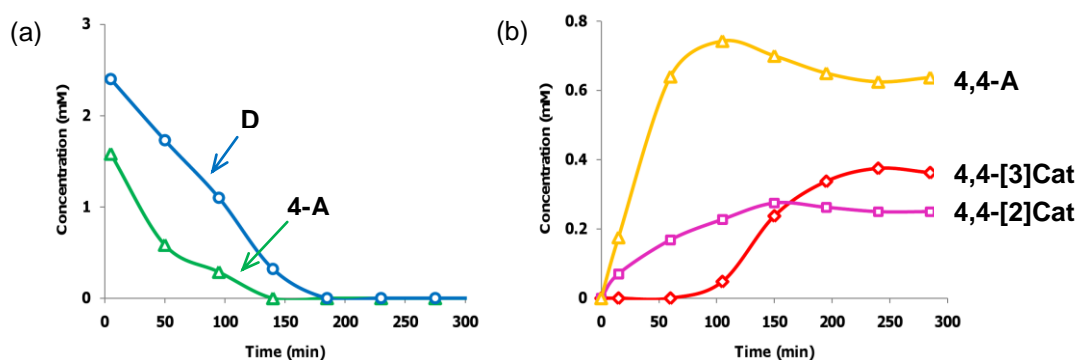


Figure 3.7. Kinetic profile (a) of the consumption of building block **4-A** (Δ) and **D2a** (\circ), and (b) of the formation of **4,4-A** (Δ), **4,4-[2]Cat** (\square) and **4,4-[3]Cat** (\diamond) in a library composed of **4-A** and **D2a** (5 mM total, 1:1 molar ratio) in water pH 8, in the presence of 1 M NaNO_3 . The concentrations were evaluated by HPLC from the peak areas of the traces shown in Figure 3.6.

Strikingly, the two building blocks do not form any mixed macrocycles, which may be rationalised by their difference in size, and the likely templation through donor-acceptor interactions of the acceptor dimer by the donor units and conversely of the donor dimer by the acceptor units. The kinetic profiles of the formation of **4,4-A**, **4,4-[2]Cat** and **4,4-[3]Cat** (Figure 3.7.b) show that the acceptor dimer **4,4-A** is threaded by two open donor dimers consecutively, forming **4,4-[2]Cat** and **4,4-[3]Cat** successively (Figure 3.8).

From this study, we concluded that the formation of the [3]catenane appears to be a stepwise process, and the library evolves until all the donor building block is fully oxidized, preventing thermodynamic equilibrium from being reached. If the disulfide exchange were to occur for a longer period of time to allow the system to reach thermodynamic equilibrium, the unthreaded residues should be recycled into **4,4-[3]Cat**, which is a kinetic trap, and may also be the thermodynamic product in this library.

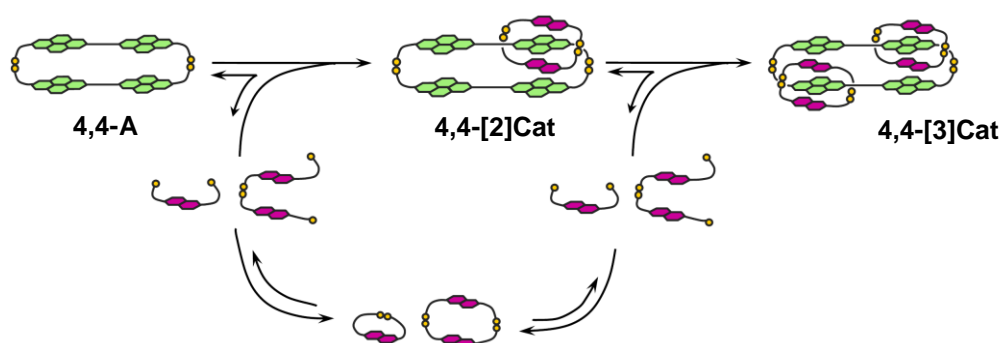


Figure 3.8. Proposed mechanism of formation of **4,4-[3]Cat**, involving the successive formation of **4,4-A**, **4,4-[2]Cat** and finally **4,4-[3]Cat**.

Consequently, the formation of the [3]catenane is limited both by the fast rate of thiol oxidation which prevents the library to reach thermodynamic equilibrium, and by the kinetic competition between the formation of the unthreaded and the threaded macrocycles.

3.4. Stepwise addition of one of the building blocks

To test this supposition, we investigated the effect of successive additions of the fresh thiol **D2a**, which reinitiates the reversible process and favours threading by providing a high acceptor/donor ratio. Two equivalents of **D2a** were added in aliquots of 0.5 equivalents every two hours to a library containing the

acceptor **4-A**. As expected, the yield of the [3]catenane increased, from 33% (one-pot procedure, Figure 3.3.a) up to 55% (stepwise procedure, Figure 3.9), with the final ratio between the building blocks equal in both cases.

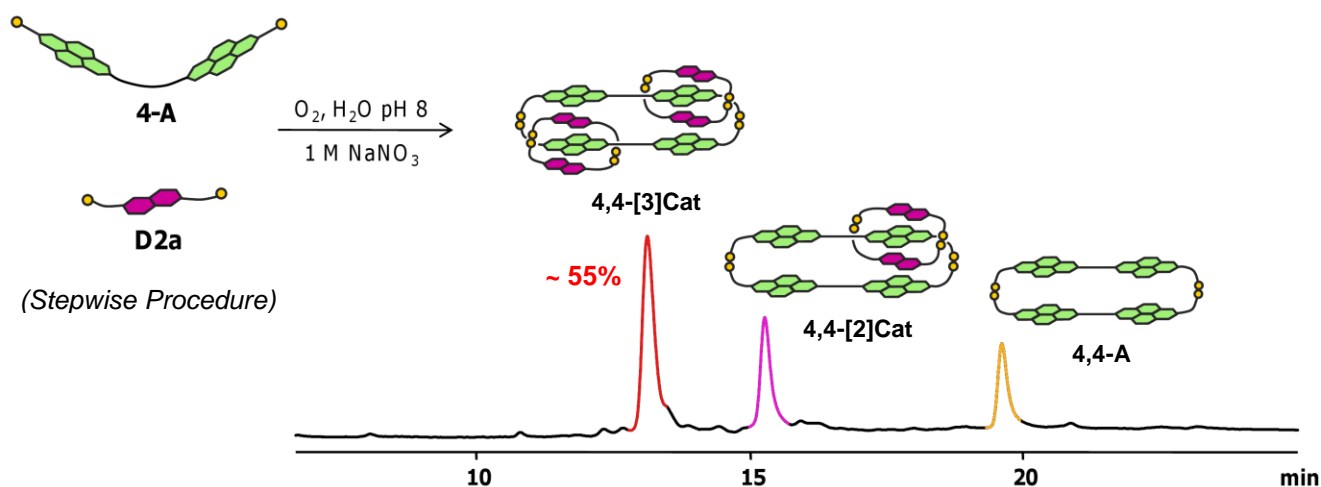


Figure 3.9. HPLC analysis of an aqueous library composed of **4-A** and **D2a** (1:2 molar ratio, 5 mM total), in the presence of 1 M of NaNO_3 . The two equivalents of **D2a** were added in fractions of 0.5 equivalents every two hours (stepwise procedure). Absorbance was recorded at 383 nm.

Unfortunately, increasing further the number of successive additions (0.25 equivalent added every two hours), or changing the time between the additions did not lead to any improvement of the [3]catenane yield, most likely due to the low overall concentration of free thiols slowing the exchange kinetics.

3.5. ^1H NMR characterisation of 4,4-[3]Cat

All the significant library members have been isolated and characterized by ^1H NMR (500 MHz, 298 K, D_2O). Macrocycle **4,4-A** and catenane **4,4-[2]Cat** display the very broad resonances characteristic of

flexible macrocycles.¹¹ The NMR behaviour of this type of large structure will be described in more detail in Chapter 4.

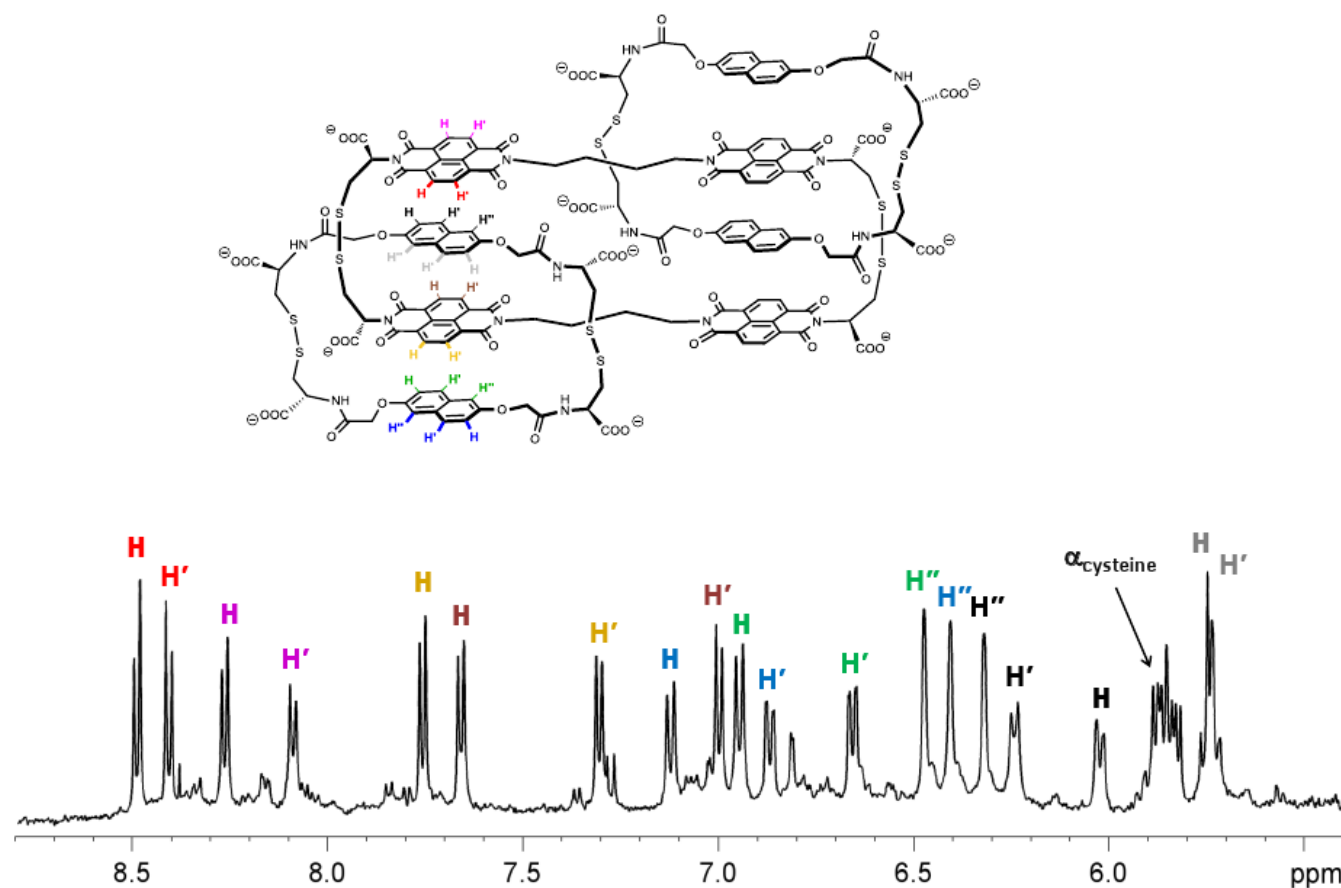


Figure 3.10. Partial ^1H NMR spectrum (D_2O , 298 K, 500 MHz) of **4,4-[3]Cat**. The solvent peak was referenced at 4.79 ppm.

On the other hand, the [3]catenane exhibits a spectrum with sharp signals in which the resonances for a single asymmetric conformation can be clearly identified by 1D (Figure 3.10) and 2D NMR (Figure 3.11): two sets of signals were assigned to the outer (8.1 to 8.6 ppm) and inner (6.9 to 7.8 ppm) acceptor

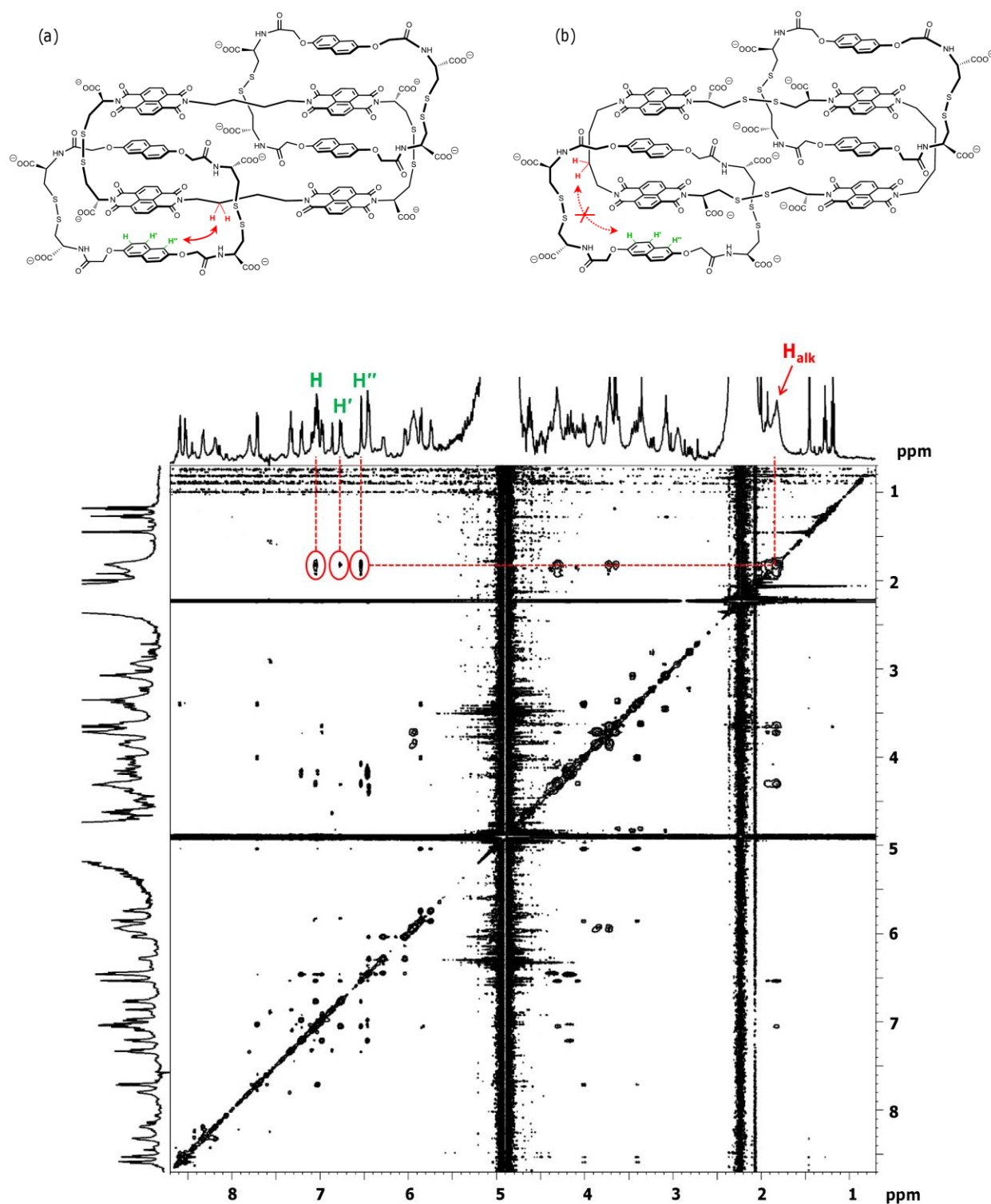


Figure 3.12. Full NOESY spectrum of 4,4-[3]Cat (D_2O , 288 K, 500 MHz, mixing time = 800 ms), highlighting the nOe correlation between the protons of the alkyl chain (H) and one of the outer donor unit (H'). From the two possible conformations of 4,4-[3]Cat represented on the top, only conformation (a) is likely to exhibit such nOe. The solvent peak was referenced at 4.79 ppm.

Amongst all the conformations that **4,4-[3]Cat** could potentially adopt, the two conformations (a) and (b) drawn in Figure 3.12 are the most likely to be found in solution. However, the NMR spectrum of **4,4-[3]Cat** shows the presence of only one conformation. The nOe correlations highlighted in the full NOESY spectrum in Figure 3.12, between the outer donors (**H**) and the protons of the aliphatic chain (**H**), suggest a close proximity which is only possible in conformation (a). Both conformations (a) and (b) can be found for larger and more flexible [3]catenanes (see Chapter 4). We attribute the fact that **4,4-[3]Cat** adopts only conformation (a) to its compact nature.

3.6. Amplification of 4,4-[3]Cat with spermine

Figure 3.13 summarises the results described in the first part of this Chapter. The first LC-MS traces show the library composed of **4-A** and **D2a** in water pH 8 in the absence of salt, recorded at (a) 260 nm and (b) 383 nm. The catenane synthesis described above appears to rely on the increased polarity of the reaction medium (1 M NaNO₃ *versus* pure water) to promote the burying of solvent-exposed hydrophobic surfaces.^{6, 9} In a salt-free reaction, **4,4-[3]Cat** is formed only in trace amounts, and the library is dominated by the homodimers **4,4-A₂** and **D₂**. Figure 3.13.c shows the same library prepared in the presence of 1 M NaNO₃, and the corresponding amplification of **4,4-[3]Cat** up to 33% (LC-MS recorded at 383 nm). As mentioned before, stepwise addition of **D2a** favours the formation of the [3]catenane, and its yield increases up to 55% (Figure 3.13.d, LC-MS recorded at 383 nm)

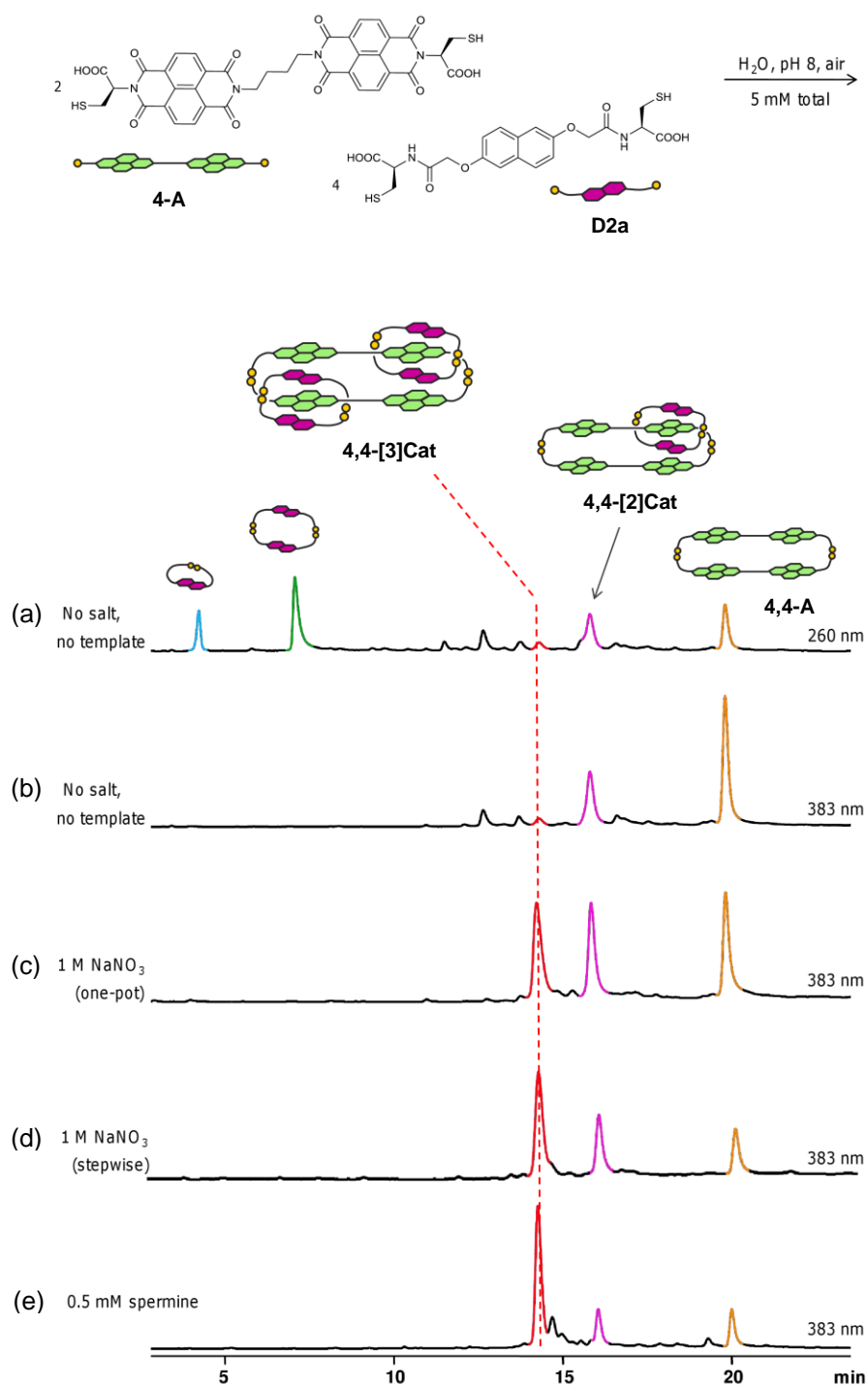


Figure 3.13. HPLC analysis of an aqueous library composed of **4-A** and **D2a** (1:2 molar ratio, 5 mM total), in the absence of NaNO_3 , recorded at (a) 383 nm and (b) 260 nm. The same library was prepared in presence of 1 M of NaNO_3 , (c) in one-pot or (d) after stepwise addition of **D2a** (absorbance recorded at 383 nm). (e) The library was also prepared in the presence of 0.5 mM of spermine (absorbance recorded at 383 nm).

Of all the library members observed in this system, the [3]catenane possesses the highest density of carboxylate groups, raising the question of whether a suitable polycation might act as a template. In Nature, polyamines such as spermine bind to the array of negative charges of the DNA backbone and play an important role in many cellular processes,¹³ prompting the development of artificial spermine binders.¹⁴ To our delight, addition of merely 0.5 mM of spermine promoted the amplification of **4,4-[3]Cat** to 60 % yield (Figure 3.13.e, LC-MS recorded at 383 nm), suggesting a strong interaction between the [3]catenane and spermine. Increasing the concentration of template does not further increase the yield of [3]catenane: it is well documented and understood, but counterintuitive, that adding too much template can lead to amplification of smaller, weaker binding receptors.¹⁵

3.7. Amplification of 4,4-[3]Cat with other polyamines

No amplification was observed in the presence of up to 1 M of NH_4Cl , implying (a) that the interaction between **[3]Cat** and spermine results from more than the sum of random carboxylate-ammonium interactions and (b) that the effect of metal salts such as NaNO_3 may be due to more than purely ionic strength effects.

The geometrical distribution, hydrophobicity and number of ammonium centres present in the polyamine are crucial for an efficient recognition as demonstrated by libraries templated by the shorter spermidine and putrescine, in which **4,4-[3]Cat** was amplified to lesser extent (Figure 3.14).

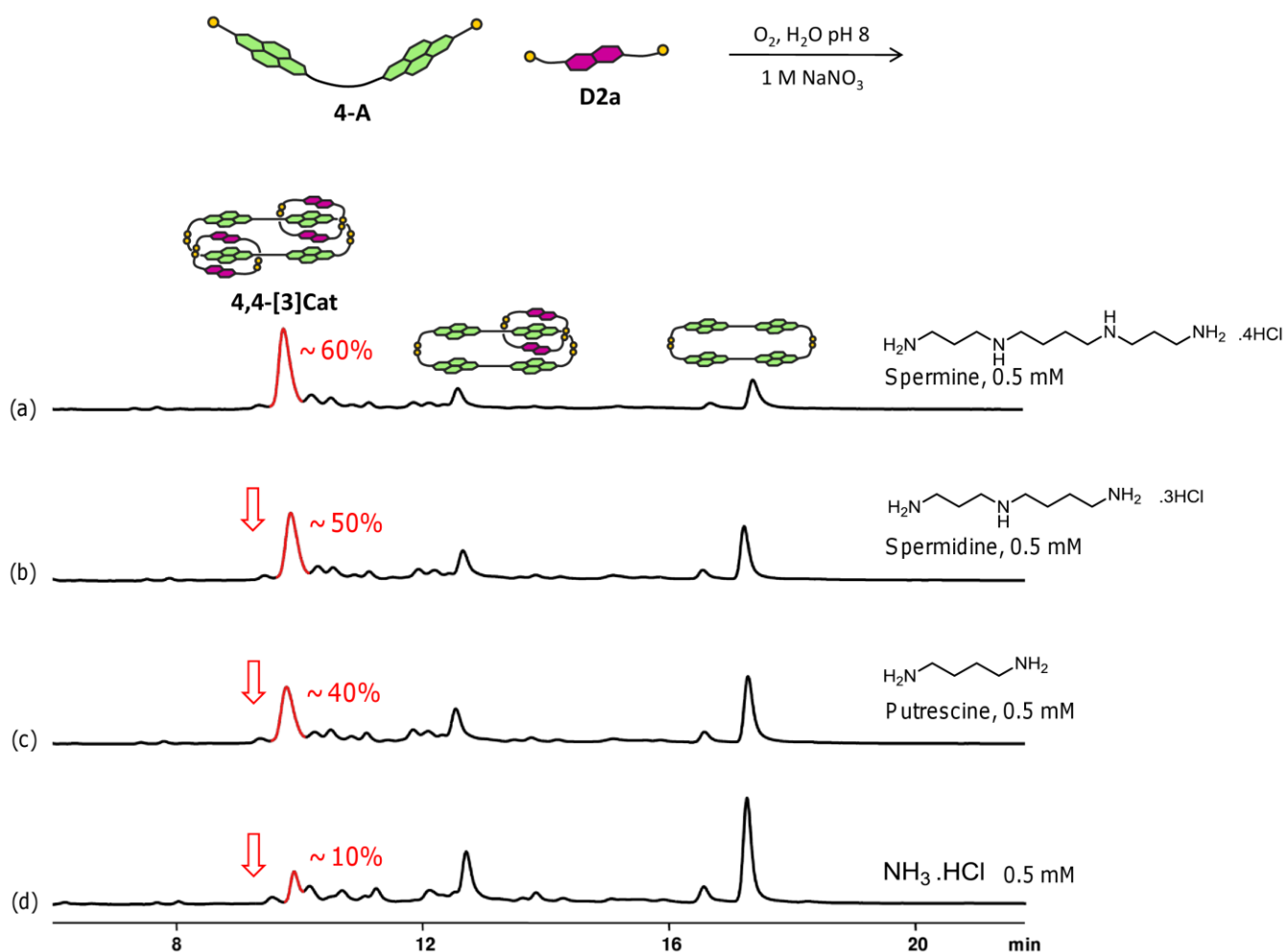


Figure 3.14. HPLC analyses of an aqueous library composed of 4-A and D2a (1:2 molar ratio, 5 mM total), in the presence of 0.5 mM of (a) spermine, (b) spermidine, (c) putrescine, and (d) NH_4Cl . Absorbance was recorded at 383 nm.

3.8. 1H NMR titration of 4,4-[3]Cat with spermine

The 4,4-[3]Cat binds spermine with an association constant of $(1.1 \pm 0.005) \times 10^5 M^{-1}$ as determined by 1H NMR titration experiments, confirming the strong interaction between the two species (Figure 3.15 and 3.16, the determination of the association constant was executed by Dr Dan Pantoş).

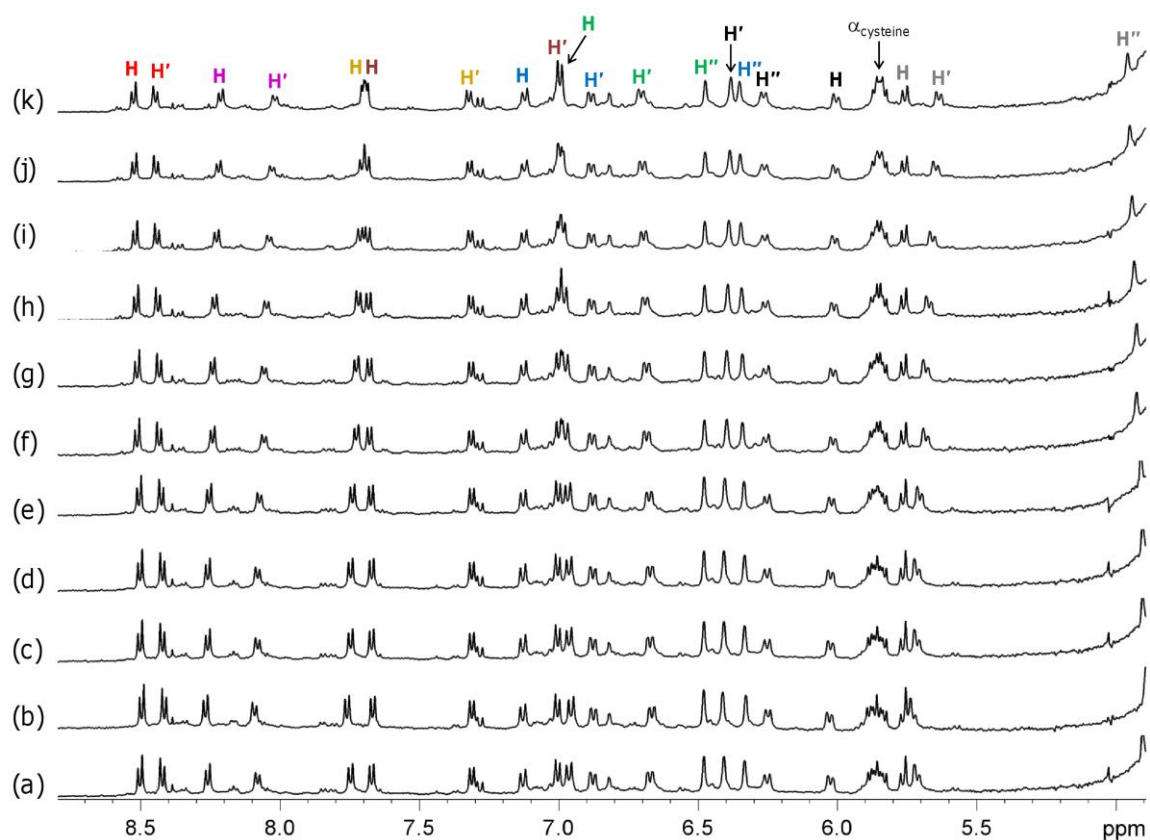


Figure 3.15. Partial ^1H NMR spectrum (D_2O , 500 MHz) of $[3]\text{Cat}$ upon addition of spermine. The solvent peak was referenced at 4.79 ppm at 298 K. Equivalents of spermine (a) 0.00, (b) 0.09 (c) 0.17 (d) 0.35 (e) 0.52 (f) 0.69 (g) 0.87 (h) 1.04 (i) 1.22 (j) 1.39 (k) 1.56.

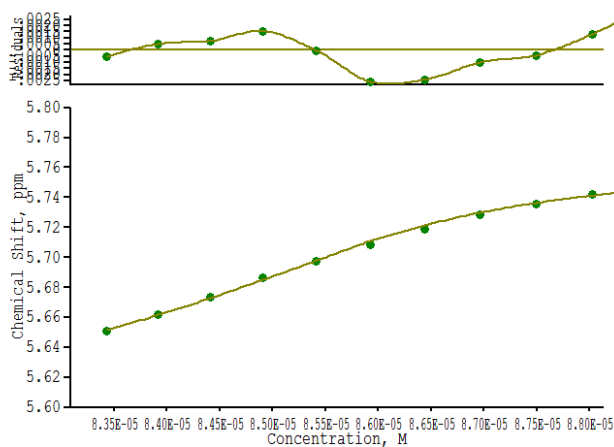


Figure 3.16. Non-linear fitting using WinEQNMR v. 2.0 of the titration of $4,4-[3]\text{Cat}$ with spermine.

Modeling,¹⁶ also performed by Dr Dan Pantoş, suggests that the aromatic moieties of the [3]catenane are too closely packed to accommodate a cavity large enough for spermine (Figure 3.17), so the template probably binds to the solvent-accessible surface of the catenane, interacting with the arrayed carboxylate ions in a manner reminiscent of its interactions with the phosphate groups of double helical DNA.

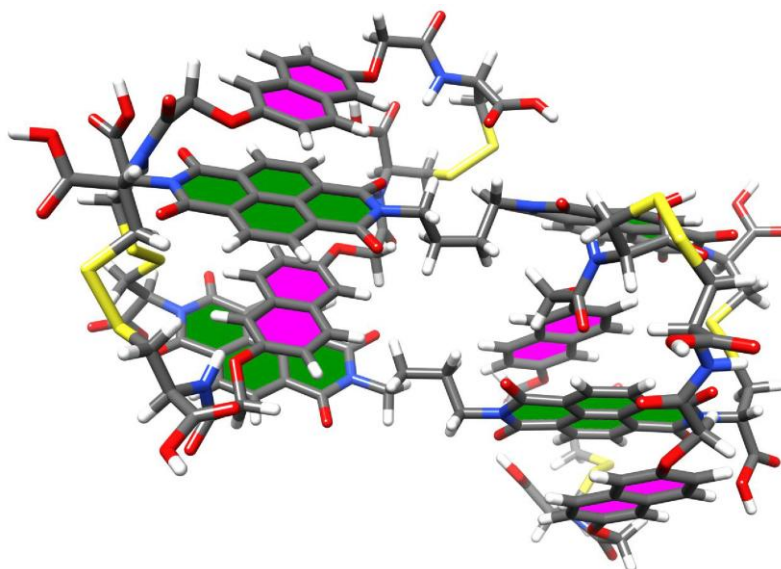


Figure 3.17. Modeling of 4,4-[3]Cat.¹⁶

3.9. Conclusion

To conclude, this work shows for the first time that acyclic units can spontaneously self-assemble into a donor-acceptor [3]catenane, either in a high polarity medium or in the presence of spermine. The amplification of the [3]catenane in the presence of spermine highlights the importance of small template molecules in the controlled assembly of large complex structures, through a multitude of seemingly weak interactions in a highly competitive medium. This work brings a new insight into the mechanism of donor-acceptor self-assembly and provides an alternative route to the efficient synthesis of

[3]catenanes. The formation of this catenane is not fully under thermodynamic control, so kinetic parameters also play a role in this process. To limit the formation of competing species, we have therefore developed a *stepwise dynamic* approach, moving away from pure dynamic combinatorial chemistry, in which the exchange continuously occurs. This approach involves the idea of an evolutionary process, with iterated cycles of selection and amplification, which is closer to the phenomena observed in biological systems.⁵

The principles developed here can be extended to access larger structures than [3]catenanes, by using building blocks containing more than one acceptor and/or donor units. This work is considered as being the first step towards the self-assembly of more complex polycatenanes.

References:

1. Sauvage, J. P.; Gaspard, P. *From Non-Covalent Assemblies to Molecular Machines*, Wiley-VCH, Weinheim, 2010.
2. (a) Patel, K.; Miljanić, O. Š.; Stoddart, J. F.; *Chem. Commun.* **2008**, 1853; (b) Ashton, P. R.; Brown, C. L.; Chrystal, E. J. T.; Goodnow, T. T.; Kaifer, A. E.; Parry, K. P.; Slawin, A. M. Z.; Spencer, N.; Stoddart, J. F.; Williams, D. J. *Angew. Chem. Int. Ed.* **1991**, *30*, 1039; (c) Coskun, A.; Spruell, J. M.; Barin, G.; Fahrenbach, A. C.; Forgan, R. S.; Colvin, M. T.; Carmieli, R.; Benítez, D.; Tkatchouk, E.; Friedman, D. C.; Sarjeant, A. A.; Wasielewski, M. R.; Goddard III, W. A.; Stoddart, J. F. *J. Am. Chem. Soc.* **2011**, *133*, 4538; (d) Spruell, J. M. et al. *Nature Chem.* **2010**, *2*, 870; (e) Ashton, P. R.; Boyd, S. E.; Claessens, C. G.; Gillard, R. E.; Menzer, S.; Stoddart, J. F.; Tolley, M. S.; White, A. J. P.; Williams, D. *J. Chem. Eur. J.* **1997**, 788.
3. (a) Blanco, V.; Chas, M.; Abella, D.; Peinador, C.; Quintela, J. M. *J. Am. Chem. Soc.* **2007**, *129*, 13978; (b) Chas, M.; Blanco, V.; Peinador, C.; Quintela, J. M. *Org. Lett.* **2007**, *9*, 675; (c) Hubbard, A. L.; Davidson, G. J. E.; Patel, R. H.; Wisner, J. A.; Loeb, S. J. *Chem. Comm.* **2004**, 138; (d) Hamilton, D. G.; Feeder, N.; Teat, S. J.; Sanders, J. K. M. *New J. Chem.* **1998**, 1019; (e) Hamilton, D. G.; Feeder, N.; Prodi, L.; Teat, S. J.; Clegg, W.; Sanders, J. K. M. *J. Am. Chem. Soc.* **1998**, *120*, 1096.
4. For other relevant self-assembled [3]catenanes, see Hori, A.; Kumazawa, K.; Kusukawa, T.; Chand, D. K.; Fujita, M.; Sakamoto, S.; Yamaguchi, K. *Chem. Eur. J.* **2001**, *7*, 4142.
5. About dynamic combinatorial chemistry, see: (a) Herrmann, A. *Org. Biomol. Chem.* **2009**, *7*, 3195; (b) Ladame, S. *Org. Biomol. Chem.* **2008**, *6*, 219; (c) Lehn, J.-M. *Chem. Soc. Rev.* **2007**, *36*, 151; (d) Rozenman, M. M.; McNaughton, B. R.; Liu, D. R. *Curr. Opin. Chem. Biol.* **2007**, *11*, 259; (e) Corbett,

- P. T.; Leclaire, J.; Vial, L.; West, K. R.; Wietor, J.-L.; Sanders, J. K. M.; Otto, S. *Chem. Rev.* **2006**, *106*, 3652; (f) de Bruin, B.; Hauwert, P.; Reek, J. N. H. *Angew. Chem. Int. Ed.* **2006**, *45*, 2660.
6. (a) Cougnon, F. B. L.; Au-Yeung, H. Y.; Pantoş, G. D.; Sanders, J. K. M. *J. Am. Chem. Soc.* **2011**, *133*, 3198; (b) Au-Yeung, H. Y.; Pantoş, G. D.; Sanders, J. K. M. *J. Org. Chem.* **2011**, *76*, 1257; (c) Au-Yeung, H. Y.; Pantoş, G. D.; Sanders, J. K. M. *Angew. Chem. Int. Ed.* **2010**, *49*, 5331; (d) Au-Yeung, H. Y.; Pantoş, G. D.; Sanders, J. K. M. *J. Am. Chem. Soc.* **2009**, *131*, 16030; (e) Au-Yeung, H. Y.; Pantoş, G. D.; Sanders, J. K. M. *Proc. Natl. Acad. Sci. USA.* **2009**, *106*, 10466.
7. For other examples of [2]catenane discovery from dynamic combinatorial chemistry: (a) Chung, M.-K.; White, P. S.; Lee, S. J.; Gagné, M. R. *Angew. Chem. Int. Ed.* **2009**, *48*, 8683; (b) West, K. R.; Ludlow, R. F.; Corbett, P. T.; Besenius, P.; Mansfeld, F. M.; Cormack, P. A. G.; Sherrington, D. G.; Goodman, J. M.; Stuart, M. C. A.; Otto, S. *J. Am. Chem. Soc.* **2008**, *130*, 12218; (c) Lam, R. T. S.; Belenguer, A.; Roberts, S. L.; Naumann, C.; Jarrosson, T.; Otto, S.; Sanders, J. K. M. *Science* **2005**, *308*, 667.
8. For the synthesis of asymmetrically substituted 1,4,5,8-naphthalenetetracarboxylic diimides, see: Tambara, K.; Ponnuswamy, N.; Hennrich, G.; Pantoş, G. D. *J. Org. Chem.* **2011**, *76*, 3338.
9. For the use of salt to increase medium polarity, see: a) Fujita, M.; Ibukuro, F.; Hagihara, H.; Ogura, K. *Nature* **1994**, *367*, 720; b) Fujita, M.; Ibukuro, F.; Ogura, K. *J. Am. Chem. Soc.* **1995**, *117*, 4175.
10. Cubberley, M. S.; Iverson, B. L. *J. Am. Chem. Soc.* **2001**, *123*, 7560.
12. Au-Yeung, H. Y.; Pengo, P.; Pantoş, G. D.; Otto, S.; Sanders, J. K. M. *Chem. Commun.* **2009**, 419.
13. (a) Tabor, C. W.; Tabor, H. *Annu. Rev. Biochem.* **1984**, *53*, 749; (b) Igarashi, K.; Kashiwagi, K. *Biochem. Biophys. Res. Commun.* **2000**, *271*, 559.

14. For examples of spermine receptors, see: (a) Pérez-Fernández, R.; Pittelkow, M.; Belenguer, A. M.; Lane, L. A.; Robinson, C. V.; Sanders, J. K. M. *Chem. Commun.* **2009**, 3708; (b) Vial, L.; Ludlow, R. F.; Leclaire, J.; Pérez-Fernández, R.; Otto, S. *J. Am. Chem. Soc.* **2006**, *128*, 10253; (c) Isobe, H.; Tomita, N.; Lee, J. W.; Kim, H. J.; Kim, K.; Nakamura, E. *Angew. Chem. Int. Ed.* **2000**, *39*, 4257; (d) Jeon, Y. M.; Whang, D.; Kim, J.; Kim, K. *Chem. Lett.* **1996**, 503.

15. (a) Severin, K. *Chem. Eur. J.* **2004**, *10*, 2565; Corbett, P. T.; Sanders, J. K. M.; Otto, S. *J. Am. Chem. Soc.* **2005**, *127*, 9390; (b) Corbett, P. T.; Sanders, J. K. M.; Otto, S. *J. Am. Chem. Soc.* **2005**, *127*, 9390.

16. Molecular modelling was performed by Dr Dan Pantoş at PM6 semi-empirical level with MOPAC2009 using the COSMO solvation model. MOPAC2009, James J. P. Stewart, Stewart Computational Chemistry, Colorado Springs, CO, USA, <http://OpenMOPAC.net> (2008).

CHAPTER 4

Versatile Formation of Donor-Acceptor [2] and [3]Catenanes in Water

This work generalises the method developed in Chapter 3 to assemble [3]catenanes, utilising hydrophobic effect and donor-acceptor interactions in aqueous dynamic combinatorial systems. Subtle variations in the building block structure, particularly the length of the alkyl chain connecting two naphthalenediimide moieties, induce important modifications to the energetic landscape of the libraries, and can ultimately be exploited to access efficiently and selectively [2] and [3]catenanes. The unexpected manifestation of an odd-even effect, with respect to the number of atoms in the alkyl chain, is particularly remarkable and dictates the library behaviour.

This work was initiated in collaboration with an undergraduate student, Nicholas A. Jenkins.

4.1. Introduction

The discovery of an assortment of new donor-acceptor [2] and [3]catenanes in dynamic combinatorial libraries is described here.¹ These catenanes were assembled from almost identical linear building blocks, whose design was based on the one developed in the previous Chapter. In the course of this study, over 30 new catenanes have been identified by LC-MS, in addition to many new giant macrocycles. This is an exploratory survey rather than an exhaustive catalogue, and only a few of these new species have been isolated and thoroughly characterized by NMR.

However, this study shows that small variations on the building blocks considerably change the energy landscape of the library and result in the selective formation of different types of catenanes. A careful study of the geometric requirements necessary for efficient catenane formation allows, in some case, a nearly quantitative assembly of these molecules.

4.1.1. Scope of this Chapter

As we have seen in earlier Chapters, donor-acceptor [2]catenanes have frequently been observed in aqueous dynamic combinatorial libraries composed of electron-deficient and electron-rich building blocks.^{2,3} In libraries composed of ‘first generation’ building blocks (Figure 4.1.a), incorporating one acceptor unit or one donor unit, the formation of [2]catenanes with the conventional alternating DADA stacking sequence was observed, as well as the previously unknown DADD, AADA and DAAD motifs (Chapter 2). The tightness of the rings was shown to dictate both the type and yield of the catenane formed: increasing ring tightness results in better overlap of the hydrophobic aromatic surfaces, thus leading to higher yields, until the rings become too small to permit threading. At the opposite extreme,

rings that are too large do not produce [2]catenanes and limit the possibility of assembling more complex concatenated structures.

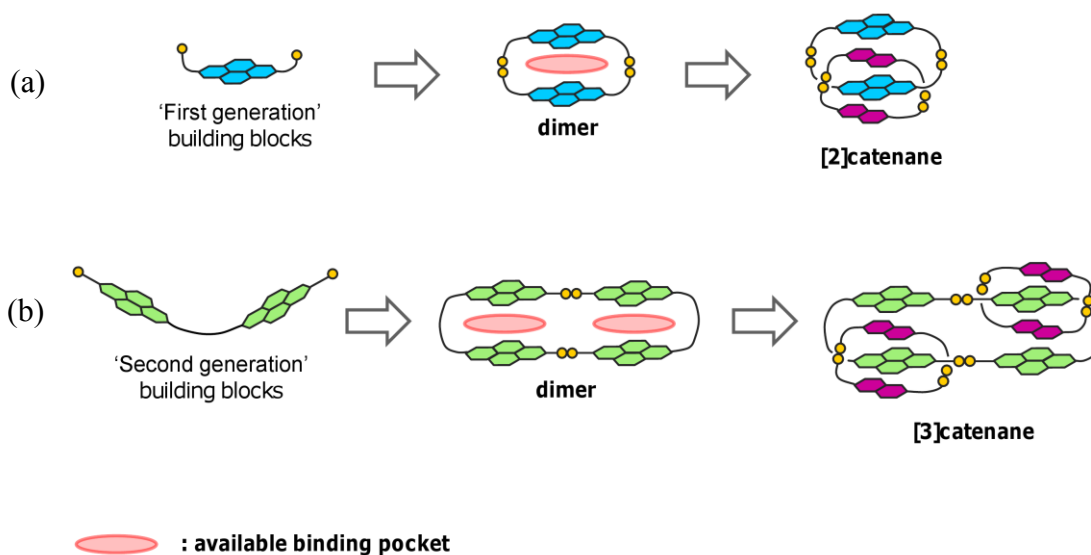


Figure 4.1. Comparison between the (a) ‘first’ and (b) ‘second generation’ acceptor building blocks, designed to form either [2] or [3]catenanes.

Based on these considerations, we developed in Chapter 3 a new strategy for accessing higher order catenanes, using a ‘second generation’ acceptor building block, containing two electron-deficient moieties instead of one (Figure 4.1.b). With this extended building block, the formation of an acceptor dimer provides two binding pockets at a limited entropic cost, allowing successive threading of up to two electron-rich moieties and formation of larger [2] and [3]catenanes (Figure 4.1.b). This pathway implies that the macrocyclisation and threading, steps which are traditionally achieved in separate low-yield reactions,^{4,5} take place *in-situ* following a classical templation mechanism.

The behaviour of libraries composed of extended acceptor building blocks is now investigated in further detail, and two key factors which govern catenane formation are studied: the length of the aliphatic chain linking the acceptor moieties, and the building block chirality.

In the previous Chapter, the use of spermine as a template in the synthesis of the first [3]-catenane was described. Apart in section 4.3.2, no further templating studies are reported here.

4.1.2. Design of the building blocks used in this Chapter

In this Chapter, the behaviour of a whole series of these ‘second generation’ acceptor building blocks (**n-A**) is explored in the presence of either an electron-rich dialkoxynaphthalene building block derived from L-cysteine, **D2a**, or its enantiomer derived from D-cysteine, **D2a'** (Figure 4.2).

The acceptor building blocks **n-A** are all based on the same design: two large hydrophobic electron-deficient π -systems (1,4,5,8-naphthalenetetracarboxylic diimide) are connected *via* a flexible aliphatic chain and terminated by L-cysteine hydrophilic side-chains. Eight consecutive diamines, from 1,2-diaminoethane to 1,9-diaminononane, were used to produce flexible aliphatic linkers of systematically increasing length. The notation **n-A** refers to the number of CH₂ of the alkyl chain linking two acceptor moieties. The extended acceptor building blocks **n-A** were initially synthesized by Nicholas A. Jenkins according to the procedure described in Chapter 3 (Scheme 4.1).⁶

Building block **D2a'** was synthesised according to the published procedure of its enantiomer **D2a** (Scheme 4.2).^{2d}

Libraries were prepared by dissolving each acceptor **n-A** with either donor **D2a** or **D2a'** to a total concentration of 5 mM (1:2 molar ratio) in water at pH 8 in the presence of 1 M NaNO₃.^{2,7} The libraries were stirred at room temperature for one day under air in capped vials to allow oxidation of the thiol building blocks and were then analyzed by LC-MS. Absorbance was recorded at the optimum wavelength for each building block: acceptor units at 383 nm, and donor units at 260 nm. This allows

easy estimation of the quantity of acceptor incorporated into each library member, which were each unambiguously identified by tandem ESI-MS and MS/MS.

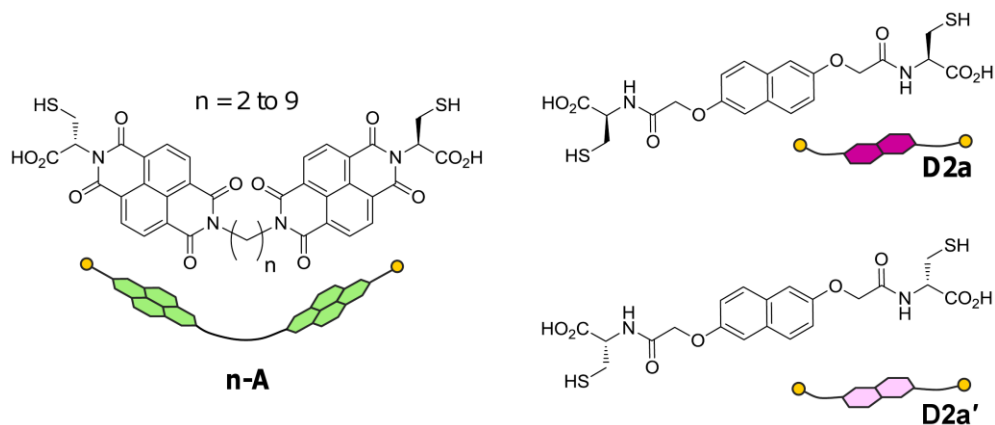
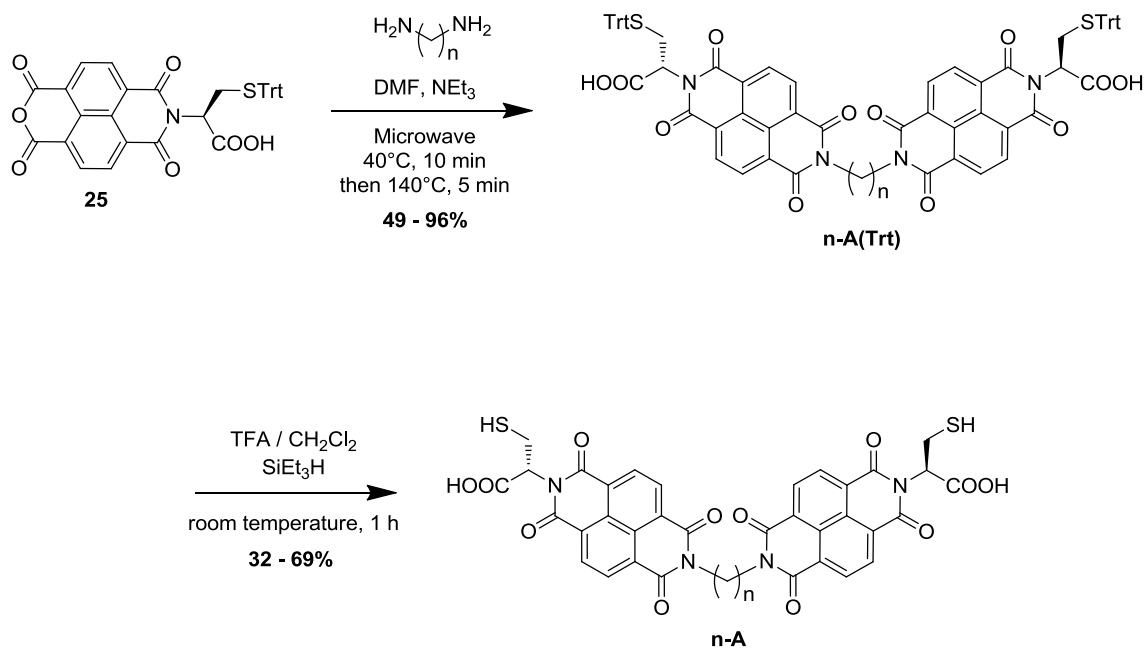
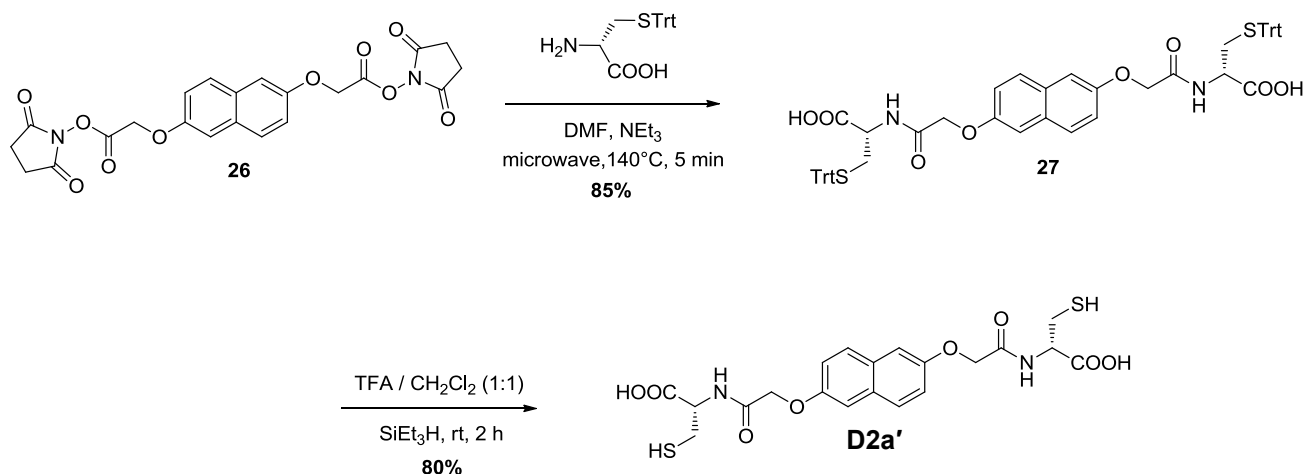


Figure 4.2. Building blocks used in this Chapter and their cartoon representations.



Scheme 4.1. Synthetic route to building block **n-A** ($n = 2$ to 9).



Scheme 4.2. Synthetic route to building block **D2a'**.

4.2. Effect of the length of the aliphatic linker

In this section, we describe the effect of the length of the aliphatic linker on the composition of libraries by comparing the behaviour of systems containing one acceptor **n-A**, reacting with the donor **D2a**. The results are shown in Figure 4.3 and schematically summarised in Figure 4.4.

The formation of [2]catenanes similar to the ‘first generation’ catenanes was observed for long aliphatic linkers ($n \geq 7$). Remarkably, when the aliphatic linker is short ($n \leq 6$), an unexpected odd-even effect⁸ dictates the library behaviour, leading either to the formation of simple libraries containing the expected [3]catenanes, or to the formation of extremely complex libraries containing larger and unusual types of [2]catenane.

In order to distinguish the different catenanes identified through this screening, the [2]catenanes were denoted either **n-[2]Cat** or **n,n-[2]Cat**, and the [3]catenanes **n,n-[3]Cat** (Figures 4.3. and 4.4). The **n-** and **n,n-** notation were chosen to indicate that these structures are based on the macrocycle composed of one and two acceptor building blocks **n-A** respectively.

4.2.1. Manifestation of an odd-even effect

It is clear in Figure 4.3 that the building blocks linked with short and even aliphatic chains ($n = 2, 4$ and 6) produced simple libraries containing in significant quantities only the respective dimer **n,n-A**, **n,n-[2]Cat** and **n,n-[3]Cat** (Figures 4.3.a, c and e). The acceptor dimer **n,n-A** appears to be a particularly stable macrocycle which, as we showed in the case of the **4-** library (Chapter 3), forms rapidly and accumulates before its conversion into **n,n-[2]Cat** and then **n,n-[3]Cat**. Other macrocycles of lower energy are not observed. The [3]catenane is likely to be the thermodynamic product of the libraries: therefore, its yield is relatively good, but the stability of **n,n-A** and **n,n-[2]Cat** limits its formation and these intermediates remain present in significant quantity in the libraries

In stark contrast, the odd libraries ($n = 3$ and 5) displayed little selectivity for any particular library member. The **3-** library is the most striking example, while the effect is less pronounced with the more flexible **5-A**, before disappearing when the length of the linker is further increased. In the odd libraries, the [3]catenane is clearly not the most stable species: other macrocyclic species are of similar stability, or are even more stable. The yield of the [3]catenane is low, and the libraries are dominated by the presence of many large macrocycles, which can also be concatenated.

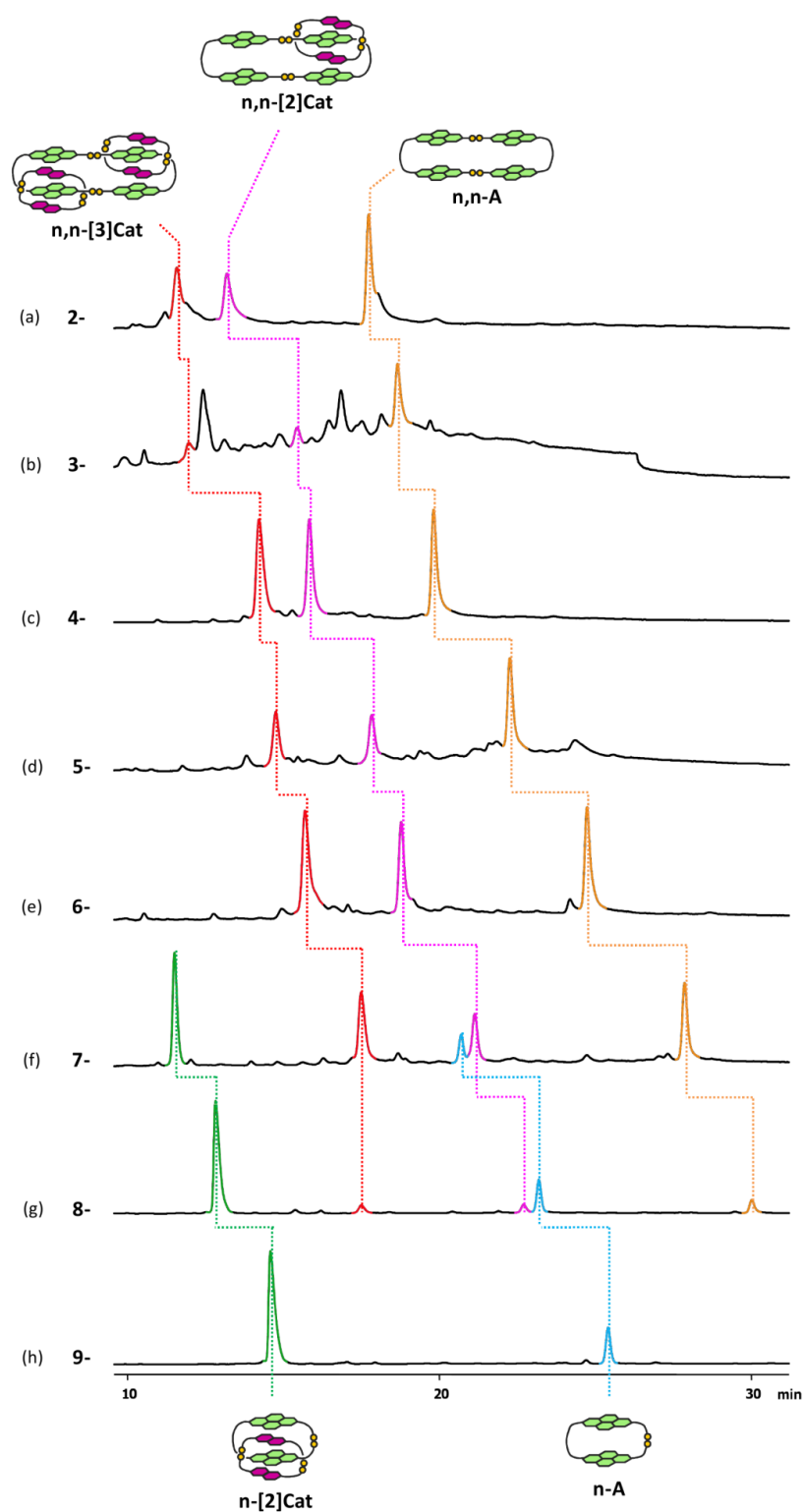


Figure 4.3. HPLC analysis of an aqueous library composed of **D2a** and (a) **2-A**, (b) **3-A**, (c) **4-A**, (d) **5-A**, (e) **6-A**, (f) **7-A**, (g) **8-A**, (h) **9-A**. These libraries were prepared in a 1:2 molar ratio (5 mM total) in the presence of 1 M of $NaNO_3$. Absorbance was recorded at 383 nm.

When the aliphatic linker is long enough, templation by the electron-rich moiety favours intramolecular closure of the acceptor building block, and results in the formation of the closed monomer and the smaller [2]catenanes **n-[2]Cat**. Our previous studies on the ‘first generation’ building blocks suggest that the formation of these [2]catenanes is possible when the aliphatic linker is longer than a cysteine-cysteine linkage, which roughly corresponds to a hexyl chain ($n > 6$).²

Upon reaching the **7-** library (Figure 4.3.f), the length of the aliphatic linker permits formation of the **7-[2]Cat**. Although the formation of **7-[2]Cat** is entropically favoured over the formation of the larger catenanes, such a high concentration of the **7,7-[2]Cat** and **7,7-[3]Cat** suggests that **7-[2]Cat** must be relatively strained and that each catenane, being a kinetic trap, accumulates as soon as it is formed.

As expected, the smaller **n-[2]Cat** becomes the dominant species with longer linkers ($n \geq 8$), and **8-[2]Cat** and **9-[2]Cat** are generated in yields of roughly 70% in otherwise simple libraries. The formation of these [2]catenanes is highly favoured by the tightness of the acceptor monomer derived from the building blocks of this study ($6 < n \leq 9$), which is in agreement with our previous observations and mechanistic proposal (Chapter 2).²

Overall, the behaviour of the ‘second generation’ acceptor building blocks is summarised in Figure 4.4.

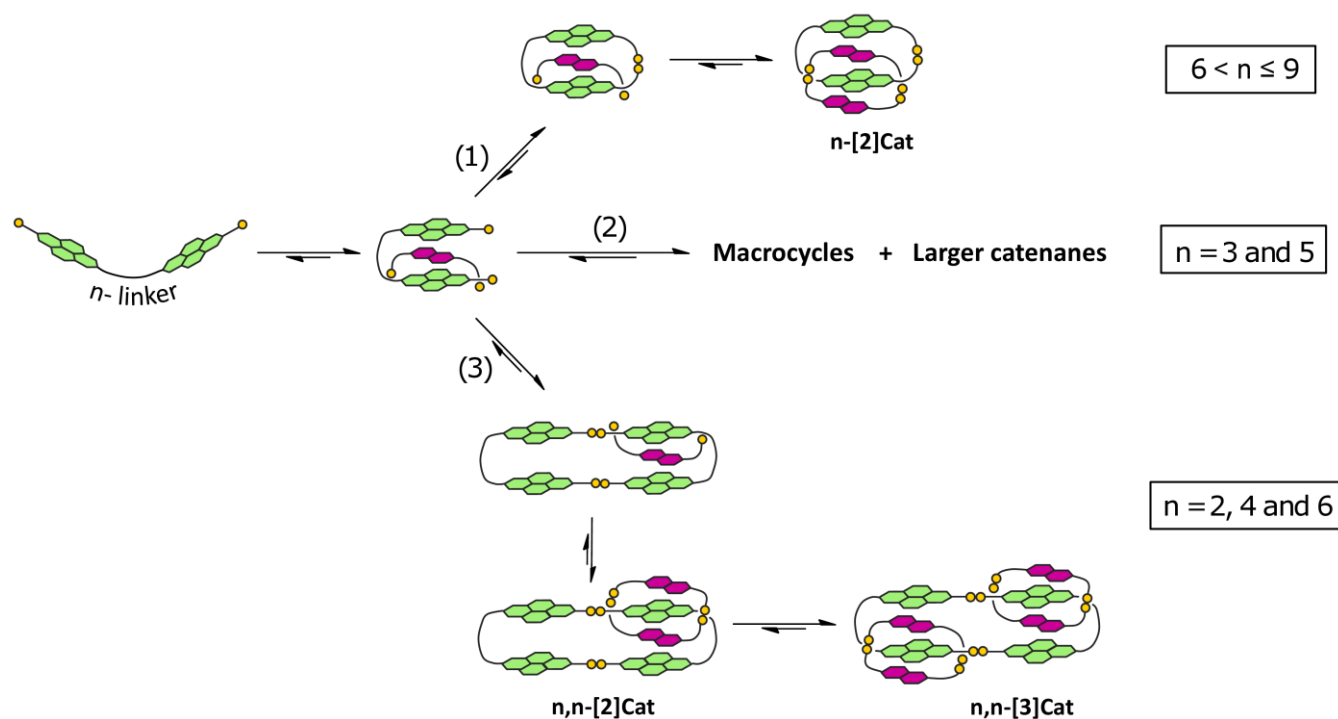


Figure 4.4. The three pathways for catenane synthesis, using ‘second generation’ acceptor building blocks: (1) intramolecular closure of the acceptor building block and formation of n -[2]Cat, (2) formation of larger macrocycles, which can also be concatenated, and (3) dimerisation of the acceptor building block and formation of n,n -[2]Cat and n,n -[3]Cat.

4.2.2. Identification of new unexpected [2]catenanes

The odd-even effect displayed by the short-linked building blocks is even more apparent in libraries prepared in a 1:1 molar ratio of the building blocks. While the even libraries still show a strong preference for the formation of the n,n -A, n,n -[2]Cat and n,n -[3]Cat in a 1:1 ratio (Figure 3.6 in the previous Chapter), the odd libraries are even more complex and multiple species with comparable peak intensities exist after full oxidation.

Figure 4.5 illustrates the complexity of the odd **3-** library in a 1:1 molar ratio. In this library, both a new unconventional [2]catenane **27** and its corresponding isomeric macrocycle **28** (Figure 4.6) were identified.

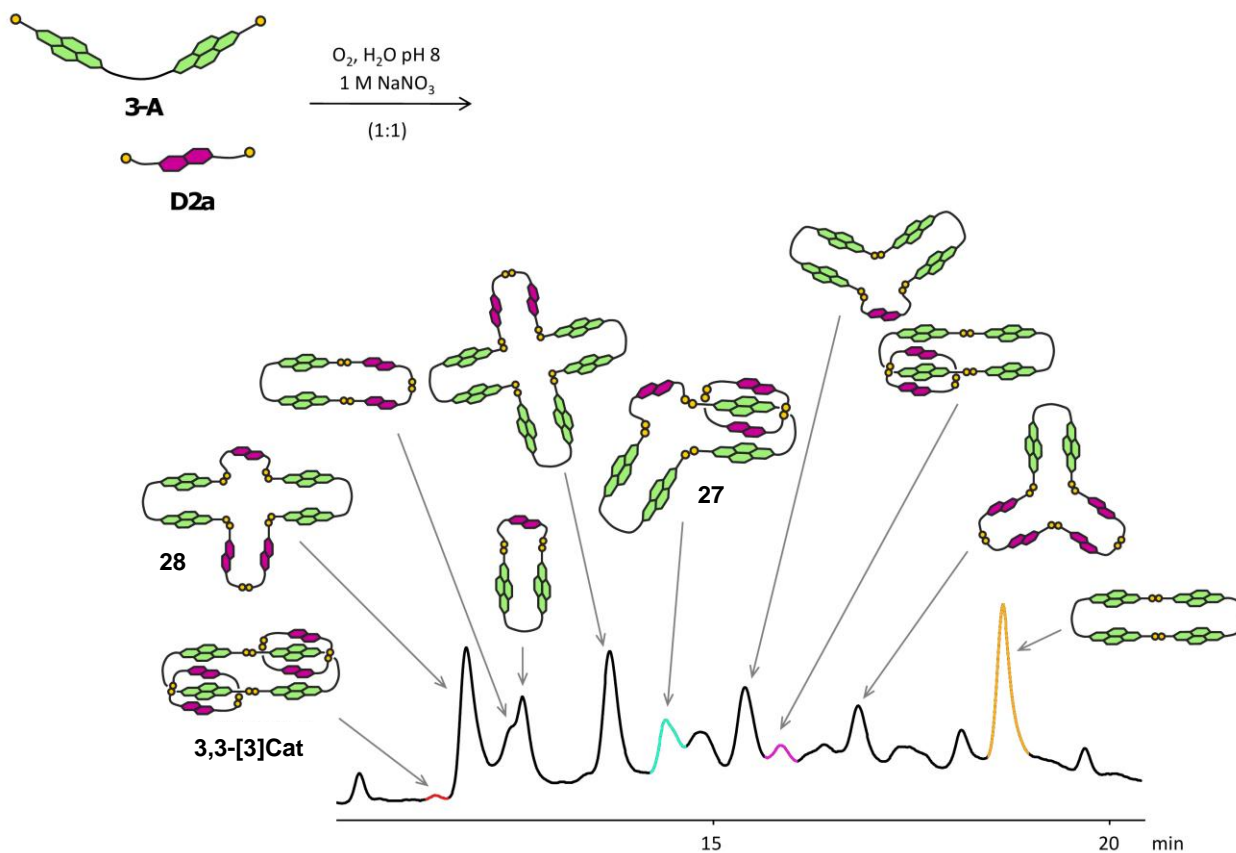


Figure 4.5. HPLC analysis of an aqueous library composed of **D2a** and **3-A** (1:1 molar ratio, 5 mM total), in the presence of 1 M of NaNO_3 .

The fragmentation pattern of **27** generated by MS/MS is consistent with the structure proposed in Figures 4.5. The soft fragmentation at 0.4 V shows a high intensity of the separated rings at m/z 2036.3 and m/z 958.9 (Figure 4.6.b). No evidence of linkage between these two fragments was found, suggesting that they are not covalently bonded to each other. The lower masses can be assigned to

fragments of these two cyclic species. As shown in Figure 4.6, the MS/MS fragmentation of the isomeric macrocycle **28** is strikingly different.

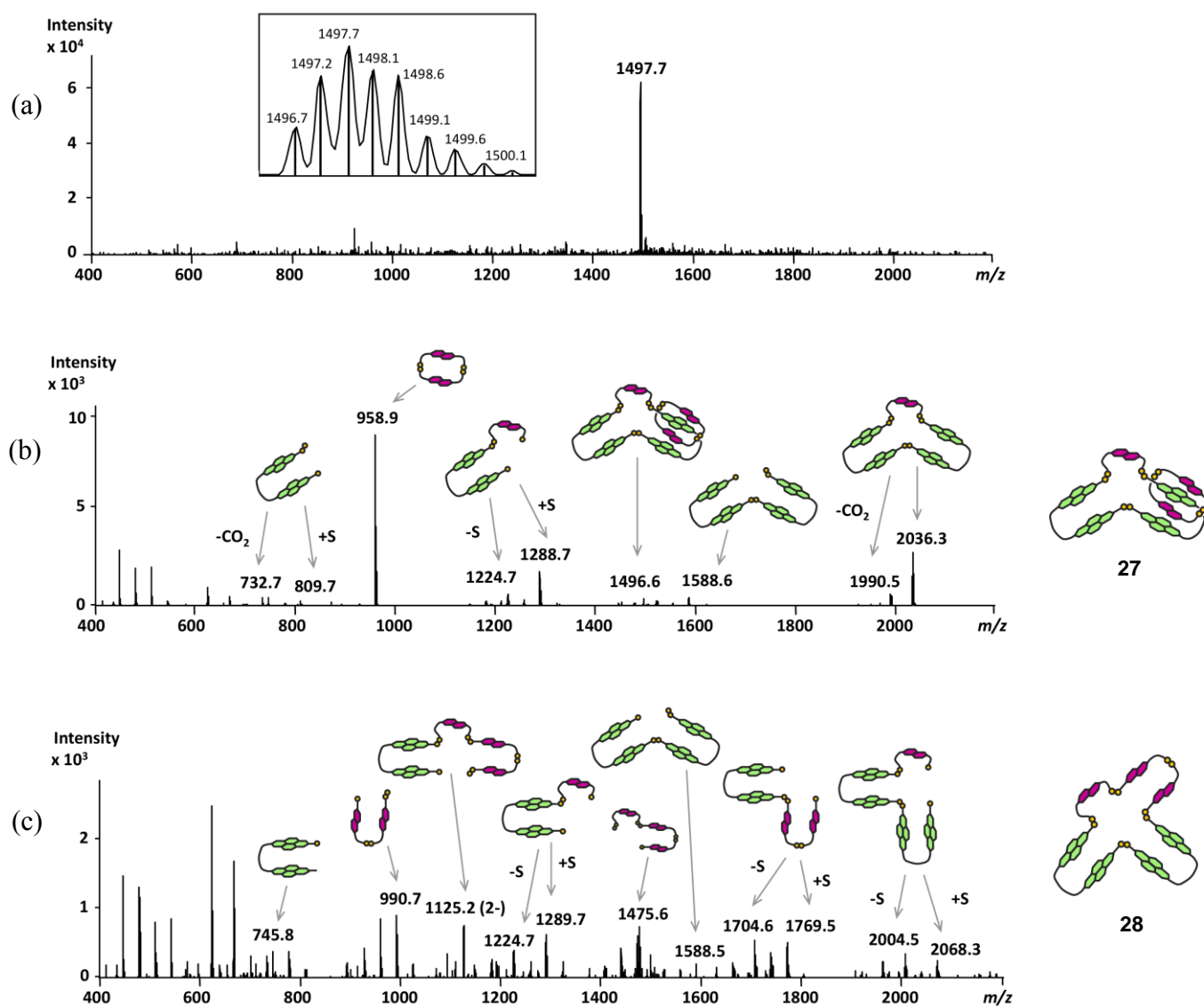


Figure 4.6. Tandem (a) MS and MS/MS fragmentation (b) of **27** and (c) of the corresponding macrocyclic isomer **28**. The cartoon yellow dots represent the sulfur atoms of the building blocks.

The **5-** library (1:1 molar ratio) is also characterized by the formation of a variety of surprisingly large macrocycles, such as macrocycle **29** (Figure 4.7). An even larger library member, **30** (m/z 1555.0, triply charged), two donor building blocks larger than **29**, was also observed.

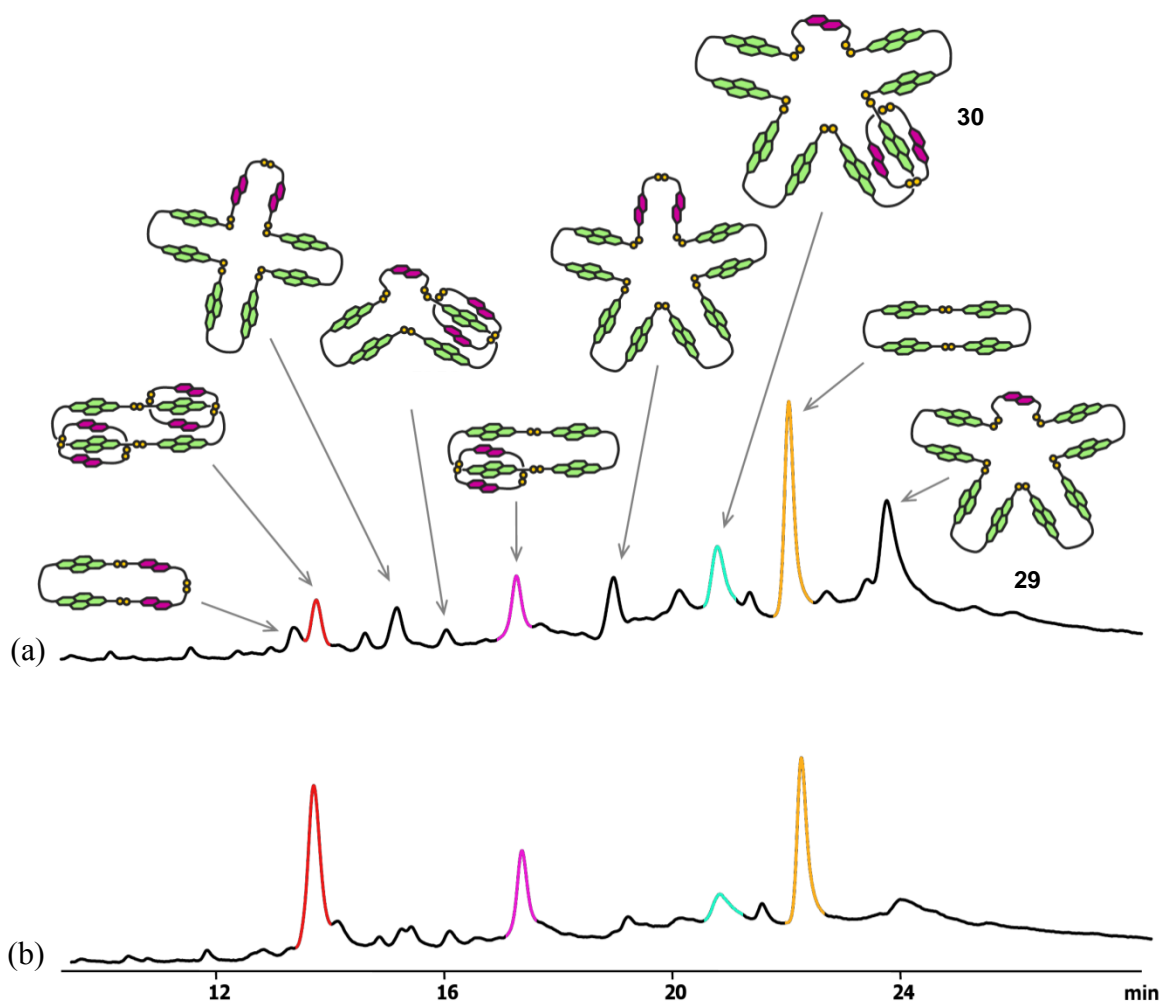


Figure 4.7. (a) HPLC analysis of an aqueous library composed of **D2a** and **5-A** (1:1 molar ratio, 5 mM total), in the presence of 1 M of NaNO_3 . (b) After full oxidation of the library, another equivalent of **D2a** was added. Absorbance was recorded at 383 nm.

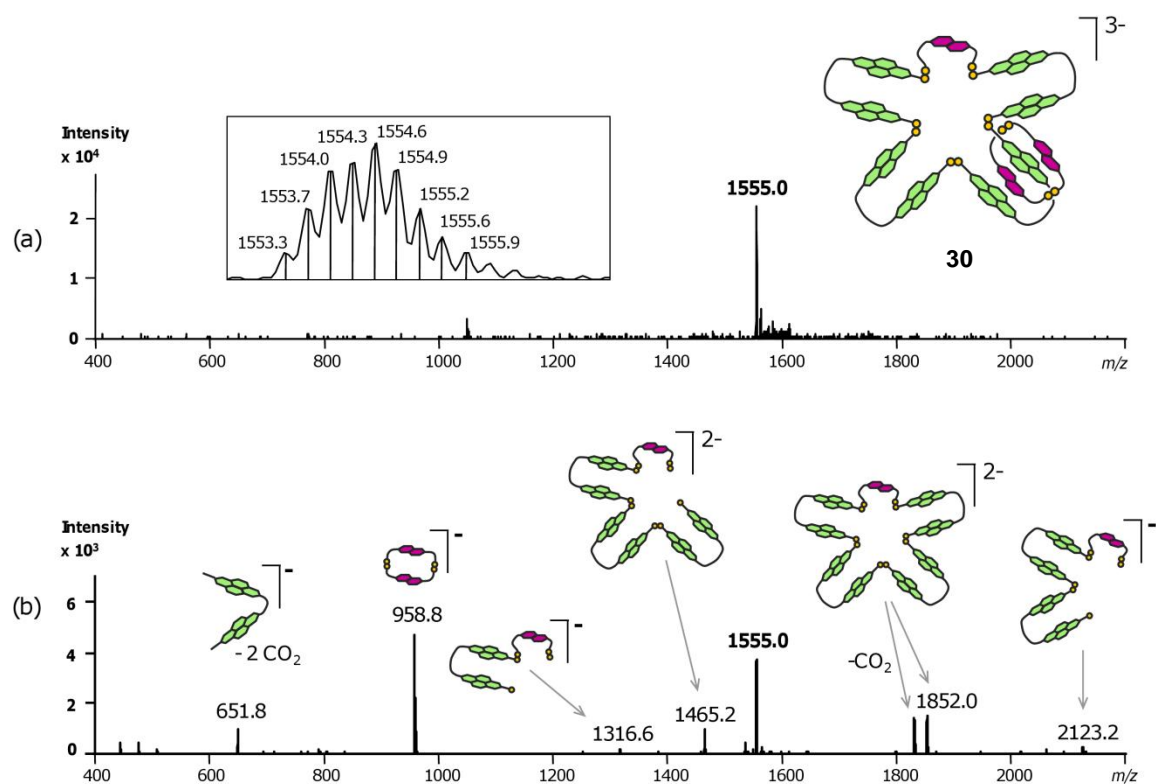


Figure 4.8. Tandem (a) MS and (b) MS/MS fragmentation of catenane **30**. The cartoon yellow dots represent the sulfur atoms of the building blocks.

Here again, the MS/MS evidence in support of a concatenated structure (Figure 4.8) is compelling. However, the expected difficulty of further characterization meant we did not examine these molecules any further. Despite this, the power of dynamic combinatorial chemistry to create unpredictable and unprecedented structures is apparent once again.

Stepwise addition of **D2a** to the **5-** library is a particularly clear example of the influence of kinetics (disulfide exchange *versus* thiol oxidation). Adding an additional equivalent of fresh thiol **D2a** to a library prepared in a 1:1 molar ratio simplified dramatically the library (Figure 4.7.a and b). Re-initiation of the reversible process led to the amplification of the more stable **5,5-[3]Cat** at the expense of the unusually large catenane **30**, suggesting that its formation is kinetically controlled. While the final

ratio between the building blocks in the ‘stepwise’ library shown in Figure 4.7.b is equal to the ratio in the ‘one-pot’ library shown in Figure 4.3.d, the stepwise procedure led to an increase of the **5,5-[3]Cat** yield from 10% to 25%. Similar experiments conducted on the **3-** library following the stepwise protocol for the addition of **D2a** led to little amplification of **3,3-[3]Cat**.

4.2.3. ¹H NMR characterisation of the isolated catenanes

The **7-** library provides a unique opportunity to compare by ¹H NMR a whole family of [2] and [3]catenanes produced by the same building blocks, thus allowing us to uncover information not only on the way these catenanes form, but also on their solution-state structure.

4.2.3.1. ¹H NMR characterisation of **7-[2]Cat**

The ¹H NMR spectrum (500 MHz, 298 K, D₂O) of **7-[2]Cat** is characteristic of a fully asymmetric catenane in which each of the aromatic protons is inequivalent (Figure 4.9). In the acceptor region (7.2 to 8.2 ppm), eight doublets were assigned by correlation spectroscopy (COSY) to the eight protons of the naphthalenediimide units: four upfield-shifted (inner acceptor) and four downfield-shifted (outer acceptor). A similar pattern was observed in the donor region (5.5 to 7.1 ppm).

A NOESY spectrum shows exchange peaks between the inner and outer NDI protons (Figure 4.10). When the acceptor rings rotate, it induces an inversion of the environment of the inner DN protons, resulting into NOESY correlations between the two sets of inner DN protons (in grey and black, Figure 4.10.b). The same pattern was observed for the outer DN protons. No exchange peaks were observed between the inner and outer donor protons.

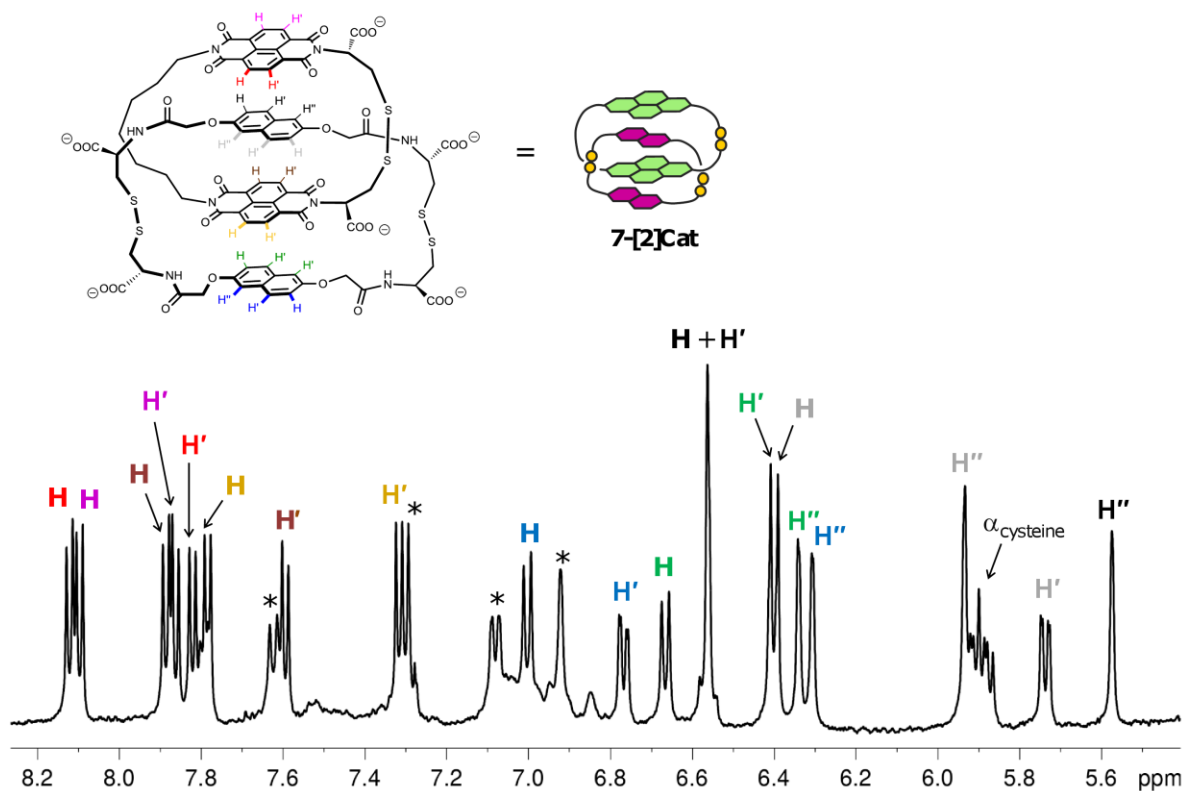


Figure 4.9. Partial ^1H NMR spectrum (D_2O , 298 K, 500 MHz) of **7-[2]Cat** (the peaks labeled with * are associated with an impurity).

Figure 4.11 highlights the expected NOESY correlations between the inner donor protons and the protons of the aliphatic chain of the acceptor ring. The NMR spectrum of **7-[2]Cat** is comparable to that of the catenane **9-[2]Cat**, which was also isolated and characterized (see the experimental section in Chapter 6).

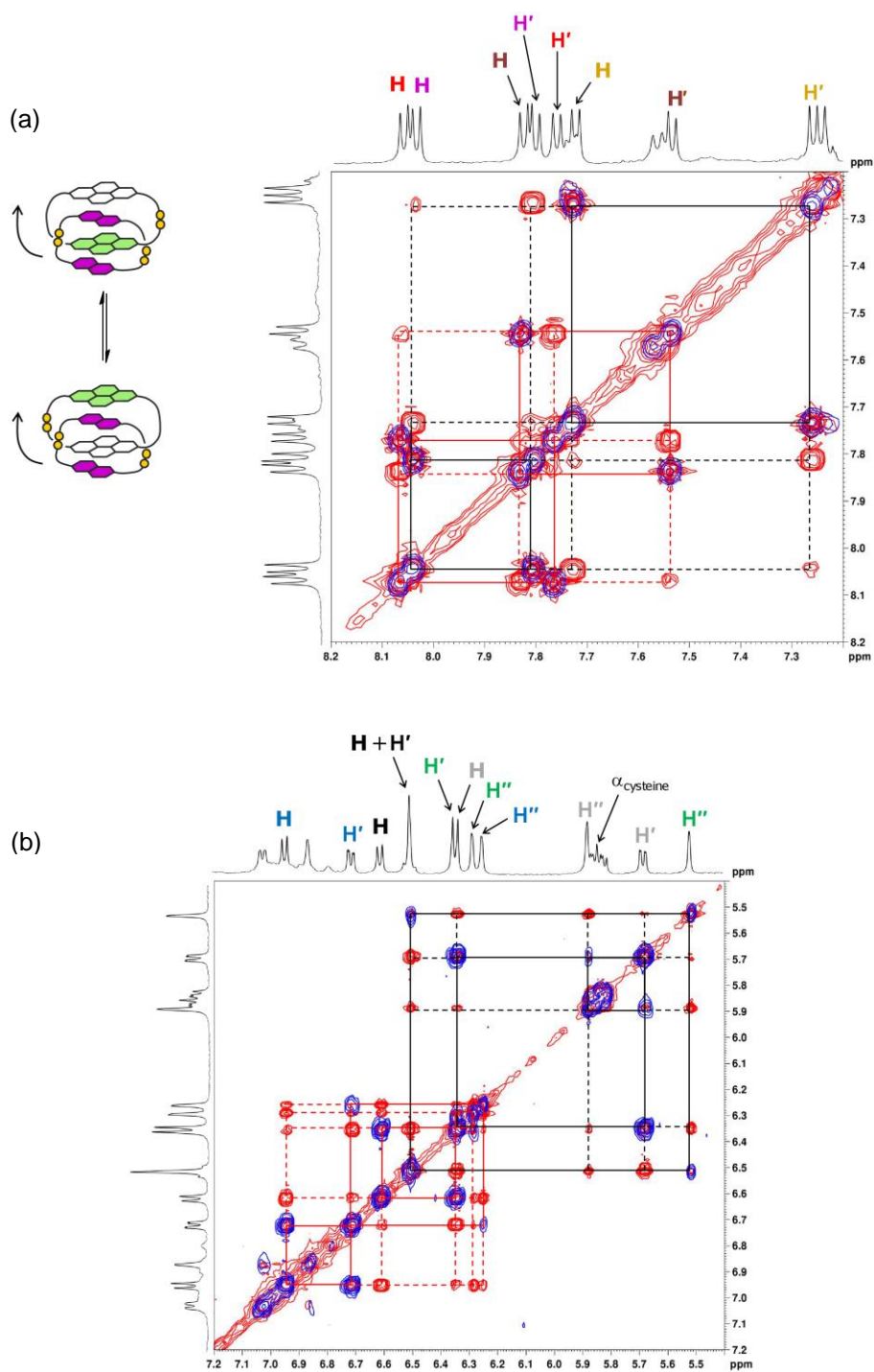


Figure 4.10. Partial COSY (blue) and NOESY (red) spectra of 7-[2]Cat between (a) 7.2 ppm and 8.20 ppm and (b) between 5.40 ppm and 7.20 ppm (D_2O , 298 K, 500 MHz, mixing time = 800 ms). The solvent peak was referenced at 4.79 ppm.

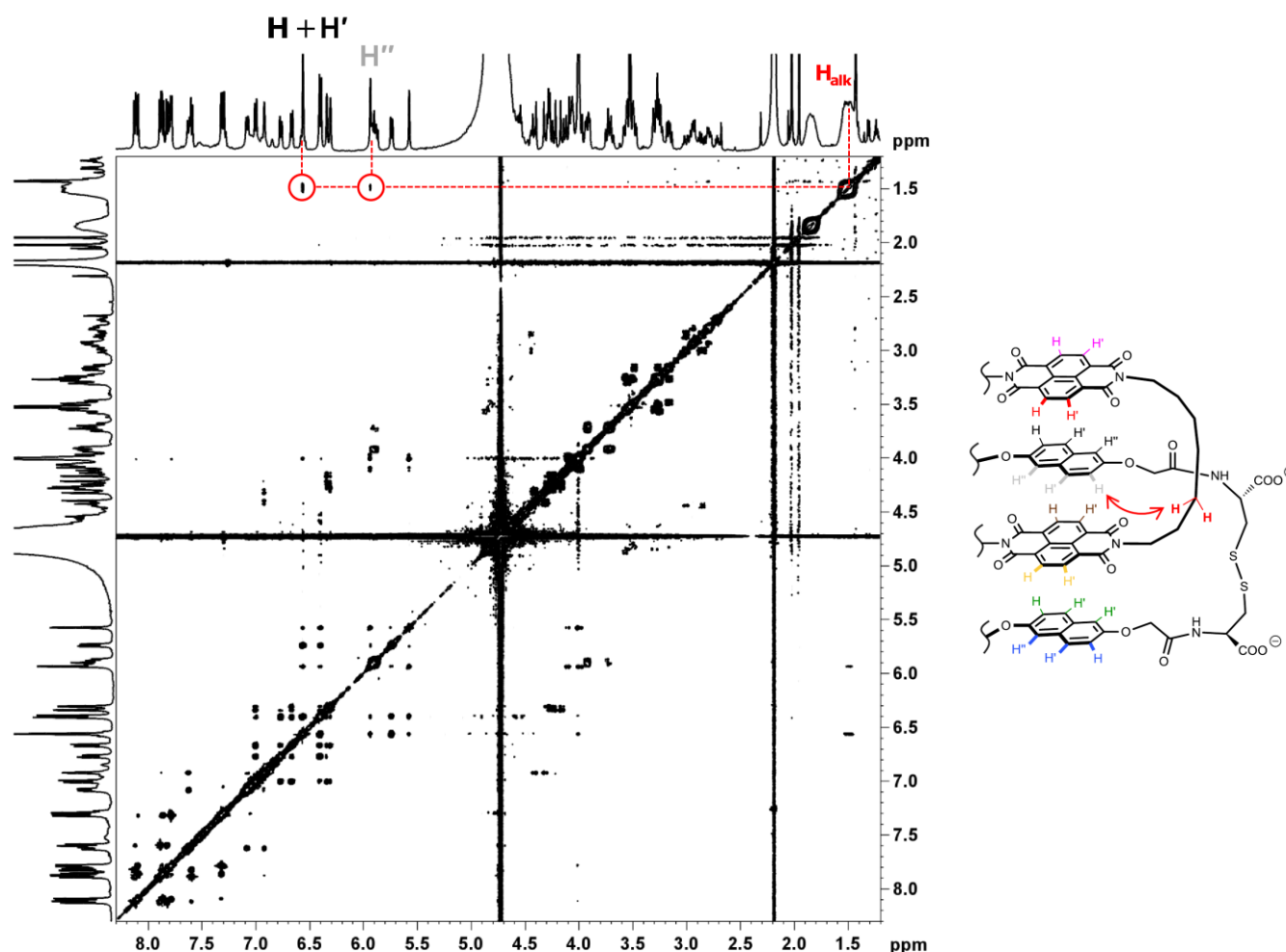


Figure 4.11. Full NOESY spectrum of 7-[2]Cat (D_2O , 298 K, 500 MHz, mixing time = 800 ms), highlighting the nOe correlation between the protons of the alkyl chain (**H**) and the inner donor units (H, H' and H''). The solvent peak was referenced at 4.79 ppm.

4.2.3.2. 1H NMR characterisation of 7,7-A, 7,7-[2]Cat and 7,7-[3]Cat

Figure 4.12 clearly illustrates how the rigidity arising from the successive threading of donor dimers around the acceptor dimer progressively sharpens the NMR signals. Macrocycle **7,7-A** displays broad resonances characteristic of large, flexible, multi-conformation macrocycles (Figure 4.12).⁹ Threading of one donor ring does not significantly constrain the flexibility of the acceptor dimer, while the donor dimer displays the expected sharp signals of a ring that freely rotates around the **7,7-A** macrocycle. The

acceptor signals are still broad and cannot be assigned. Upon threading a second donor ring, the NMR signals sharpen remarkably due to the high level of organisation of the aromatic units within **7,7-[3]Cat**.

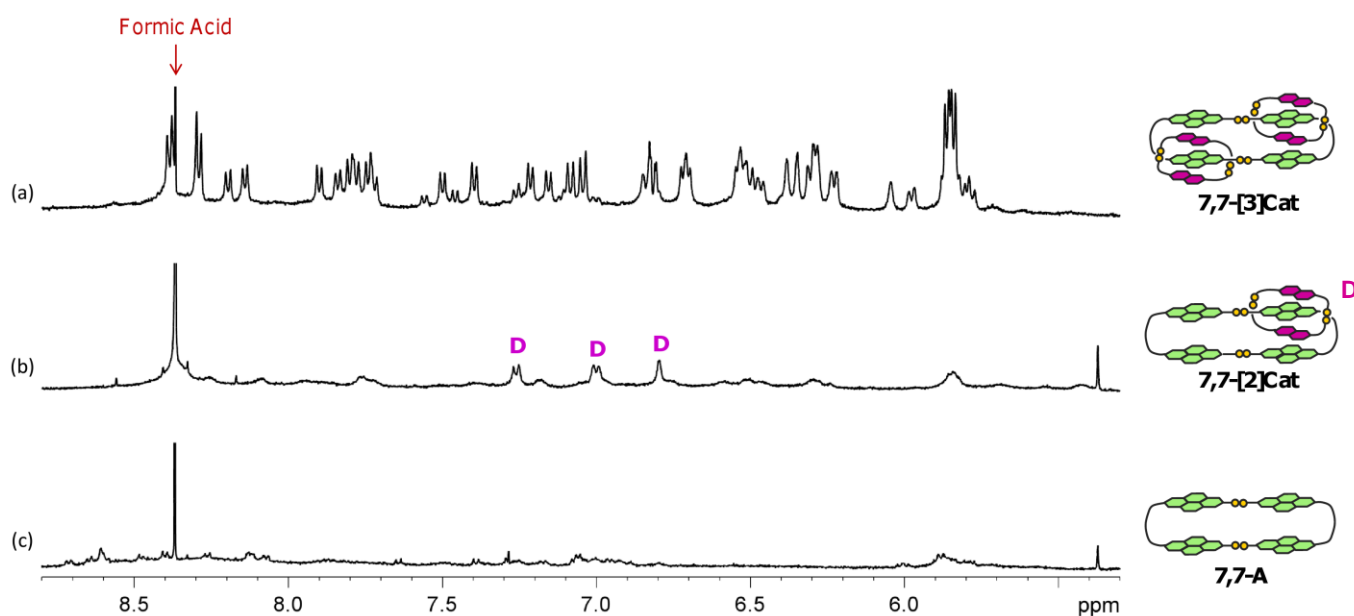


Figure 4.12. Partial ^1H NMR spectrum (D_2O , 298 K, 500 MHz) of (a) **7,7-[3]Cat**, (b) **7,7-[2]Cat** and (c) **7,7-A**.

The ^1H NMR of **7,7-[3]Cat** was studied in further detail. While only one conformation could be identified for the highly constrained **4,4-[3]Cat** (Chapter 3), two conformations in a molar ratio of 1:1 were identified for the larger **7,7-[3]Cat**. These two conformations are likely to arise, as drawn in Figure 4.13, from the two possible positions of the aliphatic linker within the catenane. Unfortunately, the presence of exchange peaks between the two conformations and also between the inner and outer aromatic units make the assignment of the individual signals impractical. However, four pairs of doublets were observed for each conformation of **7,7-[3]Cat** in the acceptor region (highlighted in

green, Figure 4.13), which is in accordance with our assignment of the simpler NMR of 4,4-[3]Cat in Chapter 3. A similar pattern was observed in the donor region (highlighted in red, Figure 4.13).

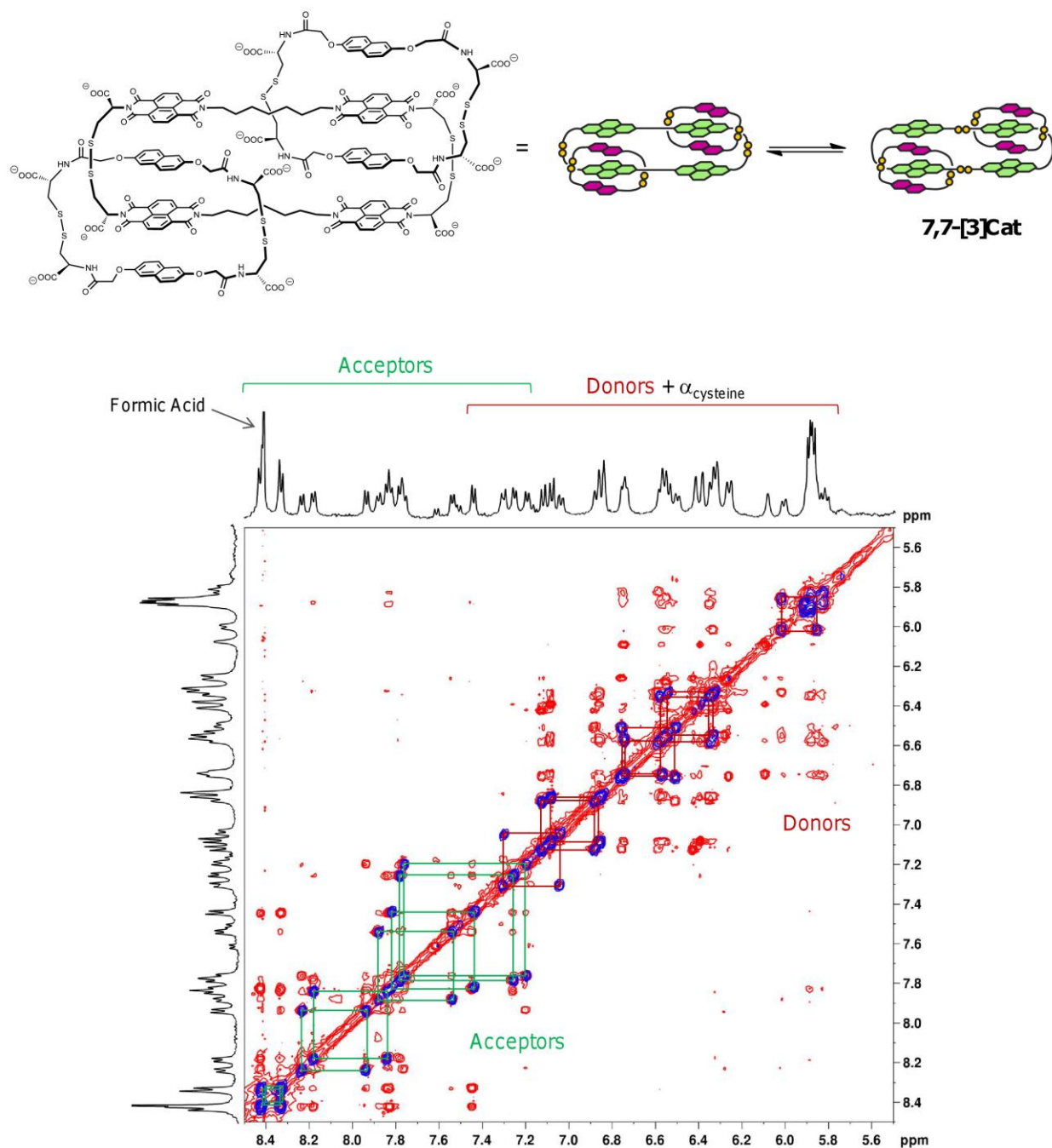


Figure 4.13. Partial COSY (blue) and NOESY (red) spectra of 7,7-[3]Cat between 5.5 ppm and 8.5 ppm (D₂O, 298 K, 500 MHz, mixing time = 800 ms). The solvent peak was referenced at 4.79 ppm.

4.3. Influence of building block chirality

The length of the aliphatic linker of the building blocks is not the only feature that can be used to control the catenanes' synthesis. In both acceptor and donor building blocks, the cysteine provides the thiol necessary for disulfide exchange and the carboxylate anions for water solubility. In compact structures such as catenanes, the negatively charged carboxylates accumulate around the disulfide bridges, potentially having an adverse effect on their formation. Changing the chirality of one of the building blocks inevitably leads to the formation of new structures,¹⁰ and may well give very different distributions of diastereomers. Therefore it can be used to adjust the energy landscape of the library in favour of a structure with a particular topology, such as a catenane.

4.3.1. Effect of chirality on the yield of catenanes

This section describes a new set of libraries each of which contains the acceptor **n-A** and the enantiomeric donor **D2a'**, derived from D-cysteine (Figure 4.14). The similarity of behaviour between the libraries containing the two enantiomeric donor building blocks confirms our previous observation on the effect of the linker length: the odd-even effect is still observable, but less clear, as macrocycles are more abundant in each **D2a'** library. To our surprise, despite the formation of overall more complex libraries, the formation of catenanes with hetero-chirality seems to be preferred compared the formation of catenanes with homo-chirality (Figure 4.15).

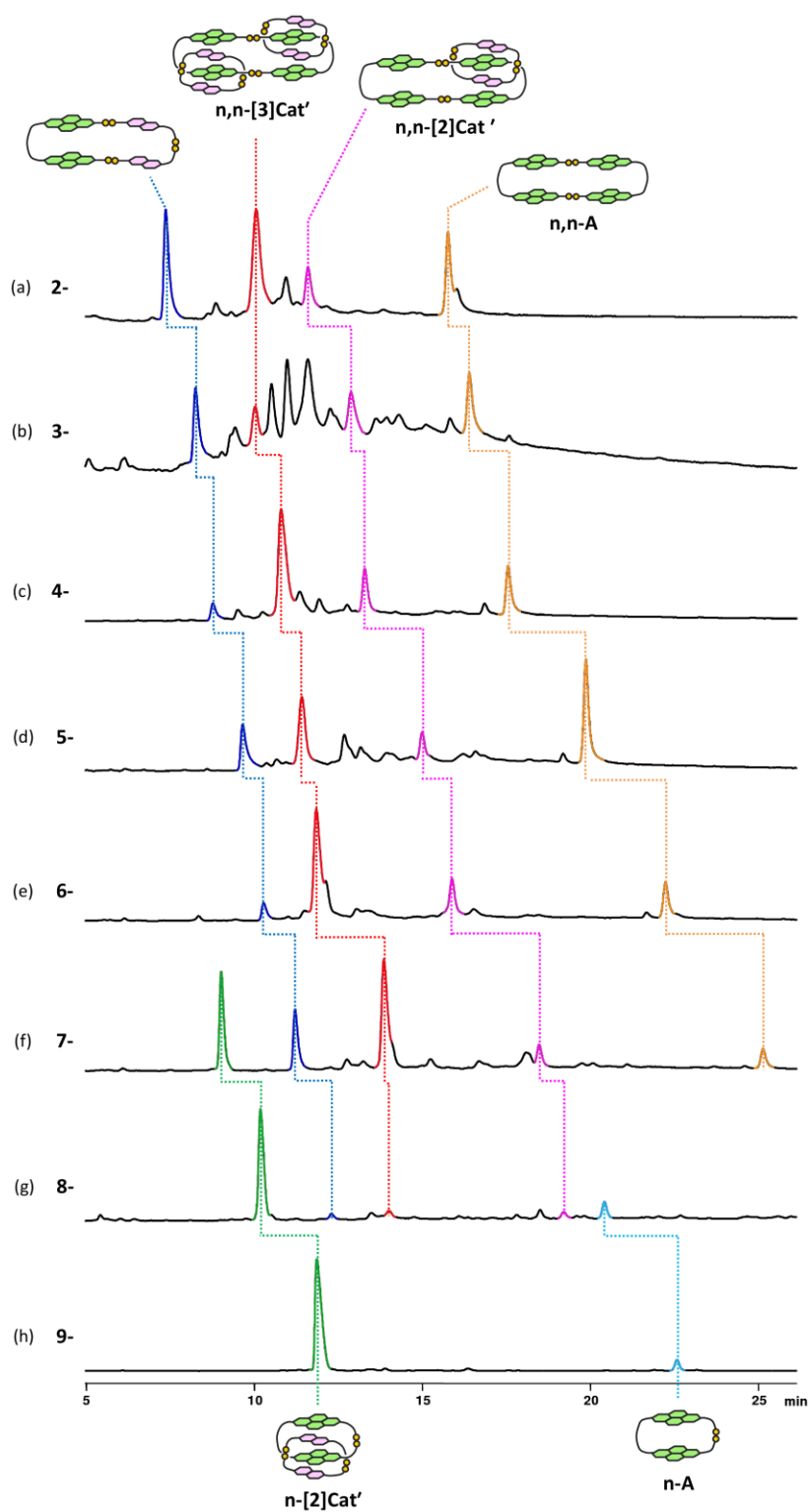


Figure 4.14. HPLC analysis of an aqueous library composed of **D2a'** and (a) **2-A**, (b) **3-A**, (c) **4-A**, (d) **5-A**, (e) **6-A**, (f) **7-A**, (g) **8-A**, (h) **9-A**. These libraries were prepared in a 1:2 molar ratio (5 mM total) in the presence of 1 M of NaNO_3 . Absorbance was recorded at 383 nm.

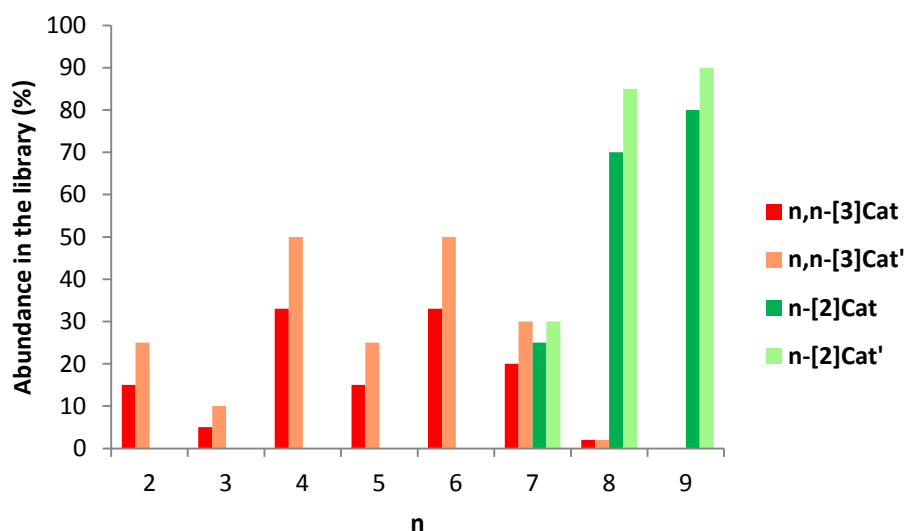


Figure 4.15. Comparison of the yield of catenanes with homo and hetero-chirality.

In the two most impressive examples, the assembly of the homo-catenane **9-[2]Cat** reached 70% (Figure 4.3.h), while the assembly of the hetero-catenane **9-[2]Cat'** is nearly quantitative (Figure 4.14.h), and the assembly of **4,4-[3]Cat'** increased to 50% (Figure 4.3.c) from the 33% observed for **4,4-[3]Cat** (Figure 4.14.c).

Although the effect of chirality on the library distribution is complex and difficult to fully understand, this same effect is recurrent in the eight libraries composed of either **D2a** or **D2a'**, and clearly indicates that the change in chirality has modified the relative energy of the catenanes compared to the macrocycles in all the libraries.

4.3.2. Exploring the differences between two diastereomeric catenanes: **4,4-[3]Cat** and **4,4-[3]Cat'**

In order to understand better the effect induced by the change in chirality on the catenanes formation, we investigated the differences between the behaviour of two diastereomeric [3]catenanes: **4,4-[3]Cat**, whose behaviour was studied in detail in the previous Chapter, and **4,4-[3]Cat'**. Their respective kinetics of formation, their ^1H NMR spectra, and the strength of their interaction with spermine were successively studied.

4.3.2.1. Kinetics of formation

A comparative kinetic study performed on two separate **4-** libraries containing either **D2a** or **D2a'** confirms that the energy landscapes of the two libraries are significantly different. As we previously described in Chapter 3 (Figure 3.6), the kinetics of formation of **4,4-[3]Cat** is surprisingly simple, and the **4,4-A**, **4,4-[2]Cat**, and **4,4-[3]Cat** are successively formed. These species are far more stable than any other macrocycles than could potentially form which consequently are not observed. Unfortunately, the high stability of the intermediates **4,4-A** and **4,4-[2]Cat**, which leads to this simple library, also limits the efficient formation of the **4,4-[3]Cat**.

On the other hand, the kinetics of formation of **4,4-[3]Cat'** (1:1 molar ratio, Figure 4.16) is governed by a radically different energy landscape characterized by the presence of intermediates and macrocyclic species of similarly low stability, which ultimately collapse into the thermodynamic sink and kinetic trap which is the [3]catenane. The kinetic studies also show that the formation of **4,4-[3]Cat'** is faster than that of **4,4-[3]Cat** (Figure 4.17).

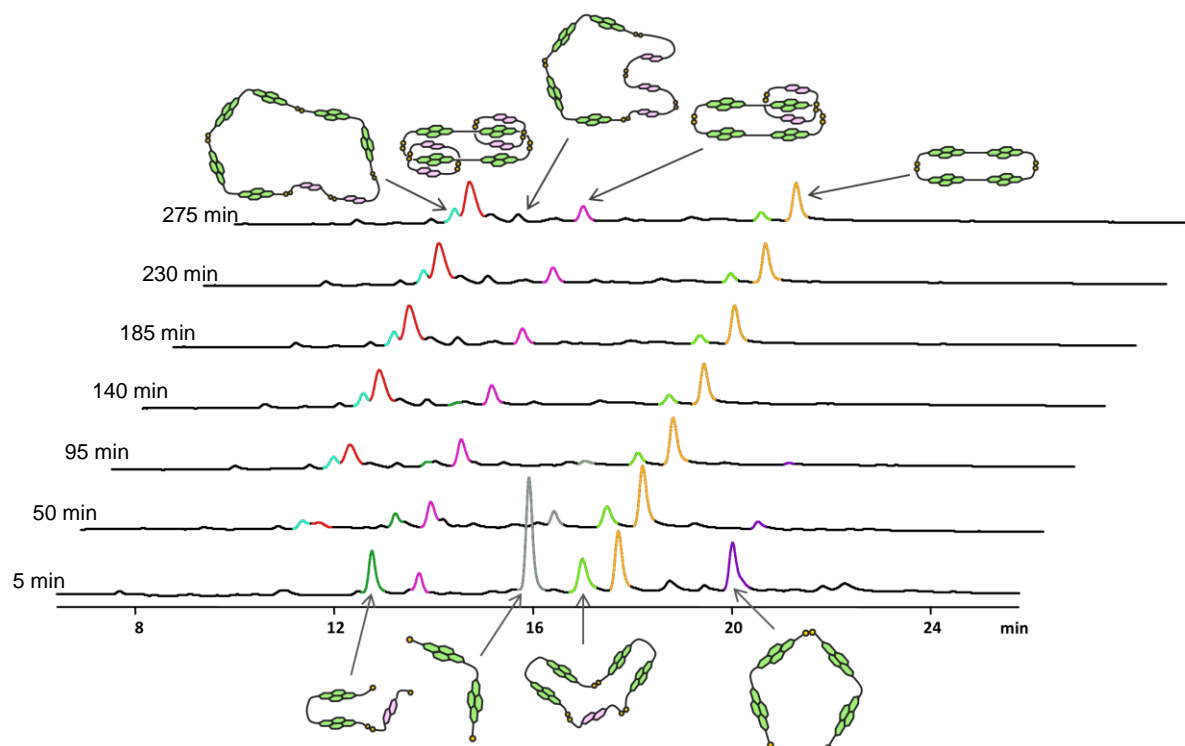


Figure 4.16. LC-MS analysis of a library composed of **4-A** and **D2a'** (5mM total, 1:1 molar ratio) at different time intervals. Absorbance was monitored at 383 nm.

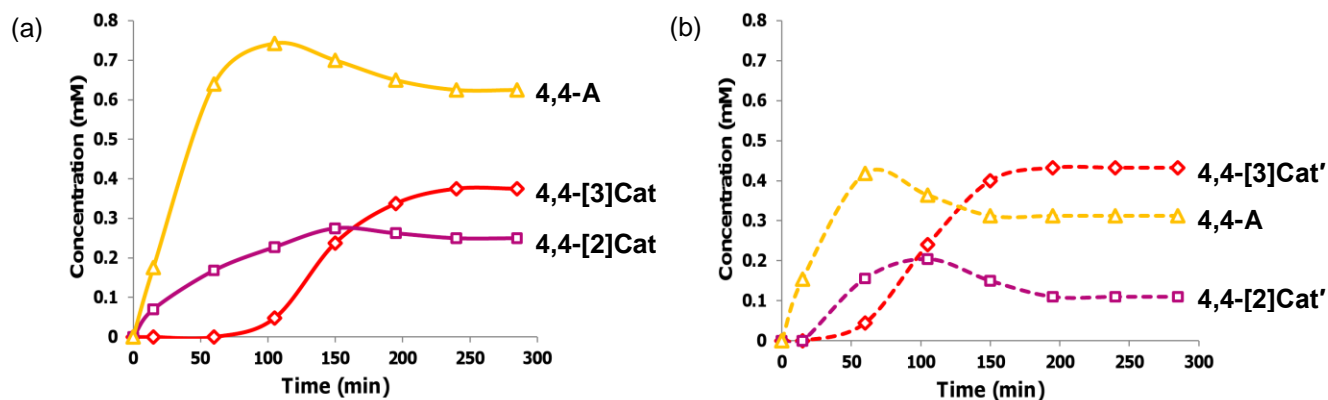


Figure 4.17. Comparison between the kinetic profile (a) of the formation of **4,4-A** (Δ), **4,4-[2]Cat** (\square) and **4,4-[3]Cat** (\diamond) in a library composed of **4-A** and **D2a** and (b) of the formation of **4,4-A** (Δ), **4,4-[2]Cat'** (\square) and **4,4-[3]Cat'** (\diamond) in a library composed of **4-A** and **D2a'**. The libraries were prepared in water pH 8, in the presence of 1 M NaNO_3 (5 mM total, 1:1 molar ratio).

These observations verify our supposition that the chirality of the building blocks may be exploited to alter the relative energy difference between the library members in favour of catenane formation. The higher stability of **4,4-[3]Cat'** compared to **4,4-[3]Cat** is tentatively attributed to changes in the relative position of the carboxylates when changing the chirality of the donor building blocks. Similar arguments can be applied when explaining the relative stability of **4,4-[3]Cat'** when compared to the **4,4-A**, **4,4-[2]Cat'** and other macrocycles present in the library.

4.3.2.2. ¹H NMR spectra

The ¹H NMR spectrum of **4,4-[3]Cat'** displays two conformations (Figure 4.18), with signals corresponding to the acceptor moieties spread over 1.3 ppm (from 7.3 to 8.5 ppm), implying a certain degree of rotational freedom for the concatenated rings.

In sharp contrast, **4,4-[3]Cat** displays only one conformation (Chapter 3), and the signals corresponding to the acceptor moieties are unusually spread over 1.7 ppm (from 6.9 to 8.6 ppm). While the rings composing the two catenanes are identical in size, these differences can only be explained by a conformational flexibility in **4,4-[3]Cat'**, perhaps due to lower carboxylate-carboxylate repulsions.

The ¹H NMR spectrum of **4,4-[3]Cat'** displays four pairs of doublets for each conformation in the acceptor region (Figure 4.19). Because the two conformations are in a molar ratio of 1:2, they can be easily distinguished (dotted and solid lines in Figure 4.19). However, we could not assign which one of the two proposed conformations is the major one or the minor one.

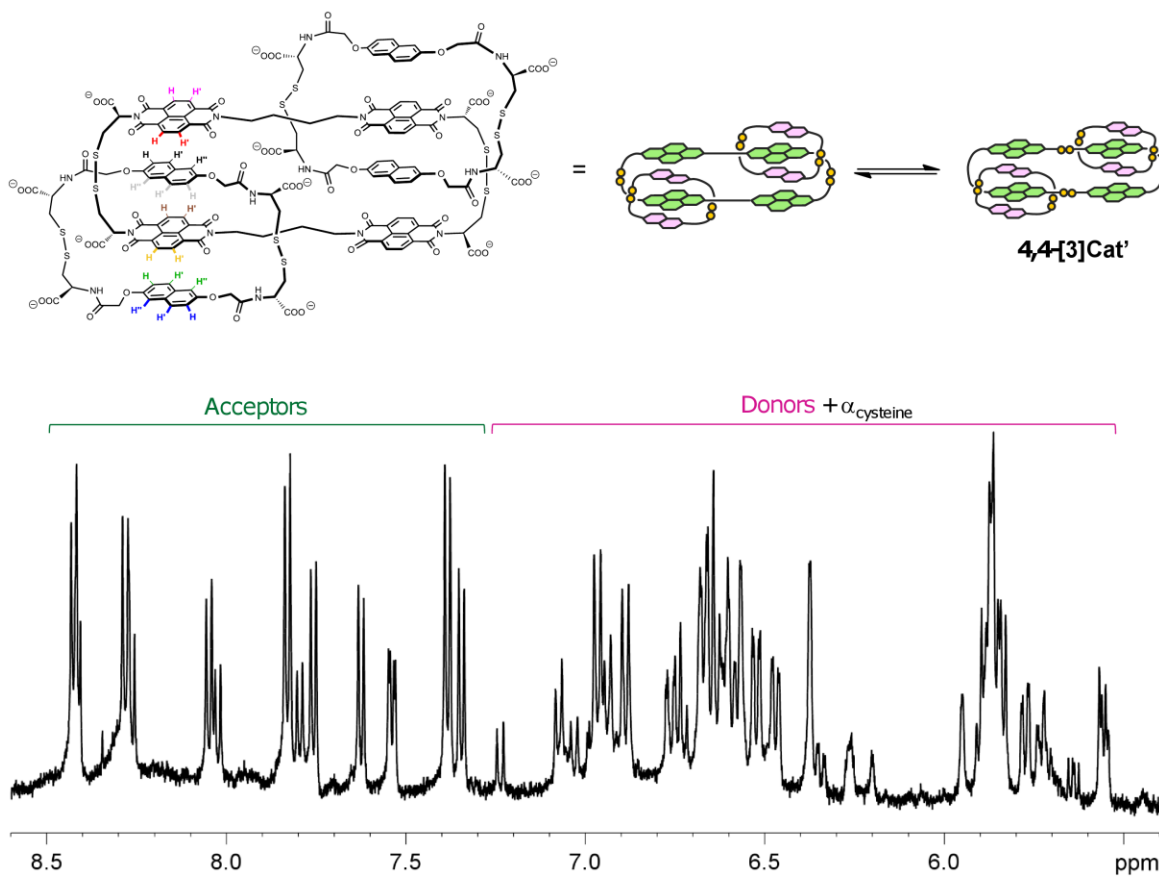


Figure 4.18. Partial ¹H NMR spectrum (D₂O, 298 K, 500 MHz) of 4,4-[3]Cat'. The solvent peak was referenced at 4.79 ppm.

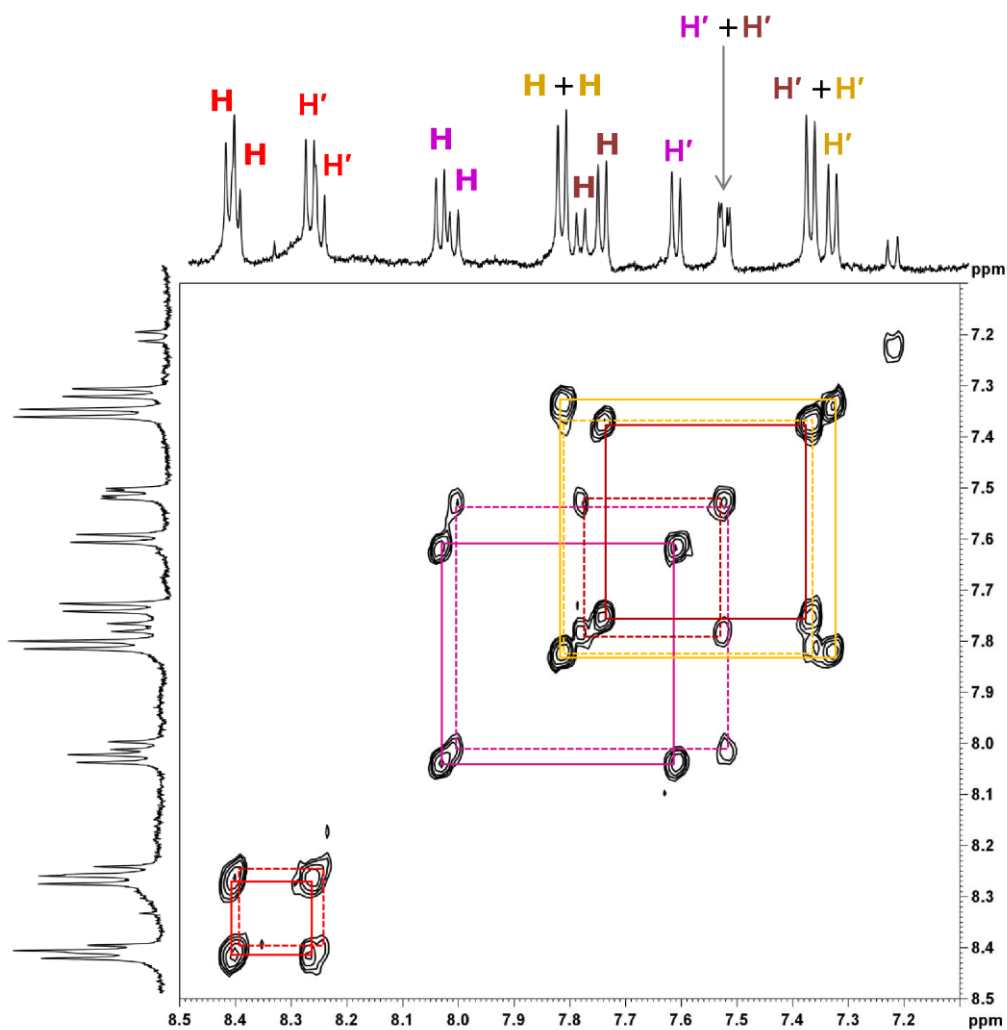


Figure 4.19. Partial COSY spectrum of **4,4-[3]Cat'** between 7.1 ppm and 8.5 ppm (D_2O , 298 K, 500 MHz). The solvent peak was referenced at 4.79 ppm.

4.3.2.3. Interaction with spermine

The correlation between the efficiency of formation of the catenanes and the position of the carboxylates is also validated by comparing the amplification of the two catenanes in the presence of salt (1 M $NaNO_3$) and of spermine (0.5 mM).

We showed in Chapter 3 that addition of either salt or spermine changes the mechanism of formation of **4,4-[3]Cat**: upon addition of salt, the increased polarity of the reaction medium encourages the burying of solvent-exposed hydrophobic surfaces; while the addition of spermine may limit the repulsion between the building blocks by binding to the array of negative charges of the carboxylates on the solvent-accessible surface of the catenane.

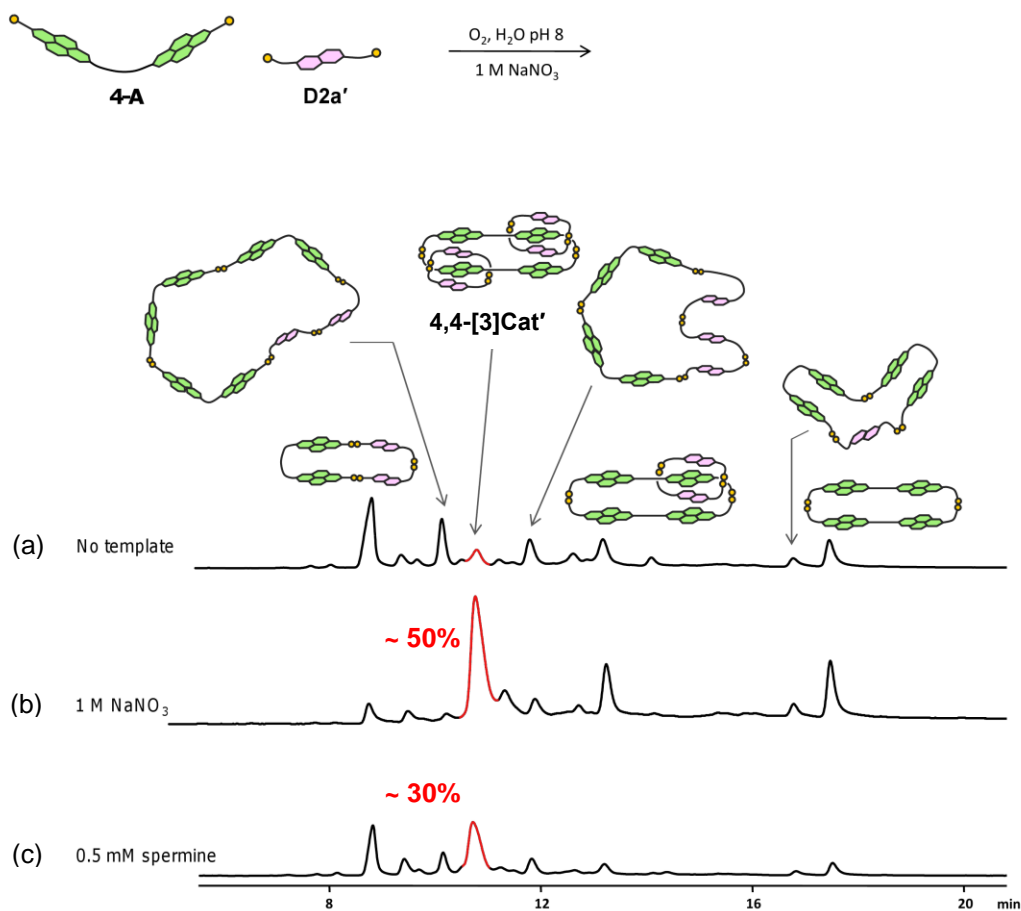


Figure 4.20. HPLC analysis of an aqueous library composed of **4-A** and **D2a'** (1:2 molar ratio, 5 mM total): (a) in the absence of $NaNO_3$, (b) in presence of 1 M of $NaNO_3$ and (c) in presence of 0.5 mM of spermine. The absorbance was recorded at 383 nm.

We have seen in Chapter 3 that **4,4-[3]Cat** is less efficiently formed upon addition of 1 M NaNO₃ (33% yield) than upon addition of spermine (60%, Figure 3.13): the increase in polarity does not prevent the repulsion between the carboxylates, while the positively charged ammoniums of spermine favourably bridges them.

Conversely, **4,4-[3]Cat'** is better amplified by the addition of salt (50%) than by addition of spermine (30%, Figure 4.20). We speculate that in this case, the position of the carboxylates, presumably situated further apart from one another, does not prevent the hydrophobic-driven assembly of the catenane as strongly, but does not interact as well with spermine.

4.3.3. Conclusion on the effect of chirality

In conclusion, changing the building blocks chirality proved to be an efficient way for increasing the yield of catenane, perhaps by minimizing the unfavoured interactions between the carboxylates. While we identified in the first series of catenanes **4-A** and **9-A** as the best acceptor building blocks to form [3] and [2]catenanes respectively (Figure 4.3), this second series allowed us to identify **D2a'** as the most favourable complementary donor building block.

The combination of **9-A** and **D2a'** leads to the nearly quantitative assembly of **9-[2]Cat'**. In a similar fashion, the combination of **4-A** and **D2a'** produces **4,4-[3]Cat'** in 50% yield, and its yield could be further improved to 70% by the stepwise addition of **D2a'** (Figure 4.21). These yields are the best yields obtained to date in dynamic combinatorial systems for the synthesis of donor-acceptor [2] and [3]catenanes.

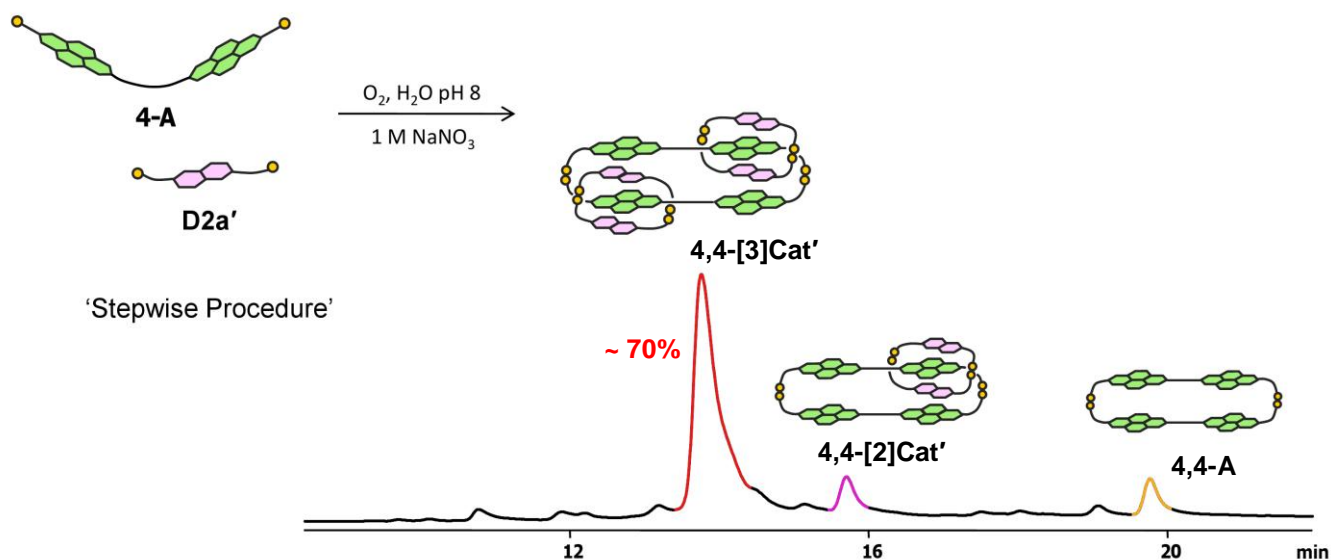


Figure 4.21. HPLC analysis of an aqueous library composed of 4-A and D2a' (1:2 molar ratio, 5 mM total), in the presence of 1 M of NaNO₃. The two equivalents of D2a' were added in fractions of 0.5 equivalents every two hours (stepwise procedure). Absorbance was recorded at 383 nm.

4.4. Conclusion

A striking variety of catenanes and macrocycles has been identified in this Chapter. Linking two acceptor units within one building block has the potential to force the system to form complex architectures and exert significant control on the distribution of the library. Short aliphatic linkers exhibit an odd-even effect, forming either clean libraries containing mostly concatenated species, or relatively iso-energetic libraries containing unexpectedly large [2]catenanes. Both the length of the aliphatic chain linker and the chirality of the building blocks dictate the effective formation of [2] or [3]catenanes.

The assembly of catenanes from linear building blocks is a delicate process, and small differences in the building block structure might result in either low or high yield of catenane. This work shows that a

simple screening of similar dynamic combinatorial systems allows fast selection and optimization of the best conditions for catenane synthesis: water-soluble donor-acceptor [2]catenanes and [3]catenanes have been synthesized with the highest yields to date of up to approximately 90% and 70% respectively.

References:

1. About dynamic combinatorial chemistry, see: (a) Herrmann, A. *Org. Biomol. Chem.* **2009**, *7*, 3195; (b) Ladame, S. *Org. Biomol. Chem.* **2008**, *6*, 219; (c) Lehn, J.-M. *Chem. Soc. Rev.* **2007**, *36*, 151; (d) Rozenman, M. M.; McNaughton, B. R.; Liu, D. R. *Curr. Opin. Chem. Biol.* **2007**, *11*, 259; (e) Corbett, P. T.; Leclaire, J.; Vial, L.; West, K. R.; Wietor, J.-L.; Sanders, J. K. M.; Otto, S. *Chem. Rev.* **2006**, *106*, 3652; (f) de Bruin, B.; Hauwert, P.; Reek, J. N. H. *Angew. Chem. Int. Ed.* **2006**, *45*, 2660.
2. (a) Cougnon, F. B. L.; Au-Yeung, H. Y.; Pantoş, G. D.; Sanders, J. K. M. *J. Am. Chem. Soc.* **2011**, *133*, 3198; (b) Au-Yeung, H. Y.; Pantoş, G. D.; Sanders, J. K. M. *J. Org. Chem.* **2011**, *76*, 1257; (c) Au-Yeung, H. Y.; Pantoş, G. D.; Sanders, J. K. M. *Angew. Chem. Int. Ed.* **2010**, *49*, 5331; (d) Au-Yeung, H. Y.; Pantoş, G. D.; Sanders, J. K. M. *J. Am. Chem. Soc.* **2009**, *131*, 16030; (e) Au-Yeung, H. Y.; Pantoş, G. D.; Sanders, J. K. M. *Proc. Natl. Acad. Sci. USA.* **2009**, *106*, 10466.
3. For other examples of [2]catenane discovery from dynamic combinatorial chemistry: (a) Chung, M.-K.; White, P. S.; Lee, S. J.; Gagné, M. R. *Angew. Chem. Int. Ed.* **2009**, *48*, 8683; (b) West, K. R.; Ludlow, R. F.; Corbett, P. T.; Besenius, P.; Mansfeld, F. M.; Cormack, P. A. G.; Sherrington, D. G.; Goodman, J. M.; Stuart, M. C. A.; Otto, S. *J. Am. Chem. Soc.* **2008**, *130*, 12218; (c) Lam, R. T. S.; Belenguer, A.; Roberts, S. L.; Naumann, C.; Jarrosson, T.; Otto, S.; Sanders, J. K. M. *Science* **2005**, *308*, 667.
4. (a) Patel, K.; Miljanić, O. Š.; Stoddart, J. F.; *Chem. Commun.* **2008**, 1853; (b) Ashton, P. R.; Brown, C. L.; Chrystal, E. J. T.; Goodnow, T. T.; Kaifer, A. E.; Parry, K. P.; Slawin, A. M. Z.; Spencer, N.; Stoddart, J. F.; Williams, D. J. *Angew. Chem. Int. Ed.* **1991**, *30*, 1039; (c) Coskun, A.; Spruell, J. M.; Barin, G.; Fahrenbach, A. C.; Forgan, R. S.; Colvin, M. T.; Carmieli, R.; Benítez, D.; Tkatchouk, E.; Friedman, D. C.; Sarjeant, A. A.; Wasielewski, M. R.; Goddard III, W. A.; Stoddart, J. F. *J. Am. Chem*

Soc. **2011**, *133*, 4538; (d) Spruell, J. M. et al. *Nature Chem.* **2010**, *2*, 870; (e) Ashton, P. R.; Boyd, S. E.; Claessens, C. G.; Gillard, R. E.; Menzer, S.; Stoodart, J. F.; Tolley, M. S.; White, A. J. P.; Williams, D. *J. Chem. Eur. J.* **1997**, 788.

5. (a) Blanco, V.; Chas, M.; Abella, D.; Peinador, C.; Quintela, J. M. *J. Am. Chem. Soc.* **2007**, *129*, 13978; (b) Chas, M.; Blanco, V.; Peinador, C.; Quintela, J. M. *Org. Lett.* **2007**, *9*, 675; (c) Hubbard, A. L.; Davidson, G. J. E.; Patel, R. H.; Wisner, J. A.; Loeb, S. J. *Chem. Comm.* **2004**, 138; (d) Hamilton, D. G.; Feeder, N.; Teat, S. J.; Sanders, J. K. M. *New J. Chem.* **1998**, 1019; (e) Hamilton, D. G.; Feeder, N.; Prodi, L.; Teat, S. J.; Clegg, W.; Sanders, J. K. M. *J. Am. Chem. Soc.* **1998**, *120*, 1096; (f) Hori, A.; Kumazawa, K.; Kusukawa, T.; Chand, D. K.; Fujita, M.; Sakamoto, S.; Yamaguchi, K. *Chem. Eur. J.* **2001**, *7*, 4142.

6. For the synthesis of asymmetrically substituted 1,4,5,8-naphthalenetetracarboxylic diimides, see: Tambara, K.; Ponnuswamy, N.; Hennrich, G.; Pantoş, G. D. *J. Org. Chem.* **2011**, *76*, 3338.

7. For the use of salt to increase medium polarity, see: (a) Fujita, M.; Ibukuro, F.; Hagihara, H.; Ogura, K. *Nature* **1994**, *367*, 720; (b) Fujita, M.; Ibukuro, F.; Ogura, K. *J. Am. Chem. Soc.* **1995**, *117*, 4175.

8. For examples of odd-even effect, see: (a) Stals, P. J. M.; Smulders, M. M. J.; Martín-Rapún, R.; Palmans, A. R. A.; Meijer, E. W. *Chem. Eur. J.* **2009**, *9*, 2071; (b) Lermo, E. R.; Langeveld-Voss, B.; Janssen, R. A. J.; Meijer, E. W. *Chem. Commun.* **1999**, 791; (c) de Jeu, W. H.; van der Veen, J. *Mol. Cryst. Liq. Cryst.* **1977**, *40*, 1; (d) Amabilino, D. B.; Serrano, J.-L.; Sierra, T.; Veciana, J. *J. Pol. Sci. Part A: Polym. Chem.* **2006**, *44*, 3161; (e) Amabilino, D. B.; Ramos, E.; Serrano, J.-L.; Sierra, T.; Veciana, J. *J. Am. Chem. Soc.* **1998**, *120*, 9126; (f) Nakashima, H.; Koe, J. R.; Torimitsu, K.; Fujiki, M. *J. Am. Chem. Soc.* **2001**, *123*, 4847; (g) Zhi, J.; Zhu, Z.; Liu, A.; Cui, J.; Wan, X.; Zhou, Q.

Macromolecules **2008**, *41*, 1594; (h) Dauselt, J.; Zhao, J.; Kind, M.; Binder, R.; Bashir, A.; Terfort, A.; Zharnikov, M. *J. Phys. Chem. C* **2011**, *115*, 2841.

9. Au-Yeung, H. Y.; Pengo, P.; Pantoş, G. D.; Otto, S.; Sanders, J. K. M. *Chem. Commun.* **2009**, 419.

10. (a) Bulos, F.; Roberts, S. L.; Furlan, R. L. E.; Sanders, J. K. M. *Chem. Commun.* **2007**, 3092; (b)

Liu, J.; West, K. R.; Bondy, C. R.; Sanders, J. K. M. *Org. Biomol. Chem.* **2007**, *5*, 778.

CHAPTER 5

Conclusion

This work describes the discovery of a new family of donor-acceptor [2]catenanes, containing the DADD, DAAD, DADA and AADA stacks, from aqueous dynamic combinatorial libraries (Chapter 2). Most of these [2]catenanes have previously been regarded as unfavourable and inaccessible. They have proved, however, to be remarkably common in aqueous libraries. In a similar fashion, the assembly of [3]catenanes from simple and linear building blocks challenges traditional routes of synthesis (Chapter 3 and 4).

Beyond the satisfaction of synthesising a variety of unprecedented catenanes, the work presented in this thesis shows that prejudices can often inhibit the imagination of chemists when building complex architectures: donor-acceptor catenanes have traditionally been regarded as difficult molecules to access, and the fear of taking less traveled roads has restricted their synthesis in many ways.

This work also highlights the fact that fundamental chemical interactions, such as hydrophobic effect and donor-acceptor interactions, are still poorly understood, and that their potential to control and direct the synthesis of large delicate structures remains largely unexplored.

CHAPTER 6

Experimental

6.1. General Information

6.1.1. Chemicals and solvents

Organic solvents were of reagent grade. Dichloromethane was distilled and dimethylformamide (DMF) was dried over 4 Å molecular sieve under N₂. Commercially available chemicals were used as received.

Building blocks **D1a**,¹ **D2a**,² **D1b**,³ **D2b**,⁴ **A1**,^{5, 6} **A2**,¹ were synthesised by Dr Ho Yu Au-Yeung according to published procedures.

6.1.2. DCL preparations

Preparation of a ‘one-pot’ library. 5 mM stock solutions of acceptor and donor building blocks were separately prepared by dissolving the building blocks in 10 mM aqueous NaOH, followed by titration with 100 mM NaOH to pH 8. The stock solutions were mixed in the relevant ratio to get the library.

When necessary, salt (NaNO_3) was added directly in solid form to give a 1 M solution. The final library solutions (0.5 mL) were stirred in close-capped vials for at least one day before LC-MS analysis.

Preparation of a ‘templated’ library. 7 mM stock solutions of acceptor and donor building blocks were separately prepared by dissolving the building blocks in 10 mM aqueous NaOH, followed by titration with 100 mM NaOH to pH 8. The stock solutions were mixed in the relevant ratio to get the library, and diluted with a concentrated aqueous stock solution of template to reach a total concentration in building blocks of 5 mM, and the appropriate concentration of template. The final library solutions (0.5 mL) were stirred in close-capped vials for at least one day before LC-MS analysis.

Preparation of a ‘stepwise addition’ library. A 5 mM stock solution (0.2 mL) was prepared by dissolving the acceptor building block in 10 mM aqueous NaOH, followed by titration with 100 mM NaOH to pH 8. NaNO_3 was added directly in solid form to give a 1 M solution. Every 2 hours, 50 μL of a freshly prepared aqueous 5 mM stock solution of donor building block (1 M NaNO_3 , pH 8) was added. The addition was repeated 4 times before LC-MS analysis.

6.1.3. NMR

^1H and ^{13}C NMR spectra were recorded on Bruker DPX-400 or Avance 500 TCI Cryo Spectrometers. All signals were internally referenced to the solvent residue. The following abbreviations are used in reporting signal multiplicity: s (singlet), d (doublet), t (triplet), q (quartet), m (multiplet) and br (broad signal). The isolated catenanes and macrocycles were solubilised in D_2O with a minimum amount of NaOD.

6.1.4. LC-MS

LC-MS grade acetonitrile (Rathburn), methanol (Fischer) and formic acid (FA) (Fluka) were used without further purification. MilliQ water was obtained from a Millipore water purification system. In general, analytical separations were achieved by injecting 5 μ l aliquots of 5 mM library solution onto a reverse phase Symmetry C₈ column (150 x 4.6 cm, 3 μ m particle size) or a Symmetry C₁₈ column (250 x 4.6 cm, 5 μ m particle size). UV/Vis absorbance was monitored at 260 nm, 292 nm, and 383 nm. Separations were achieved by running the column with acetonitrile/water or methanol/water as eluent at a flow rate of 1 ml/min at 45 °C.

LC-MS was carried out on an Agilent 1100 LC/MSD trap XCT system. Data was processed using HP ChemStation and LC/MSD trap software. Influx of analyte solution was maintained at a flow rate of 50 μ l/min and ionised with an electrospray source (ESI).

6.1.5. Preparative HPLC

Preparative DCLs were made on a 10 ml scale using the same method as the analytical libraries. Preparative separations were performed on a HP 1050 system coupled to a single variable wavelength UV detector. Samples were injected onto a reverse phase SymmetryPrep C₁₈ column (300 x 7.8 mm, 7 μ m particle size) by using a Gilson 234 auto-injector. The same elution profile as that for the analytical separation was used, with HPLC grade acetonitrile (Fischer), MilliQ water and formic acid (Romil). Fractions were manually collected and combined. Solvents were removed from the combined fractions by a rotary evaporator. The isolated samples were dried *in vacuo* and stored in the fridge.

6.1.6. UV-Vis

UV/Vis spectra were recorded using a Cary 400 UV Spectrometer at 298 K. The spectra were scanned from 250 nm to 700 nm with a 0.5 nm interval at a scan of 300 nm/min. Cells of 0.1 cm path length were used.

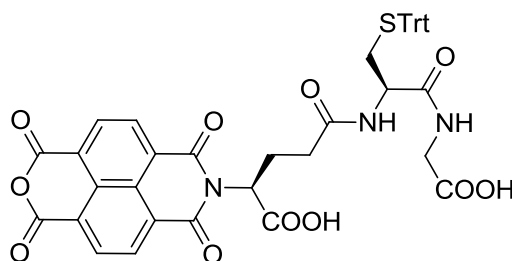
6.1.7. Other analytical methods

All high-resolution (HR) electrospray ionisation (ESI) mass spectra were recorded on Waters LCT Premier XE instrument. Melting points were measured by a Gallenkamp instrument in an open capillary. The microwave reactions were carried out in a CEM Discover system.

6.2. Synthesis of the building blocks

6.2.1. Synthesis of building block A4

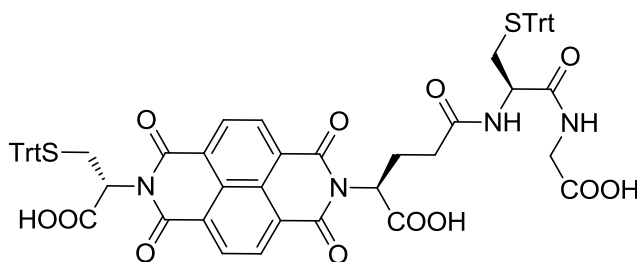
Synthesis of 21:



1,4,5,8-Naphthalenetetracarboxylic dianhydride (100 mg, 373 μmol) and the trityl protected glutathione (247 mg, 373 μmol) were suspended in 3 mL of DMF in a pressure-tight 8 mL microwave vial (the trityl protected glutathione was synthesised according to the literature).⁷ To this suspension was added 0.1 mL of dry Et_3N . The suspension was sonicated until the mixture became homogeneous. The reaction mixture was heated for 5 min at 70 ± 5 °C (direct flask temperature measurement) under microwave irradiation using a dedicated microwave system. The solvent was removed under reduced pressure. The residue was taken up into a minimum volume of acetone. This solution was added under stirring to 100 mL of 1 M HCl. The resulting suspension was filtered using a Büchner funnel. The solid was then washed with 100 mL deionized water and dried *in vacuo*. The product was obtained in the form of a yellow solid. Yield: 209 mg, 70%. M.p.: 170–172 °C (decomposed). ^1H NMR (400 MHz, $\text{DMSO-}d_6$, 300 K) δ (ppm): 13.2–12.2 (br, 2 H, COOH), 8.72 (d, $J = 8$ Hz, 2 H, NDI), 8.66 (d, $J = 8$ Hz, 2 H, NDI), 8.01 (t, $J = 6$ Hz, 1 H, NH–Gly), 7.95 (d, $J = 8$ Hz, 1 H, NH–Cys), 7.36–7.17 (m, 15 H, Trt), 5.59–5.51

(m, 1 H, α -Glu), 4.26–4.17 (m, 1 H, α -Cys), 3.17 (d, $J = 6$ Hz, 2 H, α -Gly), 2.36–2.19 (m, 6 H). $^{13}\text{C}\{^1\text{H}\}$ NMR (100 MHz, DMSO- d_6 , 300 K) δ (ppm): 171.5, 171.1, 170.2, 169.5, 163.4, 162.8, 145.4, 143.6, 132.7, 130.2, 129.2, 128.0, 127.9, 127.6, 126.9, 127.3, 124.2, 66.7, 53.5, 51.4, 40.4, 33.8, 31.9, 30.2. HRMS (ESI+) calcd. for $\text{C}_{43}\text{H}_{33}\text{N}_3\text{O}_{11}\text{SNa}$ $[\text{M}+\text{Na}]^+$ (m/z): 822.1728, found: 822.1703.

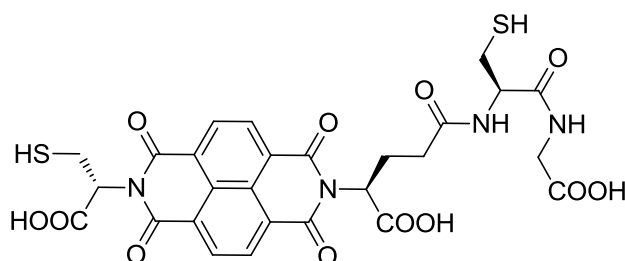
Synthesis of 22:



Compound **21** (200 mg, 250 μmol) and the trityl protected cysteine (86 mg, 250 μmol) were suspended in 4 mL of DMF in a pressure-tight 8 mL microwave vial. To this suspension was added 0.2 mL of dry Et_3N . The suspension was sonicated until the mixture became homogeneous. The reaction mixture was heated for 5 min at 140 ± 5 $^\circ\text{C}$ (direct flask temperature measurement) under microwave irradiation using a dedicated microwave system. The solvent was removed under reduced pressure. The residue was taken up into a minimum volume of acetone. This solution was added under stirring to 100 mL of 1 M HCl. The resulting suspension was filtered using a Büchner funnel. The solid was then washed with 100 mL deionized water and dried *in vacuo*. The product was obtained in the form of a yellow solid. Yield: 245 mg, 86%. M.p.: 178–182 $^\circ\text{C}$ (decomposed). ^1H NMR (400 MHz, DMSO- d_6 , 300 K) δ (ppm): 13.3–12.2 (br, 3 H, COOH), 8.70 (s, 4 H, NDI), 8.06 (t, $J = 6$ Hz, 1 H, NH-Gly), 7.93 (d, $J = 8$ Hz, 1 H, NH-Cys), 7.37–7.13 (m, 30 H, Trt), 5.62–5.53 (m, 2 H, α -Glu and α -Cys), 4.35–4.25 (m, 1 H, α -Cys), 3.63 (d, $J = 6$ Hz, 2 H, α -Gly), 3.25–2.91 (m, 2 H), 2.37–2.19 (m, 6 H). $^{13}\text{C}\{^1\text{H}\}$ NMR (100 MHz,

DMSO-*d*₆, 300 K) δ (ppm): 171.3, 170.8, 170.6, 170.1, 169.2, 162.4, 162.1, 144.4, 144.1, 131.7, 131.2, 129.2, 129.1, 128.1, 128.0, 127.9, 127.6, 126.9, 126.8, 126.5, 125.5, 66.6, 65.9, 53.2, 52.3, 51.2, 40.7, 33.9, 31.9, 30.3. HRMS (ESI+) calcd. for C₆₅H₃₃N₃O₁₁SNa [M+Na]⁺ (*m/z*): 1167.2915, found: 1167.2930.

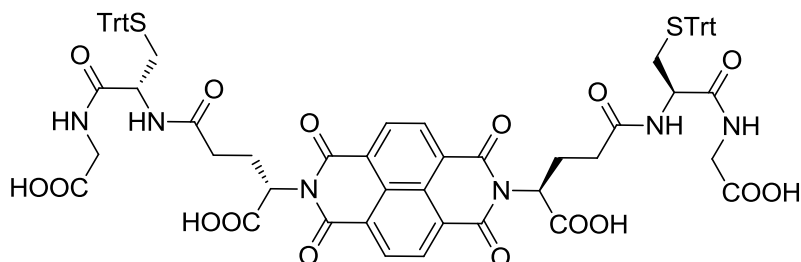
Synthesis of A4:



To a Schlenk flask charged with **22** (220 mg, 192 μ mol) was added degassed trifluoroacetic acid (5 ml), dichloromethane (5 ml), and triethylsilane (100 μ l, 873 μ mol). The solution was stirred under N₂ at room temperature. After 2 hours, all the volatiles were removed in vacuo. The residue was washed with Et₂O (20 ml) and dried *in vacuo*. Yield: 119 mg, 94 %. M.p.: 170–173 °C (decomposed). ¹H NMR (400 MHz, DMSO-*d*₆, 300 K) δ (ppm): 13.5–12.2 (br, 3 H, COOH), 8.78 (d, *J* = 8 Hz, 2 H, NDI), 8.75 (d, *J* = 8 Hz, 2 H, NDI), 8.22–8.18 (m, 1 H, NH–Gly), 7.90 (d, *J* = 8 Hz, 1 H, NH–Cys), 5.73–5.69 (m, 1 H, α –Cys), 5.60–5.56 (m, 1 H, α –Glu), 4.37–4.31 (m, 1 H, α –Cys), 3.74–3.65 (m, 2 H, α –Gly), 3.48–3.18 (m, 2 H), 2.83–2.21 (m, 6 H). ¹³C {¹H} NMR (100 MHz, DMSO-*d*₆, 300 K) δ (ppm): 171.1, 170.2, 170.4, 169.8, 169.1, 162.6, 162.2, 144.1, 143.5, 131.7, 131.1, 126.7, 126.0, 54.5, 52.8, 49.8, 40.6, 33.2, 31.0, 30.8. HRMS (ESI+) calcd. for C₂₇H₂₅N₄O₁₂S₂ [M+H]⁺ (*m/z*): 661.0905, found: 661.0974.

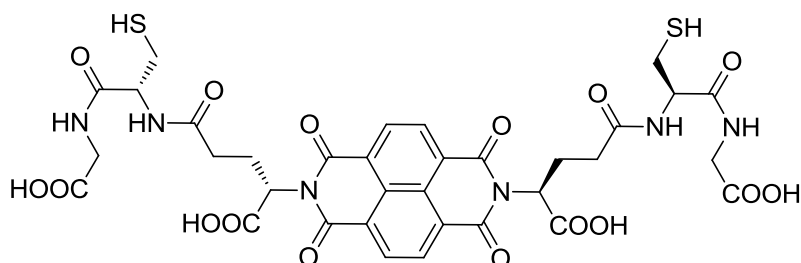
6.2.2. Synthesis of building block A5

Synthesis of 23:



1,4,5,8-Naphthalenetetracarboxylic dianhydride (80 mg, 300 μmol) and the trityl protected glutathione (396 mg, 600 μmol) were suspended in 3 mL of DMF in a pressure-tight 20-mL microwave vial. To this suspension was added 0.1 mL of dry Et_3N . The suspension was sonicated until the mixture became homogeneous. The reaction mixture was heated for 5 min at 140 ± 5 $^\circ\text{C}$ (direct flask temperature measurement) under microwave irradiation using a dedicated microwave system. The solvent was removed under reduced pressure. The residue was taken up into a minimum volume of acetone. This solution was added under stirring to 100 mL of 1 M HCl. The resulting suspension was filtered using a Büchner funnel. The solid was then washed with 100 mL deionized water and dried *in vacuo*. The product was obtained in the form of a brown solid. Yield: 306 mg, 77%. M.p.: > 250 $^\circ\text{C}$ (decomposed). ^1H NMR (400 MHz, $\text{DMSO-}d_6$, 300 K) δ (ppm): 13.1–12.3 (br, 4 H, COOH), 8.69 (s, 4 H, NDI), 8.06 (t, $J = 6$ Hz, 2 H, NH–Gly), 7.99 (d, $J = 8$ Hz, 2 H, NH–Cys), 7.33–7.11 (m, 30 H, Trt), 5.57 (dd, $J = 16$ Hz, 11 Hz, 2 H, α -Glu), 4.29 (dd, $J = 14$ Hz, 8 Hz, 2 H, α -Cys), 3.64 (d, $J = 5.6$ Hz, 4 H, Gly), 2.42–2.21 (m, 12 H). $^{13}\text{C}\{^1\text{H}\}$ NMR (100 MHz, $\text{DMSO-}d_6$, 300 K) δ (ppm): 171.6, 171.1, 170.8, 170.4, 162.7, 144.7, 131.4, 129.4, 128.7, 128.4, 127.0, 126.7, 126.4, 66.1, 53.5, 51.5, 34.2, 32.2, 31.0, 24.6. HRMS (ESI+) calcd. for $\text{C}_{72}\text{H}_{63}\text{N}_6\text{O}_{16}\text{S}_2$ $[\text{M}+\text{H}]^+$ (m/z): 1331.3736, found: 1331.3654.

Synthesis of A5:

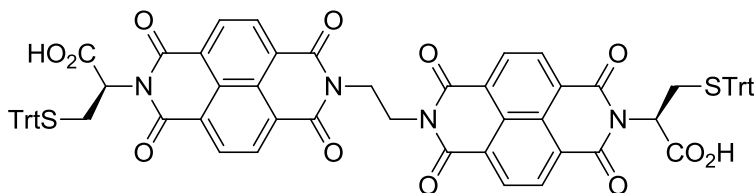


To a Schlenk flask charged with **23** (306 mg, 230 μmol) was added degassed trifluoroacetic acid (3 ml, 40 mmol), dichloromethane (3 ml), and triethylsilane (110 μl , 690 μmol). The solution was stirred under N_2 at room temperature. After 2 hours, all the volatiles were removed in vacuo. The residue was washed with Et_2O (20 ml) and dried *in vacuo*. Yield: 154 mg, 79 %. M.p.: > 250 $^\circ\text{C}$ (decomposed). ^1H NMR (400 MHz, $\text{DMSO-}d_6$, 300 K) δ (ppm): 12.85 (br, 4 H, COOH), 8.75 (s, 4 H, NDI), 8.23 (t, $J = 6$ Hz, 2 H, NH–Gly), 7.90 (d, $J = 8$ Hz, 2 H, NH–Cys), 5.58 (dd, $J = 9$ Hz, 5 Hz, 2 H, α –Glu), 4.35 (dd, $J = 13$ Hz, 7 Hz, 2 H, α –Cys), 3.73 (dd, $J = 11$ Hz, 6 Hz, 4 H, Gly), 2.80–2.63 (m, 4 H), 2.42–2.24 (m, 10 H). $^{13}\text{C}\{^1\text{H}\}$ NMR (100 MHz, $\text{DMSO-}d_6$, 300 K): 173.4, 171.8, 171.3, 170.8, 170.4, 162.8, 131.6, 65.3, 56.7, 54.8, 32.0, 26.7, 24.4, 15.5. HRMS (ESI+) calcd. for $\text{C}_{34}\text{H}_{35}\text{N}_6\text{O}_{16}\text{S}_2$ $[\text{M}+\text{H}]^+$ (m/z): 847.1545, found: 847.1571

6.2.3. Synthesis of the extended building blocks n-A

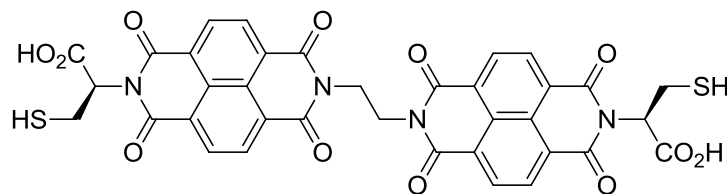
The building blocks **n-A** were initially synthesised by Nicholas A. Jenkins. Precursor **25** was synthesised according to the literature.⁸

Synthesis of 2-A(Trt):



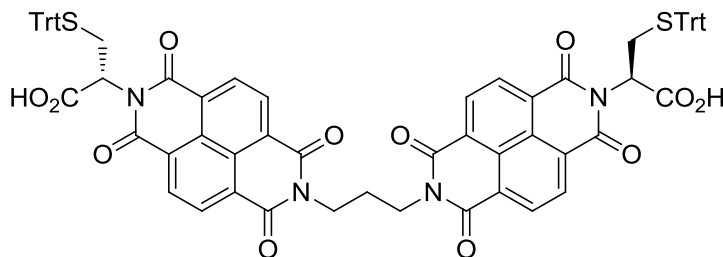
Compound **25** (200 mg, 325 μmol) was suspended in 6 ml of DMF in a pressure-tight 8 mL microwave vial. Et_3N (0.2 ml) and 1,2-diaminoethane (10.9 μl , 162 μmol) were added and the mixture was sonicated until a clear solution resulted. The mixture was then heated for 10 min at 40 ± 5 $^\circ\text{C}$ followed by 5 min at 140 ± 5 $^\circ\text{C}$ under microwave irradiation. The solvent was removed under reduced pressure and the residue was taken up into a minimum volume of acetone. This solution was added to 1 M HCl (200 ml) and the resulting suspension was filtered using a fritted glass funnel. The solid was washed with de-ionized water (100 ml) and dried *in vacuo* to yield a dull orange/brown solid. Yield: 147 mg, 73 %. M.p. 204-208 $^\circ\text{C}$ (decomposed). ^1H NMR (400 MHz, $\text{DMSO-}d_6$, 300 K) δ (ppm): 13.0 (br, 2 H, CO_2H), 8.62 (d, $J = 7.5$ Hz, 4 H, NDI), 8.58 (d, $J = 7.5$ Hz, 4 H, NDI), 7.21-7.12 (m, 30 H, Trt), 5.51 (dd, $J = 4.3, 10.7$ Hz, 2H, α -Cys), 4.55 (br, 4 H, α -Alk), 3.14 (dd, $J = 4.3, 12.7$ Hz, 2 H, β -Cys), 2.93 (dd, $J = 10.7, 12.7$ Hz, 2 H, β -Cys). $^{13}\text{C}\{^1\text{H}\}$ NMR (100 MHz, $\text{DMSO-}d_6$, 300 K) δ (ppm): 169.3, 163.0, 162.0, 144.2, 131.5, 130.8, 129.1, 128.1, 126.9, 126.5, 126.3, 126.2, 125.5, 66.6, 52.6, 38.7, 30.4, 22.2. HRMS (ESI+) calcd. for $\text{C}_{74}\text{H}_{50}\text{N}_4\text{O}_{12}\text{S}_2\text{Na}$ $[\text{M}+\text{Na}]^+$ (m/z): 1273.2759, found: 1273.2752.

Synthesis of 2-A:



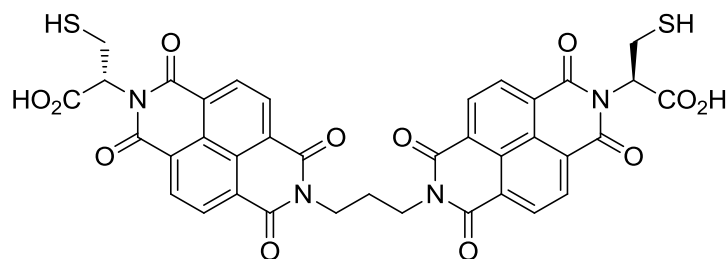
To a flask charged with **2-A(Trt)** (130 mg, 104 μmol) was added trifluoroacetic acid (2 ml), dichloromethane (2 ml), and triethylsilane (100 μl , 873 μmol). After 1 hour, all the volatiles were removed under reduced pressure. The residue was then suspended in Et₂O (30 ml), filtered with a Büchner funnel and washed with Et₂O (15 ml) and dried *in vacuo* to yield a terracotta coloured solid. Yield: 55 mg, 69 %. M.p.: 194-197 °C (decomposed). ¹H NMR (400 MHz, DMSO-*d*₆, 300 K) δ (ppm): 13.2 (br, 2 H, CO₂H), 8.73 (d, *J* = 6.2 Hz, 4 H, NDI), 8.69 (d, *J* = 6.2 Hz, 4 H, NDI), 5.71 (dd, *J* = 5.7 Hz, 9.6 Hz, 2 H, α -Cys), 4.14 (br, 4 H, α -Alk), 3.40-3.17 (m, 4 H, β -Cys), 2.70 (t, *J* = 8.9 Hz, 2 H, SH), 1.80 (br, 4 H, β -Alk). ¹³C {¹H} NMR (100 MHz, DMSO-*d*₆, 300 K) δ (ppm): 169.7, 163.2, 162.6, 131.4, 130.9, 126.5, 126.4, 126.1, 56.2, 22.9, 22.8. HRMS (ESI+) calcd. for C₃₆H₂₂N₄O₁₂S₂Na [M+Na]⁺ (*m/z*): 789.0568, found: 789.0540.

Synthesis of 3-A(Trt)



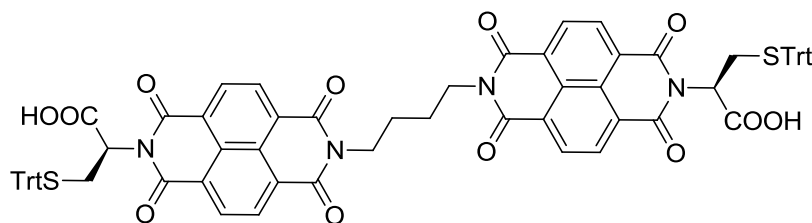
Compound **25** (200 mg, 325 μmol) was suspended in 6 ml of DMF in a pressure-tight 8 mL microwave vial. Et_3N (0.2 ml) and 1,3-diaminopropane (13.6 μl , 162 μmol) were added and the mixture was sonicated until a clear solution resulted. The mixture was then heated for 10 min at 40 ± 5 $^\circ\text{C}$ followed by 5 min at 140 ± 5 $^\circ\text{C}$ under microwave irradiation. The solvent was removed under reduced pressure and the residue was taken up into a minimum volume of acetone. This solution was added to 1 M HCl (200 ml) and the resulting suspension was filtered using a fritted glass funnel. The solid was washed with de-ionized water (100 ml) and dried *in vacuo* to yield a pale yellow solid. Yield: 110 mg, 54 %. M.p.: 198-201 $^\circ\text{C}$ (decomposed). ^1H NMR (400 MHz, $\text{DMSO-}d_6$, 300 K) δ (ppm): 13.1 (br, 2 H, CO_2H), 8.69 (s, 8 H, NDI), 7.21-7.14 (m, 30 H, Trt), 5.54 (dd, $J = 4.3, 10.4$ Hz, 2H, α -Cys), 4.22 (t, 4 H, α -Alk), 3.12 (dd, $J = 4.3, 12.5$ Hz, 2 H, β -Cys), 2.93 (dd, $J = 10.4, 12.5$ Hz, 2 H, β -Cys), 2.14 (m, 2 H, β -Alk). $^{13}\text{C}\{^1\text{H}\}$ NMR (100 MHz, $\text{DMSO-}d_6$, 300 K) δ (ppm): 169.3, 162.7, 162.1, 144.1, 131.6, 130.6, 129.1, 128.1, 127.2, 126.9, 126.5, 126.2, 125.2, 66.6, 52.4, 38.2, 30.4, 26.2. HRMS (ESI+) calcd. for $\text{C}_{75}\text{H}_{52}\text{N}_4\text{O}_{12}\text{S}_2\text{Na}$ $[\text{M}+\text{Na}]^+$ (m/z): 1287.2915, found: 1287.2931.

Synthesis of 3-A



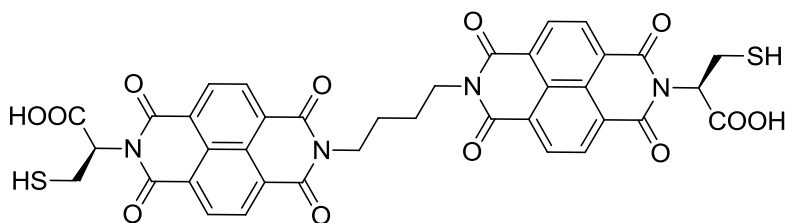
To a flask charged with **3-A(Trt)** (87 mg, 68.8 μmol) was added trifluoroacetic acid (2 ml), dichloromethane (2 ml), and triethylsilane (100 μl , 873 μmol). After 1 hour, all the volatiles were removed under reduced pressure. The residue was then suspended in Et_2O (30 ml), filtered with a Büchner funnel and washed with Et_2O (15 ml) and dried *in vacuo* to yield a light brown coloured solid. Yield: 24 mg, 45 %. M.p.: 187-190 $^{\circ}\text{C}$ (decomposed). ^1H NMR (400 MHz, $\text{DMSO-}d_6$, 300 K) δ (ppm): 13.2 (br, 2 H, CO_2H), 8.73 (d, $J = 6.2$ Hz, 4 H, NDI), 8.69 (d, $J = 6.2$ Hz, 4 H, NDI), 5.71 (dd, $J = 5.7$ Hz, 9.6 Hz, 2 H, α -Cys), 4.14 (br, 4 H, α -Alk), 3.40-3.17 (m, 4 H, β -Cys), 2.70 (t, $J = 8.9$ Hz, 2 H, SH), 1.80 (br, 4 H, β -Alk). $^{13}\text{C}\{^1\text{H}\}$ NMR (100 MHz, $\text{DMSO-}d_6$, 300 K) δ (ppm): 169.8, 162.8, 162.5, 131.3, 130.7, 127.1, 126.4, 125.5, 56.1, 25.3, 22.9. HRMS (ESI+) calcd. for $\text{C}_{37}\text{H}_{24}\text{N}_4\text{O}_{12}\text{S}_2\text{Na}$ $[\text{M}+\text{Na}]^+$ (m/z): 803.0724, found: 803.0713.

Synthesis of 4-A(Trt)



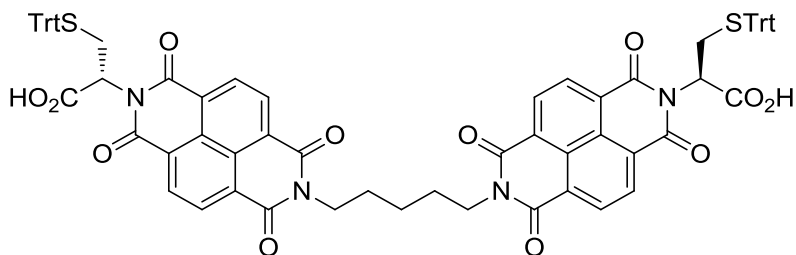
Compound **25** (200 mg, 325 μmol) was suspended in 6 ml of DMF in a pressure-tight 8 mL microwave vial. Et_3N (0.2 ml) and 1,4-diaminobutane (16.4 μl , 162 μmol) were added and the mixture was sonicated until a clear solution resulted. The mixture was then heated for 10 min at 40 ± 5 $^\circ\text{C}$ followed by 5 min at 140 ± 5 $^\circ\text{C}$ under microwave irradiation. The solvent was removed under reduced pressure and the residue was taken up into a minimum volume of acetone. This solution was added to 1 M HCl (200 ml) and the resulting suspension was filtered using a fritted glass funnel. The solid was washed with de-ionized water (100 ml) and dried *in vacuo* to yield a pale yellow solid. Yield: 170 mg, 82 %. M.p.: 198-201 $^\circ\text{C}$ (decomposed). ^1H NMR (400 MHz, $\text{DMSO-}d_6$, 300 K) δ (ppm): 13.2 (br, 2 H, CO_2H), 8.69 (s, 8 H, NDI), 7.22-7.13 (m, 30 H, Trt), 5.54 (dd, $J = 4.2$ Hz, 10.4 Hz, 2 H, α -Cys), 4.14 (br, 4 H, α -Alk), 3.12 (dd, $J = 4.2$ Hz, 12.8 Hz, 2 H, β -Cys), 2.93 (dd, $J = 10.4$ Hz, 12.8 Hz, 2 H, β -Cys), 1.80 (br, 4 H, β -Alk). $^{13}\text{C}\{^1\text{H}\}$ NMR (100 MHz, $\text{DMSO-}d_6$, 300 K) δ (ppm): 169.4, 162.8, 162.1, 144.1, 131.5, 130.6, 129.0, 128.1, 127.9, 127.3, 126.6, 126.2, 125.1, 66.5, 52.3, 39.8, 30.8, 25.1. HRMS (ESI+) calcd. for $\text{C}_{76}\text{H}_{54}\text{N}_4\text{O}_{12}\text{S}_2\text{Na}$ $[\text{M}+\text{Na}]^+$ (m/z): 1301.3072, found: 1301.3099.

Synthesis of 4-A



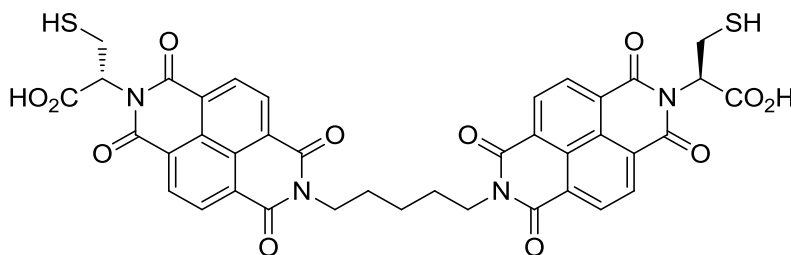
To a flask charged with **4-A(Trt)** (65 mg, 50.8 μmol) was added trifluoroacetic acid (2 ml), dichloromethane (2 ml), and triethylsilane (100 μl , 873 μmol). After 1 hour, all the volatiles were removed under reduced pressure. The residue was then suspended in Et_2O (30 ml), filtered with a Büchner funnel and washed with Et_2O (15 ml) and dried *in vacuo* to yield a cream coloured solid. Yield: 13 mg, 32 %. M.p.: 181-183 $^\circ\text{C}$ (decomposed). ^1H NMR (400 MHz, $\text{DMSO}-d_6$, 300 K) δ (ppm): 13.2 (br, 2 H, CO_2H), 8.73 (d, $J = 6.2$ Hz, 4 H, NDI), 8.69 (d, $J = 6.2$ Hz, 4 H, NDI), 5.71 (dd, $J = 5.7$ Hz, 9.6 Hz, 2 H, α -Cys), 4.14 (br, 4 H, α -Alk), 3.40-3.17 (m, 4 H, β -Cys), 2.70 (t, $J = 8.9$ Hz, 2 H, SH), 1.80 (br, 4 H, β -Alk). $^{13}\text{C}\{^1\text{H}\}$ NMR (100 MHz, $\text{DMSO}-d_6$, 300 K) δ (ppm): 169.7, 162.8, 162.6, 131.4, 130.7, 127.0, 126.4, 125.6, 56.1, 25.2, 22.9. HRMS (ESI+) calcd. for $\text{C}_{38}\text{H}_{26}\text{N}_4\text{O}_{12}\text{S}_2\text{Na}$ $[\text{M}+\text{Na}]^+$ (m/z): 817.0881, found: 817.0873.

Synthesis of 5-A(Trt)



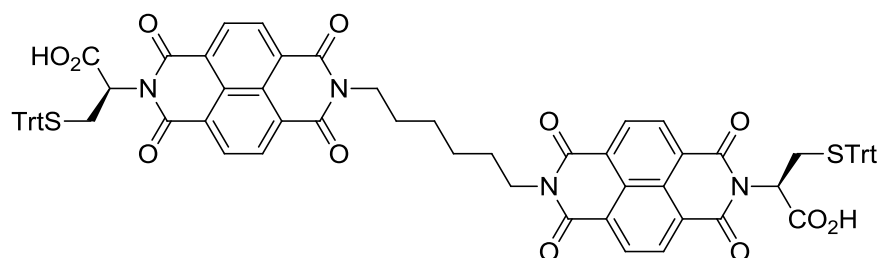
Compound **25** (200 mg, 325 μmol) was suspended in 6 ml of DMF in a pressure-tight 8 mL microwave vial. Et_3N (0.2 ml) and 1,5-diaminopentane (19.1 μl , 162 μmol) were added and the mixture was sonicated until a clear solution resulted. The mixture was then heated for 10 min at 40 ± 5 $^\circ\text{C}$ followed by 5 min at 140 ± 5 $^\circ\text{C}$ under microwave irradiation. The solvent was removed under reduced pressure and the residue was taken up into a minimum volume of acetone. This solution was added to 1 M HCl (200 ml) and the resulting suspension was filtered using a fritted glass funnel. The solid was washed with de-ionized water (100 ml) and dried *in vacuo* to yield a pale yellow solid. Yield: 102 mg, 49 %. M.p. 194-195 $^\circ\text{C}$ - decomposed). ^1H NMR (400 MHz, MeOD, 300 K) δ (ppm): 8.68 (d, $J = 7.6$ Hz, 4 H, NDI), 8.55 (d, $J = 7.6$ Hz, 4 H, NDI), 8.60-8.39 (m, 30 H, Trt), 6.97 (dd, $J = 4.5, 10.5$ Hz, 2 H, α -Cys), 5.46 (t, 4 H, α -Alk), 4.56 (dd, $J = 4.4, 13.0$ Hz, 2 H, β -Cys), 4.44 (dd, $J = 10.5, 13.0$ Hz, 2 H, β -Cys), 3.11 (quintet, 4 H, β -Alk), 2.84 (quintet, 2 H, γ -Alk). ^{13}C $\{^1\text{H}\}$ NMR (100 MHz, DMSO- d_6 , 300 K) δ (ppm): 169.3, 162.7, 162.1, 144.1, 131.6, 130.5, 129.1, 128.1, 127.3, 127.1, 126.6, 126.2, 125.1, 66.6, 52.3, 35.9, 30.4, 27.3, 24.2. HRMS (ESI+) calcd. for $\text{C}_{77}\text{H}_{56}\text{N}_4\text{O}_{12}\text{S}_2\text{Na}$ $[\text{M}+\text{Na}]^+$ (m/z): 1315.3228, found: 1315.3250.

Synthesis of 5-A



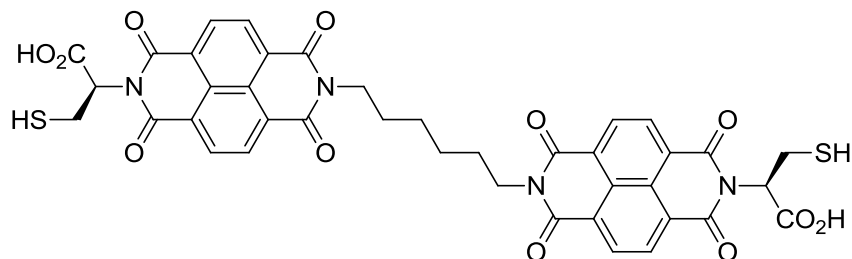
To a flask charged with **5-A(Trt)** (71 mg, 54.9 μmol) was added trifluoroacetic acid (2 ml), dichloromethane (2 ml), and triethylsilane (100 μl , 873 μmol). After 1 hour, all the volatiles were removed under reduced pressure. The residue was then suspended in Et_2O (30 ml), filtered with a Büchner funnel and washed with Et_2O (15 ml) and dried *in vacuo* to yield a yellow coloured solid. Yield: 15 mg, 34 %. M.p.: 181-184 $^\circ\text{C}$ (decomposed). ^1H NMR (400 MHz, $\text{DMSO-}d_6$, 300 K) δ (ppm): 13.2 (br, 2 H, CO_2H), 8.73 (d, $J = 6.2$ Hz, 4 H, NDI), 8.69 (d, $J = 6.2$ Hz, 4 H, NDI), 5.71 (dd, $J = 5.7$ Hz, 9.6 Hz, 2 H, α -Cys), 4.14 (br, 4 H, α -Alk), 3.40-3.17 (m, 4 H, β -Cys), 2.70 (t, $J = 8.9$ Hz, 2 H, SH), 1.80 (br, 4 H, β -Alk). $^{13}\text{C}\{^1\text{H}\}$ NMR (100 MHz, $\text{DMSO-}d_6$, 300 K) δ (ppm): 169.7, 162.6, 162.7, 131.4, 130.5, 127.0, 126.4, 125.6, 56.1, 27.5, 26.2, 30.1, 22.9. HRMS (ESI+) calcd. for $\text{C}_{39}\text{H}_{28}\text{N}_4\text{O}_{12}\text{S}_2\text{Na}$ $[\text{M}+\text{Na}]^+$ (m/z): 831.1037, found: 831.1027.

Synthesis of 6-A(Trt)



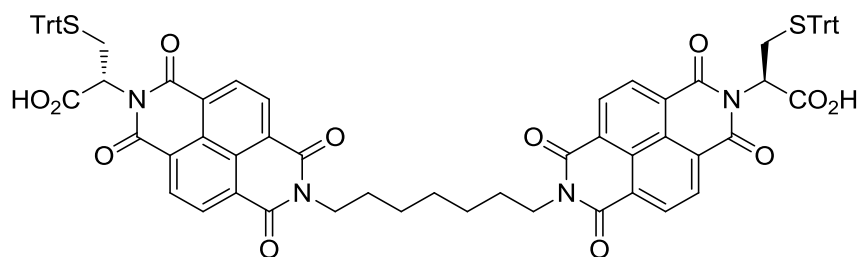
Compound **25** (200 mg, 325 μmol) was suspended in 6 ml of DMF in a pressure-tight 8 mL microwave vial. Et_3N (0.2 ml) and 1,6-diaminohexane (18.9 mg, 162 μmol) were added and the mixture was sonicated until a clear solution resulted. The mixture was then heated for 10 min at 40 ± 5 $^\circ\text{C}$ followed by 5 min at 140 ± 5 $^\circ\text{C}$ under microwave irradiation. The solvent was removed under reduced pressure and the residue was taken up into a minimum volume of acetone. This solution was added to 1 M HCl (200 ml) and the resulting suspension was filtered using a fritted glass funnel. The solid was washed with de-ionized water (100 ml) and dried *in vacuo* to yield a pale yellow solid. Yield: 135 mg, 64 %. M.p.: 191-194 $^\circ\text{C}$ (decomposed). ^1H NMR (400 MHz, CDCl_3 , 300 K) δ (ppm): 8.69 (d, $J = 7.6$ Hz, 4 H, NDI), 8.65 (d, $J = 7.6$, 4 H, NDI), 7.31-7.10 (m, 30 H, Trt), 5.51 (dd, 2 H, α -Cys), 4.18 (t, 4 H, α -Alk), 3.17-3.07 (m, 4 H, α -Cys), 1.75 (br, 4 H, β -Alk), 1.50 (br, 4 H, γ -Alk). $^{13}\text{C}\{^1\text{H}\}$ NMR (100 MHz, $\text{DMSO}-d_6$, 300 K) δ (ppm): 169.3, 162.7, 162.1, 144.1, 131.5, 130.5, 129.1, 128.1, 127.2, 126.9, 126.5, 126.2, 125.1, 66.6, 52.3, 30.4, 27.4, 26.3. HRMS (ESI+) calcd. for $\text{C}_{78}\text{H}_{58}\text{N}_4\text{O}_{12}\text{S}_2\text{Na}$ $[\text{M}+\text{Na}]^+$ (m/z): 1329.3385, found: 1329.3377.

Synthesis of 6-A



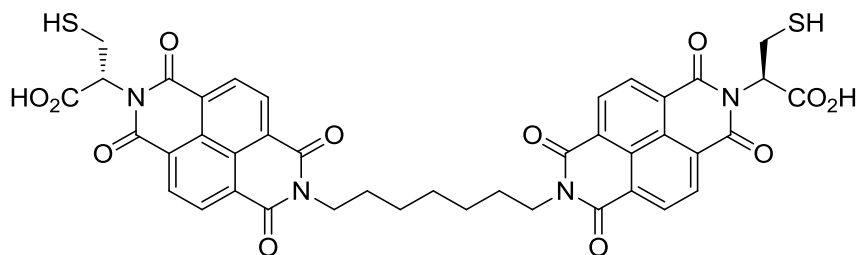
To a flask charged with **6-A(Trt)** (114 mg, 87.2 μmol) was added trifluoroacetic acid (2 ml), dichloromethane (2 ml), and triethylsilane (100 μl , 873 μmol). After 1 hour, all the volatiles were removed under reduced pressure. The residue was then suspended in Et_2O (30 ml), filtered with a Büchner funnel and washed with Et_2O (15 ml) and dried *in vacuo* to yield a pale yellow coloured solid. Yield: 48 mg, 67 %. M.p.: 179-182 $^\circ\text{C}$ (decomposed). ^1H NMR (400 MHz, $\text{DMSO-}d_6$, 300 K) δ (ppm): 13.2 (br, 2 H, CO_2H), 8.73 (d, $J = 6.2$ Hz, 4 H, NDI), 8.69 (d, $J = 6.2$ Hz, 4 H, NDI), 5.71 (dd, $J = 5.7$ Hz, 9.6 Hz, 2 H, α -Cys), 4.14 (br, 4 H, α -Alk), 3.40-3.17 (m, 4 H, β -Cys), 2.70 (t, $J = 8.9$ Hz, 2 H, SH), 1.80 (br, 4 H, β -Alk). $^{13}\text{C}\{^1\text{H}\}$ NMR (100 MHz, $\text{DMSO-}d_6$, 300 K) δ (ppm): 169.7, 162.7, 162.5, 131.4, 130.6, 127.0, 126.5, 125.6, 56.1, 27.5, 26.3, 22.9, 22.8. HRMS (ESI+) calcd. for $\text{C}_{40}\text{H}_{30}\text{N}_4\text{O}_{12}\text{S}_2\text{Na}$ $[\text{M}+\text{Na}]^+$ (m/z): 845.1194, found: 845.1192.

Synthesis of 7-A(Trt)



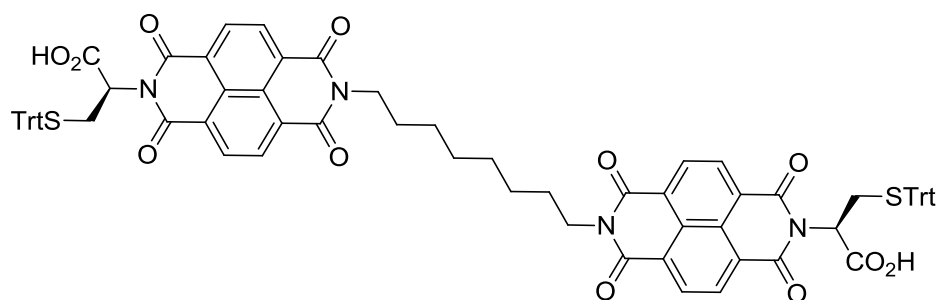
Compound **25** (400 mg, 650 μmol) was suspended in 12 ml of DMF. Et_3N (0.4 ml) and 1,7-diaminoheptane (49.5 μl , 325 μmol) were added and the mixture was sonicated until a clear solution resulted. The mixture was then heated for 10 min at 40 ± 5 $^\circ\text{C}$ followed by 5 min at 140 ± 5 $^\circ\text{C}$ under microwave irradiation. The solvent was removed under reduced pressure and the residue was taken up into a minimum volume of acetone. This solution was added to 1 M HCl (200 ml) and the resulting suspension was filtered using a fritted glass funnel. The solid was washed with de-ionized water (100 ml) and dried *in vacuo* to yield a pale yellow solid. Yield: 380 mg, 89 %. M.p.: 185-186 $^\circ\text{C}$ (decomposed). ^1H NMR (400 MHz, $\text{DMSO-}d_6$, 300 K) δ (ppm): 13.1 (br, 2 H, CO_2H), 8.69 (s, 8 H, NDI), 7.23-7.13 (m, 30 H, Trt), 5.55 (dd, $J = 4.4, 10.5$ Hz, 2 H, α -Cys), 4.07 (t, 4 H, α -Alk), 3.12 (dd, $J = 4.4, 12.7$ Hz, 2 H, β -Cys), 2.93 (dd, $J = 10.5, 12.7$ Hz, 2 H, β -Cys), 1.67 (br, 4 H, β -Alk), 1.40 (br, 6 H, γ, δ -Alk). $^{13}\text{C}\{^1\text{H}\}$ NMR (100 MHz, $\text{DMSO-}d_6$, 300 K) δ (ppm): 169.3, 162.6, 162.1, 144.1, 131.6, 130.5, 129.1, 128.1, 127.2, 126.9, 126.5, 126.2, 125.1, 66.6, 52.4, 40.2, 30.4, 28.6, 27.4, 26.5. HRMS (ESI+) calcd. for $\text{C}_{79}\text{H}_{60}\text{N}_4\text{O}_{12}\text{S}_2\text{Na}$ $[\text{M}+\text{Na}]^+$ (m/z): 1343.3541, found: 1343.3536.

Synthesis of 7-A

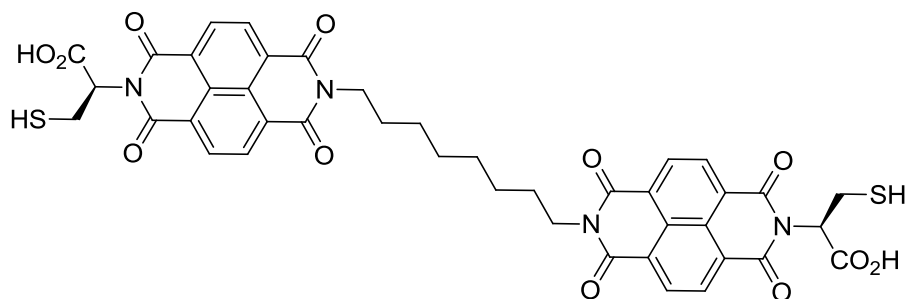


To a flask charged with **7-A(Trt)** (72 mg, 54.5 μmol) was added trifluoroacetic acid (2 ml), dichloromethane (2 ml), and triethylsilane (100 μl , 873 μmol). After 1 hour, all the volatiles were removed under reduced pressure. The residue was then suspended in Et_2O (30 ml), filtered with a Büchner funnel and washed with Et_2O (15 ml) and dried *in vacuo* to yield a pale yellow coloured solid. Yield: 28 mg, 61 %. M.p.: 175-177 $^\circ\text{C}$ (decomposed). ^1H NMR (400 MHz, $\text{DMSO}-d_6$, 300 K) δ (ppm): 13.2 (br, 2 H, CO_2H), 8.73 (d, $J = 6.2$ Hz, 4 H, NDI), 8.69 (d, $J = 6.2$ Hz, 4 H, NDI), 5.71 (dd, $J = 5.7$ Hz, 9.6 Hz, 2 H, α -Cys), 4.14 (br, 4 H, α - Alk), 3.40-3.17 (m, 4 H, β -Cys), 2.70 (t, $J = 8.9$ Hz, 2 H, SH), 1.80 (br, 4 H, β - Alk). $^{13}\text{C}\{^1\text{H}\}$ NMR (100 MHz, $\text{DMSO}-d_6$, 300 K) δ (ppm): 169.8, 162.7, 162.6, 131.5, 130.7, 127.0, 126.4, 125.7, 56.2, 28.6, 27.5, 26.5, 23.0, 22.9. HRMS (ESI+) calcd. for $\text{C}_{41}\text{H}_{32}\text{N}_4\text{O}_{12}\text{S}_2\text{Na}$ $[\text{M}+\text{Na}]^+$ (m/z): 859.1350, found: 859.1334.

Synthesis of 8-A(Trt)

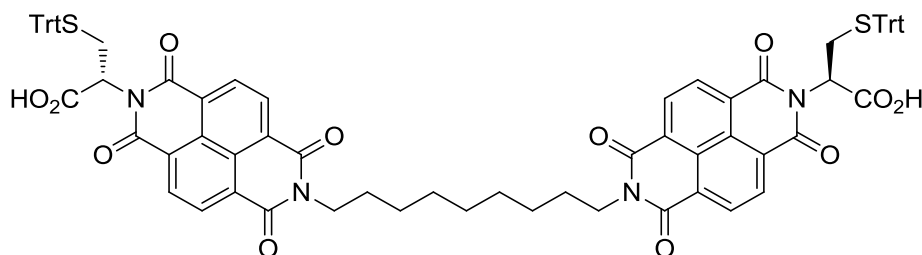


Compound **25** (200 mg, 325 μmol) was suspended in 6 ml of DMF in a pressure-tight 8 mL microwave vial. Et_3N (0.2 ml) and 1,8-diaminooctane (23.5 mg, 162 μmol) were added and the mixture was sonicated until a clear solution resulted. The mixture was then heated for 10 min at 40 ± 5 $^\circ\text{C}$ followed by 5 min at 140 ± 5 $^\circ\text{C}$ under microwave irradiation. The solvent was removed under reduced pressure and the residue was taken up into a minimum volume of acetone. This solution was added to 1 M HCl (200 ml) and the resulting suspension was filtered using a fritted glass funnel. The solid was washed with de-ionized water (100 ml) and dried *in vacuo* to yield a pale yellow solid. Yield: 218 mg, 93 %. M.p.: 180-183 $^\circ\text{C}$ (decomposed). ^1H NMR (400 MHz, $\text{DMSO-}d_6$, 300 K) δ (ppm): 13.1 (br, 2 H, CO_2H), 8.70 (s, 8 H, NDI), 7.22-7.13 (m, 30 H, Trt), 5.55 (dd, $J = 4.3, 10.5$ Hz, 2 H, α -Cys), 4.06 (t, 4 H, α -Alk), 3.12 (dd, $J = 4.3, 12.8$ Hz, 2 H, β -Cys), 2.93 (dd, $J = 10.5, 12.8$ Hz, 2 H, β -Cys), 1.66 (br, 4 H, β -Alk), 1.36 (br, 8 H, γ, δ -Alk). $^{13}\text{C}\{^1\text{H}\}$ NMR (100 MHz, $\text{DMSO-}d_6$, 300 K) δ (ppm): 169.3, 162.7, 162.1, 144.1, 131.6, 130.6, 129.1, 128.1, 127.2, 126.9, 126.5, 126.2, 125.1, 66.6, 52.3, 40.2, 30.4, 28.7, 27.4, 26.5. HRMS (ESI+) calcd. for $\text{C}_{80}\text{H}_{62}\text{N}_4\text{O}_{12}\text{S}_2\text{Na}$ $[\text{M}+\text{Na}]^+$ (m/z): 1357.3698, found: 1357.3688.

Synthesis of **8-A**

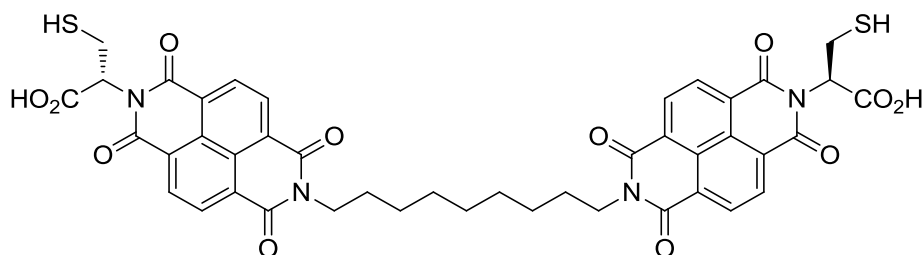
To a flask charged with **8-A(Trt)** (37 mg, 27.7 μmol) was added trifluoroacetic acid (2 ml), dichloromethane (2 ml), and triethylsilane (100 μl , 873 μmol). After 1 hour, all the volatiles were removed under reduced pressure. The residue was then suspended in Et_2O (30 ml), filtered with a Büchner funnel and washed with Et_2O (15 ml) and dried *in vacuo* to yield a pale yellow coloured solid. Yield: 8 mg, 34 %. M.p.: 169-171 $^\circ\text{C}$ (decomposed). ^1H NMR (400 MHz, $\text{DMSO}-d_6$, 300 K) δ (ppm): 13.2 (br, 2 H, CO_2H), 8.73 (d, $J = 6.2$ Hz, 4 H, NDI), 8.69 (d, $J = 6.2$ Hz, 4 H, NDI), 5.71 (dd, $J = 5.7$ Hz, 9.6 Hz, 2 H, α -Cys), 4.14 (br, 4 H, α -Alk), 3.40-3.17 (m, 4 H, β -Cys), 2.70 (t, $J = 8.9$ Hz, 2 H, SH), 1.80 (br, 4 H, β - Alk). $^{13}\text{C}\{^1\text{H}\}$ NMR (100 MHz, $\text{DMSO}-d_6$, 300 K) δ (ppm): 169.6, 162.5, 162.1, 131.3, 130.6, 127.1, 126.3, 125.6, 56.0, 28.7, 27.4, 26.5, 22.8, 22.7. HRMS (ESI+) calcd. for $\text{C}_{42}\text{H}_{34}\text{N}_4\text{O}_{12}\text{S}_2\text{Na}$ $[\text{M}+\text{Na}]^+$ (m/z): 873.1507, found: 873.1490.

Synthesis of 9-A(Trt)



Compound **25** (200 mg, 325 μmol) was suspended in 6 ml of DMF in a pressure-tight 8 mL microwave vial. Et_3N (0.2 ml) and 1,9-diaminononane (25.8 mg, 162 μmol) were added and the mixture was sonicated until a clear solution resulted. The mixture was then heated for 10 min at 40 ± 5 $^\circ\text{C}$ followed by 5 min at 140 ± 5 $^\circ\text{C}$ under microwave irradiation. The solvent was removed under reduced pressure and the residue was taken up into a minimum volume of acetone. This solution was added to 1 M HCl (200 ml) and the resulting suspension was filtered using a fritted glass funnel. The solid was washed with de-ionized water (100 ml) and dried *in vacuo* to yield a pale yellow solid. Yield: 208.6 mg, 96 %. M.p.: 180-183 $^\circ\text{C}$ (decomposed). ^1H NMR (400 MHz, $\text{DMSO-}d_6$, 300 K) δ (ppm): 13.2 (br, 2 H, CO_2H), 8.74 (s, 8 H, NDI), 7.22-7.14 (m, 30 H, Trt), 5.55 (dd, $J = 4.3, 10.5$ Hz, 2 H, $\alpha\text{-Cys}$), 4.05 (t, 4 H, $\alpha\text{-Alk}$), 3.12 (dd, $J = 4.3, 12.8$ Hz, 2 H, $\beta\text{-Cys}$), 2.93 (dd, $J = 10.5, 12.8$ Hz, 2 H, $\beta\text{-Cys}$), 1.66 (br, 4 H, $\beta\text{-Alk}$), 1.31 (br, 10 H, $\gamma, \delta, \epsilon\text{-Alk}$). $^{13}\text{C}\{^1\text{H}\}$ NMR (100 MHz, $\text{DMSO-}d_6$, 300 K) δ (ppm): 169.3, 162.6, 162.1, 144.1, 131.5, 130.5, 129.1, 128.1, 127.2, 126.9, 126.4, 126.1, 125.1, 66.6, 52.3, 40.2, 30.4, 28.9, 28.8, 28.7, 26.5. HRMS (ESI+) calcd. for $\text{C}_{81}\text{H}_{64}\text{N}_4\text{O}_{12}\text{S}_2\text{Na}$ $[\text{M}+\text{Na}]^+$ (m/z): 1371.3854, found: 1371.3844.

Synthesis of 9-A

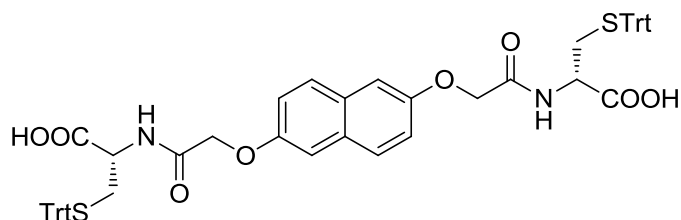


To a flask charged with **9-A(Trt)** (208 mg, 154.5 μmol) was added trifluoroacetic acid (4 ml), dichloromethane (4 ml), and triethylsilane (200 μl , 1.74 mmol). After 1 hour, all the volatiles were removed under reduced pressure. The residue was then suspended in Et_2O (30 ml), filtered with a Büchner funnel and washed with Et_2O (15 ml) and dried *in vacuo* to yield a pale yellow coloured solid. Yield: 55 mg, 41 %. M.p.: 171-172 $^\circ\text{C}$ (decomposed). ^1H NMR (400 MHz, $\text{DMSO}-d_6$, 300 K) δ (ppm): 13.2 (br, 2 H, CO_2H), 8.73 (d, $J = 6.2$ Hz, 4 H, NDI), 8.69 (d, $J = 6.2$ Hz, 4 H, NDI), 5.71 (dd, $J = 5.7$ Hz, 9.6 Hz, 2 H, α -Cys), 4.14 (br, 4 H, α -Alk), 3.40-3.17 (m, 4 H, β -Cys), 2.70 (t, $J = 8.9$ Hz, 2 H, SH), 1.80 (br, 4 H, β -Alk). $^{13}\text{C}\{^1\text{H}\}$ NMR (100 MHz, $\text{DMSO}-d_6$, 300 K) δ (ppm): 169.6, 162.6, 162.1, 131.4, 130.6, 127.2, 126.3, 125.5, 56.0, 28.7, 27.5, 26.9, 26.4, 22.9, 22.7. HRMS (ESI+) calcd. for $\text{C}_{43}\text{H}_{36}\text{N}_4\text{O}_{12}\text{S}_2\text{Na}$ $[\text{M}+\text{Na}]^+$ (m/z): 887.1663, found: 887.1646.

6.2.4. Synthesis of building block D2a'

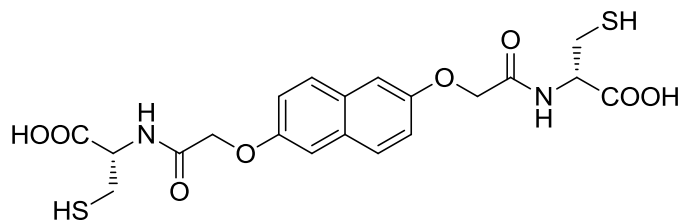
Precursor **26** was synthesised according to the literature.²

Synthesis of **27**:



To a mixture of **26** (300 mg, 637 μmol) and *R*-trityl-*D*-cysteine (481 mg, 1.4 mmol) in DMF (20 ml) was added Et_3N (0.2 ml). The solution was stirred under N_2 for 8 hours at room temperature. Solvent was removed and the residue re-dissolved in acetone (10 ml). The acetone solution was added dropwise to a vigorously stirred solution of 1 M HCl (200 ml). The yellowish-brown solid was collected by filtration and dried. Yield: 524 mg, 85%. M.p.: 173–176 $^\circ\text{C}$. ^1H NMR (400 MHz, $\text{DMSO-}d_6$, 300 K) δ (ppm): 12.88 (br, 2 H, COOH), 8.43 (d, $J = 8.2$ Hz, 2 H, NH), 7.62 (d, $J = 8.9$ Hz, 2 H, DN), 7.24–7.33 (m, 32 H, Trt, DN), 7.16 (dd, $J = 2.5$ Hz, 8.9 Hz, 2 H, DN), 4.61 (s, 4 H, OCH_2), 4.26 (dt, $J = 4.7$ Hz, 8.2 Hz, 2 H, α), 2.68 (dd, $J = 9.0$ Hz, 12.4 Hz, 2 H, β), 2.46 (d, $J = 4.7$ Hz, 2 H, β); $^{13}\text{C}\{^1\text{H}\}$ NMR (100 MHz, $\text{DMSO-}d_6$, 300 K) δ (ppm): 144.2, 129.1, 128.1, 126.8, 66.9, 51.0, 32.9. HRMS (ESI+) calcd. for $\text{C}_{58}\text{H}_{50}\text{N}_2\text{O}_8\text{S}_2\text{Na}$ $[\text{M}+\text{Na}]^+$ (m/z): 989.2906, found: 989.2873.

Synthesis of D2a':



To a Schlenk tube charged with **27** (500 mg, 517 μmol) was added degassed TFA (5 ml, 65 mmol) under N_2 . The solution was stirred at room temperature for 1.5 hour, and triethylsilane added (0.4 ml, 2.5 mmol). Immediate precipitation was observed, and the mixture was stirred for an additional 30 minutes. Volatiles were removed *in vacuo*. The resulting yellow solid was washed with Et_2O (50 ml). Yield: 199 mg, 80%. M.p.: 183–186 $^\circ\text{C}$ (decomposed). ^1H NMR (400 MHz, $\text{DMSO-}d_6$, 300 K) δ (ppm): 8.36 (d, $J = 8.0$ Hz, 2 H, NH), 7.73 (d, $J = 8.9$ Hz, 2 H, DN), 7.30 (d, $J = 2.6$ Hz, 2 H, DN), 7.24 (d, $J = 2.6$ Hz, 8.9 Hz, 2 H, DN), 4.67 (s, 4 H, OCH_2), 4.51 (dt, $J = 4.5$ Hz, 7.6 Hz, 2 H, α), 2.93–3.00 (m, 2 H, β), 2.83–2.90 (m, 2 H, β), 2.43 (t, $J = 8.5$ Hz, 2 H, SH). $^{13}\text{C}\{^1\text{H}\}$ NMR (100 MHz, $\text{DMSO-}d_6$, 300 K) δ (ppm): 171.4, 167.9, 154.2, 129.5, 128.2, 118.9, 107.8, 66.9, 54.0, 25.3. HRMS (ESI+) calcd. for $\text{C}_{20}\text{H}_{23}\text{N}_2\text{O}_8\text{S}_2$ $[\text{M}+\text{H}]^+$ (m/z): 483.0896, found: 483.0898.

6.3. LC-MS analysis of the DCLs

6.3.1. LC-MS methods for Chapter 2

ESI-MS spectra (negative ion) were acquired in ultra scan mode with drying temperature of 350 °C, nebuliser pressure of 18 psi, drying gas flow of 5 l/min. Capillary voltage was set to 4000 V. An ICC target of 20,000 ions or accumulation time of 100 ms, and a target mass of 1000 was set for the trap. Dissociation amplitude of 1 V was used for MS/MS studied.

Figure 2.5 and 2.6: the libraries were analysed using a method previously published.³

Figure 2.9: the library was analysed using *Method 1*.

Figure 2.11: the library was analysed using *Method 2*.

Figure 2.20: the libraries were analysed using methods previously published.^{2,3}

Figure 2.22: the libraries were analysed using *Method 2*.

Figure 2.29: the libraries were analysed using *Method 2*.

Figure 2.33: the libraries were analysed using *Method 3*.

Figure 2.34: the library was analysed using *Method 4*.

Method 1 (using Symmetry C₈ column):

Time/min	H ₂ O (0.1% FA)	MeOH (0.1% FA)
0	60%	40%
25	0%	100%
30	0%	100%

Method 2 (using Symmetry C₈ column):

Time/min	H ₂ O (0.1% FA)	MeOH (0.1% FA)
0	60%	40%
35	0%	100%
40	0%	100%

Method 3 (using Symmetry C₈ column):

Time/min	H ₂ O (0.1% FA)	MeOH (0.1% FA)
0	60%	40%
15	40%	60%
30	40%	60%
40	20%	80%
45	20%	80%

Method 4 (using Symmetry C₁₈ column):

Time/min	H ₂ O (0.1% FA)	MeOH (0.1% FA)
0	60%	40%
30	40%	60%
45	40%	60%

6.3.2. LC-MS method for Chapters 3 and 4

ESI-MS spectra (negative ion) were acquired in ultra scan mode with drying temperature of 350 °C, nebuliser pressure of 18 psi, drying gas flow of 8 l/min. Capillary voltage was set to 3500 V. An ICC target of 50,000 ions or accumulation time of 200 ms, and a target mass of 1200 was set for the trap. Apart when otherwise stated, dissociation amplitude of 0.6 V was used for MS/MS studied.

All the libraries were analysed using a Symmetry C₈ column.

Time/min	H ₂ O (0.1% FA)	Acetonitrile (0.1% FA)
0	70%	30%
40	10%	90%

6.4. MS and MS/MS spectra of the new catenanes

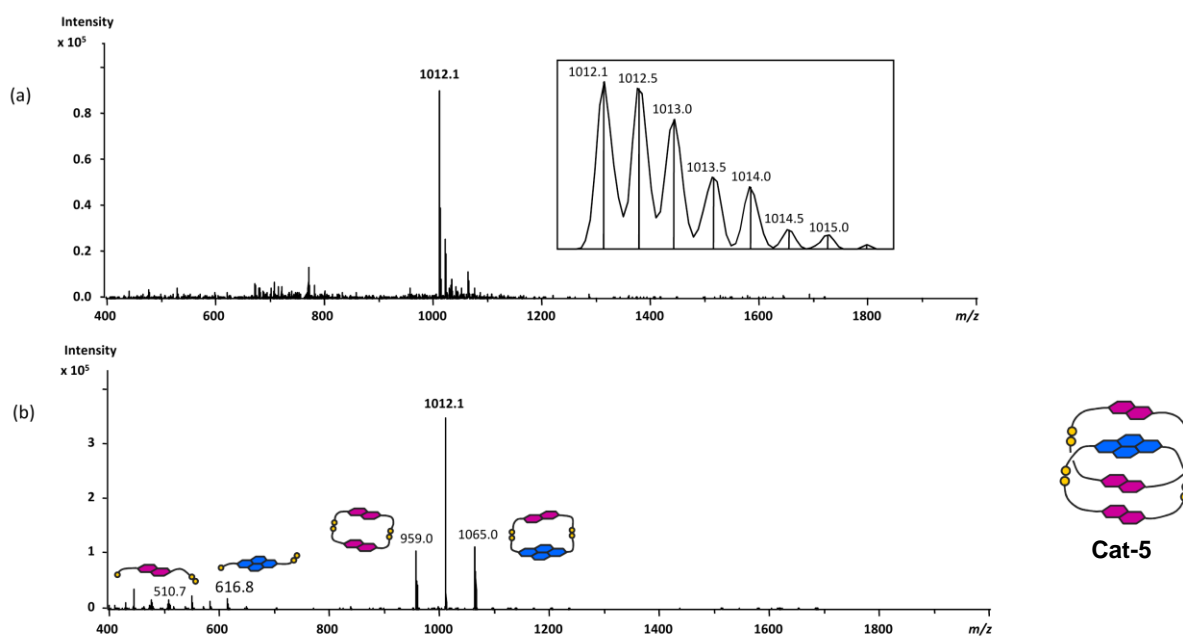


Figure 6.1. Tandem (a) MS and (b) MS/MS fragmentation of Cat-5.

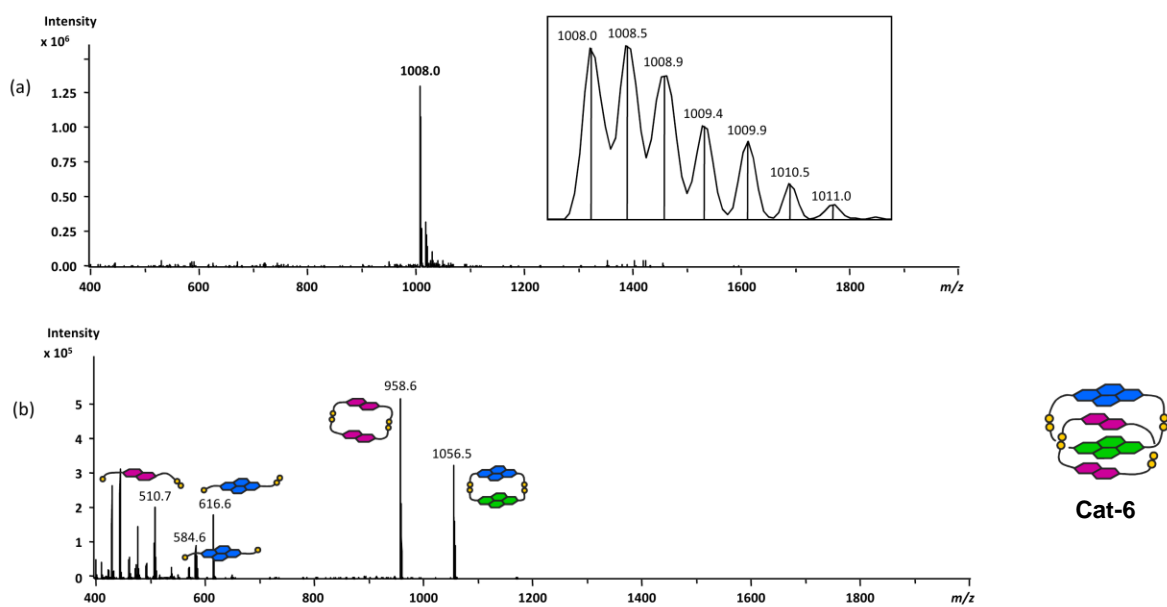


Figure 6.2. Tandem (a) MS and (b) MS/MS fragmentation of Cat-6.

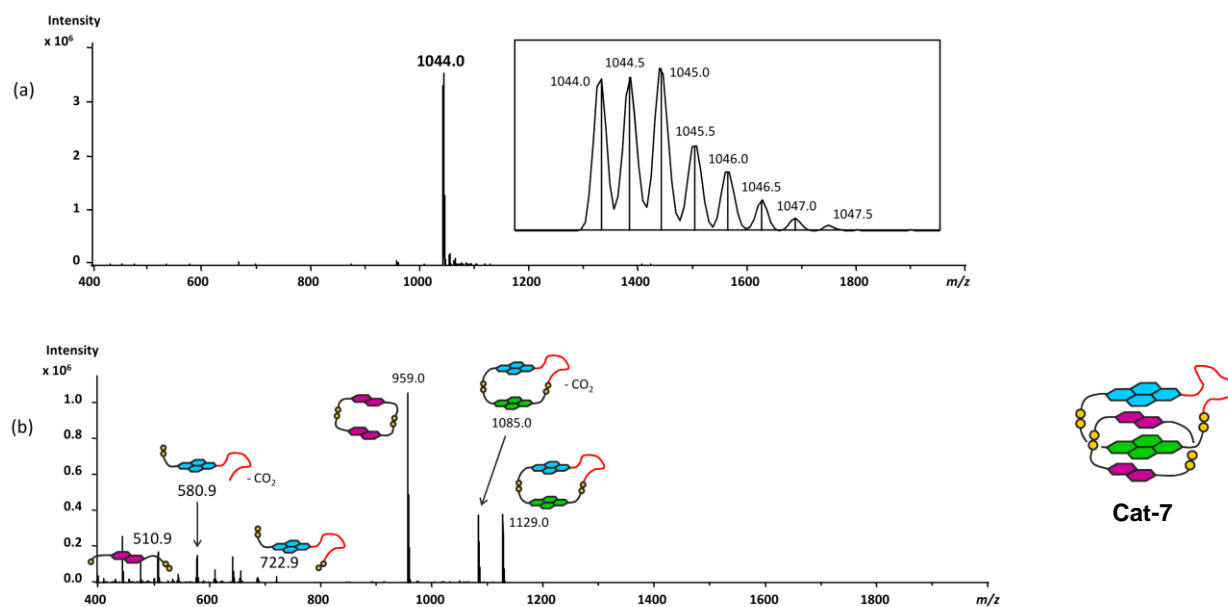


Figure 6.3. Tandem (a) MS and (b) MS/MS fragmentation of **Cat-7**.

The MS and MS/MS of **Cat-10** are identical to the ones of **Cat-8** reported in Chapter 2.

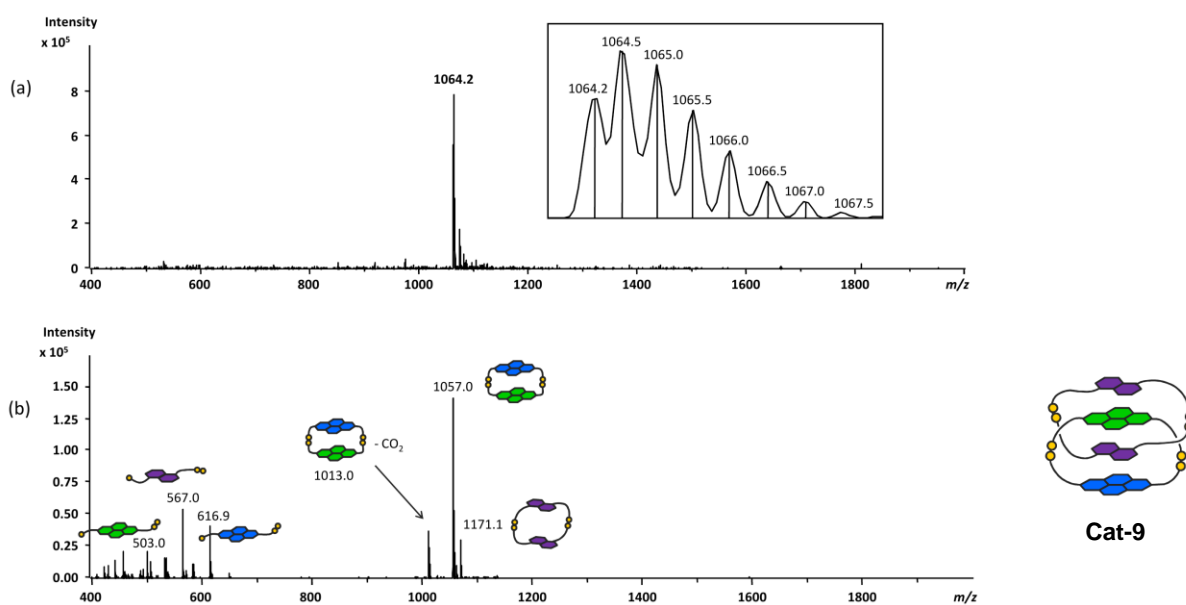


Figure 6.4. Tandem (a) MS and (b) MS/MS fragmentation of **Cat-9**. The MS and MS/MS of **Cat-11** composed of **A1**, **A2** and **D2b**, are identical to the ones of **Cat-9** (composed of **A1**, **A2** and **D1b**, shown here).

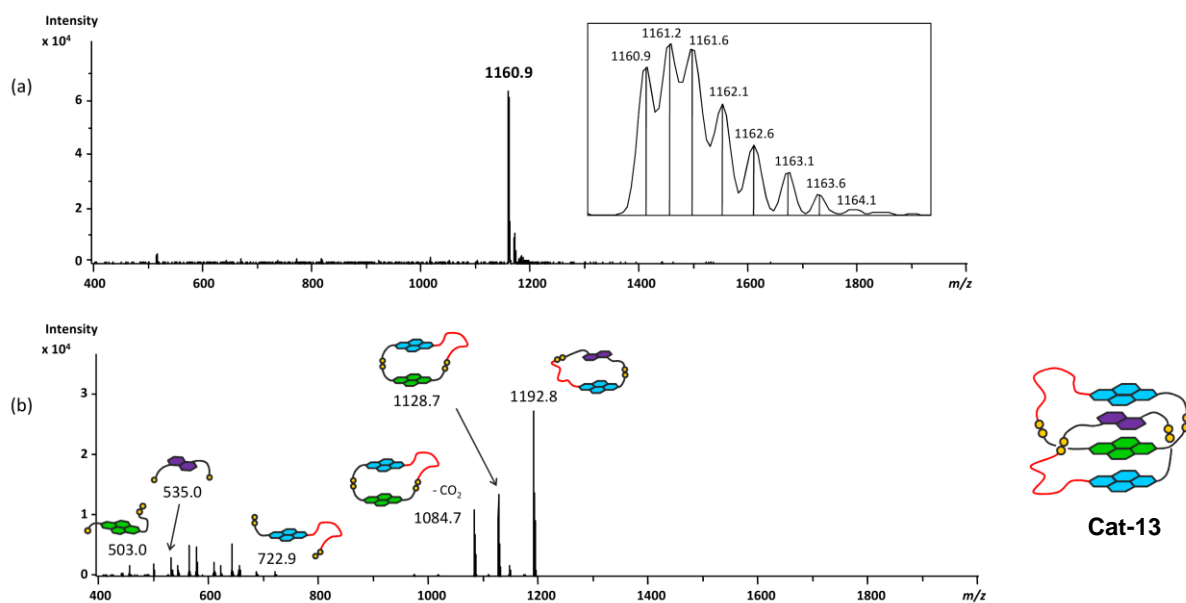


Figure 6.5. Tandem (a) MS and (b) MS/MS fragmentation of DADA catenane **Cat-13**.

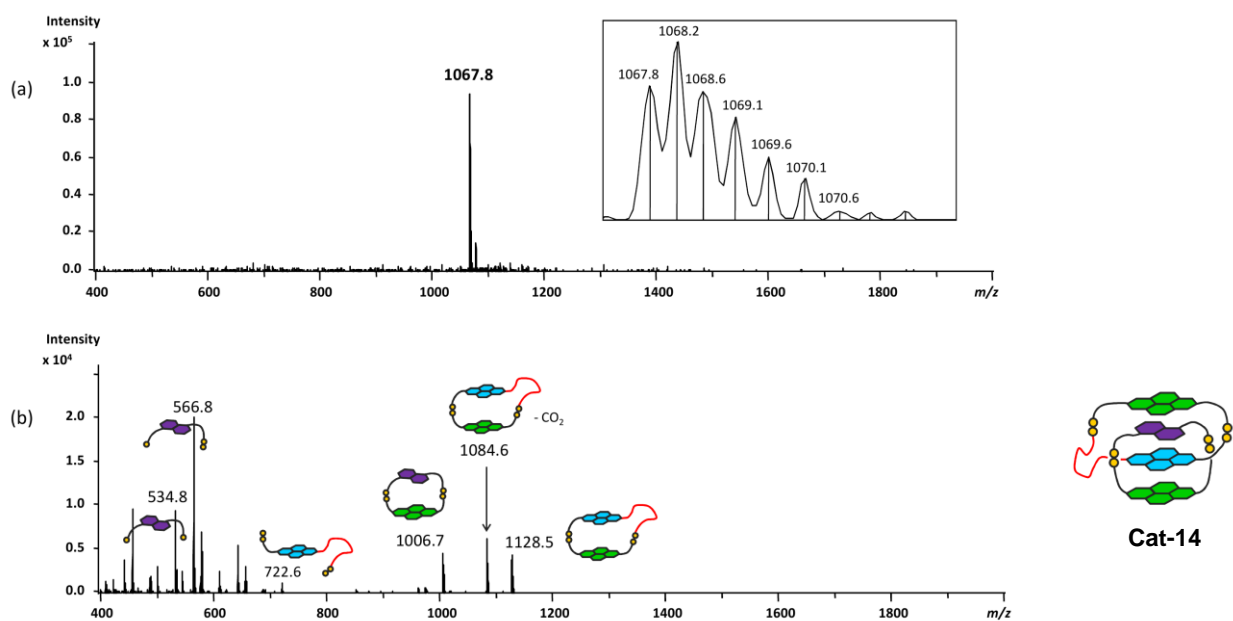


Figure 6.6. Tandem (a) MS and (b) MS/MS fragmentation of DADA catenane **Cat-14**.

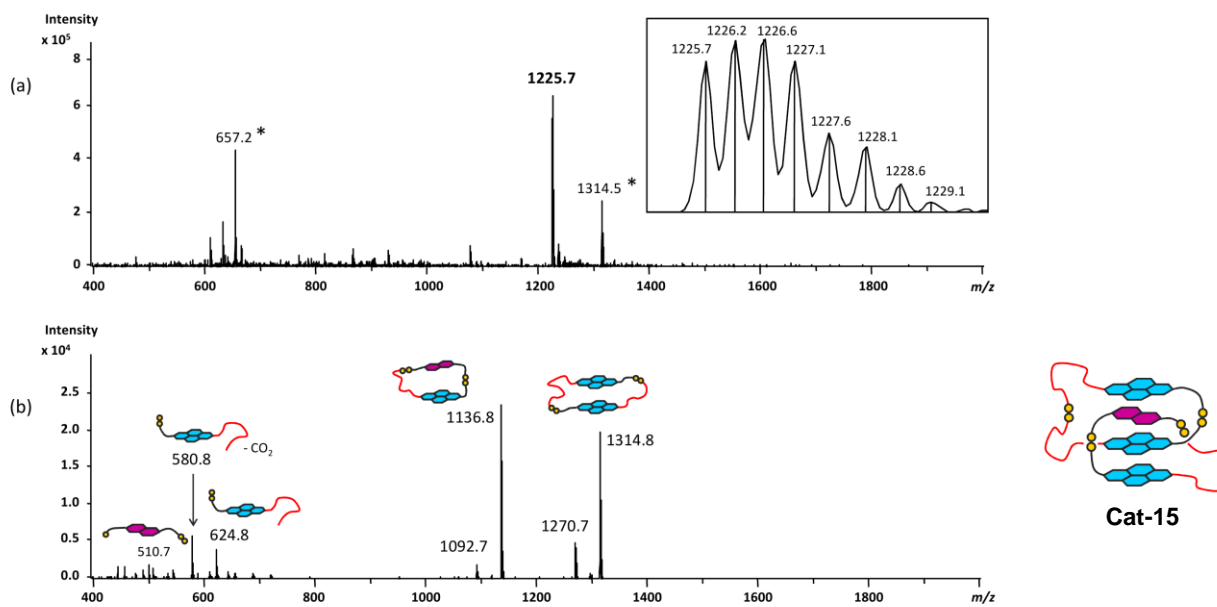


Figure 6.7. Tandem (a) MS and (b) MS/MS fragmentation of **Cat-15**. Peaks corresponding to the mass of the trimer [-A4-A4-D2a-] impurity were labeled *.

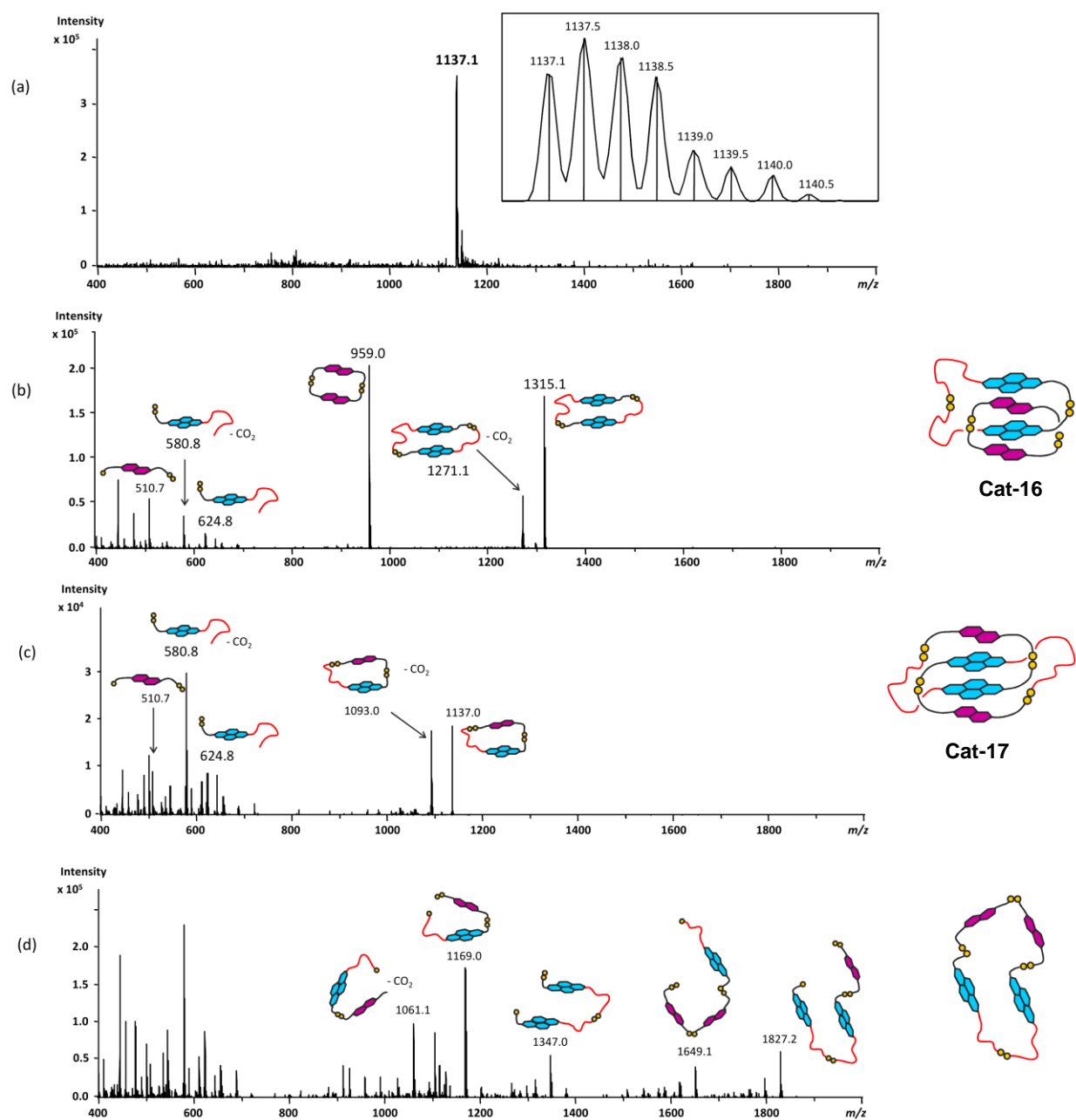


Figure 6.8. Tandem (a) MS and MS/MS fragmentation of (b) **Cat-16**, (c) **Cat-17**, (d) and of their corresponding AADD macrocyclic isomer.

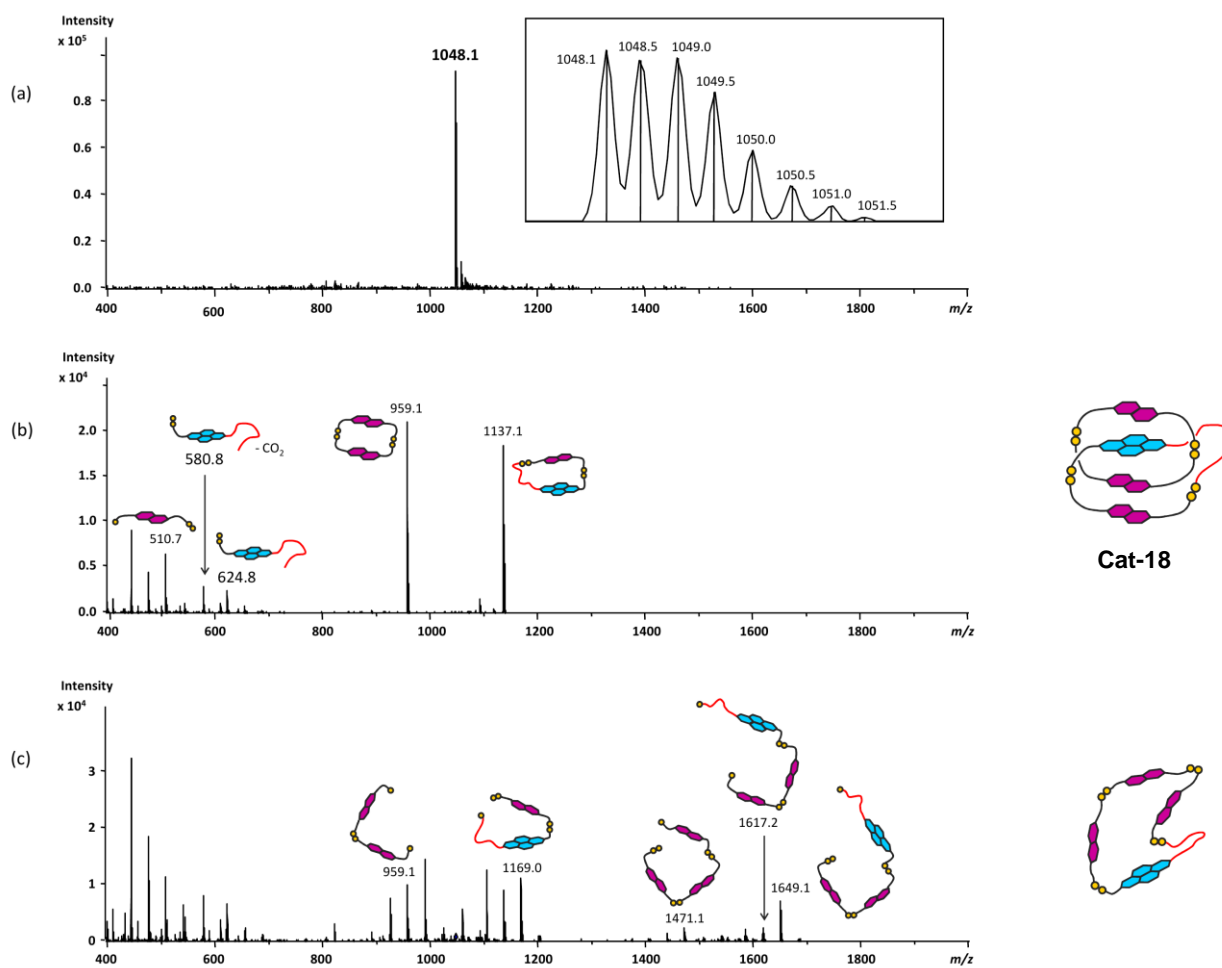


Figure 6.9. Tandem (a) MS, (b) MS/MS fragmentation of **Cat-18**, and (c) of its corresponding DDDA macrocyclic isomer.

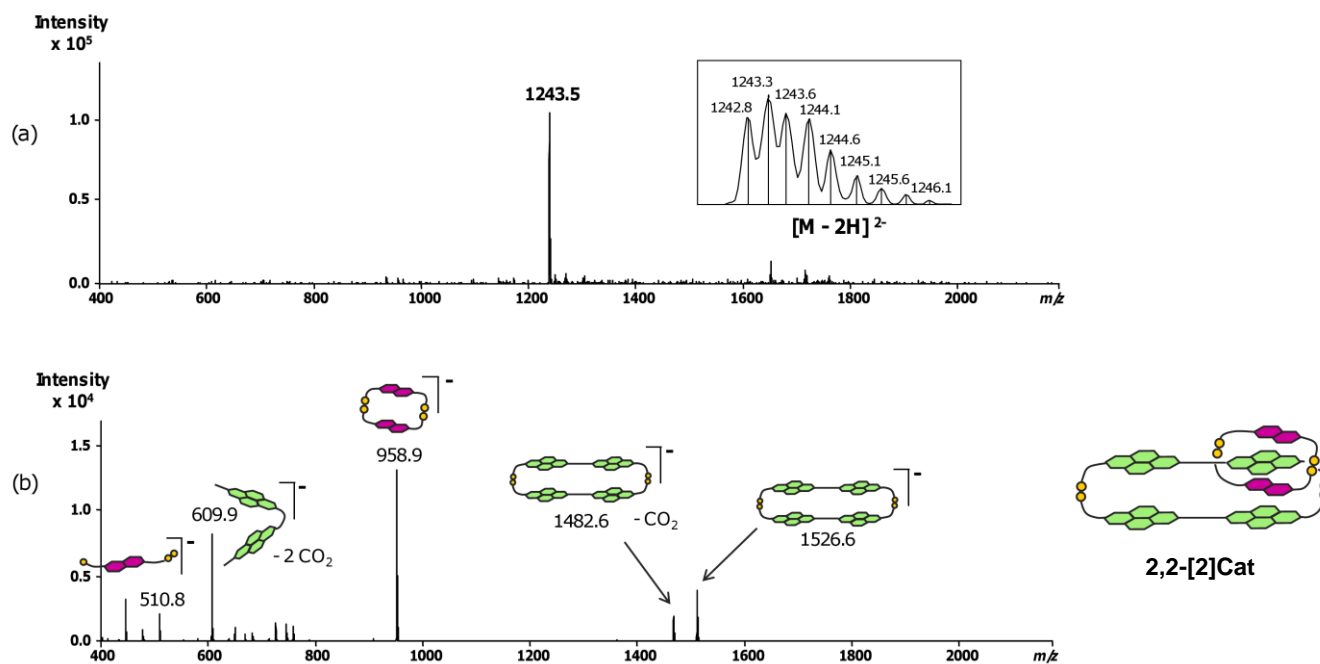


Figure 6.10. Tandem (a) MS, (b) MS/MS fragmentation of $2,2-[2]Cat$. The MS and MS/MS of $2,2-[2]Cat'$ are identical to the ones of $2,2-[2]Cat$.

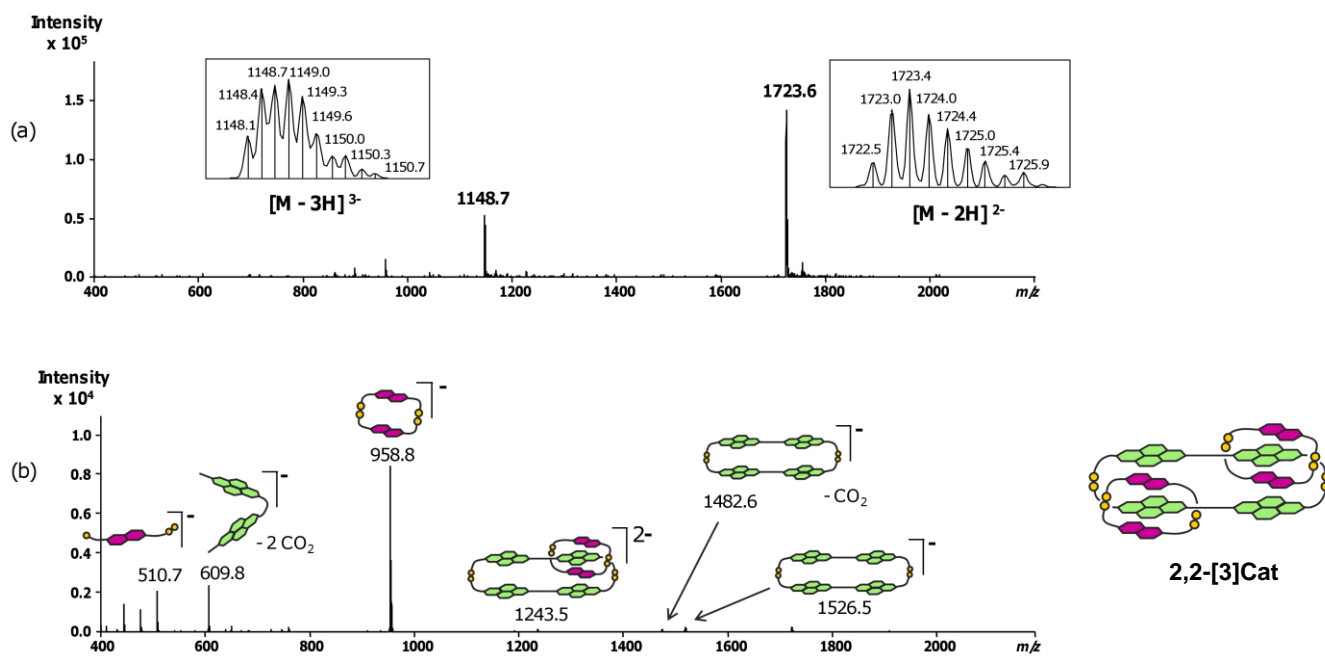


Figure 6.11. Tandem (a) MS, (b) MS/MS fragmentation of $2,2-[3]Cat$. The MS and MS/MS of $2,2-[3]Cat'$ are identical to the ones of $2,2-[3]Cat$.

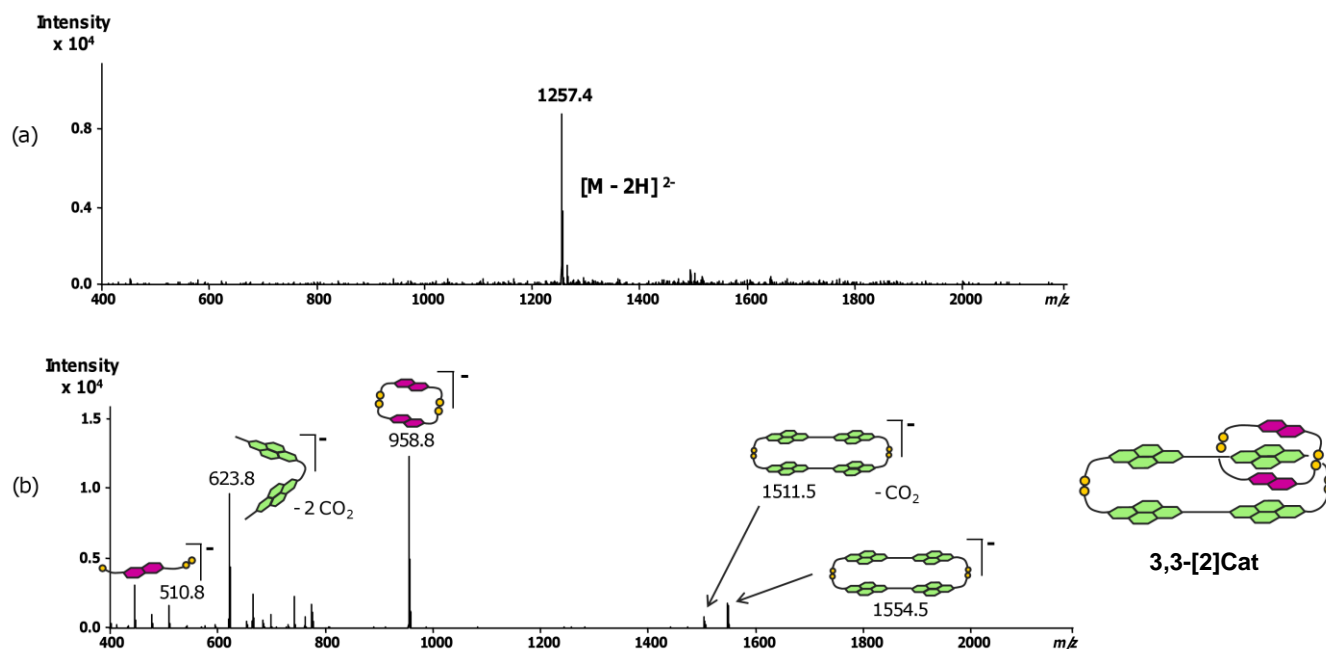


Figure 6.12. Tandem (a) MS, (b) MS/MS fragmentation of 3,3-[2]Cat. The MS and MS/MS of 3,3-[2]Cat' are identical to the ones of 3,3-[2]Cat.

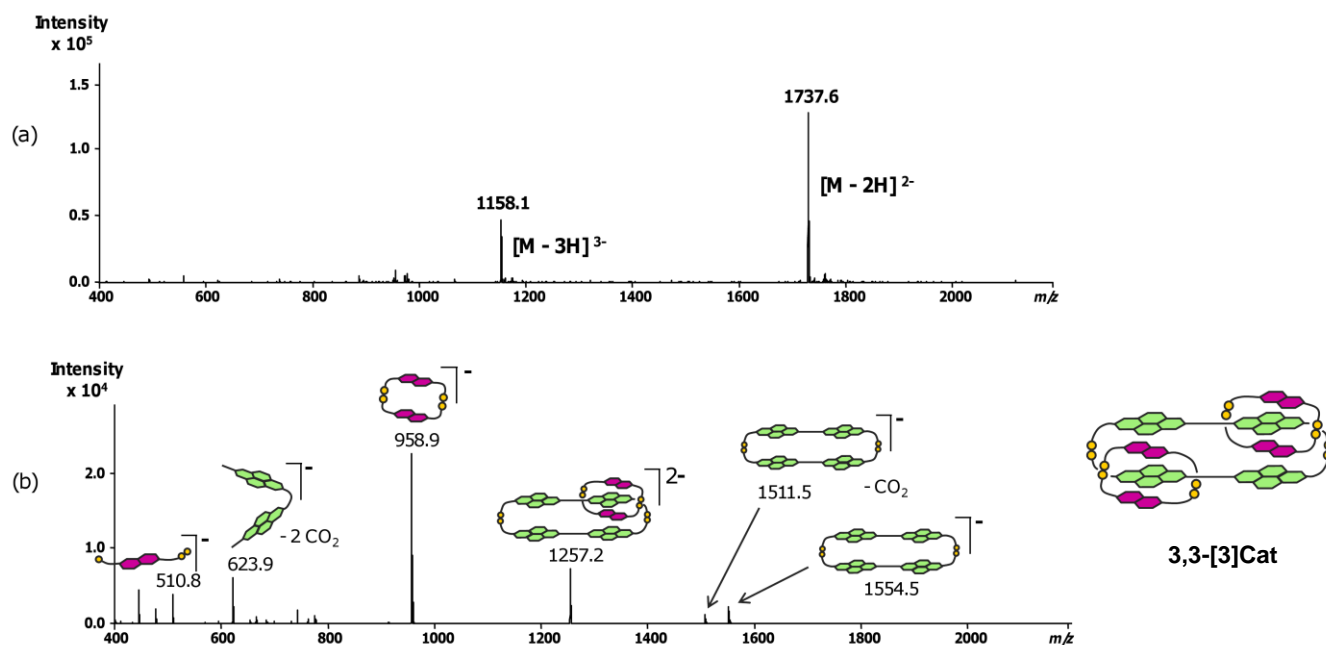


Figure 6.13. Tandem (a) MS, (b) MS/MS fragmentation of 3,3-[3]Cat. The MS and MS/MS of 3,3-[3]Cat' are identical to the ones of 3,3-[3]Cat.

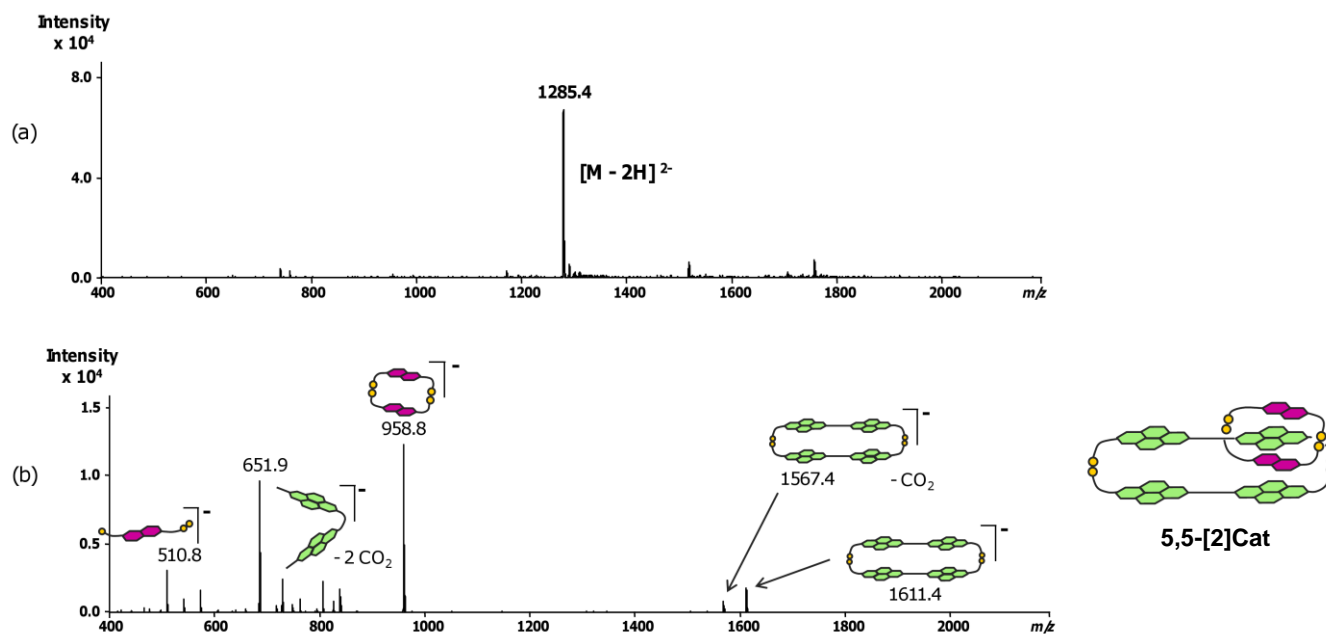


Figure 6.14. Tandem (a) MS, (b) MS/MS fragmentation of 5,5-[2]Cat. The MS and MS/MS of 5,5-[2]Cat' are identical to the ones of 5,5-[2]Cat.

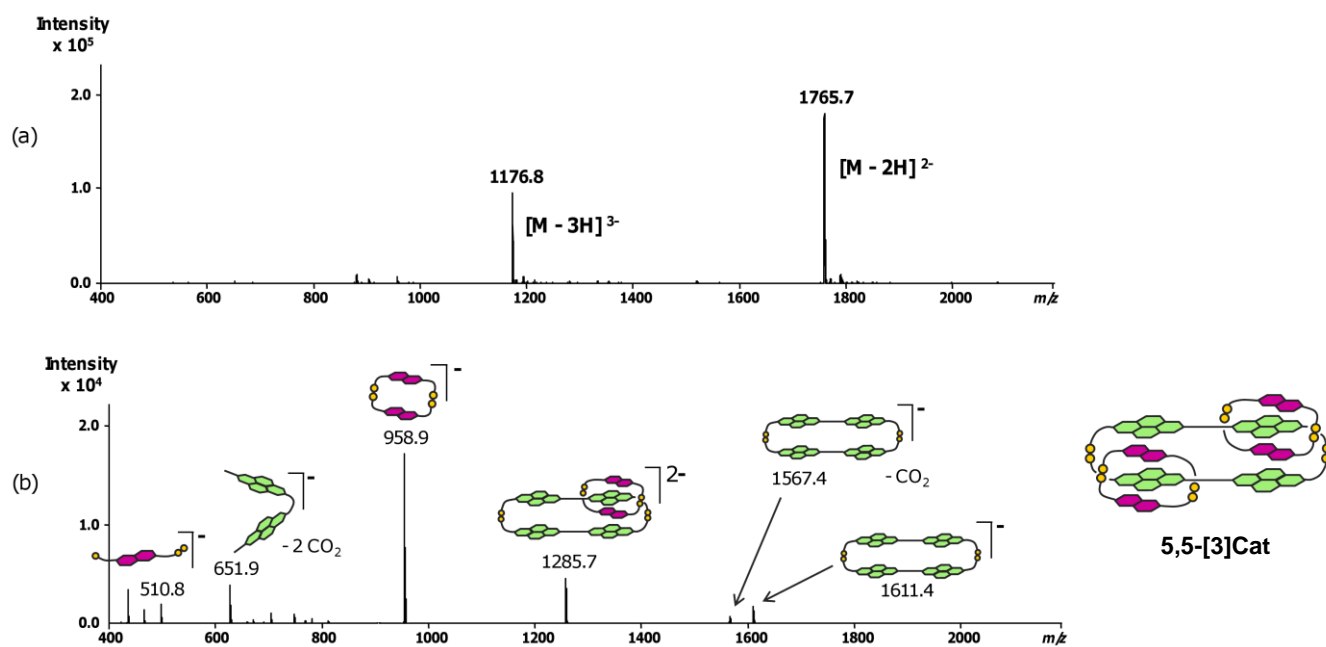


Figure 6.15. Tandem (a) MS, (b) MS/MS fragmentation of 5,5-[3]Cat. The MS and MS/MS of 5,5-[3]Cat' are identical to the ones of 5,5-[3]Cat.

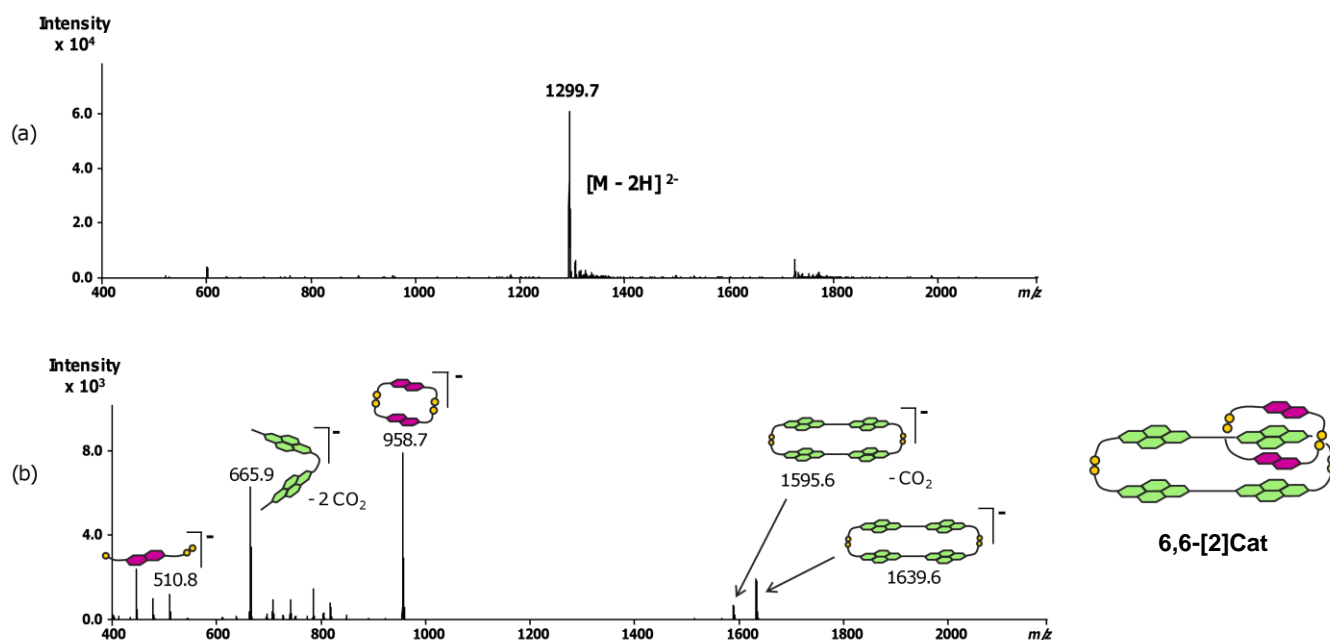


Figure 6.16. Tandem (a) MS, (b) MS/MS fragmentation of **6,6-[2]Cat**. The MS and MS/MS of **6,6-[2]Cat'** are identical to the ones of **6,6-[2]Cat**.

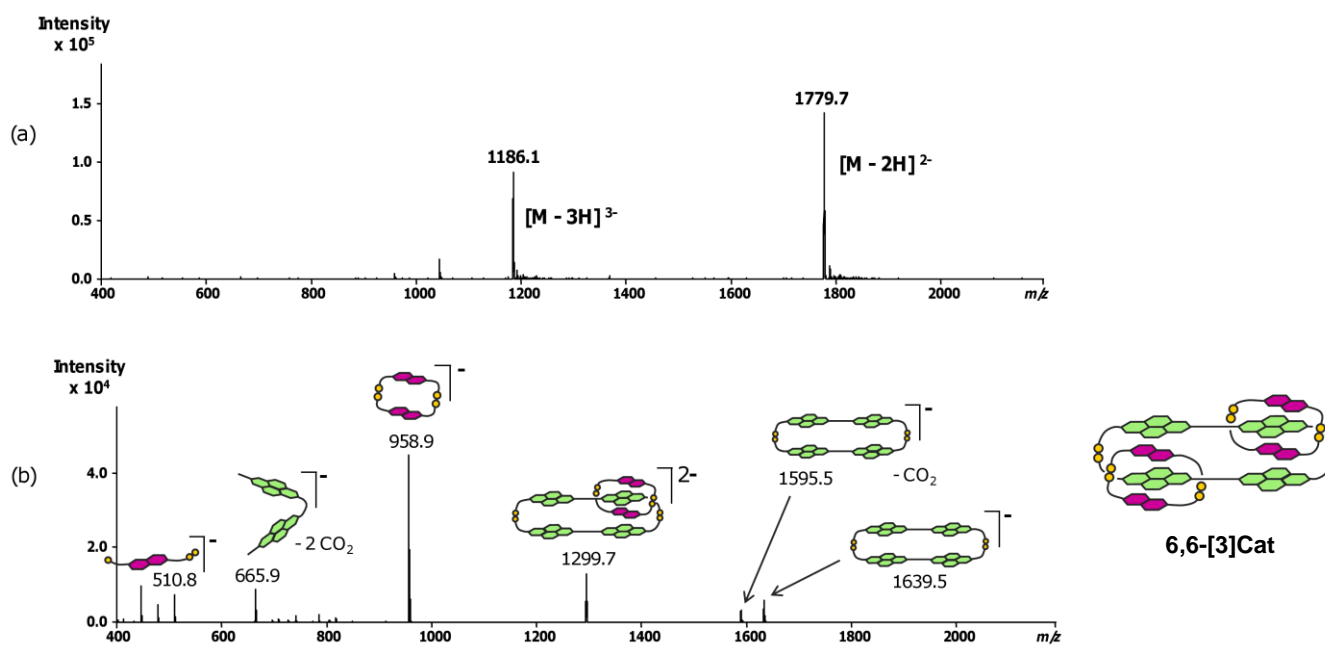


Figure 6.17. Tandem (a) MS, (b) MS/MS fragmentation of **6,6-[3]Cat**. The MS and MS/MS of **6,6-[3]Cat'** are identical to the ones of **6,6-[3]Cat**.

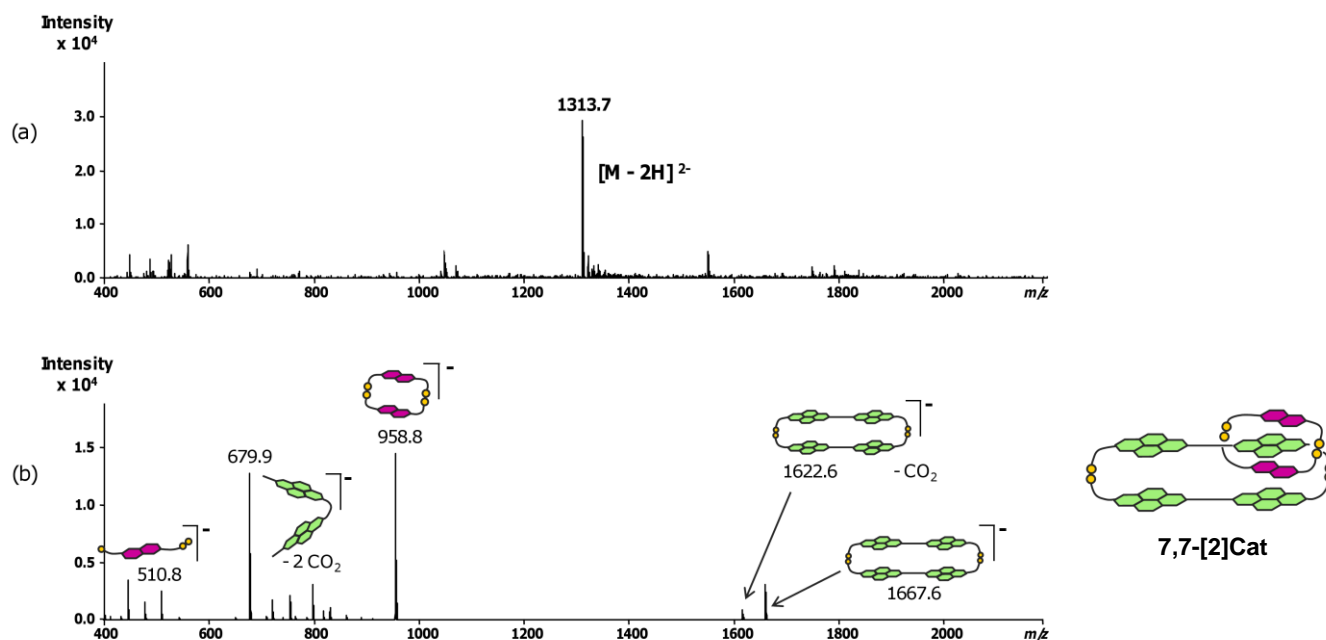


Figure 6.18. Tandem (a) MS, (b) MS/MS fragmentation of 7,7-[2]Cat. The MS and MS/MS of 7,7-[2]Cat' are identical to the ones of 7,7-[2]Cat.

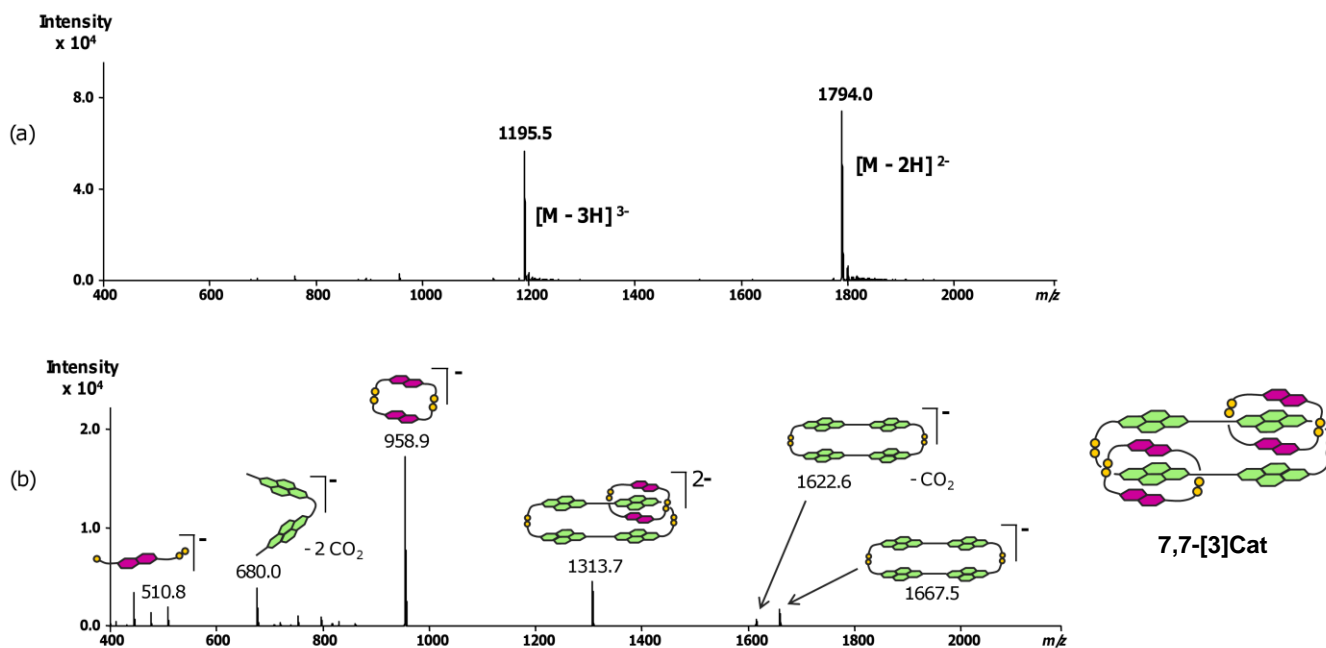


Figure 6.19. Tandem (a) MS, (b) MS/MS fragmentation of 7,7-[3]Cat. The MS and MS/MS of 7,7-[3]Cat' are identical to the ones of 7,7-[3]Cat.

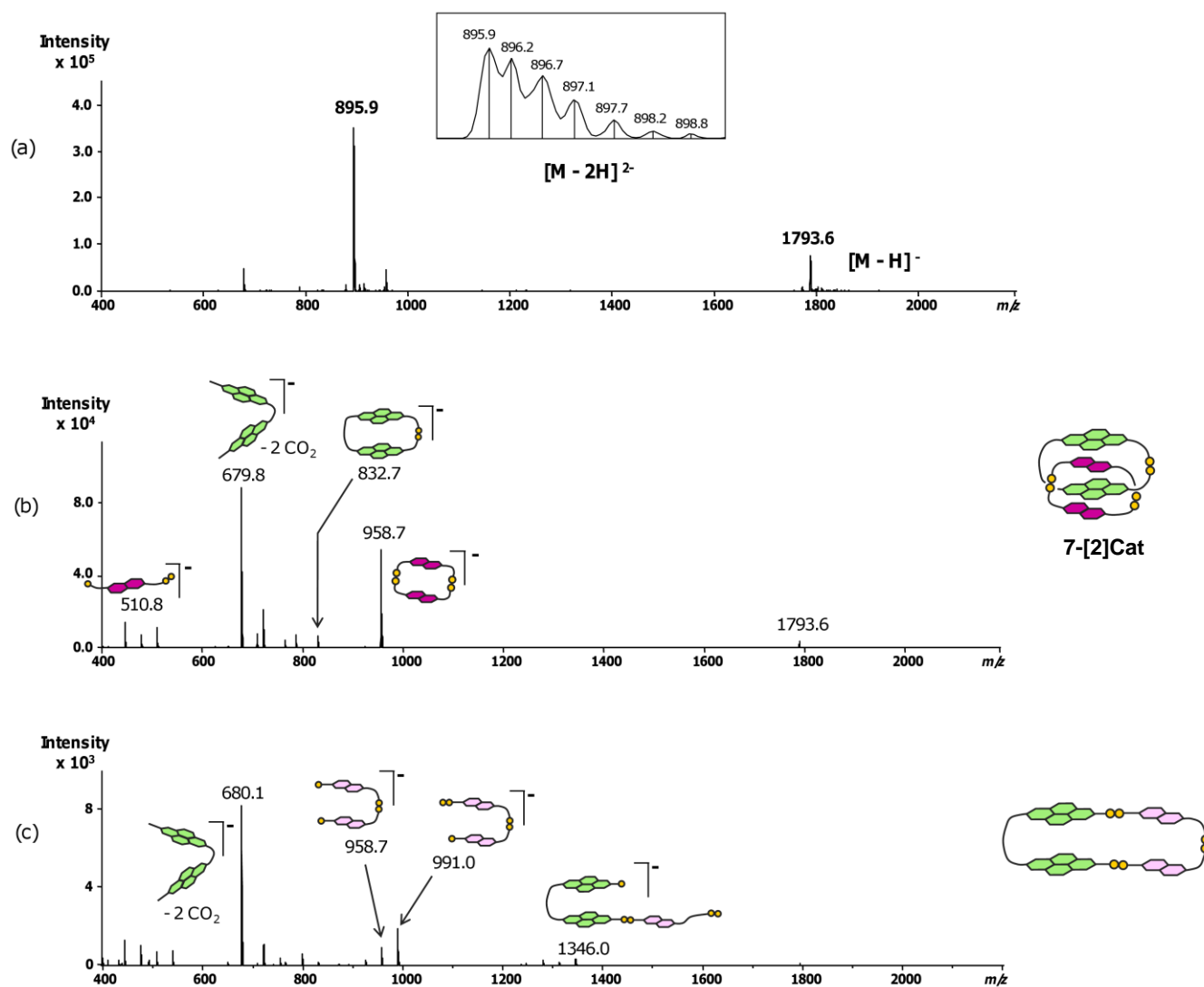


Figure 6.20. Tandem (a) MS, (b) MS/MS fragmentation of $7\text{-}[2]\text{Cat}$. The MS and MS/MS of $7\text{-}[2]\text{Cat}'$ are identical to the ones of $7\text{-}[2]\text{Cat}$. (c) MS/MS fragmentation of the macrocyclic isomer corresponding to $7\text{-}[2]\text{Cat}'$.

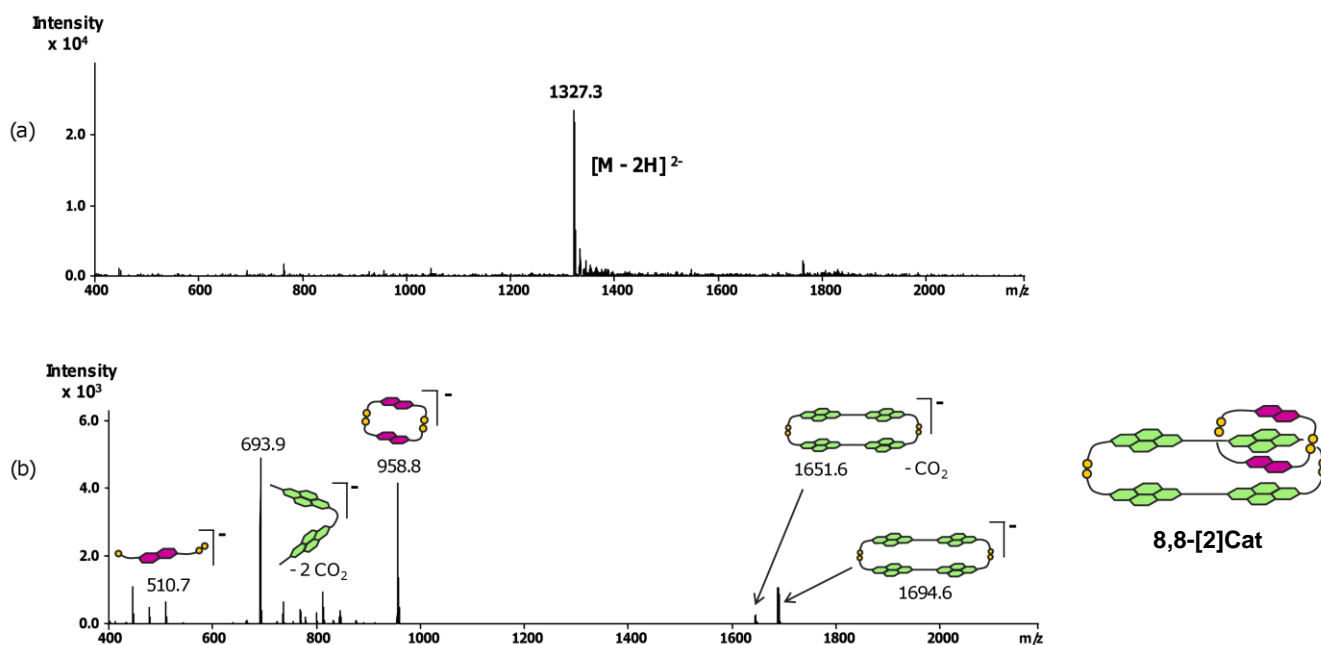


Figure 6.21. Tandem (a) MS, (b) MS/MS fragmentation of **8,8-[2]Cat**. The MS and MS/MS of **8,8-[2]Cat'** are identical to the ones of **8,8-[2]Cat**.

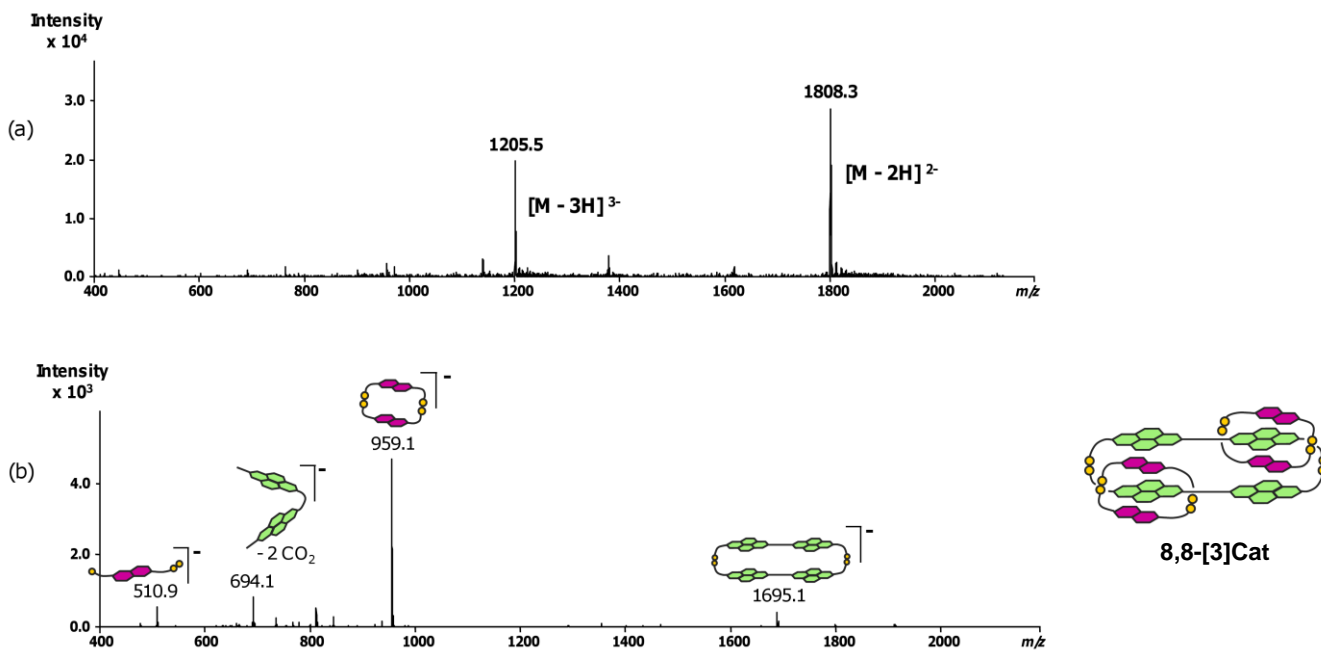


Figure 6.22. Tandem (a) MS, (b) MS/MS fragmentation of **8,8-[3]Cat**. The MS and MS/MS of **8,8-[3]Cat'** are identical to the ones of **8,8-[3]Cat**.

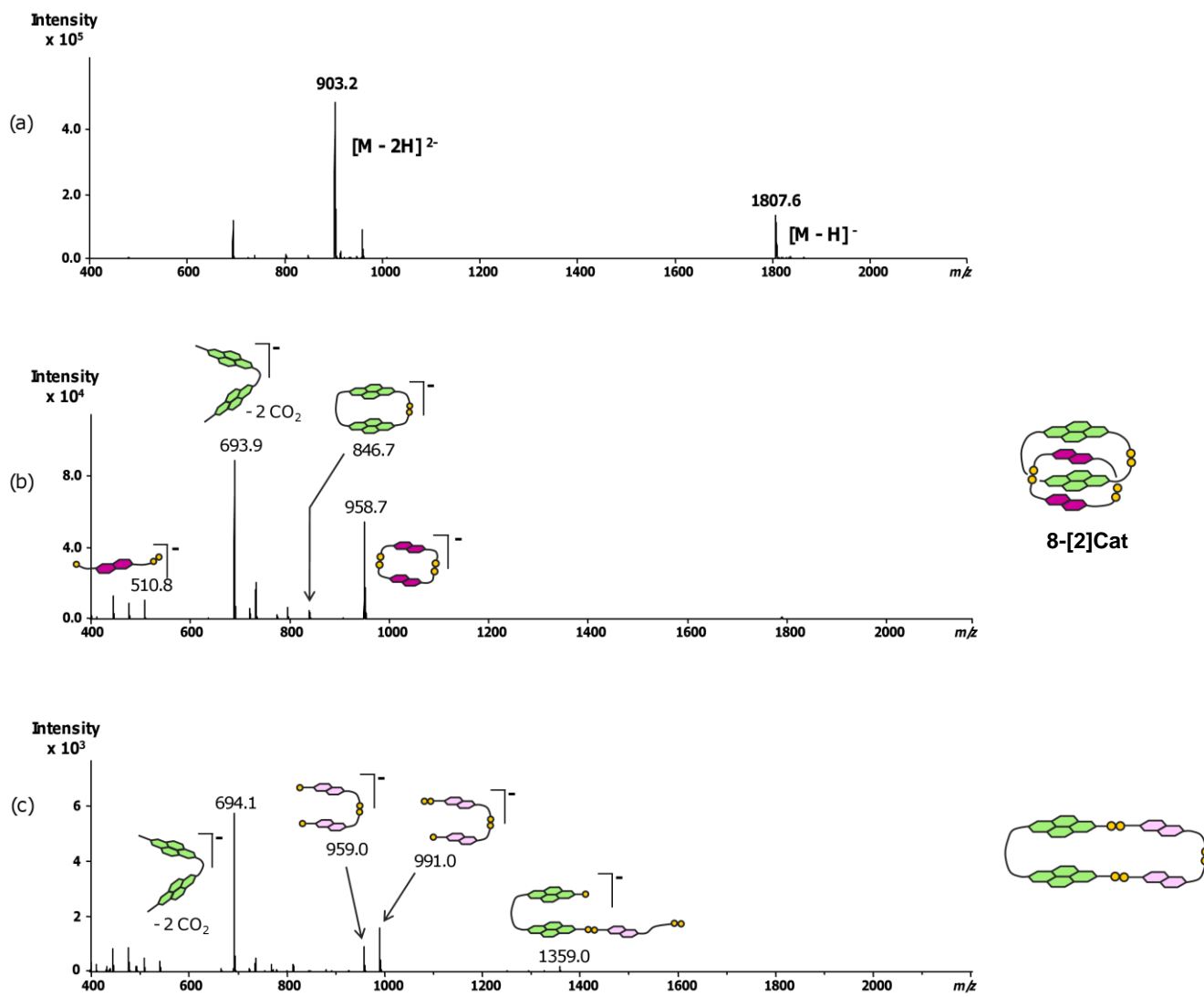


Figure 6.23. Tandem (a) MS, (b) MS/MS fragmentation of **8-[2]Cat**. The MS and MS/MS of **8-[2]Cat'** are identical to the ones of **8-[2]Cat**. (c) MS/MS fragmentation of the macrocyclic isomer corresponding to **8-[2]Cat'**.

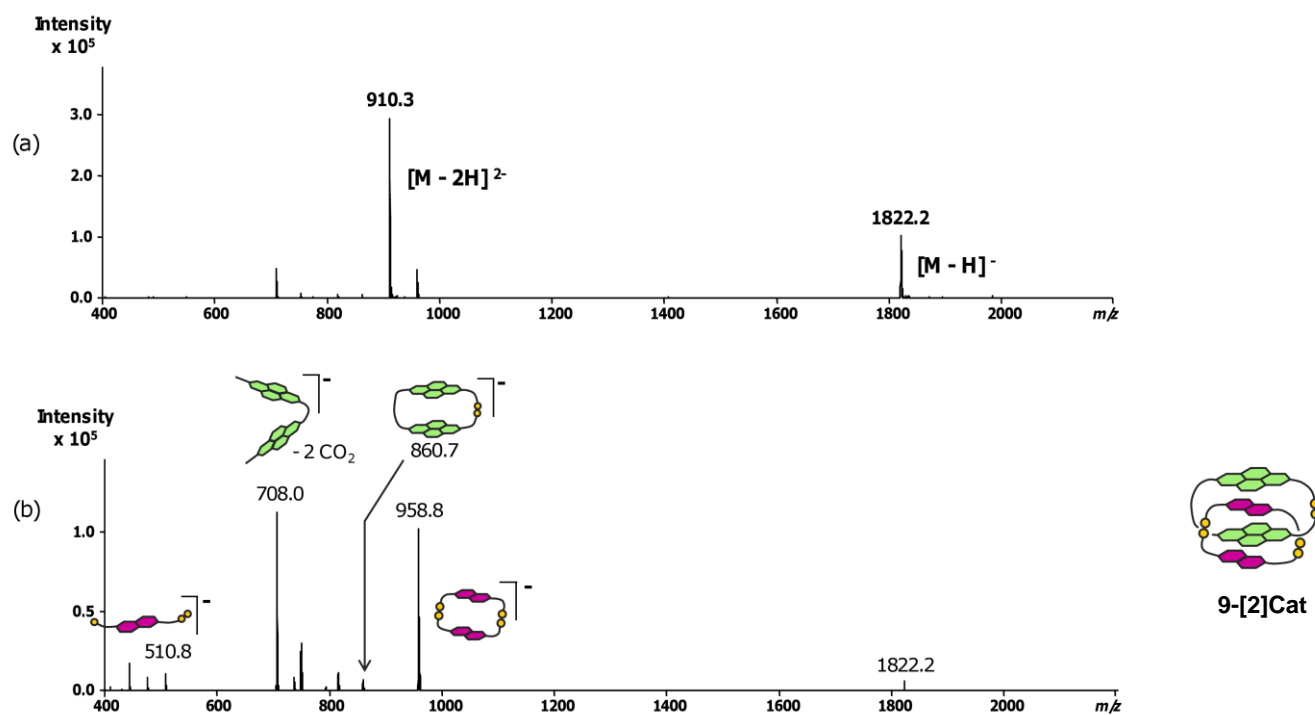
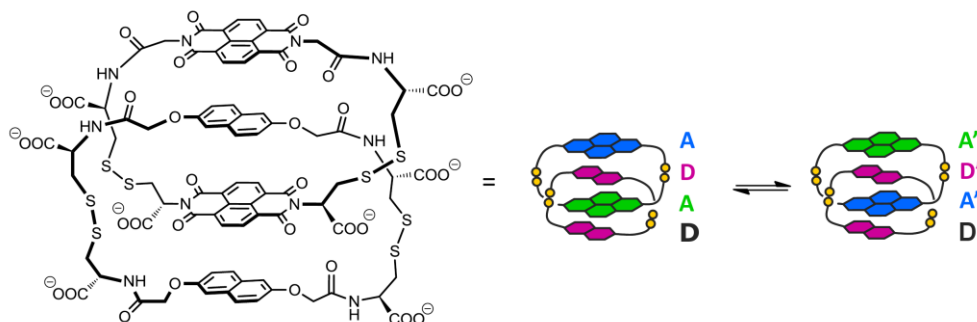


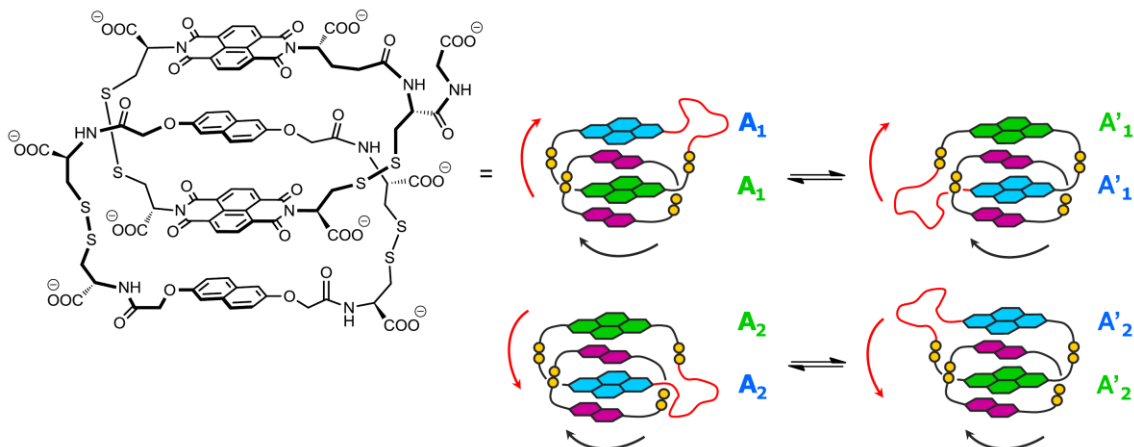
Figure 6.24. Tandem (a) MS, (b) MS/MS fragmentation of 9-[2]Cat. The MS and MS/MS of 9-[2]Cat' are identical to the ones of 9-[2]Cat.

6.5. NMR data of the isolated macrocycles and catenanes

This section lists the aromatic signals of the isolated catenanes and macrocycles that could be unambiguously assigned.

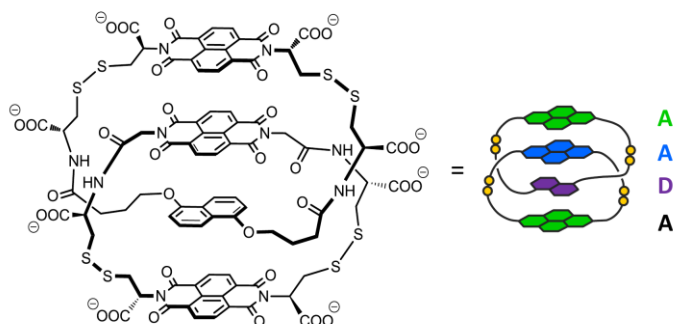


Cat-6: ^1H NMR (500 MHz, D_2O , 298 K) δ (ppm): 8.08 (d, $J = 6.0$ Hz, 2 H, **A**), 8.03 (d, $J = 6.0$ Hz, 2 H, **A**), 7.99 (s, 2 H, **A'**), 7.81 (d, $J = 7.2$ Hz, 2 H, **A**), 7.64 (m, 2 H, **A'**), 7.60 (d, $J = 7.2$ Hz, 2 H, **A**), 7.00 (d, $J = 8.3$ Hz, 2 H, **D'**), 6.77 (d, $J = 8.3$ Hz, 2 H, **D**), 6.62 (d, $J = 8.3$ Hz, 2 H, **D'**), 6.57 (d, $J = 8.3$ Hz, 2 H, **D**), 6.52 (d, $J = 8.3$ Hz, 2 H, **D'**), 6.41 (d, $J = 6.2$ Hz, 2 H, **D**), 6.30 (s, 2 H, **D'**), 6.28 (s, 2 H, **D**), 6.19 (d, $J = 8.3$ Hz, 2 H, **D'**), 6.16 (d, $J = 8.3$ Hz, 2 H, **D**), 5.72 (s, 2 H, **D**), 5.67 (s, 2 H, **D'**).

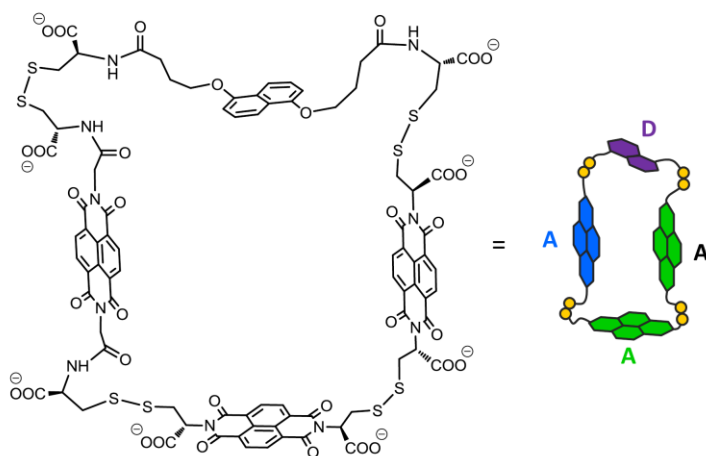


Cat-7: ^1H NMR (500 MHz, D_2O , 278 K) δ (ppm): 8.07 (d, $J = 7.7$ Hz, 2 H, **A₁**), 8.02 (m, 2 H, **A₂**), 8.01 (m, 2 H, **A'₂**), 7.89 (d, $J = 6.4$ Hz, 2 H, **A'₁**), 7.76 (m, 2 H, **A₂**), 7.75 (d, $J = 7.7$ Hz, 2 H, **A₁**), 7.71 (d, $J =$

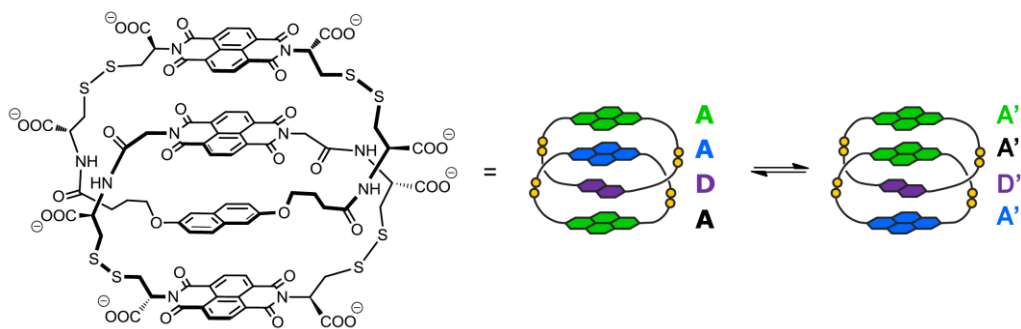
7.7 Hz, 2 H, **A'**₁), 7.63 (d, $J = 7.7$ Hz, 2 H, **A**₂), 7.62 (d, $J = 7.5$ Hz, 2 H, **A'**₂), 7.57 (m, 2 H, **A'**₂), 7.56 (d, $J = 6.4$ Hz, 2 H, **A'**₁), 7.55 (d, $J = 7.7$ Hz, 2 H, **A**₁), 7.45 (d, $J = 7.5$ Hz, 2 H, **A'**₂), 7.42 (d, $J = 7.7$ Hz, 2 H, **A'**₁), 7.22 (d, $J = 7.7$ Hz, 2 H, **A**₂), 7.20 (d, $J = 7.7$ Hz, 2 H, **A**₁).



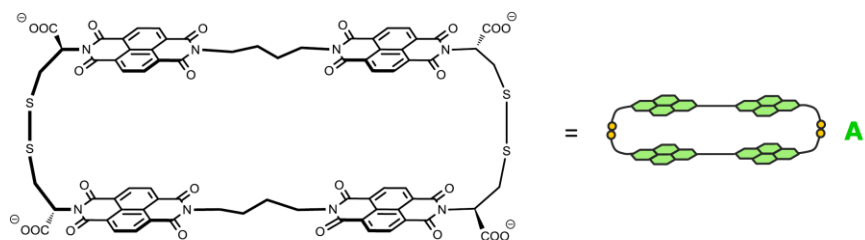
Cat-8: ¹H NMR (500 MHz, D₂O, 333 K) δ (ppm): 8.44 (d, $J = 7.6$ Hz, 2 H, **A**), 8.34 (s, 4 H, **A**), 8.24 (d, $J = 5.7$ Hz, 2 H, **A**), 8.18 (d, $J = 7.6$ Hz, 2 H, **A**), 8.08 (d, $J = 5.7$ Hz, 2 H, **A**), 6.81 (t, $J = 7.6$ Hz, 7.6 Hz, 2 H, **D**), 6.67 (d, $J = 7.6$ Hz, 2 H, **D**), 5.98 (d, $J = 7.6$ Hz, 2 H, **D**).



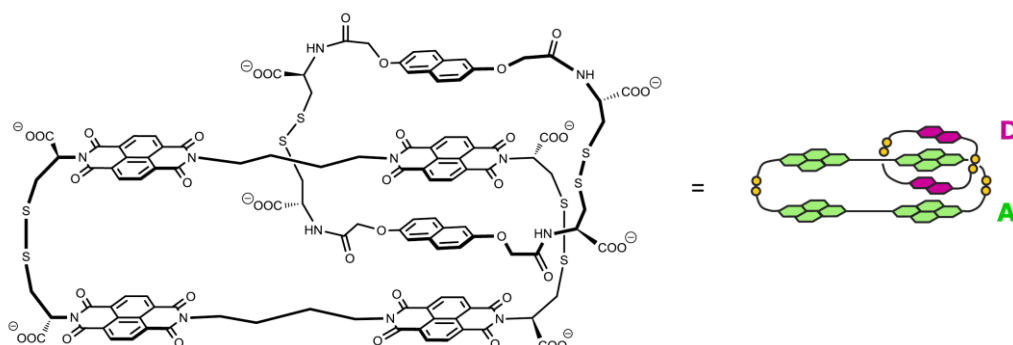
24: ¹H NMR (500 MHz, D₂O, 298 K) δ (ppm): very broad signals, not assignable. ¹H NMR (500 MHz, D₂O, 353 K) δ (ppm): 9.04 (d, $J = 7.6$ Hz, 2 H, **A**), 8.94 (d, $J = 7.6$ Hz, 2 H, **A**), 8.13 (d, $J = 7.7$ Hz, 2 H, **A**), 8.08 (s, 4 H, **A**), 8.07 (d, $J = 7.7$ Hz, 2 H, **A**), 6.37 (d, $J = 7.8$ Hz, 2 H, **D**), 6.27 (t, $J = 7.8$ Hz, 7.8 Hz, 2 H, **D**), 5.64 (d, $J = 7.8$ Hz, 2 H, **D**).



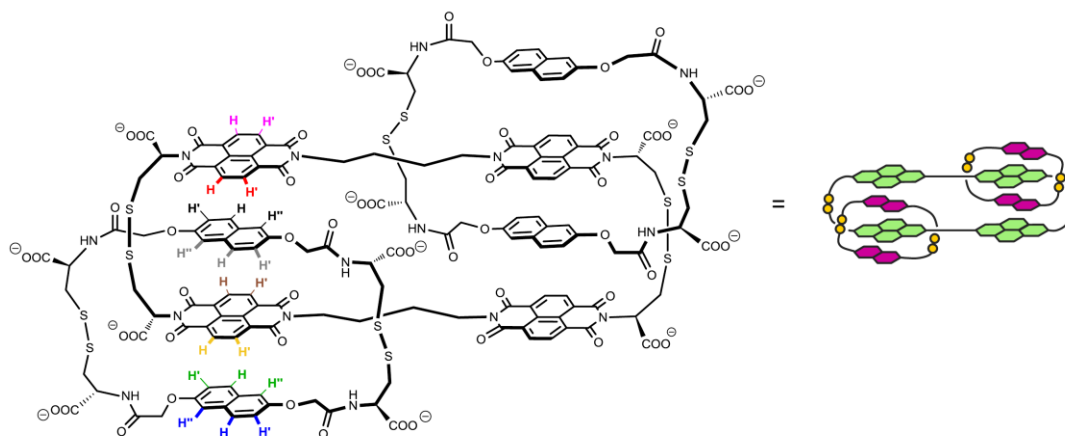
Cat-10: 8.00 (d, $J = 7.5$ Hz, 2 H, **A'**), 7.96 (d, $J = 7.5$ Hz, 2 H, **A'**), 7.95 (m, 4 H, **A'**), 7.64 (d, $J = 7.6$ Hz, 2 H, **A'**), 7.89 (m, 4 H, **A**), 7.87 (m, 4 H, **A**), 7.70 (d, $J = 7.3$ Hz, 2 H, **A**), 7.62 (d, $J = 7.3$ Hz, 2 H, **A**), 7.60 (d, $J = 7.6$ Hz, 2 H, **A'**), 6.17 (d, $J = 8.3$ Hz, 2 H, **D**), 6.04 (s, 4 H, **D'**), 5.77 (d, $J = 8.3$ Hz, 2 H, **D**), 5.58 (s, 2 H, **D**), 5.22 (s, 2 H, **D'**).



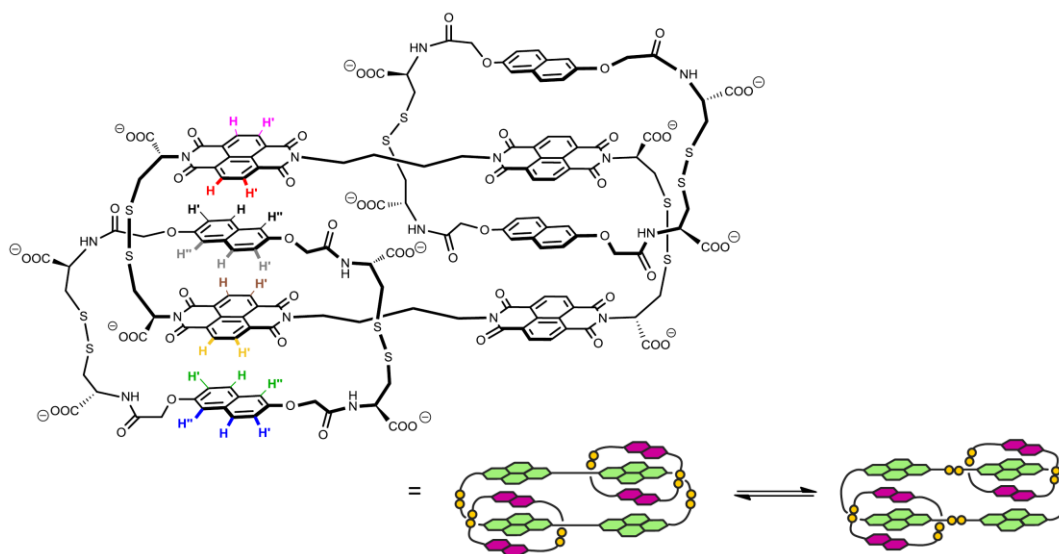
4,4-A: ^1H NMR (500 MHz, D_2O , 310 K) δ (ppm): very broad signals, not assignable. ^1H NMR (500 MHz, D_2O , 353 K) δ (ppm): 8.43-8.62 (m, 16 H, **A**).



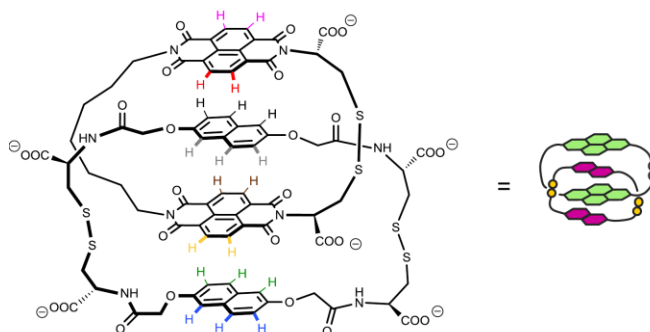
4,4-[2]Cat: ^1H NMR (500 MHz, D_2O , 310 K) δ (ppm): Acceptor signals - 7.61-8.70 (m, 16 H, **A**) very broad signals, not assignable. Donor signals - 7.44 (d, $J = 8.0$ Hz, 4 H, **D**), 7.14 (d, $J = 8.0$ Hz, 4 H, **D**), 6.97 (s, 4 H, **D**).



4,4-[3]Cat: ^1H NMR (500 MHz, D_2O , 298 K) δ (ppm): Acceptor signals - 8.49 (d, $J = 8.1$ Hz, 2 H, **H**), 8.41 (d, $J = 8.1$ Hz, 2 H, **H'**), 8.27 (d, $J = 8.1$ Hz, 2 H, **H**), 8.10 (d, $J = 8.1$ Hz, 2 H, **H'**), 7.75 (d, $J = 8.1$ Hz, 2 H, **H**), 7.65 (d, $J = 8.1$ Hz, 2 H, **H**), 7.29 (d, $J = 8.1$ Hz, 2 H, **H''**), 6.99 (d, $J = 8.1$ Hz, 2 H, **H'**). Donor signals - 7.13 (d, $J = 8.9$ Hz, 2 H, **H**), 6.95 (d, $J = 8.9$ Hz, 2 H, **H**), 6.87 (dd, $J = 8.9$ Hz, 1.8 Hz, 2 H, **H'**), 6.66 (dd, $J = 8.9$ Hz, 2.0 Hz, 2 H, **H'**), 6.47 (d, $J = 2.0$ Hz, 2 H, **H''**), 6.41 (d, $J = 1.8$ Hz, 2 H, **H''**), 6.32 (s, 2 H, **H''**), 6.22 (d, $J = 9.0$ Hz, 2 H, **H'**), 6.00 (d, $J = 9.0$ Hz, 2 H, **H**), 5.76 (d, $J = 9.0$ Hz, 2 H, **H**), 5.72 (d, $J = 9.0$ Hz, 2 H, **H'**), 5.02 (s, 2 H, **H''**).

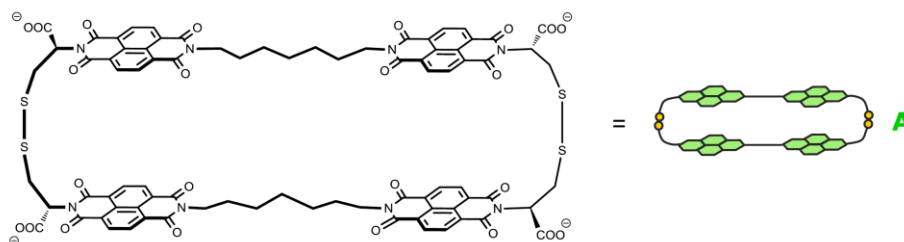


4,4-[3]Cat': ^1H NMR (500 MHz, D_2O , 298 K) δ (ppm): Acceptor signals, conformation a - 8.43 (d, $J = 7.4$ Hz, 2 H, **H**), 8.28 (d, $J = 7.4$ Hz, 2 H, **H'**), 8.05 (d, $J = 8.5$ Hz, 2 H, **H**), 7.83 (d, $J = 8.1$ Hz, 2 H, **H**), 7.76 (d, $J = 7.5$ Hz, 2 H, **H**), 7.62 (d, $J = 8.5$ Hz, 2 H, **H'**), 7.38 (d, $J = 7.5$ Hz, 2 H, **H'**), 7.35 (d, $J = 8.1$ Hz, 2 H, **H'**). Acceptor signals, conformation b - 8.41 (d, $J = 7.1$ Hz, 2 H, **H**), 8.26 (d, $J = 7.1$ Hz, 2 H, **H'**), 8.02 (d, $J = 8.1$ Hz, 2 H, **H**), 7.83 (m, 2 H, **H**), 7.79 (d, $J = 8.1$ Hz, 2 H, **H**), 7.59 (d, $J = 8.1$ Hz, 2 H, **H'**), 7.55 (d, $J = 8.1$ Hz, 2 H, **H'**), 7.39 (m, 2 H, **H'**). The two conformations could not be assigned.

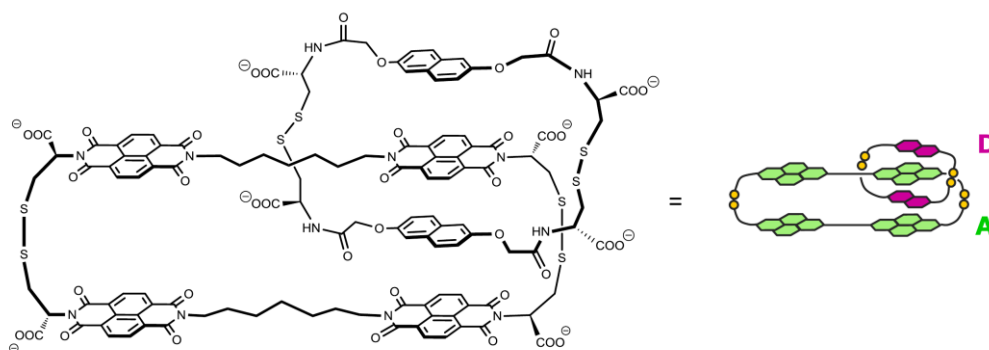


7-[2]Cat: ^1H NMR (500 MHz, D_2O , 298 K) δ (ppm): Acceptor signals - 8.08 (d, $J = 7.5$ Hz, 1 H, **H**), 8.05 (d, $J = 7.5$ Hz, 1 H, **H**), 7.84 (d, $J = 7.5$ Hz, 1 H, **H**), 7.82 (d, $J = 7.5$ Hz, 1 H, **H'**), 7.78 (d, $J = 7.5$ Hz, 1 H, **H'**), 7.74 (d, $J = 7.5$ Hz, 1 H, **H**), 7.55 (d, $J = 7.5$ Hz, 1 H, **H'**), 7.28 (d, $J = 7.5$ Hz, 1 H, **H'**). Donor signals - 6.96 (d, $J = 8.8$ Hz, 1 H, **H**), 6.72 (dd, $J = 8.8$ Hz, 2.2 Hz, 1 H, **H'**), 6.62 (d, $J = 8.7$ Hz,

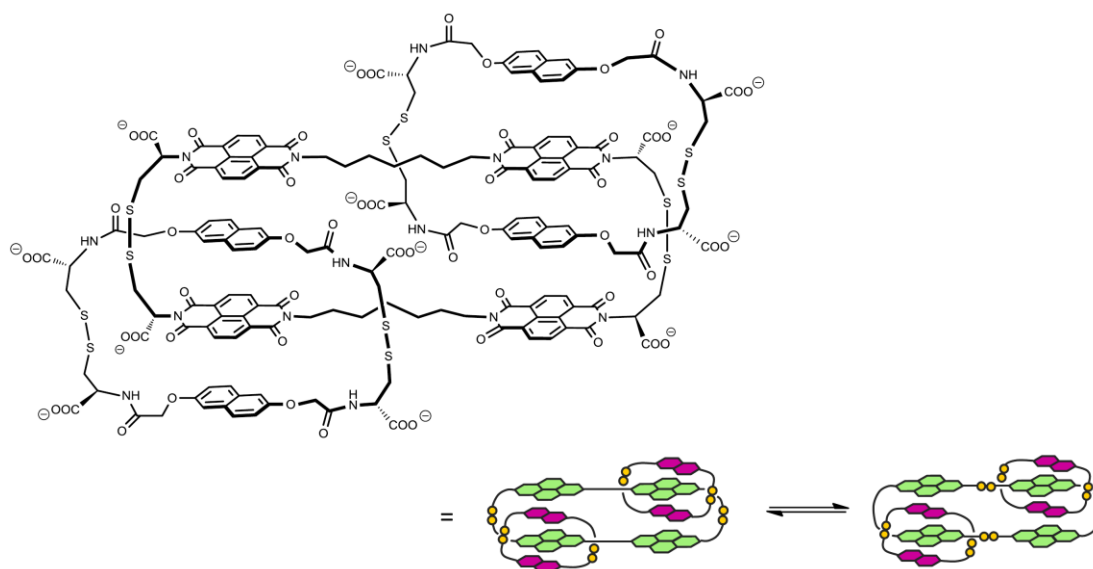
1 H, **H**), 6.52 (s, 2 H, **H** + **H'**), 6.36 (d, $J = 8.7$ Hz, 1 H, **H'**), 6.35 (d, $J = 8.8$ Hz, 1 H, **H**), 6.29 (s, 1 H, **H''**), 6.26 (d, $J = 2.2$ Hz, 1 H, **H''**), 5.90 (d, $J = 2.0$ Hz, 1 H, **H''**), 5.69 (dd, $J = 8.8$ Hz, 2.0 Hz, 1 H, **H'**), 5.53 (s, 1 H, **H''**).



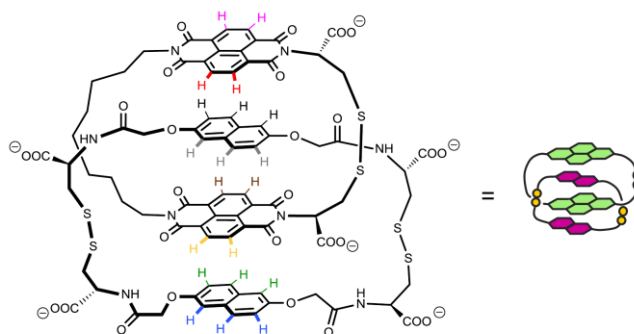
7,7-A: ^1H NMR (500 MHz, D_2O , 310 K) δ (ppm): very broad signals, not assignable.



7,7-[2]Cat: ^1H NMR (500 MHz, D_2O , 310 K) δ (ppm): Acceptor signals - very broad signals, not assignable. Donor signals – 7.27 (d, $J = 8.1$ Hz, 4 H, **D**), 6.98 (d, $J = 8.1$ Hz, 4 H, **D**), 6.78 (s, 4 H, **D**).



7,7-[3]Cat: ^1H NMR (500 MHz, D_2O , 298 K) δ (ppm): Acceptor signals, conformations a and b – 8 pairs of doublets, labelled from H_1 to H_8 . 8.47 (d, $J = 9.0$ Hz, 2 H, \mathbf{H}_1), 8.47 (d, $J = 9.0$ Hz, 2 H, \mathbf{H}_2), 8.38 (d, $J = 9.0$ Hz, 2 H, \mathbf{H}_1), 8.38 (d, $J = 9.0$ Hz, 2 H, \mathbf{H}_2), 8.28 (d, $J = 8.0$ Hz, 2 H, \mathbf{H}_3), 8.23 (d, $J = 8.0$ Hz, 2 H, \mathbf{H}_4), 7.98 (d, $J = 8.0$ Hz, 2 H, \mathbf{H}_3), 7.93 (d, $J = 8.0$ Hz, 2 H, \mathbf{H}_5), 7.89 (d, $J = 8.0$ Hz, 2 H, \mathbf{H}_4), 7.87 (d, $J = 8.0$ Hz, 2 H, \mathbf{H}_6), 7.83 (d, $J = 8.0$ Hz, 2 H, \mathbf{H}_7), 7.81 (d, $J = 8.0$ Hz, 2 H, \mathbf{H}_8), 7.59 (d, $J = 8.0$ Hz, 2 H, \mathbf{H}_5), 7.49 (d, $J = 8.0$ Hz, 2 H, \mathbf{H}_6), 7.30 (d, $J = 8.0$ Hz, 2 H, \mathbf{H}_7), 7.25 (d, $J = 8.0$ Hz, 2 H, \mathbf{H}_8).



9-[2]Cat: ^1H NMR (500 MHz, D_2O , 298 K) δ (ppm): Acceptor signals – 8.18 (d, $J = 7.9$ Hz, 1 H, \mathbf{H}), 8.06 (d, $J = 7.9$ Hz, 1 H, \mathbf{H}), 8.00 (d, $J = 7.9$ Hz, 1 H, \mathbf{H}), 7.95 (d, $J = 7.9$ Hz, 1 H, \mathbf{H}'), 7.75 (d, $J = 7.9$ Hz, 1 H, \mathbf{H}), 7.66 (d, $J = 7.9$ Hz, 1 H, \mathbf{H}'), 7.62 (d, $J = 7.9$ Hz, 1 H, \mathbf{H}'), 7.16 (d, $J = 7.9$ Hz, 1 H, \mathbf{H}').

Donor signals – 6.90 (d, $J = 10.6$ Hz, 1 H, **H**), 6.72 (d, $J = 10.6$ Hz, 1 H, **H'**), 6.62 (d, $J = 10.6$ Hz, 1 H, **H**), 6.46 (d, $J = 10.6$ Hz, 1 H, **H'**), 6.44 (d, $J = 10.5$ Hz, 1 H, **H**), 6.25 (s, 1 H, **H''**), 6.21 (s, 1 H, **H''**), 6.20 (d, $J = 10.5$ Hz, 1 H, **H'**), 5.90 (s, 1 H, **H''**), 5.62 (d, $J = 8.8$ Hz, 1 H, **H**), 5.59 (d, $J = 8.8$ Hz, 1 H, **H'**), 4.89 (s, 1 H, **H''**).

6.6. UV-Vis spectra of the isolated macrocycles and catenanes

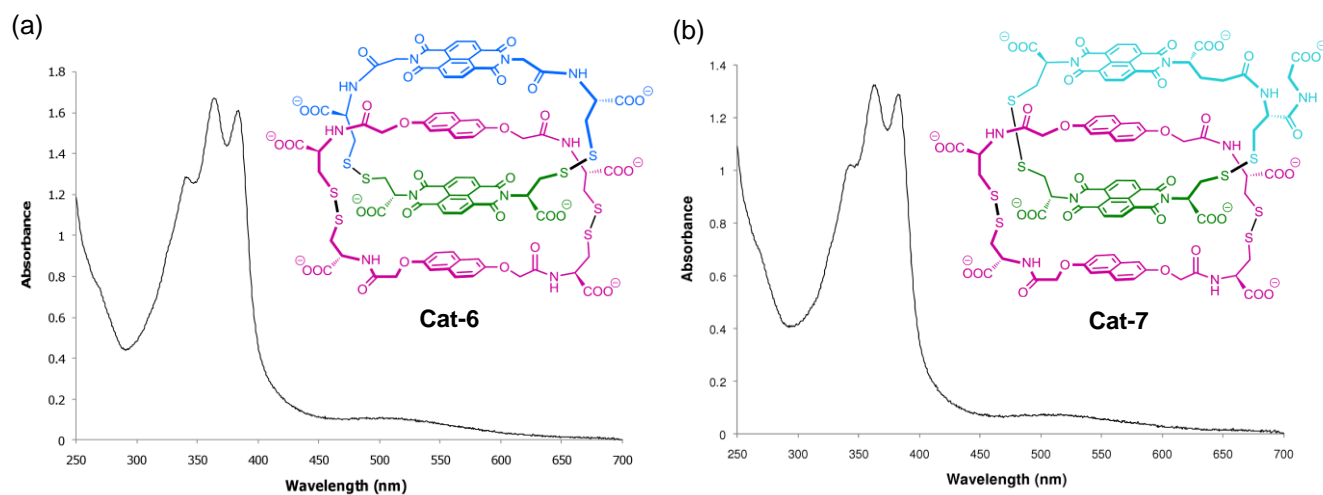


Figure 6.25. UV-Vis spectrum of (a) Cat-6 and (b) Cat-7 (H₂O, 298K).

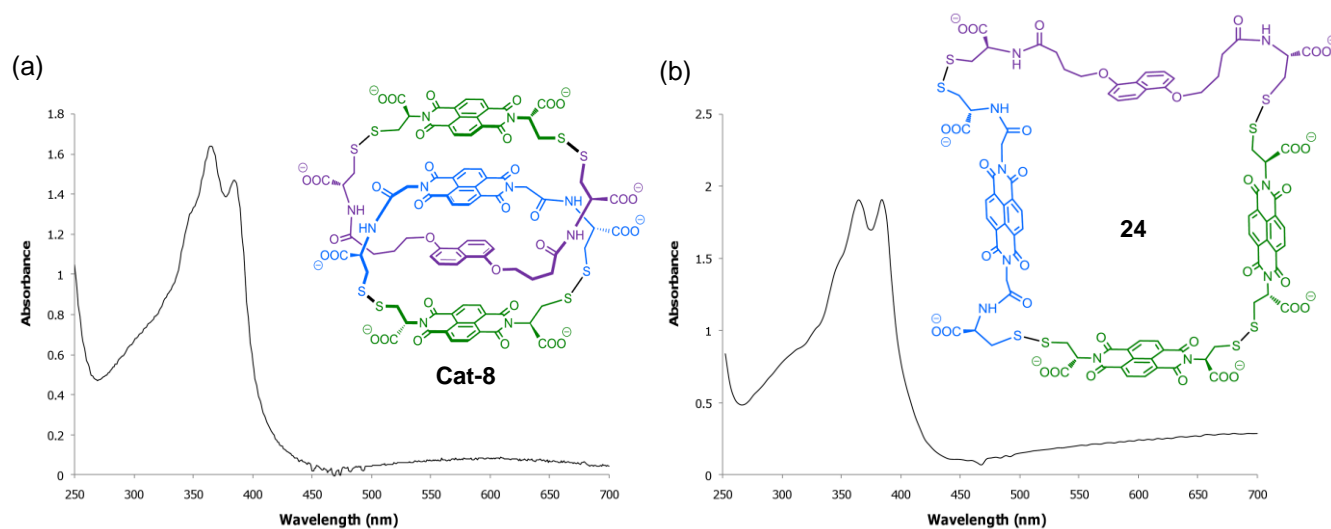


Figure 6.26. UV-Vis spectrum of (a) Cat-8 and (b) macrocycle 24 (H₂O, 298K).

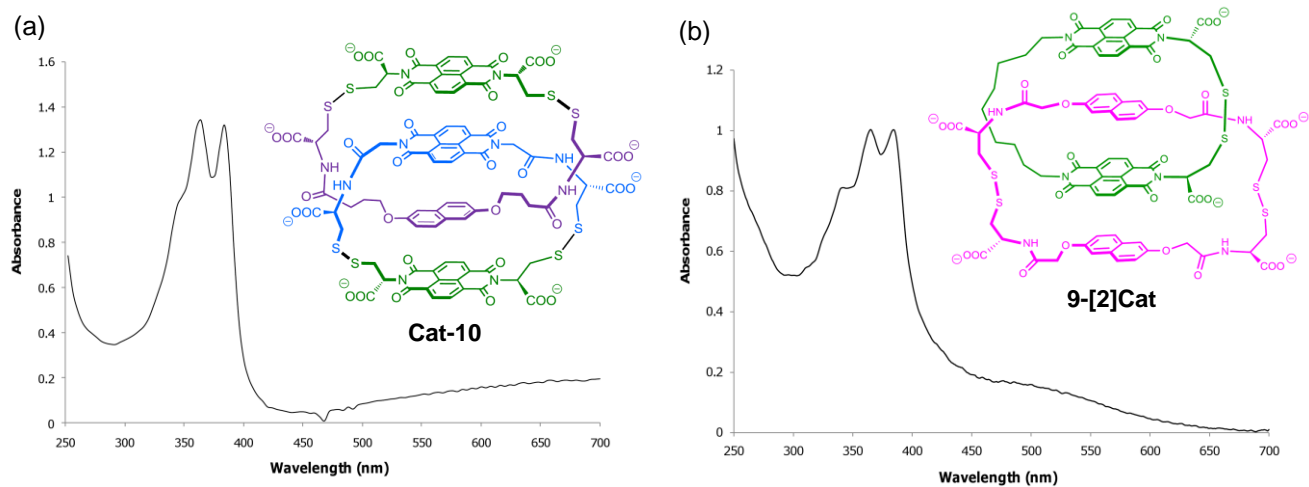


Figure 6.27. UV-Vis spectrum of (a) **Cat-10** and (b) **9-[2]Cat** (H_2O , 298K).

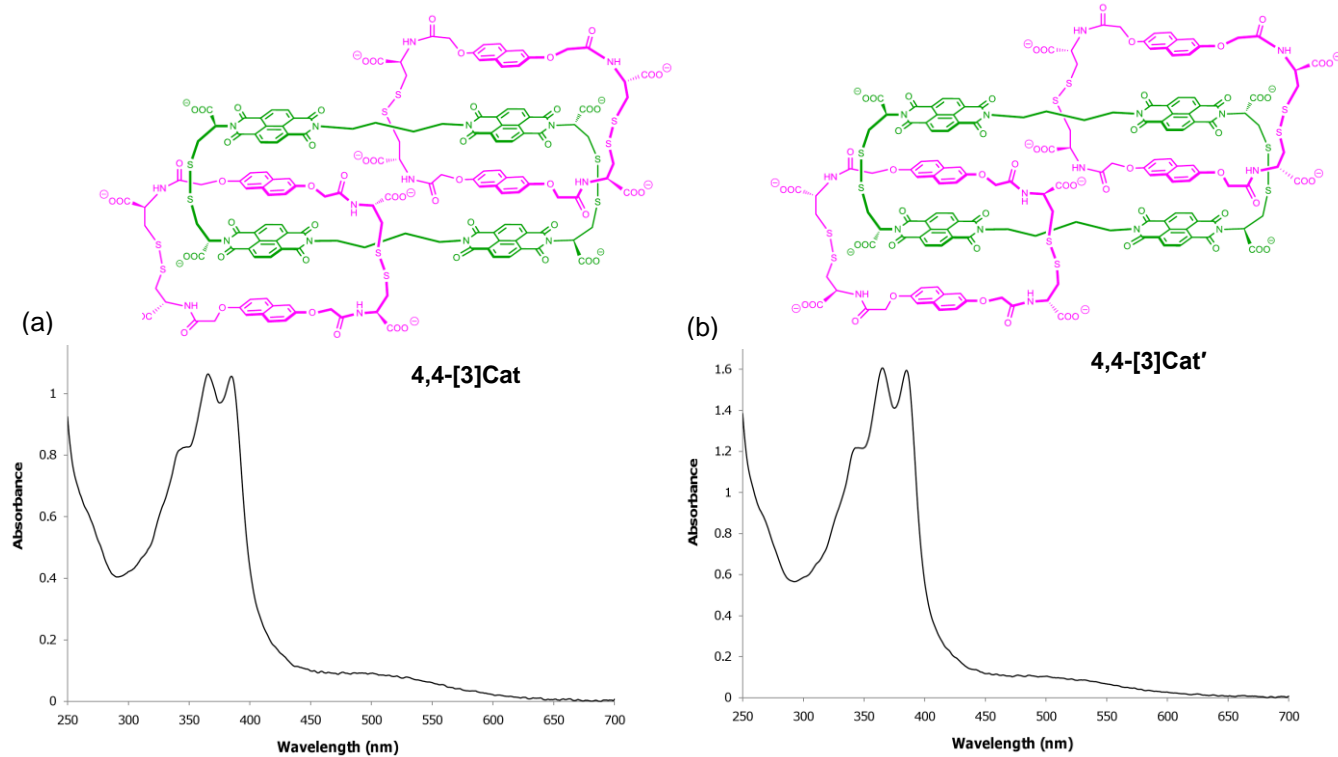


Figure 6.28. UV-Vis spectrum of (a) **4,4-[3]Cat** and (b) **4,4-[3]Cat'** (H_2O , 298K).

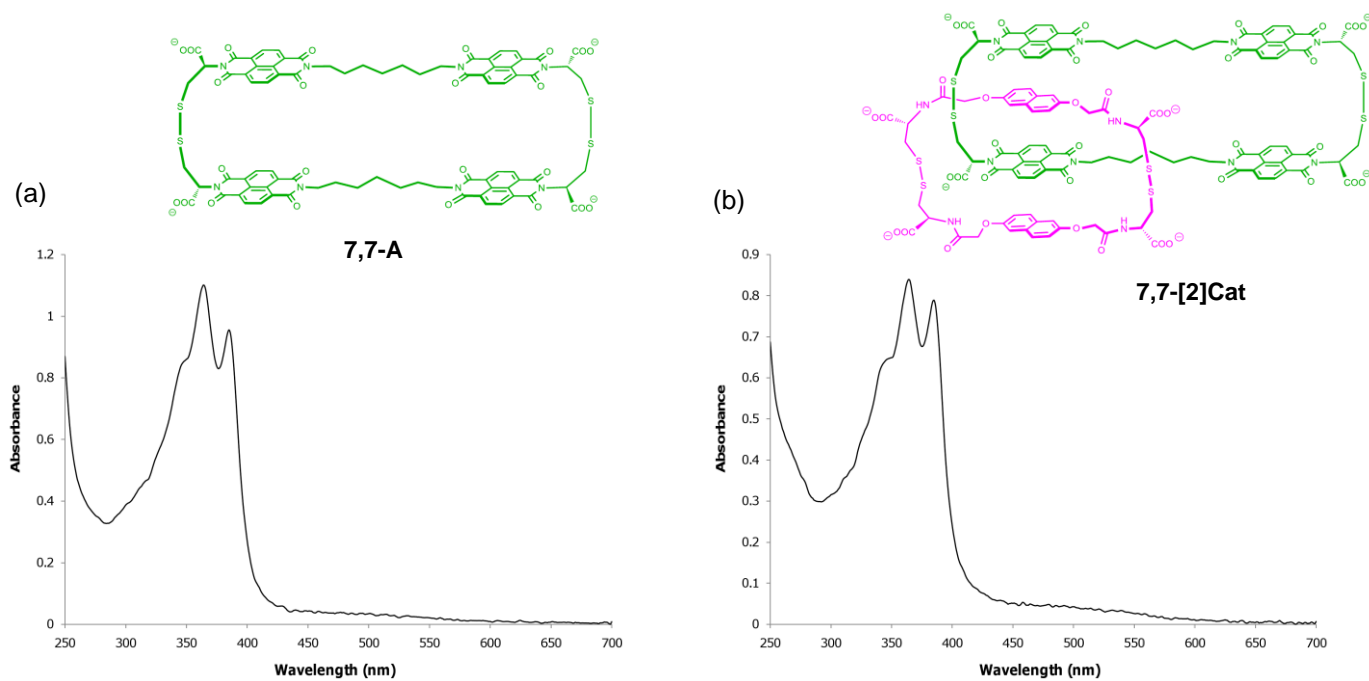


Figure 6.29. UV-Vis spectrum of (a) 7,7-A and (b) 7,7-[2]Cat (H₂O, 298K).

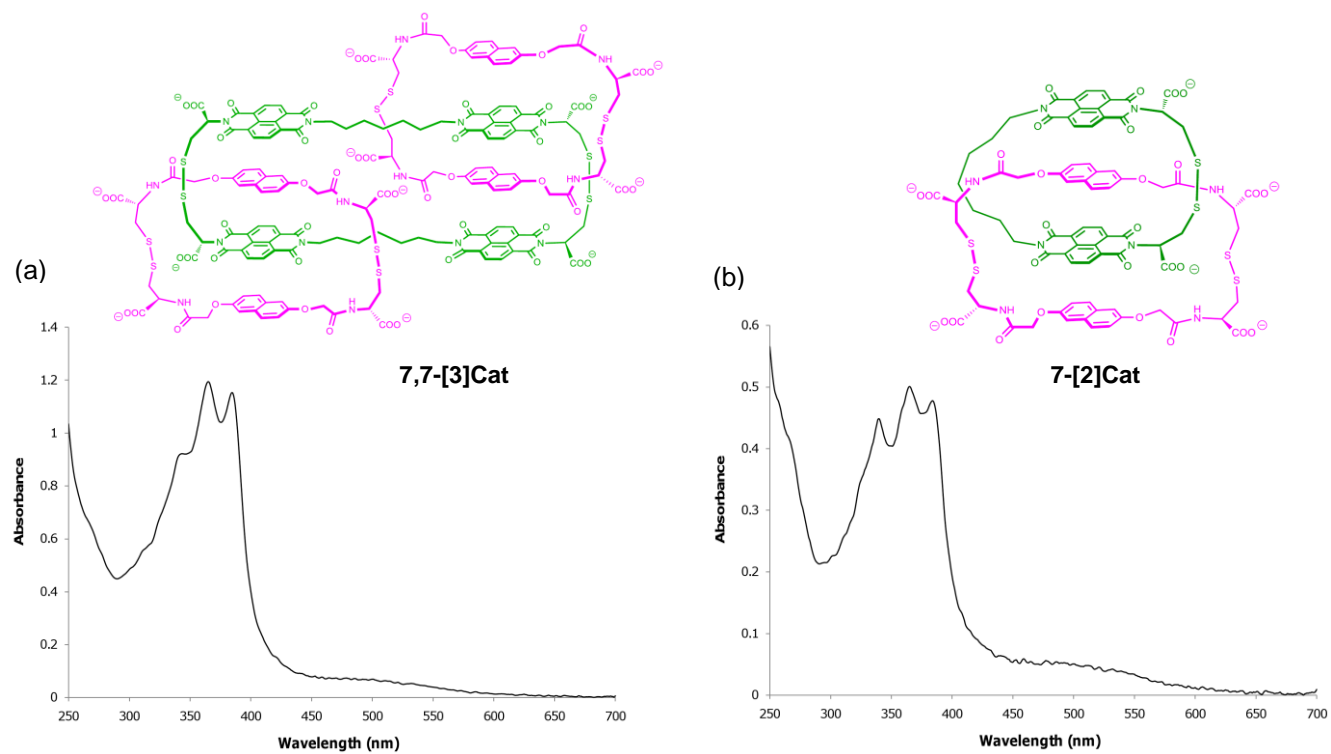


Figure 6.30. UV-Vis spectrum of (a) 7,7-[3]Cat and (b) 7-[2]Cat (H₂O, 298K).

References:

1. Au-Yeung, H. Y.; Cougnon, F. B. L.; Otto, S.; Pantoş, G. D.; Sanders, J. K. M. *Chem. Sci.* **2010**, 567.
2. Au-Yeung, H. Y.; Pantoş, G. D.; Sanders, J. K. M. *J. Am. Chem. Soc.* **2009**, 131, 16030.
3. Au-Yeung, H. Y.; Pantoş, G. D.; Sanders, J. K. M. *Proc. Natl. Acad. Sci. U.S.A.* **2009**, 106, 10466.
4. Au-Yeung, H. Y.; Pantoş, G. D.; Sanders, J. K. M. *Angew. Chem. Int. Ed.* **2010**, 49, 5331.
5. Pengo, P.; Pantoş, G. D.; Otto, S.; Sanders, J. K. M. *J. Org. Chem.* **2006**, 71, 7063.
6. Au-Yeung, H. Y.; Pantoş, G. D.; Sanders, J. K. M. *Chem. Commun.* **2009**, 419.
7. Crunch, D.; Krishnamurthy, V.; Brebion, F.; Karatholuvhu, M.; Subramanian, V.; Hutton, T. K. *J. Am. Chem. Soc.* **2007**, 129, 10282.
8. Tambara, K.; Ponnuswamy, N.; Hennrich, G.; Pantoş, G. D. *J. Org. Chem.* **2011**, 76, 3338.